MULTIPLE ROLES FOR UNC-53/NAV2 IN CELL MIGRATION, TRAFFICKING AND INNATE IMMUNITY IN *CAENORHABDITIS ELEGANS*

by

Kristopher Lee Schmidt

M.Sc., University of British Columbia, 2005
B.Sc., Trinity Western University, 2001

THESIS SUBMITTED IN PARTIAL FULFILLMENT OF
THE REQUIREMENTS FOR THE DEGREE OF

DOCTOR OF PHILOSOPHY

in the
Department of Molecular Biology and Biochemistry
Faculty of Science

SIMON FRASER UNIVERSITY

Summer 2012

APPROVAL

Name: **Kristopher Lee Schmidt**

Degree: **Doctor of Philosophy**

Title of Thesis: **Multiple roles for UNC-53/NAV2 in cell migration, trafficking, and innate immunity in *Caenorhabditis elegans.***

Examining Committee:

Chair: Dr. Barry Honda, Ph.D.
Professor, Department of Molecular Biology and Biochemistry

_____

Dr. Eve Stringham, Ph.D.
Co-Senior Supervisor
Professor, Department of Biology, Trinity Western University

_____

Dr. Nancy Hawkins, Ph.D.
Senior Supervisor
Associate Professor, Department of Molecular Biology and Biochemistry

_____

Dr. Christopher Beh, Ph.D.
Supervisor
Associate Professor, Department of Molecular Biology and Biochemistry

_____

Dr. Nicholas Harden, Ph.D.
Supervisor
Associate Professor, Department of Molecular Biology and Biochemistry

_____

Dr. Harald Hutter, Ph.D.
Internal Examiner
Professor, Department of Biological Sciences

_____

Dr. Nathalie Pujol, Ph.D.
External Examiner
Project Leader, Centre d'Immunologie de Marseille-Luminy

_____

Date Defended/Approved: June 1, 2012

Partial Copyright Licence

ABSTRACT

unc-53 is the *Caenorhabditis elegans* homolog of *Nav2*, and a member of the Neuron Navigator protein family, a group of cytoskeletal binding proteins with conserved roles in the guidance and outgrowth of cells and cellular processes. The signalling pathways that employ UNC-53 during development, and the role of UNC-53 after development is complete, are largely unknown.

A proteomics screen for interactors of UNC-53 identified that UNC-53 interacts with ABI-1. The Calponin Homology domain unique to the long-isoform of UNC-53 is sufficient to bind ABI-1 *in vitro* and is required *in vivo* for longitudinal migration. ABI-1 and UNC-53 are co-expressed, and *abi-1* genetic loss causes many of the same migration defects as *unc-53* mutants. *abi-1* and *unc-53* function cell-autonomously and in a common genetic pathway in the posterior migration of the excretory canals, and genetically inactivating *abi-1* interactors (*nck-1*, *wve-1*, *arx-2*) resulted in phenotypes similar to *unc-53* and *abi-1*. *abi-1* and *unc-53* are also required for endocytosis as measured by assaying the *in vivo* uptake of GFP into coelomocytes and primary oocytes. Lastly, *abi-1* mutants have *unc-53* independent migration defects, and ABI-1 binds to MIG-10A through its SH3 domain, thereby demonstrating that ABI-1 interacts with two proteins that function cell-autonomously in the longitudinal migration of the excretory canals.

To identify a post-developmental role for *unc-53*, a potential role for *unc-53* in innate immunity was assessed. *unc-53* mutants are susceptible to the human and nematode pathogen *Pseudomonas aeruginosa* PA14. *unc-53* mutants are hypersensitive to Aldicarb and have increased RNA levels of the *daf-16* antagonist *ins-7* as well as decreased nuclear DAF-16 localization following recovery from cellular stress, suggesting that *unc-53* functions in the *daf-16* pathway. Loss of function and null alleles of *daf-2* and *ins-7* only partially suppress *unc-53* in immunity, and a null *pmk-1* mutant does not enhance *unc-53*. Together, this data suggests that *unc-53* participates in innate immunity through multiple tissues, isoforms and genetic pathways.

These findings expand on the varied functions of *unc-53* and the signal transduction pathways that it controls, opening up new prospects for future areas of research.

Keywords: *C. elegans*; UNC-53; Neuron Navigators; ABI-1; cell migration; innate immunity

“Our modern world has fantastic power and knowledge. Man has conquered the moon, delved into the secret of matter, and discovered immense energies. But the only real knowledge necessary for the survival of the human race is lacking: the knowledge of how to transform violence and hatred into tenderness and forgiveness; how to stop the chain of aggression against the weak; how to see differences as a value rather than as a threat; how to stop people from envying those who have more and incite them to share with those who have less.”

~ Jean Vanier

~To my Mom

Without your dedication and sacrifice I would have never come this far.

ACKNOWLEDGEMENTS

"My Grace is sufficient for you because you are made strong in weakness"

(2 Corinthians 12:9)

My time during this degree program has been alive with reminders of my dependency on the strength and help of others. I am especially indebted to my thesis supervisor Dr. E. Stringham for steering me towards *C. elegans* as an undergraduate in 1998, and for offering me patience and grace as I developed into a scientist. Thank you also to my exceptional committee (Dr. C. Beh, Dr. N. Harden, and Dr. N. Hawkins). Your individual and collective insights have sharpened me and contributed substantially to this work. Thank you to my many friends and colleagues at Trinity Western University, Simon Fraser University, the Menno Simons Centre (PCDA), the University of British Columbia, Douglas College, and the *C. elegans* research community. Your support and contributions are unmatched, and you provide clear evidence that a strong and healthy community brings wellness to its members. I am especially indebted to Dr. A. Adeleye, Dr. N. Marcus, Dr. J. Webber, Dr. D. Baillie, D. Tu, Dr. S. Alper, E. Kreiter, C. Grypma, and Dr. E. Ryder, for either technical assistance or formal collaboration.

Finally, thank you to my family, and especially my wife Kathryn. You have supported me with kindness, compassion, and loving care. Thank you for your love.

TABLE OF CONTENTS

LIST OF FIGURES

LIST OF TABLES

LIST OF ABBREVIATIONS

AAA	ATPase associated with diverse cellular activities
ABI-1	Abelson interactor-1
ABL	Abelson tyrosine kinase
ABLIM	Actin binding LIM
AD	Alzheimer's disease
AGE-1	PI3K
AP2	Adaptor protein 2
APF	Actin polymerizing factor
ARP	Actin-related protein
at-Ra	all-trans Retinoic acid
CAM	Cell-adhesion molecule
Cdc42	Cell division control protein 42
CFZ	*C. elegans* Frizzled
CH	Calponin Homology
clec	C-lectin
CME	Clathrin mediated endocytosis
CN	Cranial nerve
Comm	Commisureless
CRIB	Cdc42 Rac Interaction
CRMP-2	Collapsin response mediator protein 2
CTCL	common primary cutaneous T-cell lymphoma
CUP	Coelomocyte uptake
CWN	*C. elegans* WNT
DAF	Dauer defective
DAF-16	Dauer defective-16/FOXO
DAF-18	Dauer defective-PTEN
DAF-2	Dauer defecting-Insuling receptor
DCC	Deleted in colorectal cancer/Frazzled
dFADD	Drosophila Fas-associated death domain
DGK	Diacylglycerol kinase
DIAP2	Drosophila Inhibitor of Apoptosis Protein DIAP2
DIG-1	Displaced gonad-1
Dredd	Death related ced-3/Nedd2-like
EB1	End Binding 1
ECM	Extracellular matrix
EGL	Egg-laying defective

EMS	Ethyl methanesulfonate
Ena	Enabled/Vasp
ERK	Extracellular receptor kinase
ESP	Enhanced sensitivity to pathogens
EVH	Enabled/VASP Homology
EVL	Ena Vasp Like
ExC	Excretory cell
FGF	Fibroblast growth factor
FGFR	Fibroblast growth factor receptor
FOXO	Forkhead box
FUDR	Fluorodeoxyuridine
FZ	Frizzled
GAP	GTPase activating protein
GD	Gonad-dependent
GDI	GTPase dissociation inhibitor
GDR	Gonad dependent repulsion
GEF	Guanine nucleotide exchange factor
GEX-2	Gut on exterior-SRA1
GEX-3	Gut on exterior-NAP1
GF	Gain of function
GFP	Green Fluorescent Protein
GID	Gonad-independent
GnRHR	Gonadotropic releasing hormone receptor
GTP	guanosine triphosphate
HSN	Hemaphrodite specific neuron
IL	Interleukin
IMD	Immune deficiency pathway
INS	Insulin
IRAK	Interleukin-1 receptor associated kinases
IRF3	Immune regulatory factor-3
IRSp53	Insulin receptor tyrosine kinase substrate of 53-kDa protein
JNK	June nuclear kinase
LET-60	Lethal-60-Ras
LpD	Lamellipodin
LPS	Lipopolysaccharide
MAP	Mitogen activated proteins
MDIA	Mammalian Diaphanous
MENA	Mammalian Enabled
MIG-10	Migration-10-Lammelipodin
MRL	MIG-10-RIAM-Lamellipodin
MT	Microtubules
MyD88	Myeloid differentiation factor 88
NAV	Neuron Navigator

NB	Neuroblastoma
Nck/Dock	Non-Catalytic region of tyrosine kinase
NF-kB	Nuclear factor-kappa beta
NMJ	Neuromuscular junction
NTP	Nucleotide Triphosphate
N-WASP	Neural-WASP (Wiskott Aldrich Syndrome Protein)
PAMP	Pathogen associated molecular pattern
PCD	Programmed cell death
PDGF	Platelet derived growth factor
PFT	Pore forming toxin
PGRP-LC	Peptidoglycan recognition protein-LC
PI3K	Phosphatidyl inositol-3 kinase
PIK-1	Pelle IRAK kinase homolog
PKC	Protein Kinase C
PKD	Protein Kinase D
PRR	Pathogen recognition receptors
qPCR	Quantitative PCR
Relish	NF-kB
Rho	Ras homology gene member
RIP1	Receptor interacting protein 1
RME-2	Receptor mediated endocytosis-2
RNAi	RNA-interference
Robo	Roundabout
ROS	Reactive oxygen species
RPIP-8	Rap2-interacting protein 8
RTK	Receptor tyrosine kinase
SAX-3	ROBO
SEM-5	Sex myoblast migration-5-GRB2
SL	Spliced-leader
SLT-1	SLIT
SM	Sex myoblasts
SPLT	Subcutaneous panniculitis-like T-cell lymphoma
TF	Transcription factor
TGF-B	Transforming Growth Factor
TIR	Toll-interleukin Receptor
TOCA	Transducer of Cdc42-dependent actin assembly
TRF-1	TRAF homolog
TRIF	TIR-domain-containing adapter-inducing interferon-β
UNC	Uncoordinated
UNC-115	Ablim
UNC-129	TGF-B
UNC-34	Enabled/Vasp
UNC-40	DCC/Frazzled

UNC-44	Akyrynin
UNC-54	Myosin
UNC-6	Netrin
UNC-64	Syntaxin
UNC-71	ADAM
UNC-73	TRIO
VAB-8	Kinesin-like
VASP	Enabled/Vasp
VCA	Verprolin Cofilin Acidic
WASP	Wiskott Aldrich Syndrome Protein
WAVE	WASP family Verprolin-homologous protein
WH1	Wasp Homology 1
WHD	Wave Homology Domain
WVE	WAVE
YP170	Yolk-protein 170

CONTRIBUTIONS

This work was a collaboration between myself and many others. Chapter 2 was mostly published or submitted in the following (in order of relevance):

Schmidt KL, Marcus-Gueret N, Adeleye A, Webber J, Baillie D, Stringham EG. The cell migration molecule UNC-53/NAV2 is linked to the ARP2/3 complex by ABI-1. *Development*. 2009. 136(4):563-74.

Stringham EG, **Schmidt KL**. Navigating the cell: UNC-53 and the navigators, a family of cytoskeletal regulators with multiple roles in cell migration, outgrowth and trafficking. Cell Adh Migr. 2009:342-6.

McShea MA, **Schmidt KL**, Dubuke ML, Baldiga CE, Zhang S, O'Toole SM, Gosselin J, Kuhlwein M, Hashmi S, Stringham EG, Ryder EF. Abelson interactor-1 (ABI-1) interacts with MRL adaptor protein MIG-10 and is required in guided cell migrations and process outgrowth in *C.elegans*. *Submitted.* 2012.

Marcus-Gueret N, **Schmidt KL**, Stringham EG. Distinct cell guidance pathways controlled by the Rac and Rho GEF domains of UNC-73/TRIO in *Caenorhabditis elegans*. Genetics. 2012. 190(1):129-42.

I am the first author on the *Development* publication (Schmidt et al., 2009) with the following co-authors: Dr. N. Marcus, Dr. A. Adeleye, Dr. J. Webber, Dr. D. Baillie and Dr. E. Stringham. I performed all the experiments in this publication with the following exceptions: Dr. A. Adeleye performed the yeast two-hybrid screen identifying UNC-53N and ABI-1 as interactors, produced the polyclonal antibody PAB-UNC-53N, and conducted some of the immunostaining. Dr. D. Baillie (with D. Tu performing injections) produced the strains BC12924, BC10129 and BC14371. Dr. N. Marcus and I conducted the experiments and data collection together for Figure 15, Figure 16 and Figure 23, while Dr. N Marcus sequenced the allele *unc-53 (n166)*, and established that *unc-53 (n166)* is a null allele. Dr. J. Webber and I conducted the experiments for Figure 12 together. Dr. E. Stringham co-wrote this publication and assisted with the experiments. I wrote ~80% of this paper. I am second author on the *Cell Adhesion and Migration* publication (Stringham and Schmidt, 2009) along with Dr. E. Stringham, and I am responsible for the data and figures generated in this publication, and I wrote part of

the paper (~50% of the writing). The submitted manuscript McShea *et al.* (2012) includes me as a second author. For this study, I generated the plasmids and conducted the experiments determining that full-length ABI-1 and full-length MIG-10A interact by yeast two-hybrid, and mapped the binding domain of ABI-1 of MIG-10A. I also produced the plasmid pVA700 which was used in subsequent experiments to establish the cell-autonomy of *mig-10a* in excretory canal elongation. I performed a minority of the writing for this manuscript (~10%). I am second author on the *Genetics* publication. For this publication I contributed to the production of the clone pVA700 and the clone pVA705 which was used to show a cell non-autonomous role for *vab-8* in the longitudinal migration of the excretory canals. I also generated some of the crosses that were used in this publication. I did not contribute to any of the writing.

Chapter 3 includes work done by myself, Dr. S. Alper, Dr. Ivana Yung, and Dr. E. Stringham. I co-designed these experiments with Dr. E. Stringham and Dr. S. Alper and performed all of the experiments in this work with the following exceptions: Dr. I Yung performed the microarray experiments. Dr. S. Alper performed the qPCR analysis and and the post-processing analysis including significance and fold-change determinations and the Kegg, Transfac, and Ingenuity Pathway Analysis (IPA). I performed a majority of the writing (~95%).

1: INTRODUCTION TO UNC-53 AND THE NEURON NAVIGATORS

While much has been uncovered with respect to the signalling events that control cell guidance (see Section 2.2) and the changes in the cytoskeleton that initiate migration and outgrowth (see Section 2.2.4), less is known about the proteins that integrate these processes. One family of proteins that coordinate upstream signals to changes in the cytoskeleton are the Neuron Navigators (NAVs). The purpose of this thesis is to expand what is known about UNC-53/NAV2 in development and after development is complete. Chapter 1 introduces the *C. elegans* protein UNC-53/NAV2 (see Section 1.1) and the NAV homologs (see Section 1.2), and provides an overview of the subsequent sections of the thesis (see Section 1.3).

1.1 Prior research on UNC-53 from *C. elegans*

unc-53 (*unc*oordinated-53) is the *C. elegans* homolog of NAV2, and a member of the NAV family of proteins (see Section 1.2) with conserved roles in cytoskeletal binding and cell migration (Stringham et al., 2002; Stringham and Schmidt, 2009). *unc-53* was originally isolated through the early ethyl methanesulfonate (EMS) mutagenesis screens carried out by Sydney Brenner that identified several genes based on a limited number of phenotypes observable with a dissecting microscope including “unc” or “uncoordinated”, selecting mutant animals that displayed abnormal movement compared to the elegant sinusoidal movement patterns observed in wild-type (Brenner, 1974). Uncoordinated phenotypes are relatively non-specific and have been attributed to genes controlling multiple processes including axonal guidance (e.g. *unc-6/Netrin)*, muscle function (e.g. *unc-54/Myosin)*, and synaptic vesicle trafficking (e.g *unc-64/Syntaxin*). Several years later, additional alleles of *unc-53* were identified in a screen for egg-laying defective (“Egl”) animals, and *unc-53* was observed to be resistant to serotonin and imaprine, suggesting that the Egl phenotype resulted from defects in vulva development or function rather than the induction of egg-laying (Trent et al., 1983). The Unc and Egl phenotypes remain as two of the most obvious features of most *unc-53* mutants.

unc-53 is needed for the migration of axons and cellular extensions along the anteroposterior axis in *C. elegans*, with only minor defects so far observed in migration

along the dorsoventral axis (Hekimi and Kershaw, 1993; Stringham et al., 2002). Some of the axonal projections requiring *unc-53* include the anterior projections of the mechanosensory touch receptor neurons (ALML/R, PLML/R, AVM, and PVM), the ALNL/R and PLNL/R, (Hekimi and Kershaw, 1993; Siddiqui and Culotti, 1991; Stringham et al., 2002), the anterior and posterior processes of the PDEL/R, and the anterior processes of the HSNL/R and AVKL/R (Wightman et al., 1997). Posterior longitudinal migration was also recently shown to be defective in the ALA neuron in *unc-53* (Marcus-Gueret et al., 2012). Figure 1 shows examples of some of the extensions that are abnormal in *unc-53* mutants. In addition to the longitudinal migration of axons, *unc-53* is required for the anterior and posterior migration of the excretory canal processes (Stringham et al., 2002). The excretory cell (ExC) functions as the nematode equivalent of the kidney (Nelson et al., 1983; Nelson and Riddle, 1984) and is the largest cell in *C. elegans*, serving as an excellent model for the study of cell migration and tube formation (Buechner, 2002). During its development, the ExC extends two canals dorsoventrally from its anterior position in the head towards the lateral hypodermis, followed by a bifurcation of the canals and an anterior and posterior extension so that the canals run the entire length of the animal (Buechner, 2002; Zhao et al., 2005). In *unc-53* mutants, both the anterior and posterior processes fail to reach their wild-type positions while the dorsoventral migrations appear to be normal (Stringham et al., 2002). Only a minimal contribution to guidance along the dorsoventral axis is attributed to *unc-53*. Dorsoventral motorneuron axon outgrowth and guidance were previously observed to be normal for the DD and VD neurons as were the dorsoventral projections of the mechanosensory neurons and ventral projection of the HSN and PDEs, and DA and AS dorsoventral projections were only sometimes observed to be altered, with variable phenotypes and expressivity (Hekimi and Kershaw, 1993; Siddiqui and Culotti, 1991; Stringham et al., 2002). The lack of dorsoventral defects in *unc-53* could be the result of the presence of several overlapping genetic pathways controlling dorsoventral migrations. Previous studies using the excretory cell as a model indicate that *unc-53* is required in a genetic pathway parallel to *unc-71/Adam* and *unc-5* in the control of the dorsally directed migrations of the excretory cell (Roelens, 2002). Other defects observed in *unc-53* mutants include defasiculation of the dorsal, ventral and sublateral nerve cords including the frequent absence of some portions of the nerve cords, as well as midline guidance defects in neurons and other cells (Hekimi and Kershaw, 1993).

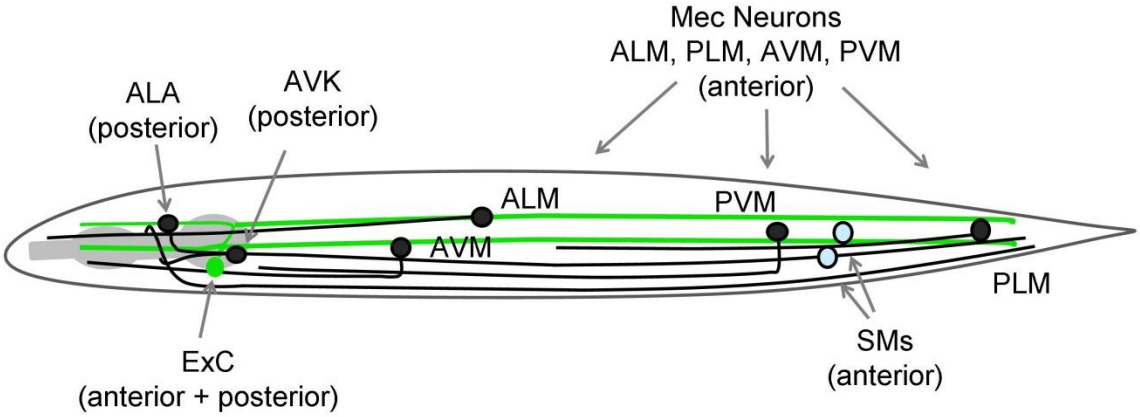

Figure 1. Summary of the migrations affected by *unc-53*

Examples of some of the cells and cellular processes controlled by *unc-53* in *C. elegans* are shown. *unc-53* affects the migration of cells and cellular processes along the longitudinal axis. Neuronal cell bodies and axons are in black, the excretory cell (ExC) and associated canals are in green, and the sex myoblasts (SMs) are shown in blue. Note that the migrations and trajectories are all oriented along the anteroposterior axis, and *unc-53* controls both anterior and posterior migration.

unc-53 also controls the positioning of cells, as evidenced by its role in the anterior migration of the sex myoblasts (SMs). The SMs are a pair of muscle precursor cells that originate within the ventral midposterior region of the animal during early larval development and undergo a sexually dimorphic migration under the control of the *Hox* gene *mab-5* (Burdine et al., 1997; Chen et al., 1997), migrating posteriorly in males, or anteriorly along the ventral muscle quadrants towards the center of the developing gonad in hermaphrodites, at which point they divide and differentiate to become the sixteen vulval and uterine muscle cells (Sternberg, 2005). The anterior migration of the SMs in hermaphrodites is under the control of both gonad-dependent (GD) and gonad-independent (GID) genetic pathways. Eliminating the GD pathway by laser ablating the Z1 and Z4 gonadal precursor cells disrupts the anterior migration of the SMs, as does the use of *dig-1* mutants with dorsally displaced gonads that similarly position the SMs dorsally with respect wild-type, suggesting the gonad secretes an attractive cue responsible for SM anterior migration. Numerous members of the GD pathway have been identified including EGL-17/FGF expressed and secreted from the dorsal uterine cells of the somatic gonad, and EGL-15/FGFR which is expressed in the migrating SMs (see Section 2.2.2). Subsequent to the earlier screens identifying *unc-53* as Egl (Trent

et al., 1983), Chen *et al.* (1997) recognized that *unc-53* is a regulator of vulval and uterine muscle cell positioning through its effects on the gonad-independent pathway. To define GID pathway genes, they carried out an enhancer screen for defects in the anterior migration of the SMs using *sem-5 (n1779)* animals lacking the GD pathway. This screen identified three GID genes: the disintegrin and metalloprotease *unc-71/Adam*, the Rac-GEF *unc-73/Trio*, and *unc-53* (Chen et al., 1997). These findings suggest that UNC-53 may function with UNC-71 and UNC-73 in SM migration. It was recently shown that both *unc-71* and *unc-73* are expressed in the excretory cell and function in a genetic pathway together with *unc-53* in the control of the posterior migration of the excretory canals (Marcus-Gueret et al., 2012). Importantly, while UNC-53 was identified as functioning in the GID pathway, Chen *et al.* (1997) also observed that *unc-53; sem-5* and *unc-53; let-60/Ras* animals have enhanced anterior SM migration defects compared to *unc-53* gonad-ablated animals. An enhancement of the SM defects in the absence of a gonad suggest that *sem-5* and *let-60/Ras* may have a larger role in the GID pathway. The observation that UNC-53 binds SEM-5 *in vitro* supports this assertion (Stringham et al., 2002). Therefore, studies of cell migration of the SMs implicate UNC-53 in SEM-5, LET-60, UNC-71 and UNC-73 signalling pathways in the large-scale migrations of the SMs. In addition to the large-scale movements of the SMs, *unc-53* also appears to be required for some of the later muscle cell extensions required for the development of the adult vulva. Once the SMs have migrated to the position of the future vulva, the SMs undergo three cell divisions to give rise to the 16 VMs and UMs. Following this division, the lateral extensions fail to migrate properly, contributing to the underlying egl defect (Stringham et al., 2002).

unc-53 interacts genetically with *vab*-8, a gene encoding a *C. elegans* kinesin-like molecule needed to traffic guidance receptors (see Section 2.2.2) (Levy-Strumpf and Culotti, 2007; Watari-Goshima et al., 2007). *vab-8* is required for the posterior migration of neuronal cell bodies and their cellular extensions (Wightman et al., 1996; Wightman et al., 1997; Wolf et al., 1998), as well as the anterior and posterior migration of the excretory canals (Marcus-Gueret et al., 2012). So far, it is suggested that *unc-53* may either antagonize *vab-8* or function independently of *vab-8*, depending on the migration event involved. Two lines of evidence suggest that *unc-53* may antagonize *vab-8* in some cells. The first is that *unc-53* genetic loss suppresses the weak allele *vab-8 (ev411)* in the posterior migration of the CAN neurons (Dr. G. Garriga, personal

communication). Secondly, when the long transcript of *vab-8* is ectopically expressed in the mechanosensory neurons using a *pmec-7::vab-8L::gfp* construct, the ALM mechanosensory neuron that normally extends anteriorly is rerouted posteriorly, exactly 180° relative to their usual route a majority of the time, suggesting that VAB-8L is able to direct axons to the posterior direction cell-autonomously, probably by altering the site of outgrowth at the cell body (Wolf, 1998). Importantly, this rerouting is enhanced in *unc-53 (n152)* mutants, indicating *unc-53* may normally act in opposition to *vab-8* for posterior directed migrations. Two possible models explain these latter results: 1) UNC-53 negatively regulates VAB-8, and the genetic removal of UNC-53 allows VAB-8 to constitutively direct posterior outgrowth of the ALM process; 2) UNC-53 and VAB-8 operate in separate pathways to control outgrowth. In the second model, the role of UNC-53 is to drive the anterior outgrowth of the ALM and removal of UNC-53 removes the anterior driving force and allows ectopic expression of VAB-8 to drive posterior migration unabated (Wolf, 1998). Recent genetic studies aimed towards understanding the relationship between UNC-53 and VAB-8 in migrations of the excretory cell show that *vab-8* and *unc-53* mutants both have defects in the posterior migration of the excretory canals, and that double mutant *unc-53; vab-8* animals have enhanced posterior excretory canal defects, suggesting that these genes function in separate pathways in the posterior migration of the ExC and that both pathways employ UNC-73 (Marcus-Gueret et al., 2012).

Even though some of the developmental roles and genetic interactions of *unc-53* have been described, it is only somewhat recently that the molecular nature of *unc-53* has been examined. The *unc-53* genetic locus is large and complex, consisting of 23 exons spanning 31kb of genomic DNA, and subject to SL1 transplicing as well as alternative splicing to produce a total of six predicted isoforms (Stringham et al., 2002); the longest transcript encodes a 1583 amino acid protein. So far, two internal promoters have been described that together drive the expression of *unc-53* in many tissues including several populations of neurons, the excretory cell, vulval and uterine cells, intestinal and anal muscles, and distal tip cells (Stringham et al., 2002). One promoter is composed of intronic DNA contained between exons 5-8 (*punc-53SA*) and another is found between exons 8-13 (*punc-53SB*). These internal promoters drive *unc-53* expression independently to confer tissue and isoform specificity to *unc-53* (Stringham et al., 2002). The *punc-53SA* promoter, which conferes expression in the excretory cell,

rescues the posterior ExC canal migration defects, while the *punc-53SB* promoter is expressed in the vulva and uterine cells and rescues the Egl defect (Stringham et al., 2002). Given that each promoter is only able to rescue in the cells where it is expressed suggest that *unc-53* functions cell-autonomously in cell migration and outgrowth. A cell-autonomous role for *unc-53* is also supported by the observation that overexpression of *unc-53* under the control of muscle promoter (*punc-54::unc-53*) results in elongated body muscles and lethality (Stringham et al., 2002).

unc-53 encodes proteins containing domains that suggest a role for UNC-53 in signal transduction and cytoskeletal binding. Several protein motifs are shared between UNC-53 and the Navigators including a calponin homology (CH) domain in the N-terminus, several coiled-coil regions, polyproline rich SH3 binding motifs, and an ATPases associated with diverse cellular activities domain (AAA domain) (Figure 2). The UNC-53 CH domain is located at its N-terminus, situated at amino acids 11 to 109 (Stringham et al., 2002). The CH domain is present in various actin-binding proteins, including α-actinin and dystrophin, which have been implicated in regulating actin and cell shape dynamics (Broderick and Winder, 2005), as well as proteins implicated in scaffolding functions in signal transduction (Galkin et al., 2006; Gimona et al., 2002; Korenbaum and Rivero, 2002). Adjacent to the CH domain is an additional putative actin-binding site with an LKK consensus motif from amino acids 114 to 133 and a second LKK motif from amino acids 1097 to 1116. Importantly, UNC-53 was shown to co-sediment with F-actin *in vitro* (Stringham, unpublished results). It also contains two polyproline rich sequences at residues 487-495 and 537-545 that are expected to bind SH3 domain containing proteins (Reebye et al., 2012). Two regions towards the C-terminus of UNC-53 (890-923 and 1078-1113) are putative coiled-coil domains that may mediate homomeric or heteromeric protein-protein interactions (Maes et al., 2002; Stringham et al., 2002). Another identified region accompanying amino acids 837-1065 directs localization with the microtubule cytoskeleton (Muley et al., 2008). Finally, the C-terminal AAA has a nucleotide (NTP) binding site that can propagate changes in conformational state to target substrates in response to NTP binding in processes such as transport, disaggregation and dissassembly (Hanson and Whiteheart, 2005; Stringham et al., 2002).

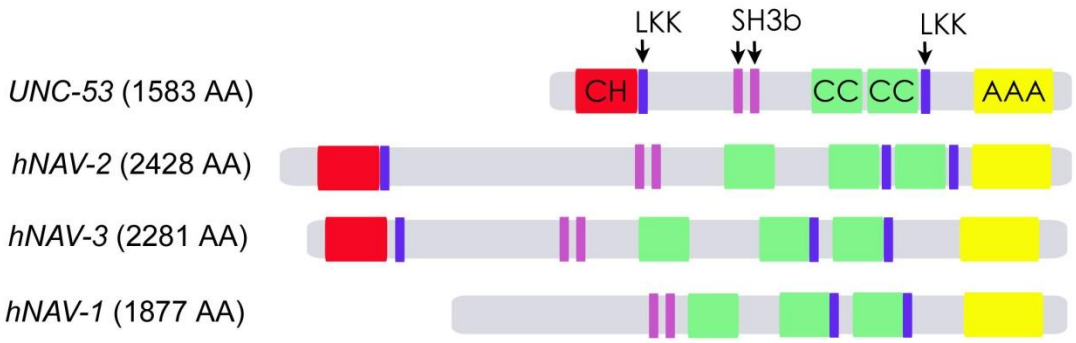

Figure 2. General domain organization of Neuron Navigator family proteins

General domain organization of NAVs. NAVs display a highly conserved domain organization containing multiple domains involved in signal transduction and cytoskeletal binding. Domains include a Calponin Homology domain (CH, Red), LKK actin-binding motifs (LKK, Blue), polyproline rich SH3 binding motifs (SH3b, Purple), Coiled Coil domains (CC, Green), and a AAA ATPase associated with diverse cellular activities (AAA, Yellow) (Stringham and Schmidt, 2009). Note that NAV1 differs substantially from NAV2/3 and UNC-53 because it lacks an N-terminal CH domain.

1.2 Insights from the Neuron Navigators, UNC-53 homologs

unc-53 homologs have been identified across organisms, including insects, fish, amphibians and mammals (Maes et al., 2002). The genomic composition of the *Nav* genes has only been formally examined for the human *Navs* (*Nav-1,2,3*). Human *Nav* genomic loci are remarkably similar to *unc-53*, spanning large segments of genomic DNA, and composed of multiple exons with large intervening introns (Maes et al., 2002). Like *unc-53*, they are also subject to alternative splicing of RNA transcripts that give rise to multiple protein isoforms expressed in tissue-specific ways (Maes et al., 2002). Several protein motifs are shared between UNC-53 and the NAVs (Figure 2), including the CH domain, coiled-coil regions, SH3 binding motifs, and a C-terminal AAA domain. Microtubule binding domains have also been identified in NAV homologs (Martinez-Lopez et al., 2005; Muley et al., 2008; van Haren et al., 2009). UNC-53 is most closely related to NAV2 (56% and 41% similar to the N-terminal and C-terminal regions respectively) (Stringham et al., 2002) while NAV1 is most divergent from UNC-53, NAV2, and NAV3 (Maes et al., 2002) as NAV1 lacks the actin-binding CH domain found in the

long-isoform of UNC-53 and the other NAVs. The apparent divergence of *Nav1* from *Nav2* and *Nav3* resulted from an ancient genome duplication that isolated these loci (Maes et al., 2002).

The mammalian NAVs are expressed both during development and after development is complete. Multiple alternatively spliced transcripts of human *Nav1* and *Nav2* but not *Nav3* are observed in the developing brain (Maes et al., 2002), and additional expression of *Nav2* has been observed in developing heart, cerebellum, bladder, aorta, jejunum and interventricular septum (Merrill et al., 2002), arguing that *Nav2* may control the development of non-neuronal tissues. *Nav1* expression persists in the adult heart and placenta but appears to be low in nervous tissue after development, suggesting a developmentally controlled role for this gene. Interestingly, while *Nav1* expression is low in the adult brain, it appears to be upregulated in pathological conditions, as increased *Nav1* transcripts are observed in cases of oligodendrogliomas, and all of the *Navs* are expressed in numerous cancer derived cell lines (Maes et al., 2002). After development, *Nav2* is found in kidney and brain (Maes et al., 2002) as well as the stomach, spinal cord, uterus, prostate, thyroid and mammary gland (Merrill et al., 2002). One study observed that human *Nav3* expression appears to be restricted to the adult brain (Maes et al., 2002), suggesting a specific post-developmental role for *Nav3* in the brain, at least in humans, though *Nav3* mRNA is also associated with synapses at neuromuscular junctions (Kishi et al., 2005), and *Nav3* expression was also observed in normal peripheral blood lymphocytes and activated T-lymphocytes (Karenko et al., 2005) in adult tissue. Mammalian navigators also appear to be expressed in migrating neurons *in situ*, as mNAV1 positive cells originating from the neural crest and along several migratory pathways including the intermediate zone (IZ) and pontine migratory stream (PMS) were observed (Martinez-Lopez et al., 2005). Multiple tissue northern blots for *Nav2* in rats are positive for brain and spinal cord in rat embryos, and *in situ* hybridization showed *Nav2* expression correlating with the production of the *atRA* (all-trans retinoic acid), a vitamin-A metabolite required for neuronal migration and specification (Clagett-Dame and Knutson, 2011), and Vitamin-A deficient or *atRA* deficient animals have less *Nav2* and display hindbrain developmental defects (McNeill et al., 2010; Merrill et al., 2002).

Studies in mammalian genetic model systems reveal a role for the *Navs* in neurodevelopment, specifically in the control of neuronal outgrowth and directionality. Murine NAVs (*mNav-1,2,3*) are nearly identical to their human *Nav* counterparts (Peeters et al., 2004), and like the human *Navs*, the *mNAVs* are expressed during development and post-developmentally (Martinez-Lopez et al., 2005; Merrill et al., 2002; Muley et al., 2008; Peeters et al., 2004). A single *mNAV* knockout mouse line (*mNav2*, C57BL/6-Tyrc-Brd unc53H2) has been developed that lacks the long-isoform of *mNav2* while leaving the shorter isoforms (lacking the CH domain, similar to the shorter isoforms of *unc-53*) intact (Peeters et al., 2004). *mNav2* mice are hypomorphic but exhibit multiple phenotypes including decreased post-natal survival (McNeill et al., 2010) and multiple sensory defects including reduced smell, hearing and visual acuity (Peeters et al., 2004). Of particular interest is that the defects in visual acuity follow from hypoplasia of the optic nerve, consistent with a role for *mNav2* in migration and neurodevelopment (Peeters et al., 2004). *mNav-2* mice also have substantial hindbrain development defects including decreased nerve fiber density along the mesencephalic tract and dorsal root ganglia, and axonal elongation and fasciculation defects in cranial nerves (CN) IX and X that result in a decreased baroreceptor response (McNeill et al., 2010). Importantly the development of the hindbrain as well as CN IX and X are under the control of atRA (McNeill et al., 2010; Merrill et al., 2002; Muley et al., 2008). *Nav2* expression is rapidly increased (~4hrs for up to 2 days) in SH-SY5Y neuroblastoma (NB) cells following treatment by atRA (all-trans retinoic acid), (Merrill et al., 2002), and *atRA* induced neurite outgrowth in NB cells is eliminated by *shmNAV2* (Muley et al., 2008), placing the *mNAV-2* as a key mediator of *atRA* controlled developmental processes. The human *Navs* are also shown to induce neurite-like extensions in non-neuronal cells (Martinez-Lopez et al., 2005; van Haren et al., 2009). In addition to its role in neurite outgrowth, the *Navs* also appear to contribute to growth cone directionality as RNA interference of *mNav-1* abolishes the directional outgrowth of rat pontine neurons grown in the presence of a *Netrin-1* gradient (Martinez-Lopez et al., 2005). A role for human *Nav2* in neuronal migration has also been suggested through studies in *C. elegans* as *Nav2* expressed under the control of the mechanosensory neuron specific promoter *pmec-7* rescues the *unc-53 (e404)* PLM outgrowth defect (Muley et al., 2008), evidence that *Nav2* functions cell-autonomously and is the functional equivalent of *unc-53*.

While it is understood that the *Navs* function in neuronal outgrowth during development, it is only recently that the cell biology of the *Navs* has started to be uncovered. *Nav* family proteins are cytoskeletal binding proteins and are associated with F-actin, intermediate filaments (Muley et al., 2008) and microtubules (Martinez-Lopez et al., 2005; Muley et al., 2008; van Haren et al., 2009). The subcellular distribution of the *Navs* appears to depend partially on the cell type examined and the *in vitro* conditions. Muley *et al.* (2008) identify that endogenous NAV2 is distributed in a punctate fashion in the cytoplasm and along neurites in unstimulated SH-SY5Y cells, and that in response to *atRA*, NAV2 redistibutes towards the perinuclear region and neurites where it overlaps with phosphorylated neurofilaments but not either alpha-tubulin or the +TIP protein EB1 (Muley et al., 2008). Alternatively, NAV2 overexpressed in COS-1 cells shows that NAV2 is highly associated with alpha–tubulin, and has a domain-specific for tubulin-interactions (van Haren et al., 2009). van Haren *et al*. (2009) found that all of the NAVs localize to the plus-ends of MT-tips, with NAV1 also found to be associated with unidentified granular structures and NAV2 and NAV3, and to be associated with membrane ruffles. Pan-NAV antisera shows colocalization of the NAVs with the +TIP EB1, and overexpression of UNC-53 displaces CLIP-170 and p150glued which have CAP_GLY motifs that allow MT interaction, suggesting an overlap of these proteins at MT plus ends. NAV overexpression is able to induce neurite extension in non-neuronal cells, and this polarization is continuous with the formation of acetylated tubulin, suggestive of stabilized MTs. For at least NAV1, the capacity to induce the polarized membrane protrusions was dependent on its ATPase activity, as a mutation in the AAA cassette that abolishes nucleotide binding virtually eliminated the formation of ectopic extensions, coupling NAV outgrowth and polarization to its ATPase function. Importantly, while NAV2 expression follows that of alpha-tubulin, it does not appear to be directly involved with microtubule assembly *per se* as its association with microtubules lagged behind polymerization (van Haren et al., 2009). Similar observation for *mNav1* are observed. mNAV1-GFP contructs were produced and expressed in non-neuronal COS-1 cells and comet-like tails were observed (Martinez-Lopez et al., 2005); the subcellular expression pattern depended on the expression levels: low levels resulted in expression on microtubule tips, intermediate expression along shafts of microtubules, and high expression caused bundling. mNAV1 and alpha-tubulin coimmunoprecipitated, and colocalization of mNAV1 was observed with the plus end proteins CLIP-170 and CLIP-115, and these authors also found a minimal region in mNAV1 that is needed for

MT binding and bundling (Martinez-Lopez et al., 2005). Additional evidence for mNAV1 in neuronal migration and outgrowth extends from the finding that expression of *mNav-1* was observed in neurons, particularly as granules in neurite extension, and in a high density at distal ends, branching points, and growth cones (Martinez-Lopez et al., 2005).

While much information has been gained about the role of UNC-53 homologous proteins in neurodevelopment and as proteins that interact with the cytoskeleton, several questions remain. Of particular interest is the extent to which UNC-53 and the NAVs function after development is complete. *Nav* expression persists following development. *Nav3* mRNA was observed to be concentrated to the post-synaptic regions at neuromuscular junctions, which could suggest a role for NAV3 at the synapse, possibly in endocytosis (Kishi et al., 2005). It has also been suggested that *unc-53* or the NAVs may function in immunity (Alper et al., 2008; Foley and O'Farrell, 2004). *C. elegans unc-53* was recently found to be needed for the full intestinal expression of the worm C-lectin *clec-85* in a whole-genome RNAi screen (Alper et al., 2008). A genome-wide RNAi screen in *Drosophila* S2 cell culture revealed the *unc-53* homolog *Sickie* as a novel member of the IMD pathway as an activator of the *caspase-8* homolog *Dredd*, required for *Relish* nuclear translocation (see Section 3.3.1) (Foley and O'Farrell, 2004). There is also some evidence from mammals to suggest a potential role for the NAVs in immunity. Genetic silencing of *Nav-3* in Jurkat T-cells as well as primary lymphocytes increases the expression of the interleukin-2 (IL-2) with no changes in IL-4, suggesting that *Nav-3* may alter the cytokine profile from a Th-1 to a Th-2 type response (Karenko et al., 2005). A recent microarray experiment examining *Nav3* silenced primary human epidermal keratinocytes revealed alterations in genes mostly implicated in inflammation (Maliniemi et al., 2011). In addition, treatment of corneal fibroblasts with the anti-inflammatory dexamethasone decreases the expression of *Nav2* (Liu et al., 2011).

Navs have also been implicated in cancer and neuropathological states. *Nav3* has been suggested by many groups to function in cancer development as a tumor suppressor (Carlsson et al., 2012; Coy et al., 2002; Karenko et al., 2005; Maliniemi et al., 2011). Evidence for this role comes from numerous cytological studies that have examined tumor tissue and cancer cell lines. In one study, fifty percent (50%) of patients with early Sézary syndrome, a common primary cutaneous T-cell lymphoma (CTCL), had lesions carrying a deletion of *Nav3* while 85% of patients with advanced disease

had *Nav3* deleted (Karenko et al., 2005). A similar study found allelic aberrations in 44% of subcutaneous panniculitis-like T-cell lymphoma (SPLT) (Hahtola et al., 2008), and low copy-numbers of *Nav3* are also observed in a significant number of basal cell and squamous cell carcinomas and related cancer cell lines (Maliniemi et al., 2011). Finally, a very recent study showed that *Nav3* is deleted in a number of carcinomas and cancer cell lines, and that *Nav3* silencing causes the upregulation of the gonadotropic releasing hormone receptor (GnRHR) and the IL-23 receptor, which are correlated to tumor staging and lymph node metastases (Carlsson et al., 2012). Neuron Navigators have been implicated in neuropathology in two studies. One study identified that *Nav1* mRNA is decreased in the prefrontal cortex of patients with schizophrenia, and that *Nav1* levels correlate with the levels of the presynaptic plasticity marker dysbindin known to be abnormal in schizophrenic patients (Fung et al., 2011). A second study aimed at identifying the underlying pathological implication of aberrant miRNA expression in neurodegenerative diseases and found miR-29a to be decreased in the brains of Alzheimer's disease (AD) patients, resulting in increased *Nav3* mRNA levels and increased NAV3 in degenerating pyramidal neurones in the cerebral cortex of AD (Shioya et al., 2010). Interestingly, miR-29 family members target genes known to play an important role in cancer development, so it is possible that the miR-29 family of miRNAs may target proteins involved in both neurodegenerative diseases and cancer, and that these diseases may share common mechanisms of genetic and molecular abnormalities (Du and Pertsemlidis, 2011).

1.3 Thesis overview

UNC-53 and the NAVs have conserved roles in the guidance and outgrowth of cells and cellular processes in both *C. elegans* and mammals, and evidence suggests that these proteins may function as molecular links between upstream signals and changes in the cytoskeleton. The goal of this project was to further clarify the role of UNC-53 in *C. elegans*. Two approaches follow this aim. In the first approach (Chapter 2), a previously identified physical interaction between a portion of the long-isoform of UNC-53 and ABI-1 (Abelson interactor-1) is pursued, identifying that these two proteins function together and independently in various processes including cell migration and endocytosis. This approach extends the migration pathway involving UNC-53 and contributes to what is known about UNC-53 during development. In the second approach (Chapter 3), a potential role for *unc-53* in the control of the innate immune

response is explored. It is found that *unc-53* is required for protection against the human and nematode pathogen *Pseudomonas aeruginosa* PA14, and that *unc-53* may function in multiple tissues and genetic pathways in pathogen resistance.

Chapter 2 investigates the role of the longest isoform of UNC-53, and provides evidence that UNC-53 and ABI-1 function together to control longitudinal migration. The long isoform of UNC-53 is expressed in many cells that require UNC-53, and RNAi targeting the long isoform, or overexpression of the CH domain of UNC-53 is sufficient to generate phenotypes reminiscent of UNC-53 genetic loss. UNC-53 physically interacts with ABI-1 *in vitro*, and binding between UNC-53 and ABI-1 is refined to the UNC-53 CH domain and ABI-1 residues 260-427. *abi-1* and *unc-53* mutants possess many of the same phenotypes, including the posterior migration of the excretory canals, the anterior migration of the PLM axons, and the dorsoventral axons of the ventral cord motor neurons, UNC-53 and ABI-1 are coexpressed in some of the same cells, they interact genetically, and the cell-autonomous expression of both UNC-53 and ABI-1 in the excretory cell is sufficient to rescue their posterior ExC canal migration defect. In addition, several interactors that function with ABI-1 (*nck-1/Nck*, *wve-1/Wave*, *arx-2*/*Arp2*) are needed for posterior excretory canal migration. UNC-53 and ABI-1 also participate in endocytosis in *C. elegans*, suggesting that the ABI-1-UNC-53 interaction is important to more than only migration. Lastly, it is shown that in addition to interacting with UNC-53, ABI-1 interacts with MIG-10A, showing that ABI-1 functions with two proteins that function cell-autonomously in the development of the ExC

Chapter 3 presents an investigation into a potential post-developmental role for UNC-53 in innate immunity. In addition to being expressed during development, UNC-53 expression persists in many cells in adult animals, including the intestine and neurons, two tissues needed for pathogen resistance. UNC-53 affects resistance to the human and nematode pathogen *P.aeruginosa* and this requirement is independent of its earlier role during development. Using a pharmacological approach, it is observed that *unc-53* affects synaptic transmission as measured by Aldicarb. *unc-53* mutants have increased levels of the pathogen-induced *daf-2* agonist *ins-7/insulin-7*, and UNC-53 is needed for DAF-16-GFP nuclear localization following recovery from heat-stress. *daf-2* and *ins-7* mutants do not completely suppress the *unc-53* immunity defect, and a *unc-53; pmk-1* double mutant combination suggest that *unc-53* may function in a PMK-1

pathway. Studies towards identifying the relevant tissues involved in *unc-53* function in immunity suggest a requirement for multiple tissues or isoforms. A microarray analysis of *unc-53* mutants subjected to *P. aeruginosa* PA14 was also performed that could be used for the identification of future *unc-53* target genes relevant to innate immunity.

2: THE CELL MIGRATION MOLECULE UNC-53/NAV-2 IS LINKED TO THE ARP2/3 COMPLEX BY ABI-1

2.1 Abstract

The shape changes that are required to position a cell to migrate or grow out in a particular direction involve the coordinated reorganization of the actin cytoskeleton in response to guidance cues. While it is known that the ARP2/3 complex nucleates actin filament assembly, exactly how the information from guidance cues is integrated to elicit ARP2/3 mediated remodeling during outgrowth remains unknown. Previous studies have shown that *C. elegans* UNC-53 and its vertebrate homolog NAVs are required for the migration of cells and neuronal processes. Here ABI-1 is identified as a novel molecular partner of UNC-53 and a restricted CH domain of UNC-53 is shown to be sufficient to bind full-length ABI-1 and a restricted portion of ABI-1 (260-427). ABI-1 and UNC-53 are expressed in some of the same cells, and display similar migration phenotypes in the posterior migration of the excretory canals, the anterior migration of PLM axons and the dorsoventral migration of motor neurons. Consistent with their physical interaction, *unc-53* and *abi-1* both function cell-autonomously in the excretory cell and participate in a common genetic pathway. *abi-1* is also required for several *unc-53* independent migrations. Migration defects were also observed when genes known to function with *abi-1* in actin dynamics including *nck-1*, *wve-1* and *arx-2* were eliminated or reduced genetically. Additionally, *unc-53* and *abi-1* are both observed to be required for endocytosis in *C. elegans*, suggesting that *unc-53* and *abi-1* may function together in numerous cellular processes. Lastly *abi-1* is shown to bind a second protein required cell-autonomously for the longitudinal migration of the excretory canals, MIG-10a. A model is proposed to suggest how UNC-53, ABI-1 and MIG-10 participate in cell migration through the control of actin-mediated events.

2.2 Introduction

2.2.1 Growth cones and cell migration

The migration of cells and cellular processes is indispensible for many biological processes, including: organogenesis (Guillemot and Zimmer, 2011), wound healing (Sonnemann and Bement, 2011), immune responses (Collington et al., 2011), and tissue remodeling (Windoffer et al., 2011); defects in cell migration contribute to pathogenic processes including metastatic cancers and diseases of the immune system (Blundell et al., 2010; Palmer et al., 2011). The importance of migration is underscored in neurodevelopment, where billions of precise points of connectivity between neurons, myoblasts, and glial cells are required to accomplish even simple tasks.

During the development of the nervous system, each neuron has the incredible assignment of elongating an axon from its birthplace to a terminal position, followed by the development of extensive synaptic connections. The outgrowth of cellular processes like axons are dependent on growth cones (Figure 3), the leading-edge active zones of extending cellular processes that are dynamic and highly motile, rich in ligand-binding receptors, signalling complexes, and cytoskeletal rearrangements (Lowery and Van Vactor, 2009). Growth cones consist of numerous filipodial projections separated by lamellipodial sheets, with each structure containing an underlying microtubule and actin substratum necessary to its function and responsible for the steering and motility of the growth cone (Insall and Machesky, 2009). The thin, sheet-like lamellipodium, contain a dense cross-linked actin mesh where most of the filaments have their plus ends close to the plasma membrane while the filipodia are composed of strong bundled actin filaments (Figure 3A,B). Filipodial protrusions orient with their plus ends pointing outward, helping to probe the environment and find the correct path to its target. Activation of receptors at filopodial tips by interaction with ligands generate signals that are transduced as a stabilizing signal in the case of an attractant, or a destabilizing signal in the case of a repellent, while the lamellipodia provide the driving force for the migration (Dent et al., 2011). If a cue is encountered, growth cones responds through a three-step process of protrusion, consolidation and engorgement in the direction of the cue (Lowery and Van Vactor, 2009). While actin-networks form the underlying layer of cytoskeleton underneath the plasma membrane, the shaft of filipodia and the sheets of lamellipodia also contain a dynamic underlying microtubule network that undergoes depolymerization

and repolymerization during outgrowth (Lowery and Van Vactor, 2009). The microtubules (MT) have numerous roles in the outgrowth of cellular processes. They provide a stabilizing mechanism during outgrowth (Witte et al., 2008), and can mediate branching, while also providing for the production of secondary growth cones from existing outgrowing membranes (Lowery and Van Vactor, 2009; Lundquist, 2003). They also serve as a basic transport thoroughfare on which membrane components including guidance receptors can be transported to the membrane (Dent et al., 2011).

Migration and outgrowth is achieved by sensing, integrating and responding to specific cues (Lowery and Van Vactor, 2009). Using this model, migration begins with a growth cone sensing a guidance cue through precise ligand-receptor interactions (e.g. secreted UNC-6/Netrin binds UNC-40/DCC), followed by integration through the activation of specific effectors in the form of Rho family GTPases (e.g. Rho, Rac, Cdc42), and finally by responding through the initiation of changes in the cytoskeleton (e.g. actin polymerization). While the basic model of 'sense-integrate-respond' (Lowery and Van Vactor, 2009) holds true, there are many complexities along the way, and the details of these events are still fragmentary. In addition to cues and their receptors, Rho family GTPases, and cytoskeletal proteins, there are a range of intermediate signalling molecules and cellular processes that modify signalling. These molecules include co-receptors, lipids, trafficking proteins (e.g. RABs), proteins that affect the activation of GTPases (e.g. GEFs and GAPs), as well as those proteins that can promote the polymerization of actin (e.g. ARP2/3 complex, WAVE, VASP/Enabled), and those proteins that promote the disassembly of actin polymers (e.g. Cofilin) to allow for continued dynamic outgrowth. There are also many intermediate cellular processes including, for example, receptor trafficking, endocytosis, proteolytic processing, secondary messenger systems, and kinase cascades, that contribute to how guidance cues are interpreted and acted upon (Bashaw and Klein, 2010). Current research by many groups is directed towards understanding the precise proteins and processes that connect upstream guidance cues to changes in the cytoskeleton at a molecular level.

The following sections will introduce some of the genes required for successful cell migration and outgrowth in a range of organisms, but focussing on *C. elegans*, including: guidance cues and their receptors (see Section 2.2.2), Rho family GTPases

(see Section 2.2.3), and proteins that control the polymerization of actin (see Section 2.2.4). We will also discuss studies of endocytosis in *C. elegans* (see Section 2.2.5).

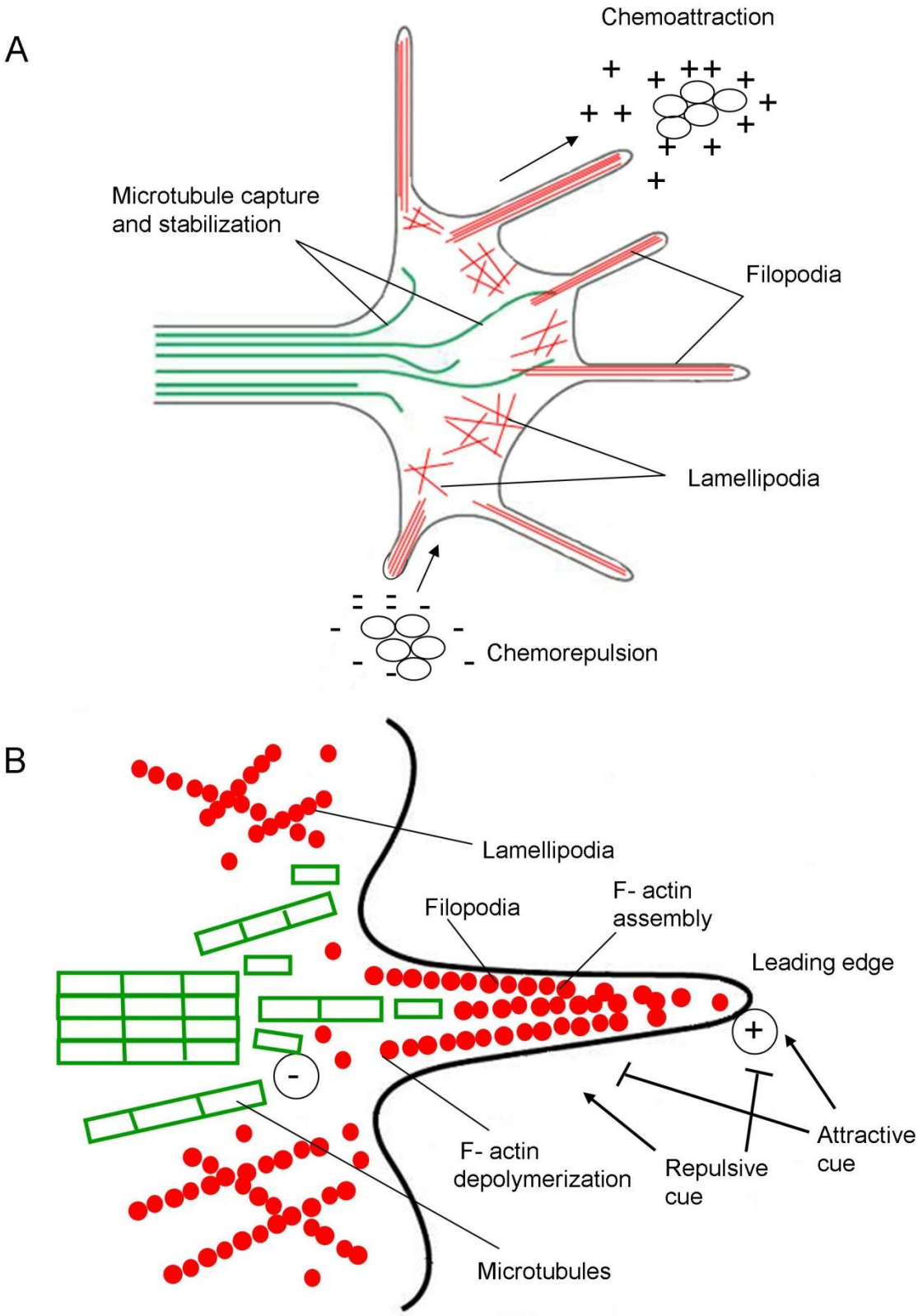
A
Chemoattraction
Microtubule capture
and stabilization
Filopodia
Lamellipodia
Chemorepulsion
B
Lamellipodia
Filopodia
F- actin
assembly
Leading edge
F- actin
depolymerization
Repulsive
cue
Attractive
cue
Microtubules

Figure 3. Growing axons respond to their environment through growth cones

(A) Axon growth and steering are directed by both attractive (+) and repulsive (-) cues that mediate their effects through growth cones. Lamellipodia are composed of a branched actin network while filipodia contain linear arrays of actin bundles. Microtubules in the axon shaft stabilize specific filipodia through microtubule capture and can mediate axon turning and branching (Adapted from (Lundquist et al., 2001)). (B) Attractive cues will cause outgrowth in specific areas of a growth cone and that can be blocked at that lack an attractive signal or are under the influence of a repellent (Adapted from (Huber et al., 2003)). G-actin units are red circles, microtubule subunits are green rectangles. The filopodia extend and retract through regulation of the rates of actin polymerization and depolymerization. The MT network serves to stabilize the growth cone and contributes to growth-cone steering and guidance decisions.

2.2.2 Guidance cues and their receptors

Successful migration is dependent on the ability of the cell or cellular process to respond to chemotropic guidance cues during migration and to make adhesive contacts with either cells or with the underlying extracellular matrix (ECM) during its journey (Lowery and Van Vactor, 2009). Several signals and receptors reported to control cell migration in vertebrates have been described in *C. elegans*, including: UNC-6/NETRIN and its receptors UNC-40/DCC and UNC-5 (Hedgecock et al., 1990; Ishii et al., 1992), the SLT-1/SLIT cue (Hao et al., 2001) and its receptor SAX-3/ROBO (Ghenea et al., 2005; Levy-Strumpf and Culotti, 2007; Zallen et al., 1998), WNTs and their associated FZ receptors (Pan et al., 2006), and growth factors such as EGL-17/FGF (Burdine et al., 1997) and its receptor EGL-15/FGFR (Birnbaum et al., 2005; Bulow et al., 2004; DeVore et al., 1995). Several of these molecules are shown to have roles dorsoventral or anteroposterior migrations. However, in contrast to the migration cues that control dorsoventral migration in *C. elegans* and other organisms, less is known about the molecules that control migration in the anteroposterior axis, due potentially to functional redundancy in these pathways (Killeen and Sybingco, 2008). The gradients of some of the known ligands in *C. elegans* are given in Figure 4.

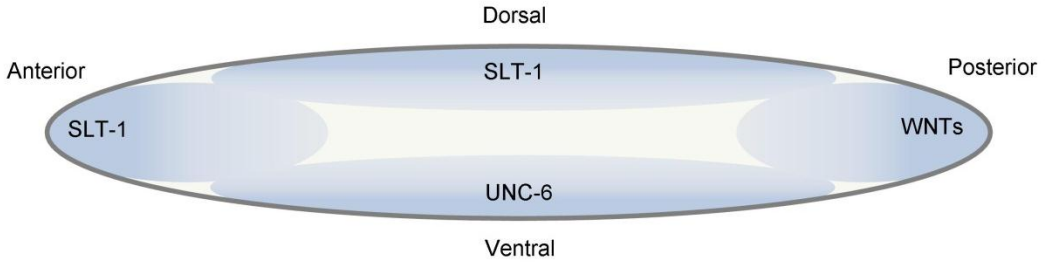

Figure 4. Examples of major guidance cues known in *C. elegans*

Guidance cues are expressed in specific gradients in *C. elegans* as shown (worm orientation indicated). Specific details about the expression are found in the text. Adapted from (Killeen and Sybingco, 2008).

UNC-6, UNC-40, UNC-5

The netrins are a family of secreted and membrane tethered proteins that are similar to the basement membrane protein laminin (Kennedy et al., 1994), with conserved roles in axon guidance. Evidence for Netrins controlling axon guidance across species is numerous with pioneering studies showing that Netrins are necessary for the attraction of commissural axons in mice and chicks to the floor plate during development (Kennedy et al., 1994; Serafini et al., 1994), for the guidance of CNS commissural axons and peripheral motor neurons in *Drosophila* (Mitchell et al., 1996), and in the directional turning of *Xenopus* spinal and retinal axons (de la Torre et al., 1997; Hong et al., 1999). Studies of the *C. elegans* Netrin guidance cue UNC-6 and its associated receptors UNC-40/DCC and UNC-5 have contributed substantially to what is understood about this guidance system (Wadsworth, 2002).

UNC-6 was first isolated by Sydney Brenner in his screens for Unc mutants (along with UNC-40 and UNC-5) (Brenner, 1974), but it was later studies that characterized UNC-6 as required for both the dorsal and ventral projections of pioneering commissural neurons, with UNC-40 being mostly required for the ventralward and anteroposterior migrations of cells and processes (Chan et al., 1996), and UNC-5 being required in the dorsal direction, and that guidance, but not motility, was affected by mutations in these genes (Hedgecock et al., 1990; Ishii et al., 1992). Defects in all of the major dorsoventral projections occur including motorneuron commissures and the

dorsoventral projections of the mechanosensory neurons (Chan et al., 1996; Colavita and Culotti, 1998; Norris and Lundquist, 2011). UNC-6 is expressed in neuroglia, neurons, and epidermoblasts along the ventral surface of worms (Figure 4) (Hedgecock et al., 1990; Ishii et al., 1992), and attracts UNC-40 expressing axons while repelling axons that express UNC-5, independent of UNC-40 expression. Evidence suggests that UNC-6 binding to UNC-5 switches UNC-40 axons from being attracted to being repulsed. In *Xenopus* spinal axons, which are attracted to UNC-40, expression of UNC-5 in the presence of UNC-6 allows for the formation of an UNC-40/UNC-5 complex that allows UNC-5 to compete with UNC-40 for UNC-6 binding, promoting repulsion (Hong et al., 1999). Ectopic expression of UNC-5 is able to redirect cells and axons in dorsal directions in a cell-autonomous manner that is dependent on several genes including *unc-6*, *unc-34/Ena/Vasp*, *unc-44/Ankyrin*, *unc-129/TGF-B* (Colavita and Culotti, 1998). UNC-34 is the *C. elegans* Enabled/VASP homolog normally required for actin cytoskeleton dynamics (see Section 2.2.4), and UNC-44 is an ankyrin, a type of adaptor protein that links integral membrane proteins to the actin cytoskeleton. The identification of these supressors suggests that UNC-5 function is mediated in part through its effect on the cytoskeleton. It has been suggested that the UNC-6/5/40 signalling group functions by inducing the polarization of axons, resulting in asymmetric neuronal growth and axon protrusiveness (Norris and Lundquist, 2011). In a well-designed set of experiments into the polarization of the ventral projecting HSN axon, it is shown that UNC-6 and UNC-40 polarize the axon, and that as polarization proceeds, MIG-10/LpD, required for actin-dependent outgrowth (see Section 2.2.4), is brought to the membrane to drive polarization through an AGE-1/PI3K signalling mechanism requiring DAF-18/PTEN (Adler et al., 2006; Chang et al., 2006). The small GTPase CED-10/Rac (see Section 2.2.3), is necessary for the asymmetric localization of MIG-10 as well as microtubules and F-actin downstream of UNC-6 (Quinn et al., 2006; Quinn and Wadsworth, 2008; Quinn et al., 2008). More recent evidence confirms that the UNC-6/5/40 signalling module is required for the development of polarity in migrating axons and that it exerts profound effects on the growth cones by affecting the degree of axon protrusion through the enrichment of F-actin (Norris et al., 2009). In this paradigm, Rac functions downstream of the guidance receptor UNC-40. It has also been shown that GTPases function upstream of UNC-40 to determine its localization at membrane sites for outgrowth (Levy-Strumpf and Culotti, 2007).

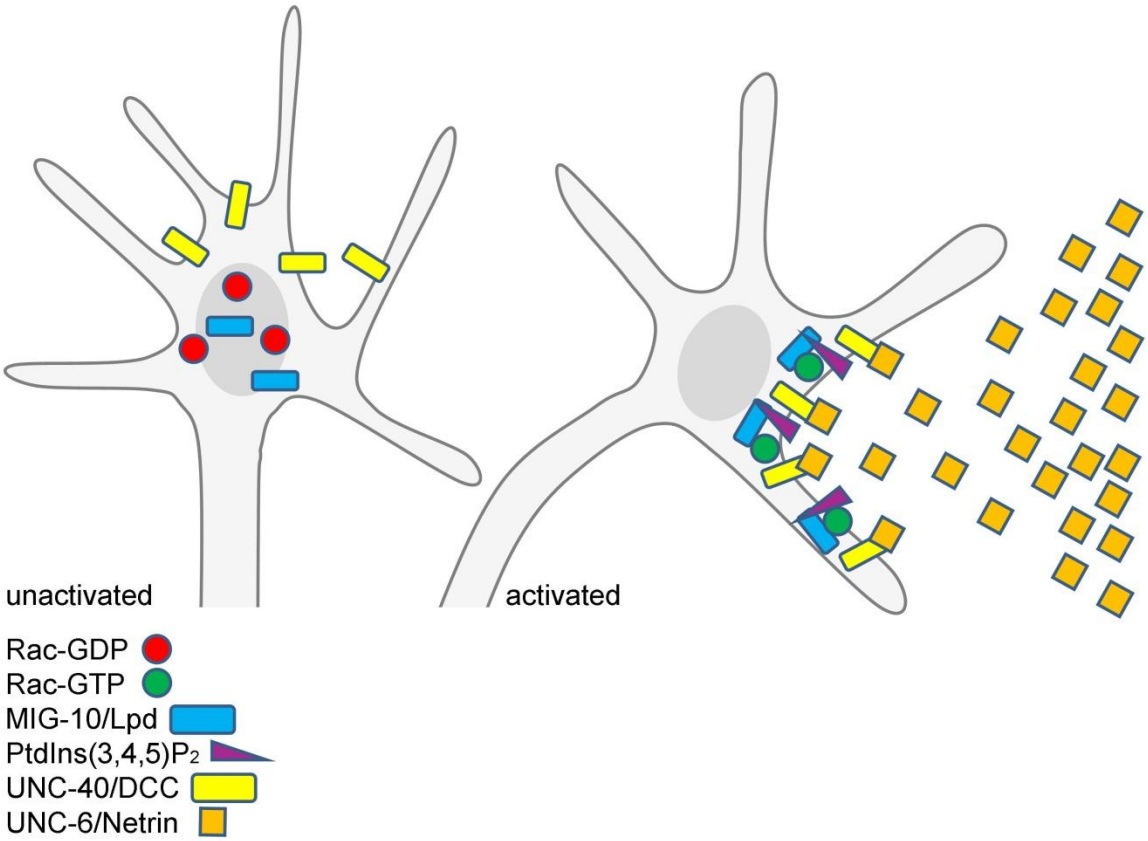

Figure 5. Model for the polarization of an outgrowing axon in response to a guidance cue.

The turning of an axon in response to an attractive cue is shown. In an unactivated state, UNC-40 and MIG-10 are evenly distributed throughout the growth cone. Activation by UNC-6 induces the polarization of the growth cone through the receptor UNC-40. This induces the asymmetric localization of MIG-10, which binds to PIP_2 and depends on activated Rac-GTP. Polarization of the growth cone results in directed actin polymerization. The various proteins required for this process are shown. Adapted from (Quinn and Wadsworth, 2008).

SLT-1, SAX-3, EVA-1

In *C. elegans,* SLT-1 is expressed in dorsal body-wall muscle as well as anterior regions of the embryo and repels SAX-3 expressing neurons (Hao et al., 2001; Zallen et al., 1998). Slit-Robo mediated guidance functions in parallel to the UNC-6/5/40 signalling pathway in a complementary way, repelling axons to promote ventrally directed axonal guidance (Hao et al., 2001). Also, SAX-3 physically interacts with UNC-40 and *unc-40* supresses *slt-1* gain-of-function (gf) mutations, suggesting that SAX-3

signalling is potentiated by an association between UNC-40 and SAX-3 (Yu et al., 2002). Migration defects are observed in a number of cells under the control of SLT-1 including the ventral projections of the AVM and the positioning of the sex myoblasts to ventral muscle quadrants in developing larva (Branda and Stern, 1999; Hao et al., 2001). Like the UNC-6/5/40 pathway, SLT-1 and SAX-3 depend on MIG-10 and UNC-34 (see Section 2.2.4) to promote axon polarization during guidance (Chang et al., 2006; Quinn et al., 2006). SLT-1 mediated repulsion of SAX-3 depends on a third protein, the co-receptor EVA-1 (Fujisawa et al., 2007). *eva-1* is found in the same genetic pathway as *slt-1* and *sax-3* in the guidance of the AVM neuron and EVA-1 coexpression with SAX-3 permits SLT-1 responsiveness (Fujisawa et al., 2007). SLT-1 and SAX-3 also appear to function in anteroposterior migration as defects are observed in the longitudinal migration of the CAN neurons, and overexpression of SAX-3 is able to cause a posterior rerouting phenotype in anteriorly directed AVM axons that is dependent on UNC-73 and VAB-8L (Watari-Goshima et al., 2007). In this migration, VAB-8L targets SAX-3 to the membrane downstream of UNC-73 and MIG-2/RhoG. In addition to its role in axon guidance, *sax-3* has additional roles in gastrulation cleft closure and ventral epidermal enclosure with *vab-1*/Eph in parallel to *slt-1* (Ghenea et al., 2005).

WNTs, FZs

WNTs are a group of small and secreted cysteine rich glycoproteins with conserved roles in cell polarity, cell fate and cell migration among many other functions (Hardin and King, 2008). Studies of Wnt signalling in migration in *C. elegans* have been particularly fruitful because the degree of functional redundancy is less in worms compared to other organism due to the comparably lower number of cues and receptors (Pan et al., 2006). Several studies have described a role for Wnts in migration, and have shown that Wnts can control anteroposterior migration as either guidance cues or by controlling the expression of the *Hox* gene *mab-5*. One of the most interesting and powerful series of experiments showing a role for Wnts in migration was conducted by Maloof *et al.* (1999) who examined the migrations of the QL and QR neuroblasts in their responsiveness to EGL-20/WNT (Maloof et al., 1999). Due to left-right asymetrical differences, the expression of *mab-5* in the QL neuroblast promotes a posteriorly directed migration while the absence of *mab-5* promotes an anteriorly directed migration. Mutants in EGL-20 as well as BAR-1/B-catenin result in QR like QL neuroblasts that are therefore directed anteriorly like their QR counterparts (Maloof et al., 1999). In addition

to this effect on *mab-5* expression, it appears as though the WNTs also function as guidance cues in migration, with primarily redundant roles. *Pan et al.* (2006) examined the full complement of WNTs and FZ receptors in the migrations of the HSNs as well as the AVM and PVM mechanosensory neurons. Of the WNTs and FZs examined, *egl-20/wnt* and *mig-1/fz* appeared to have the strongest phenotypes, but double mutant combinations, revealed a role for all these proteins. This study also examined the expression pattern and cell-autonomy of these proteins and observed that three WNT signals (EGL-20, CWN-1, LIN-44) are expressed in the tail and that EGL-20 functions as a repellent, which is different from what might be expected from mammalian systems. In addition, it was observed that MIG-1 functioned cell autonomously in the migration of the HSN, suggesting that the observed defects in HSN migration are not related to MIG-1 function in distant tissues (Pan and Garriga, 2008).

FGF, FGFR

FGFs (Fibroblast growth factor) and their receptor tyrosine kinase fibroblast growth factor receptors (FGFRs) are implicated in cell migration across organisms (Guillemot and Zimmer, 2011). *egl-17* and *egl-15* are homologous to FGF and FGFR respectively (Burdine et al., 1997; DeVore et al., 1995) and these proteins are shown to have roles in the migration of individual cells, axons, and membrane extensions (Bulow et al., 2004; Chen et al., 1997; Dixon et al., 2006; Fleming et al., 2005). One example of the role of EGL-15/17 is in the migration of the SMs, which are a pair of muscle precursor cells that originate within the ventral midposterior region of the animal during early larval development and undergo a sexually dimorphic migration under the control of the *Hox* gene *mab-5* (Burdine et al., 1997; Chen et al., 1997), migrating posteriorly in males, or anteriorly along the ventral muscle quadrants towards the center of the developing gonad in hermaphrodites, at which point they divide and differentiate to become the sixteen vulval and uterine muscle cells (Sternberg, 2005). The anterior migration of the SMs in hermaphrodites is under the control of both gonad-dependent (GD) and gonad-independent (GID) genetic pathways (see Section 1.1). Eliminating the GD pathway by laser ablating the Z1 and Z4 gonadal precursor cells disrupts the anterior migration of the SMs, as does the use of *dig-1* mutants with dorsally displaced gonads that similarly position the SMs dorsally with respect wild-type, suggesting the gonad secretes an attractive cue responsible for SM anterior migration. Genetic analysis performed alongside laser ablation studies have defined several members of

the GD pathway including EGL-17 expressed and secreted from the dorsal uterine cells of the somatic gonad, and EGL-15 which is expressed in the migrating SMs (Burdine et al., 1997). Other GD pathway genes include the SH2/SH3 adaptor protein SEM-5 that interacts with the EGL-15, as well as *let-60*/Ras and *let-341*/Sos-1 (Burdine et al., 1997). Numerous other genes controlling SM migration have been identified including those that control gonad-dependent repulsion (GDR): *unc-14/RPIP-8*, *unc-33/Crmp-2*, *unc-44/Ankyrin*, *unc-51*. Importantly, even in the absence of a gonad or null mutants of GD pathway genes, SMs maintain a partial anterior migration, evidence of a GID pathway. Enhancer screens conducted with the GD pathway eliminated to reveal potential GID pathway members identified *unc-53*, *unc-73*, and *unc-71* (see Section 1.1) (Chen et al., 1997).

2.2.3 **Rho family of small GTPases**

The Rho family GTPases are a subfamily of the Ras superfamily of proteins that control diverse signal transduction pathways to regulate actin dynamics and cell motility. Their functionality lies in their ability to mediate GTP-hydrolysis as molecular switches that exist in active GTP-bound “on” conformations and GDP-bound inactive “off” conformations. The precise regulation of GTPases in space and time is controlled by Guanine nucleotide exchange factors (GEFs) that favor the active GTP-bound state, GTPase activating proteins (GAPs) that favour an inactive GDP-bound state, and GTPase dissociation inhibitors (GDIs) that inhibit GTPase associations with the membranes where they function (Spiering and Hodgson, 2011). The three members of the Rho family of GTPases are Rac, Rho, and Cdc42. Rho GTPases have specific roles with respect to the cytoskeleton during cell motility and attachment: Rac regulates lamellipodia formation and ruffling; Rho controls stress fiber formation; and Cdc42 forms filipodia (Nobes and Hall, 1994; Nobes and Hall, 1995; Nobes et al., 1995; Spiering and Hodgson, 2011; Symons, 1996). The interactors and downstream targets of this protein familiy are well described and numerous and include kinases, formins, WASP family proteins (Spiering and Hodgson, 2011).

Rac-like genes are conserved across organisms and exhibit essential and redundant functions in the formation of lamellipodia and filipodia as well as membrane ruffles. Racs function by receiving signals from upstream receptors that include growth factors and cell guidance receptors (Symons, 1996) that travel through intermediates

(e.g. PI3K) that initiate GEFs (Welch et al., 2003). Several mammalian Racs have been identified that differ in their expression: Rac2 and Rac3 are expressed in hematopoetic cells and the brain respectively while Rac1 is ubiquitously expressed (Bosco et al., 2009). Rac1 localizes to the actin-rich tips of lamellipodia and filipodia in cultured cells that are rich in PIP_2 and PIP_3 (Ehrlich et al., 2002). Constituitive Rac activation or loss of function exert profound axonal defects (Lundquist, 2003; Luo, 2000). Cells lacking Rac1 or expressing a dominant-negative form of Rac1 show deficiencies in the formation of lamellipodia and filipodia while the overexpression of Rac can result in aberrant outgrowth (Lundquist, 2003; Symons, 1996). For example, constitutively active Rac(G12V) expressed in neurons in *C. elegans* causes the formation of ectopic lamellipodia and filipodia in addition to axon outgrowth and guidance defects (Struckhoff and Lundquist, 2003)

C. elegans has several Rho family homologs: *rho-1*, *cdc-42*, *ced-10*, *rac-2*, and *mig-2*. *rho-1* and *cdc-42* have roles in *C. elegans* in cytokinesis, embryo elongation, apical cell polarity and ventral hypodermal enclosure (Lundquist, 2006). The three worm Racs are *ced-10* and *rac-2* which are homologous to mammalian Rac1, and *mig-2* which is similar to RhoG. These molecules participate in several processes including cell migration, vulva development, and cell-engulfment (Lundquist, 2003). *ced-10* is required for phagocytosis during programmed cell death and for migration of the distal tip cells of the somatic gonad (Zhou et al., 2001). *rac-2*, *mig-2* and *ced-10* regulate CAN and PDE axon pathfinding and CAN cell migration, and affect axon outgrowth and branching, producing defects in the control of unnecessary axon branch formation (Lundquist et al., 2001; Lundquist, 2003). There is also functional redundancy among these genes. Lundquist *et al.* (2001) show that loss of *ced-10*, *mig-2,* or *rac-2* alone are wild-type or have very slight defects in the migration of the CAN, VD neurons, DD neurons or the distal tip cells alone, but showed marked defects when double mutants were constructed (Lundquist et al., 2001). *ced-10* and *mig-2* show overlapping control of P cell migration and axon outgrowth of D type motoneurons (Wu et al., 2002), and *mig-2, rac-2* and *ced-10* function redundantly to regulate CAN and PDE axon pathfinding (Lundquist et al., 2001; Struckhoff and Lundquist, 2003).

C. elegans Racs affect the activity of guidance receptors and APFs. When constitutively active Rac(G12V) is expressed in neurons it causes the formation of

ectopic lamellipodia and filipodia and axon outgrowth and guidance defects (Struckhoff and Lundquist, 2003) that are suppressed by actin-polymerization factors (APFs) WASP and WAVE (Shakir et al., 2008), suggesting that Racs functions upstream of APFs (see Section 2.2.4). *ced-10* and *mig-2* have defects in epidermal migration in *C. elegans* including defects that are shared with *wve-1*, *gex-2*, and *gex-3*, arguing for a conserved role for these Rho family GTPases in actin-polymerization during embryogenesis (Lundquist et al., 2001; Soto et al., 2002). Several studies have identified guidance molecules that function alongside these proteins in *C. elegans.* Mutations in *ced-10* function downstream of the guidance receptor UNC-40, and CED-10 binds MIG-10 in the development of axonal polarity (Chang et al., 2006; Quinn et al., 2006; Quinn and Wadsworth, 2008; Quinn et al., 2008) (see Section 2.2.2). Roles for CED-10 and MIG-2 upstream of receptors are also observed as SAX-3 and UNC-40 membrane targeting appears to be dependent on these proteins (Levy-Strumpf and Culotti, 2007; Watari-Goshima et al., 2007). Several studies have implicated the Rac-GEF UNC-73 in Rac function (Lundquist, 2003). *C. elegans unc-73* mutants display the full range of axon development defects (outgrowth, guidance, branch formation and branch suppression defects), and each of these defects is enhanced by Rac loss of function (Struckhoff and Lundquist, 2003). Furthermore, *unc-73* mutations are suppressed by Rac overactivation, indicating that Racs act downstream of *unc-73* (Lundquist et al., 2001; Lundquist, 2003; Lundquist, 2006).

2.2.4 **Regulation of actin polymerization**

Actin polymerization is fundamental to the outgrowth of cellular processes during development, and its polymerization is tightly regulated. The basic unit of polymerized filamentous-actin (F-actin) is globular actin (G-actin). Actin monomers contain a central cavity that binds both ATP and ADP. In the growth cone, ATP-bound actin is added to the 'plus' end of a growing filament (also called the barbed end) while ADP bound actin (following hydrolysis) is lost from the 'minus' end. When polymerized, actin microfilaments have the appearance of a double helix, as two linear strands of polymerized actin rotate 166° around each other, with approximately 13.5 actin monomers per turn. The balance of actin assembly versus disassembly influences the tendency of a cellular process to grow out in a given direction. Actin filaments grow in a polarized manner through the addition of ATP-actin monomers to the barbed end

through the assistance of actin nucleator proteins such as the ARP2/3 complex and formins (Machesky and Insall, 1998).

ARP2/3 Complex

Several actin-nucleating proteins have been discovered including formins (Firat-Karalar and Welch, 2011) and the Arp2/3 complex (Ibarra et al., 2005). Both protein complexes synthesize actin polymers, though formins are able to generate linear polymers, like for example in stress fibers and in the linear polymers found in filipodia (Firat-Karalar and Welch, 2011) while the ARP2/3 complex catalyzes the polymerization of branched actin microfilaments by synthesizing daughter polymers at 70° angles onto the side of an already existing mother filament (Kurisu and Takenawa, 2009) (Figure 6). The highly conserved ARP2/3 complex polymerizes actin through its ability to mimic the structure of actin, as actin polymerization is made possible when actin monomers form a trimeric arrangement (Takenawa and Suetsugu, 2007). The ARP2/3 complex is a seven-subunit structure, two of which (ARP2 and ARP3) are structurally similar to actin monomers (forming a pseudodimer) that together with an actin monomer forms an actin-like trimer that induces actin polymerization.

WASP and WAVE

When the ARP2/3 complex was originally isolated, it was observed that it was unable to efficiently polymerize actin on its own, and instead required the involvement APFs (Insall and Machesky, 2009). Several APFs have been discovered including WAVE and WASP family proteins (Kurisu and Takenawa, 2009) which are found in *C. elegans*, and others such as WASH, WHAMM, and JMY that are not (Rottner et al., 2010).

Mammals have two WASP proteins, WASP and N-WASP, that are downstream effectors of the Rho family GTPase Cdc42 (Kurisu and Takenawa, 2009). These effectors are structurally similar but are differentially expressed, with WASP expression restricted to hematopoetic cells and N-WASP expressed ubiquitously (Disanza and Scita, 2008). Specific mutation in WASP result in the disorder Wiskott-Aldrich Syndrome, an autoimmune syndrome characterized by defects in hematopoetic cell function including defects in cell proliferation, phagocytosis, cell adhesion and migration, and immune synapse formation that can result in autoimmune diseases, cancers, and

uncontrolled infections (Blundell et al., 2010). WASP and N-WASP have a similar domain organization including an N-terminal WASP homology domain 1 (WH1) domain, an internal basic region, a CRIB (Cdc42/Rac Interactive Binding domain) domain, an internal stretch of proline residues and a C-terminal VCA domain (Figure 6). The V domain is the Verprolin-homology region, the C domain is the Central or Cofilin domain and the A region is the acidic region. The CA region of WASP and N-WASP bind to the ARP2/3 complex while the V region binds to globular actin (Kurisu and Takenawa, 2009). The N-terminal WH1 domain mediates WASP/N-WASP protein-protein interactions with the verprolin family of proteins (e.g. WIRE/WICH, CR16, WIP) that regulate the activity of WASP, stabilize WASP levels and effect its subcellular localization (Aspenstrom, 2005; Sawa and Takenawa, 2006). The internal basic region of WASP/N-WASP binds PIP_2 which recruits WASP to the membrane for activation (Sechi and Wehland, 2000). The CRIB domain is needed for Cdc42 binding, resulting in the activation of the ARP2/3 complex (Spiering and Hodgson, 2011). In an unactivated state, the CRIB domain of WASP interacts specifically with the C region of the VCA domain, preventing ARP2/3 interaction with WASP. Cdc42-GTP binding to the CRIB domain, or PIP_2 to the basic region relieves this auto-inhibition and allows for ARP2/3 mediated actin polymerization *in vitro* (Kurisu and Takenawa, 2009). Additionally, the internal proline region allows for binding to SH3 domain containing proteins that can modify the activity, phoshorylation state and localization of WASP/N-WASP, and include numerous SH3 domain containing proteins including NCK, GRB2, ABI1 and others (Carlier et al., 2000; Innocenti et al., 2005; Rivera et al., 2004). In this way, WASP proteins serve as pathway relays between the PIP_2, Cdc42-GTP, and SH3 domain containing proteins and the polymerization of actin through the ARP2/3 complex. In *C. elegans* WASP is shown to function alongside the Racs, and ARP2/3 complex, mediating processes such as epidermal migration during ventral closure as well as axon guidance and outgrowth (Shakir et al., 2008; Sheffield et al., 2007; Withee et al., 2004).

Three WAVE proteins (WAVE1,2,3) have been identified in mammals and one WAVE (WVE-1) is present in *C. elegans* (Kurisu and Takenawa, 2009; Patel et al., 2008). WAVE was originally isolated as the protein SCAR from *Dictyostelium* (Bear et al., 1998), and WAVE proteins have since been shown to be powerful downstream effectors of Rac (Innocenti et al., 2002; Innocenti et al., 2004; Scita et al., 1999; Stradal et al., 2004). Treating cells with growth factors or the expression of constitutively active

Rac induces endogenous WAVE localization to membrane ruffles (Innocenti et al., 2002; Innocenti et al., 2004). WAVE has an N-terminal WAVE homology domain (WHD), a basic region, a proline-rich region, and a C-terminal VCA domain (Figure 6). Similar to N-WASP, the VCA domain of WAVE binds to and activates Arp2/3. Unlike WASP, WAVE does not have a CRIB domain to bind Cdc42 (Takenawa and Suetsugu, 2007). Instead the WHD domain allows for the formation of the pentameric WAVE complex between WAVE and its associated members, that include SRA1, NAP1, ABI1 and HSPC300 (Innocenti et al., 2004). Steffen *et al.* (2004) show that ABI and HSPC300 bind to WAVE directly through the WHD domain, and NAP1 SRA interact with ABI in the complex, and sequester the VCA domain to prevent binding with the ARP2/3 complex and actin. ABI1 interaction with WAVE is mediated through the coiled-coil regions of ABI, and serves as a link to upstream cues (Echarri et al., 2004). ABI interacts with the tyrosine-kinase Abelson, and in response to ABL signalling allows for the translocation of WAVE to lamellipodia upon stimulation (Leng et al., 2005). The activating mechanism of the WAVE complex is somewhat controversial as some studies have suggested WAVE is constitutively active and that its activation is localization dependent through Rac-GTP activation (Takenawa and Suetsugu, 2007) while others have suggested that WAVE is essentially inhibited in a basal state (Kurisu and Takenawa, 2009). Despite these different understandings of the activation of the WAVE complex, it is appreciated that WAVE is activated and localized by Rac-GTP. SRA1, NAP1, WAVE2 and Abi-1 translocate to the tips of membrane protrusions after microinjection of constitutively active Rac, and removal of components of the WAVE complex abrogate the formation of Rac-dependent lamellipodia induced by growth factor stimulation (Steffen et al., 2004). WAVE is also able to be activated through an interaction between the SH3 domain of IRSp53 which draws the WAVE complex to filipodia and lamellipodia. WAVE is also initiated by the clustering effect of the lipid PIP_3 which is generated by PI3K, and that Rac, IRSp53, and PIP_3 function synergistically on the activation and recruitment of WAVE to the plasma membrane (Kurisu and Takenawa, 2009).

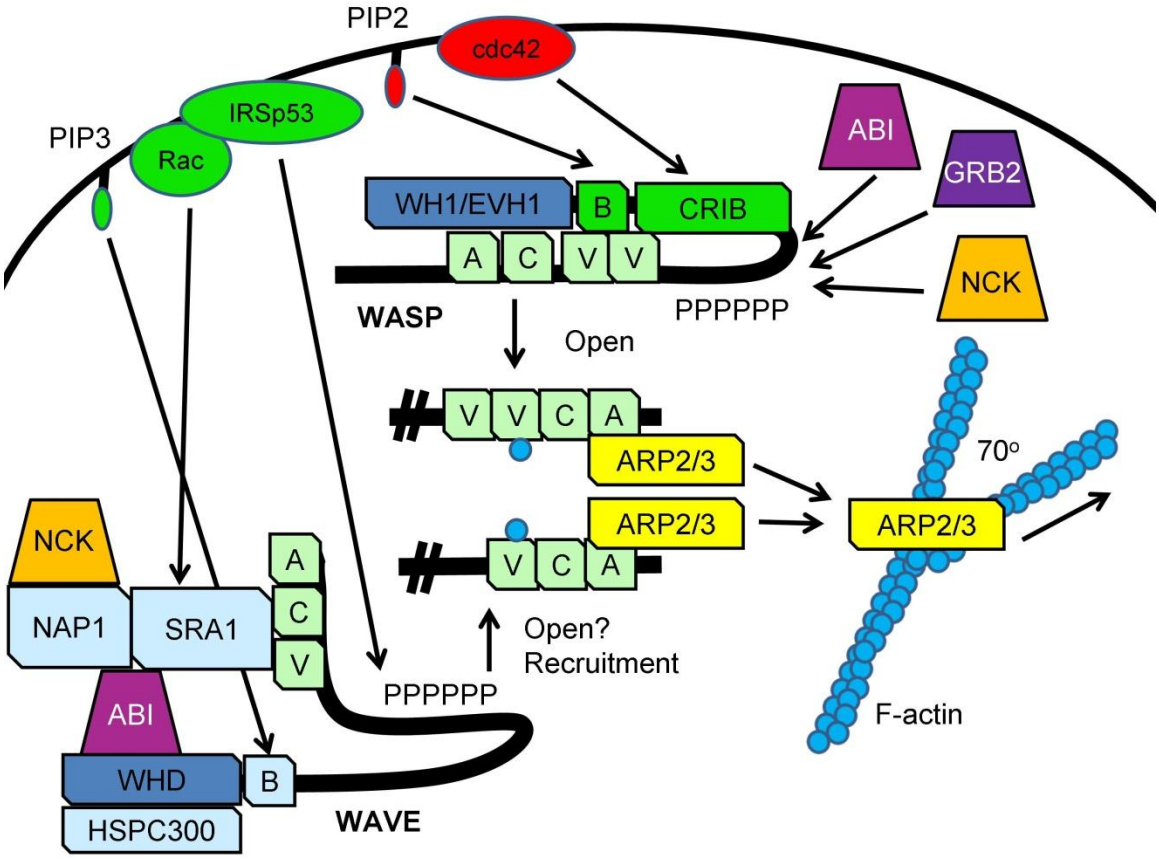

Figure 6. Control of the ARP2/3 Complex by WAVE and WASP

The control of actin polymerization by the ARP2/3 complex is mediated through both WASP and WAVE. In an unactivated state WASP is autoinhibited through interactions between its CRIB domain and the VCA region that interacts with the ARP2/3 complex and actin. In response to Cdc42 and PIP_2 through the CRIB and basic region "B" respectively, or through binding the polyproline regions and SH3 domain containing proteins (ABI, GRB2, NCK), WASP obtains an open conformation and can interact with the ARP2/3 complex to promote actin polymerization. WAVE is similarly autoinhibited through interactions between the VCA domain and SRA1. Release of inhibition by Rac-GTP and PIP_3 with SRA1 and the basic "B" region respectively are able to either open the WAVE complex to interact with the ARP2/3 complex through its VCA domain and/or recruit WAVE to sites of actin polymerization. Adapted from (Kurisu and Takenawa, 2009). The double dash symbol indicates that the N-terminal portion of activated WASP and WAVE is not shown.

The role of the ARP2/3 complex, WASP, and WAVE in development have all been pursued to varying degrees in *C. elegans* and other organisms. In *Drosophila*, the Arp2/3 complex and its regulators SCAR/WAVE and Kette are required for proper axon pathfinding, actin-contractility during myoblast formation, and the outgrowth of retinal axons (Bogdan and Klambt, 2003; Bogdan et al., 2004; Nord et al., 2009). Most work in

C. elegans has focussed on the role of the ARP2/3 complex and its regulators during embryogenesis, showing that these proteins have conserved roles in actin-mediation. GEX-2 and GEX-3 colocalize to cell boundaries during embryogenesis and interact physically, and loss of either WVE-1, the GEXs, or ABI-1 results in defective hypodermal cell migration (Patel et al., 2008; Soto et al., 2002) and these animals have ventral enclosure defects reminiscent of those found in RAC and ARP2/3 mutant animals (Lundquist, 2006; Sawa et al., 2003; Sawa and Takenawa, 2006; Soto et al., 2002), suggesting that a conserved pathway involving Rac, the WAVE complex and ARP2/3 is maintained during embryogenesis in *C. elegans* . More recent studies in *C. elegans* show that the Arp2/3 regulators *wve-1*, *gex-2*, *gex-3* and *wsp-1* are required for proper axon guidance (Norris et al., 2009; Shakir et al., 2008; Withee et al., 2004), and that the WASP and WAVE homologs act in parallel upstream of the ARP2/3 complex in several migrations of the dorsoventral neurons in these animals, and that WASP and WAVE display specific genetic interactions with Rac activators (Shakir et al., 2008). MIG-2/Rho functions specifically through a pathway that involves WSP-1, while CED-10/Rac controls migration through a WVE-1 mediated complex. What is novel about this work is GEX-2 and GEX-3 appear to be involved in both pathways, which is a contrast from what is observed in studies of the actin regulators from other systems. Additionally, Shakir *et al.* (2008) show that WASP and WAVE function in parallel to the actin-binding protein UNC-115/Ablim and UNC-34. This redundancy observed between *unc-34*, *wve-1*, and *wsp-1* is reminiscent of the redundancy observed between these genes in embryogenesis (Withee et al., 2004).

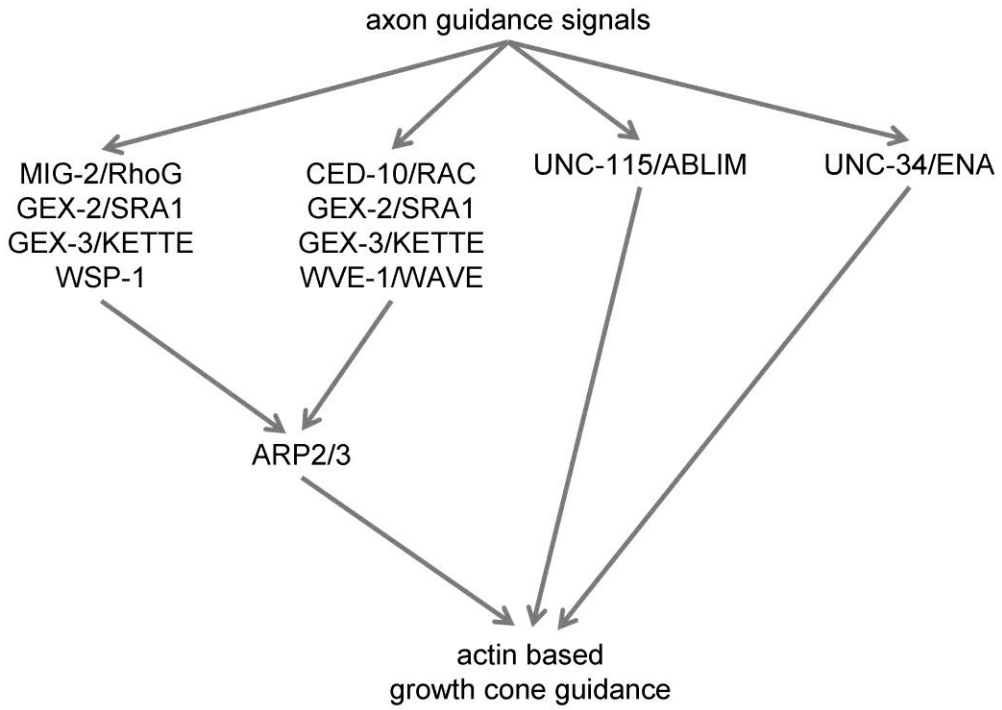

Figure 7. Genetic interactions between actin regulators in axonal guidance in *C. elegans*.

Genetic interactions between the actin regulators in *C. elegans* are shown (Shakir et al., 2008). UNC-34/ENA and UNC-115/ABLIM function in parallel to the APFs WASP and WAVE, which function upstream of the ARP2/3 complex. Note that GEX-2/SRA1 and GEX-3/NAP1 function with both WASP and WAVE in this model.

ABI-1/ABI

ABI (Abelson-interactor) proteins have emerged as central regulators of actin and membrane dynamics at the leading edge of cells. There are three mammalian ABI proteins, ABI1, ABI2, and NESH/ABI3, while *Drosophila* and *C. elegans* have only one each, dABI and ABI-1 respectively that are homologous to ABI1/2 (Echarri et al., 2004). Less is known about NESH/ABI3, except that it is similar to ABI1/2 by way of sequence homology but does not bind ABL (Abelson) (Hirao et al., 2006). ABI1/2 contains multiple protein domains including: an N-terminal WAVE-homology binding domain to bind the WAVE complex, together with an overlapping SNARE domain that binds Syntaxin and SNAP-25 (Echarri et al., 2004), an HHR (homeodomain homologous region), internal

proline-rich segment that binds the SH3 of ABL, and a C-terminal SH3 domain that mediates many of its interactions including numerous actin regulators such as ENA/VASP and WASP (Courtney et al., 2000; Grove et al., 2004; Ibarra et al., 2005). Studies into the ABI proteins began following the observation that murine ABI1 and ABI2 bound the oncogene Abelson (ABL), and that ABI1/2 are kinase substrates, and dual regulators of ABL (Shi et al., 1995; Taki et al., 1998). Subsequent studies show that chromosomal translocations involving ABI occur in patients with acute myelogenous leukemia (Taki et al., 1998).

ABI proteins are expressed in ways that are consistent with a role for these proteins in controlling actin dynamics during development. Mouse ABI1 and ABI2 localize to the actin-rich tips of growth cones in lamellipodia and filipodia in outgrowing neurites where they are widely expressed in the cortical regions of the nervous system (Grove et al., 2004). Later in development they exhibit punctate expression throughout axons and dendritic spines (Courtney et al., 2000; Stradal et al., 2001). Decreasing ABI expression in mice results in midgestational lethality with abnormalities in placental and cardiovascular development, as well as defects in adherens junction formation in the eye and brain, and abnormal dendritic spine morphology and density together with severe deficits in short and long-term memory and learning (Grove et al., 2004). As a part of the WAVE complex in *C. elegans*, ABI-1 is found at the actin rich rips of migrating hypodermal cells during ventral enclosure (Patel et al., 2008; Soto et al., 2002), and later in apical junctions in intestinal cells where it is needed to maintain apical junctions with ARP2/3 (Bernadskaya et al., 2011).

ABI function is mediated in part through its interaction with Abelson (ABL), a non-receptor tyrosine kinase that is activated and localized to actin-rich lamellipodia and membrane ruffles in response to growth factor stimulation (Juang and Hoffmann, 1999; Leng et al., 2005), where it promotes actin assembly/disassembly (Leng et al., 2005). ABI and ABL reciprocally interact through their SH3 domains and respective poly-proline regions, and ABI and ABL proteins have been shown either to activate or suppress each other depending on the context (Comer et al., 1998; Comer et al., 1998; Juang and Hoffmann, 1999). Studies of ABI and Mammalian Ena (Mena) show that ABI binds Mena and that they colocalize at the leading edge directly and that specific tyrosine phosphorylation allow for Abl phoshorylation of Mena and their downstream activity (Tani

et al., 2003). ABI also seems to be needed for the direct phosphorylation of WAVE by ABL and their interaction localizes WAVE2 to actin-rich zones, allowing cell spreading and ruffling (Leng et al., 2005). So it appears that ABI functions as an adaptor for ABL function in directing the activity of proteins involved in actin dynamics. However, while ABI is observed to be a positive regulator of ABL in some circumstances it is not in others. For example, reducing dABI dosage by half rescues defects in dABL mutants such as pupal lethality, axonal guidance defects and locomotion deficits (Lin et al., 2009).

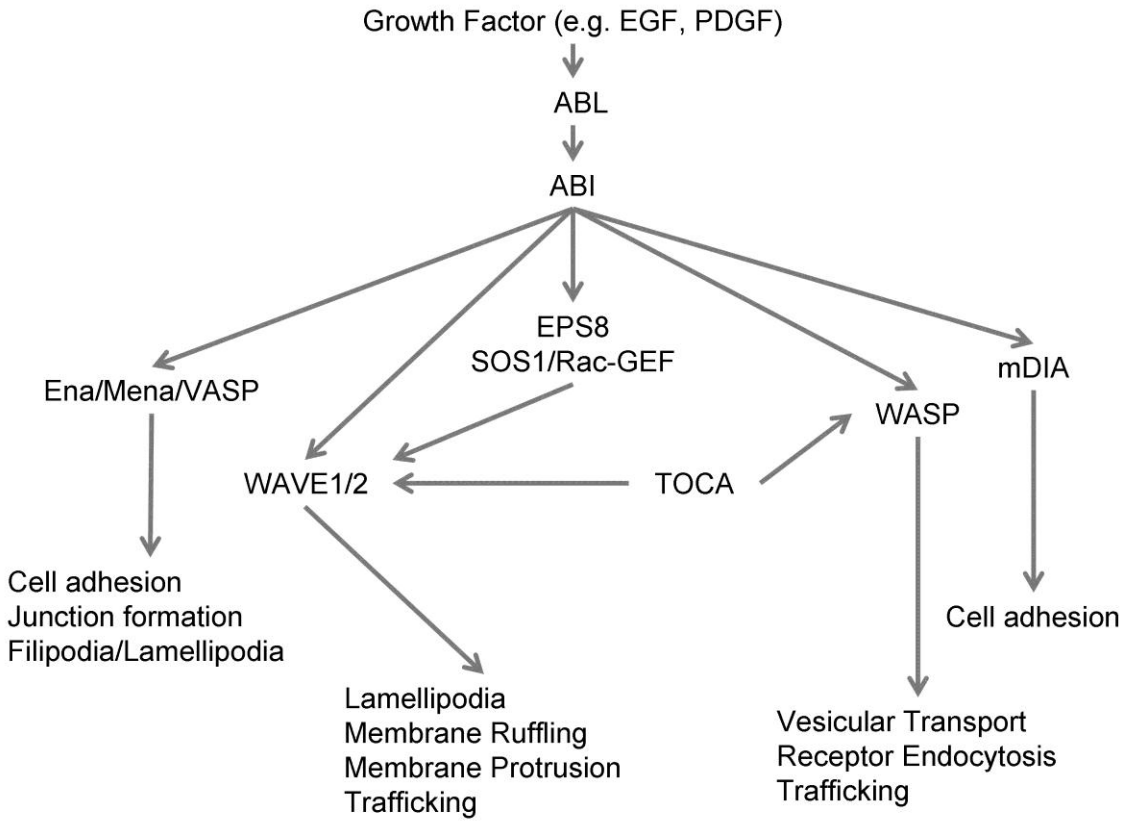

Figure 8. Diverse functions for ABI with Actin Regulators

Some of the diverse interactions of ABI proteins with actin regulators are shown. ABI interacts with Ena/Mena/VASP, WAVE, WASP and mDIA. ABI-1 induces the Rac-GEF activity of SOS-1 through EPS8. Interaction between the WASP and WAVE complex along with ABI-1 work with the TOCA proteins to inititiate changes in membrane dynamics alongside changes in actin mediation. Details are provided in text.

ABI proteins are also shown to interact with signalling molecules that direct Rac dependent cytoskeletal changes. ABI is required for PDGF induced membrane ruffling and in the transduction of signals from Ras to Rac by binding SOS-1 through its SH3 domain to allow the formation of a tricomplex together with EPS-8 and SOS-1, that exhibits Rac-specific GEF activity (Innocenti et al., 2002; Scita et al., 1999), and subsequent work showed that this complex synergizes with with IRSp53 and PI3K in Rac activation (Funato et al., 2004; Katso et al., 2006). As previously described, ABI is a part of the pentameric WAVE complex together with NAP-1, PIR121/SRA-1, HSPC300 and WAVE, shown to mediate actin remodeling through ARP2/3 (Bompard and Caron, 2004; Takenawa and Suetsugu, 2007). ABI/WAVE complex functions downstream of EGFR signalling in *Drosophila* (Stephan et al., 2008) and *C. elegans* ABI-1 is required for maintaining the integrity of the WAVE complex (Soto et al., 2002).

ABI functions independently of WAVE with WASP. In *Drosophila,* dABI genetic loss results in defective bristle formation while overexpression results in the production of ectopic bristles (Bogdan et al., 2005). Bristle development is under the control of WASP; overexpression of dABI forms ectopic bristles through EGFR signalling that can be suppressed by WASP and not WAVE mutations (Bogdan et al., 2005). While ABI functions with WAVE in Rac-dependent membrane protrusion (Innocenti et al., 2004) it functions with N-WASP, but not WAVE, in the regulation of actin-based vesicular transport, epidermal growth factor receptor (EGFR) endocytosis, and EGFR and transferrin receptor (TfR) cell-surface distribution (Innocenti et al., 2005). ABI-1 also functions with the formin mDIA independent of ARP2/3. ABI functions through the WAVE complex to sequester mDIA to prevent filipodia formation during the induction of membrane ruffling (Beli et al., 2008). Also, active mDia1 localized to cell-cell junctions rescues the abnormal junctions induced by depletion of Abi in epithelial cells, suggesting a link between junctional adhesion and the regulation of actin dynamics through an Abi/mDia1 complex (Ryu et al., 2009).

A role for ABI-1 has also been suggested in controlling endocytic processes through F-Bar containing proteins (Fricke et al., 2009; Giuliani et al., 2009). In Drosophila, Cip4 recruits both WASP and WAVE complexes to the membrane to allow for actin comet-based vesicle recruitment that is dependent on both WASP and WAVE (Fricke et al., 2009). Similarly, an analysis of TOCA-1/2 from *C. elegans* showed that

TOCA proteins function through both WASP and WAVE, with the WAVE interaction being mediated by ABI-1 (Giuliani et al., 2009). ABI-1 contains a SNARE domain towards its N-terminus (Echarri et al., 2004), and ABI-1 has been observed to interact with several proteins involved in regulating trafficking, including synaptojanin, dynamin and syntaxin (Echarri et al., 2004; So et al., 2000), and ABI functions in vesicle trafficking in a WASP dependent fashion (Innocenti et al., 2005). A role for ABI-1 in synaptic processes is also shown as it is expressed in synapses and in growth cone particles (Courtney et al., 2000). It is also possible that an endocytic process may involved *abi-1* in the process of endocytosis during cell corpse engulfment (Hurwitz et al., 2009). Two parallel pathways have been described in cell corpse engulfment during *C. elegans* development: a membrane recruitment pathway involving CED-1 and a second pathway involving CED-10/Rac. Double mutants of *abi-1* with genes from either of these engulfment pathways results in an increased engulfment defect, suggesting that abi-1 functions in parallel to each of these pathways (Hurwitz et al., 2009).

UNC-34/Ena

UNC-34 is a member of the Ena/VASP family of proteins that have conserved roles in axonal guidance (Bear and Gertler, 2009; Krause et al., 2003). Three mammalian Ena proteins are known, including Mena, VASP and Ena-Vasp (Evl), and these proteins all contain conserved domains that include an N-terminal Ena/VASP homology (EVH1) domain, a central proline rich stretch and a C-terminal EVH2 domain that allows for interactions with actin. Ena appears to function in actin dynamics in a number of different ways, including as an anti-capping protein that allows for actin polymerization, and also in the control of actin branching and bundling, and the recruitment of profilin (Bear and Gertler, 2009). *unc-34* functions in a diverse set migrations and functions in determining polarity during axon outgrowth (Adler et al., 2006; Chang et al., 2006; Fleming et al., 2010). For example, *unc-34* functions alongside MIG-10 in establishing the polarity of the HSN axon in response to SLT-1 and UNC-6. Lack of UNC-34 results in decreased ventrally directed filipodia during these migration (Adler et al., 2006). UNC-34 localizes to apical junctions during development, and is needed for the establishment of neuronal polarity along the anteroposterior axis as well (Fleming et al., 2010). UNC-34 has been previously observed to function in parallel to *wsp-1* and *wve-1* in gastrulation and morphogenesis as well as neuronal cell

migration, and in a parallel pathway to *abl-1* which antagonizes its function (Sheffield et al., 2007; Withee et al., 2004).

MIG-10/Lamellipodin (Lpd)

MIG-10 is a member of the MRL (MIG-10/RIAM/Lamellipodin) family of cytoplasmic proteins that are necessary for the polymerization of actin and cell polarization during axonal outgrowth (Fleming et al., 2010; Krause et al., 2004; Quinn et al., 2008). MIG-10 contains a Pleckstrin Homology domain akin to those found in the mammalian SH2 domain proteins Grb7 and Grb10 that bind PIP_2. In addition, MIG-10 contains polyproline repeats and an EVH1 domain that allow MIG-10 and its homologs to interact with Ena/VASP proteins (Manser et al., 1997). Studies of mammalian Lpd in cell culture show that it is required for actin outgrowth, as overexpression of Lpd in PDGF stimulated fibroblasts results in increased actin protrusion while eliminating Lpd reduces lamellipodia formation and causes decreases in F-actin content (Krause et al., 2004). *mig-10* causes multiple cell migration defects in *C. elegans* including defects in the longitudinal migration of the CAN neurons and the posterior canals of the excretory cell (Manser and Wood, 1990; Manser et al., 1997), as well as the ventral migrations of the PVM, AVM and HSN axons (Quinn et al., 2006; Quinn and Wadsworth, 2008; Quinn et al., 2008). Overexpression of MIG-10 results in a multipolar phenotype in neurons that are normally monopolar, suggesting a role for MIG-10 in polarity determination in axon outgrowth. Support for this observation comes from the finding that MIG-10 is assymetrically localized in response to UNC-6. In the presence of UNC-6, the UNC-40 receptor localizes to the ventral HSN neuron, resulting in a CED-10 dependent localization of MIG-10 toward UNC-6. Elimination of MIG-10 or CED-10 results in a lack of polarity and outgrowth (Quinn et al., 2006; Quinn et al., 2008). Lpd and its homolog MIG-10 interact with Rac, Ena, and the lipid PIP_2 (Krause et al., 2004; Quinn et al., 2006). Defects in either *ced-10*, *unc-34*, *age-1* or *daf-18* are similar to *mig-10*. Interestingly, while MIG-10 binds UNC-34 it appears as though defects in *mig-10* are worse than *unc-34* defects, suggesting additional effector functions for *mig-10* that are independent of *unc-34*, and *mig-10; unc-34* double mutants result in embryonic arrest (Chang et al., 2006), suggesting separate pathways for these gene in embryonic function in *C. elegans*.

2.2.5 **Studies of endocytosis in *C. elegans***

Endocytosis drives the internalization of the outermost plasma membrane and allows for the intake and recycling of extracellular and transmembrane proteins, nutrients, and membrane lipids; clathrin-mediated endocytosis (CME) is the most well-studied type of endocytosis in *C. elegans* (Grant and Sato, 2006). One way to order the steps of CME is by the sequential processes of initiation, cargo selection, coat assembly, scission and uncoating (Boettner et al., 2011). CME is intitated at presumptive invaginations sites that are rich in PIP_2 suggesting a role for lipid phosphorylation by inositol kinases, recruiting the clathrin adaptor protein AP2 through AP2 interations with cargo and membrane lipids (Boettner et al., 2011). AP2 then recruits clathrin from the cytosol to membrane sites of invagination which is thought to drive the formation of the vesicle bud. The GTPase dynamin buds the membrane and disassembly and clathrin uncoating follows, mediated by auxilin and heat shock cognate 70 (HSC70). Endosomal trafficking and cargo recycling to the plasma membrane complete the cycle (Grant and Sato, 2006).

Studies in yeast and mammals have identified several proteins required for endocytosis, many of which are involved in actin dynamics, and electron microscopy shows that sites of membrane invagination contain actin associated proteins (Galletta and Cooper, 2009). Endocytosis appears to require branched actin filament assembly, which is dependent on the Arp2/3 complex, and the presence of F-actin at CME sites occurs in the active of vesicle invagination (Galletta et al., 2010). N-WASP appears to be a central in both yeast and mammals (Bierne et al., 2005; Boettner et al., 2011; Innocenti et al., 2005; Stradal et al., 2004). N-WASP appears together with Arp3 and actin at approximately the same time and propels clathrin coated vesicles into the cytoplasm (Merrifield et al., 2004). Knocking down N-WASP results in decreased EGFR internalization (Galovic et al., 2011). Other evidence for WASP in actin polymerization during endocytosis come from its observed interactions with F-Bar domain containing proteins. Cdc42 and N-WASP form a complex together with TOCA-1 in vesicle and tubule formation (Bu et al., 2010), and a complex involving Cdc42-WASP-TOCA-1 links endocytosis to filipodia formation (Bu et al., 2009).

Two assays have been principally employed to study endocytosis in *C. elegans*: the coelomocyte uptake assay (CUP) and the yolk protein uptake assay (Fares and

Greenwald, 2001; Grant and Sato, 2006) (Figure 9). Both of these assays monitor the amount of GFP able to be endocytosed in a normal physiological way, though more is known about the processes controlling uptake into oocytes (Fares and Grant, 2002; Grant and Sato, 2006). In the yolk-uptake assay, the yolk-protein YP170 (VIT-2) is tagged with GFP and is secreted into the pseudocoelom from the intestine where it is produced endogenously. Following its secretion into the intestine it is taken up by developing oocytes. YP170-GFP is bound for endocytosis by RME-2, a receptor from the low-density lipoprotein receptor superfamily (Grant and Hirsh, 1999). Uptake of YP170-GFP requires many of the *C. elegans* homologs of the CME pathway including clathrin, members of the AP2 complex and dynamin (Grant and Hirsh, 1999) as well as HSC70 (Greener et al., 2001). In addition, YP170 uptake depends on the *C. elegans* homologs of *rab-5, rab-7* and *rab-11* which control some of the major endocytic sorting steps (Olkkonen and Stenmark, 1997), suggesting a specific role for these *Rabs*, though not all of the putative *rabs* were tested (Grant and Hirsh, 1999). Also, disruption of the major secretory pathways disrupted YP170-GFP uptake, probably by affecting the trafficking of RME-2 (Grant and Hirsh, 1999). Disruption of the secretory pathway generated several additional phenotypes that knockdown of the endocytic mediators did not, which is helpful for distinguishing the relevant involvement each of these processes could be playing in YP170-GFP uptake (Grant and Hirsh, 1999). In addition to endocytic and secretory associated trafficking, a general requirement for polarity proteins for YP170-GFP uptake into oocytes was found. A genome-wide RNAi screen identified proteins previously implicated in the generation of polarity in other systems such as PAR-3, PAR-6, PKC-3 and CDC-42 in YP170-GFP uptake into oocytes, and that these proteins were also necessary for endocytic uptake in Hela cells (Balklava et al., 2007). Cdc42 associates with N-WASP in actin polymerization during trafficking (Innocenti et al., 2005), and subsequent work investigating a role for Cdc42 identified that the F-bar containing proteins TOCA-1 and TOCA-2 were necessary for YP170-GFP uptake through mechanisms that was dependent on the APFs WASP and WAVE, suggesting a conserved role for actin polymerization during oocyte uptake (Giuliani et al., 2009).

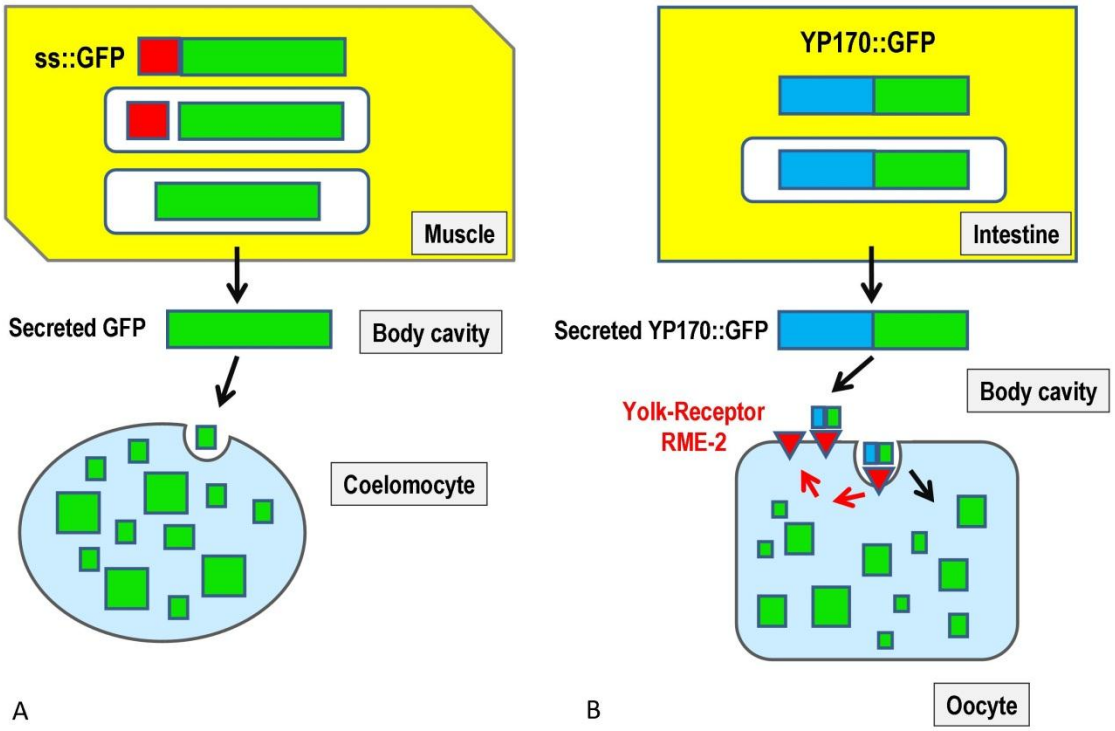

Figure 9. Two assays used to assess endocytosis in *C. elegans.*

Two assays are used to measure endocytosis in *C. elegans* including the coelomocytes uptake assay (A) and the YP170-GFP uptake assay into oocytes (oocyte uptake assay) (B). Both of these assays measure the relevant abundance of the uptake of GFP in the cell of interest (coelomocytes or oocyte) compared to residual GFP in the pseudocoelom. Adapted from (Grant and Sato, 2006).

2.2.6 Overview

The actin cytoskeleton is responsible for a wide variety of cellular functions including processes such as cell migration and endocytosis. Although it is known that the ARP2/3 complex nucleates actin filament assembly, exactly how it is linked to these processes is not fully understood. In this portion of the study, a role for UNC-53 and ABI-1, a known regulator of the ARP2/3 complex in both cell migration and endocytosis, was examined.

The largest UNC-53 isoforms are found to be expressed in several migrating cells in which UNC-53 is required, as well as in adult cells. Additionally, it is shown that

UNC-53 binds the *C. elegans* ABI-1 homolog, and that loss of *abi-1* leads to migration defects similar to those found when *unc-53, wve-1, nck-1* and *arx-2* (*arp2*) are removed. UNC-53 and ABI-1 have an overlapping pattern of expression. Also, it is shown that both *abi-1* and *unc-53* are required for endocytosis using the coelomocytes uptake and oocyte uptake assays as reporters. Finally, *abi-1* functions independently from *unc-53* for some migrations, and that ABI-1 binds MIG-10A, another protein that functions cell-autonomously in excretory canal extension.

2.3 Results

2.3.1 Expression pattern of the long-isoform of *unc-53*

The *unc-53* locus is large, spanning 31kb of genomic DNA (II:11089398..11058043 bp), and containing 23 exons. Previous work showed that *unc-53* undergoes alternative SL1 trans-splicing and cis-splicing and contains two alternatively spliced exons (17 and 18) (Figure 10A) (Stringham et al., 2002). Six isoforms have so far been identified: four large isoforms each beginning at a separate SL1 trans-splice site (labelled LA, LB, LC and LD) which will be collectively refer to as UNC-53L, and two small isoforms beginning at the internal SL1 sites of *unc-53* (labelled SA and SB), referred to as UNC-53S. Two intronic promoters for *unc-53* have been described that convey tissue and isoform specificity: *punc-53SA* (also called pA) upstream of the SL1 site at exon 7, coding for UNC-53SA, and *punc-53SB* (also called pB) that is found upstream of exon 9 and codes for UNC-53SB (Stringham et al., 2002). Several protein motifs are shared between UNC-53 and its orthologs including a CH domain, two putative actin binding sites of the LKK motif, two coiled-coil regions, two polyproline rich SH3 binding motifs, and a AAA (Figure 10B)(Stringham et al., 2002). The short isoforms lack the CH domain and first LKK motif found in the longest isoform of *unc-53*.

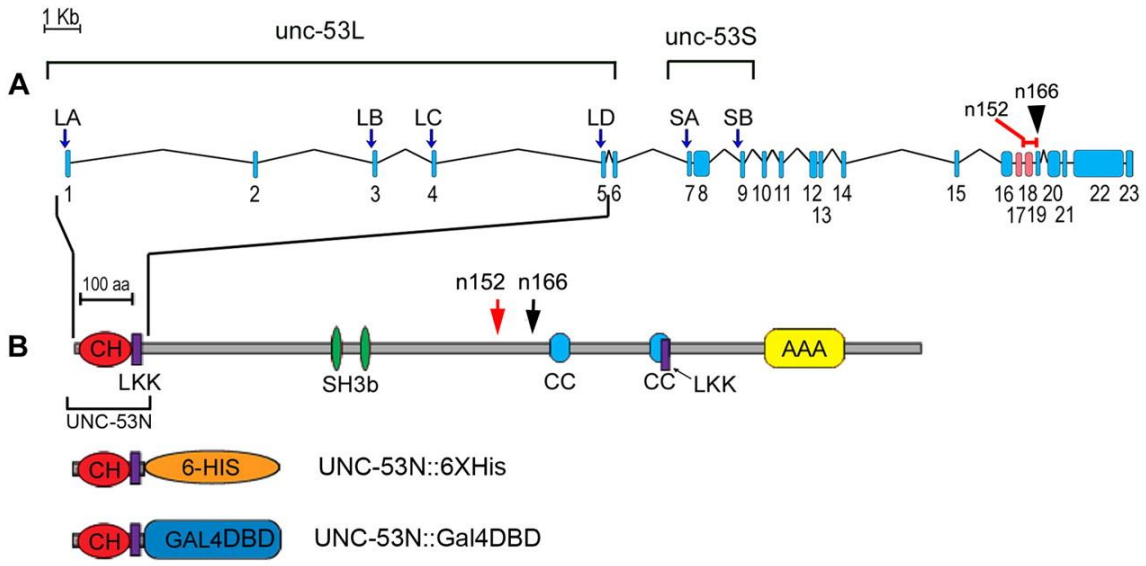

Figure 10. Molecular organization of the *C. elegans unc-53* gene and protein.

(A) Structure of the *unc-53* locus. The start of the various *unc-53* trans-splice sites are indicated by arrows. The promoter for *unc-53SA* is found between exons 5 and 8, and the promoter for *unc-53SB* was determined by using a genomic fragment containing exons 8 and 13 (Stringham et al., 2002). A 2.9 kb promoter region upstream of the most 5'SL1 site of UNC-53LA was used to construct *punc-53L::gfp*. Alternatively spliced exons are shown in pink. *unc-53(n152)* is a 319-bp deletion removing parts of exons 18 and 19, producing a stop codon in exon 20 (Stringham et al., 2002), and *n166* is a single nucleotide C to T transition in exon 19 that introduces a premature stop codon. (B) The longest polypeptide, UNC-53LA, is 1583 amino acids and contains a calponin homology domain (CH, red; amino acids 11-109), two LKK motifs (LKK, purple; 114-133 and 1097-1116), two proline-rich SH3-binding motifs (SH3b, green; 487-495 and 537-545), two coiled-coil regions (CC, blue; 890-923 and 1078-1113) and an AAA domain (yellow; 1292-1425). *n166* introduces a premature stop codon at amino acid 949. Both *n152* and *n166* remove the coiled-coil, LKK and AAA domains from all isoforms. The first five exons of UNC-53 (UNC-53N; amino acids 1-139) were used for the production of PAB-UNC-53N antisera and the GAL4 DNA-binding domain (GAL4DBD) in pVA200 for yeast two-hybrid studies.

Previous attempts to identify the expression of the longest isoform of *unc-53* were carried out using a 2.3kb promoter region upstream of the most 5' SL1 splice site but only produced expression in a few unidentified neurons in the head that did not correlate well with the observed phenotypes of *unc-53* (Stringham et al., 2002). To better determine the expression of the UNC-53L isoforms, a promoter region 2.9 kb upstream of the most 5' SL1 splice site of *unc-53* was used, and strong GFP expression was observed in embryos, larva, and adult animals. Expression was found in the excretory cell, neurons in head and tail ganglia, and several classes of ventral cord

motorneurons, as well as the vulval cells and sex myoblasts (Figure 11A-F). Immunostaining with an antibody raised against the translated product of the first 5 exons of *unc-53* (Figure 10B) supported the expression observed by the transcriptional reporter, and revealed UNC-53L protein localized to the excretory cell and coelomocytes (Figure 11G,H) as well as the sex myoblasts, anal muscles and neurons (Adeleye, 2002).

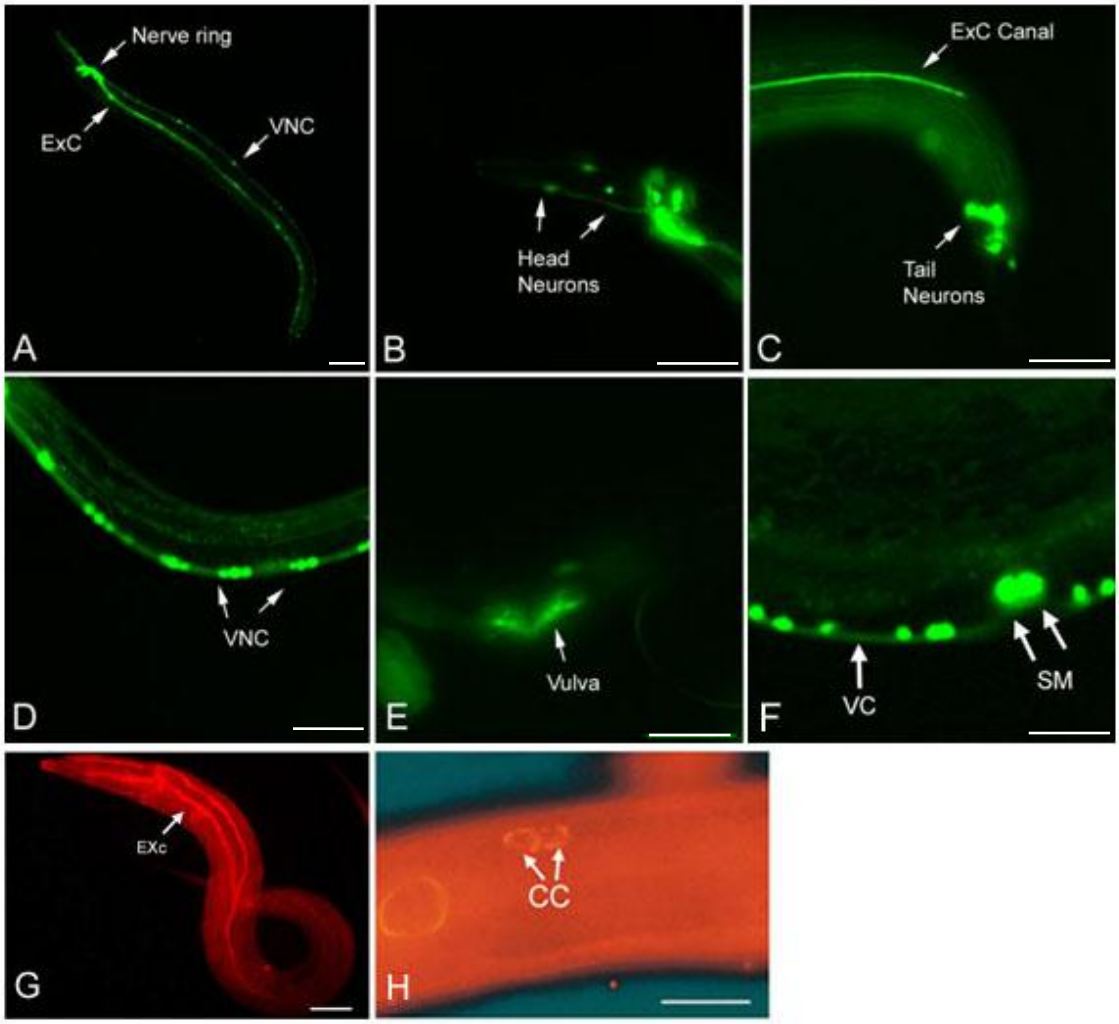

Figure 11. Expression pattern of the long-isoform of *unc-53*

(A-F) Expression pattern using *punc-53::gfp* (BC14371). (A) Adult hermaphrodite (anterior is left), showing GFP expression in several neurons in the head (nerve ring), the excretory cell (ExC) and ventral nerve cord (VNC) (B) Head of an adult animal showing neurons in the head including the nerve ring. (C) Several neurons in the tail of an adult worm as well as the posterior canal of the excretory cell (ExC). (D) Midbody of

an adult worm showing *unc-53* expression in the ventral nerve cord (VNC) (E) Midbody of an adult worm showing *unc-53* expression in the uterine and muscle cells making up the adult vulva. (F) Expression of *unc-53* in the ventral cord VC, same as VNC) and sex myoblasts (SM) as shown. (G-H) Expression pattern using *PAb-UNC-53N* antisera. (G) Expression of UNC-53 throughout the excretory cell (EXc) canals. (H) UNC-53 expression in a pair of coelomocytes (CC). Scale bar is 100 μm.

2.3.2 **UNC-53L interacts with Abelson Interactor-1 (ABI-1)**

Previous studies suggest that UNC-53 is involved in signal transduction during migration and may function as a link between upstream signalling cues and the cytoskeleton (see Section 1.1) (Stringham et al., 2002). Despite this, few molecules known to interact directly with UNC-53 have been identified. Moreover, a cDNA devoid of the first 4 exons was observed to partially rescue the Unc and Egl phenotypes of *unc-53* mutants (Stringham et al., 2002), suggesting that the shorter isoforms driven by the internal promoters are sufficient to convey some of the function of *unc-53*. We were interested in understanding the role of the longest isoform of UNC-53 and wondered what molecules might interact with its N-terminus, as this region is conserved in the mammalian NAVs, NAV2 and NAV3 (Maes et al., 2002). To answer this question, a screen for interactors using a *C. elegans* yeast two-hybrid library together with the N-terminus of UNC-53 including the CH domain and the first LKK motif (UNC-53N) as bait was conducted (Figure 10B). Of the candidate cDNAs isolated, six corresponded to the B0336.6 genomic locus, the *C. elegans abi-1* (Abelson Interactor-1) homolog (Figure 12A). Of the *abi-1* clones isolated, the smallest cDNA encoded amino acids 16-427, excluding the SH3 region of ABI-1 as a required domain for UNC-53 binding (Figure 13). Moreover, the UNC-53 bait contained only the first 139 amino acids of UNC-53L, devoid of the polyproline repeats that are typical of SH3 binding domains. Therefore, the interaction between ABI-1 and UNC-53 does not appear to require SH3 binding. The yeast two hybrid data was further confirmed by GST pulldown (Figure 12B), demonstrating that the interaction between ABI-1 and UNC-53 is direct.

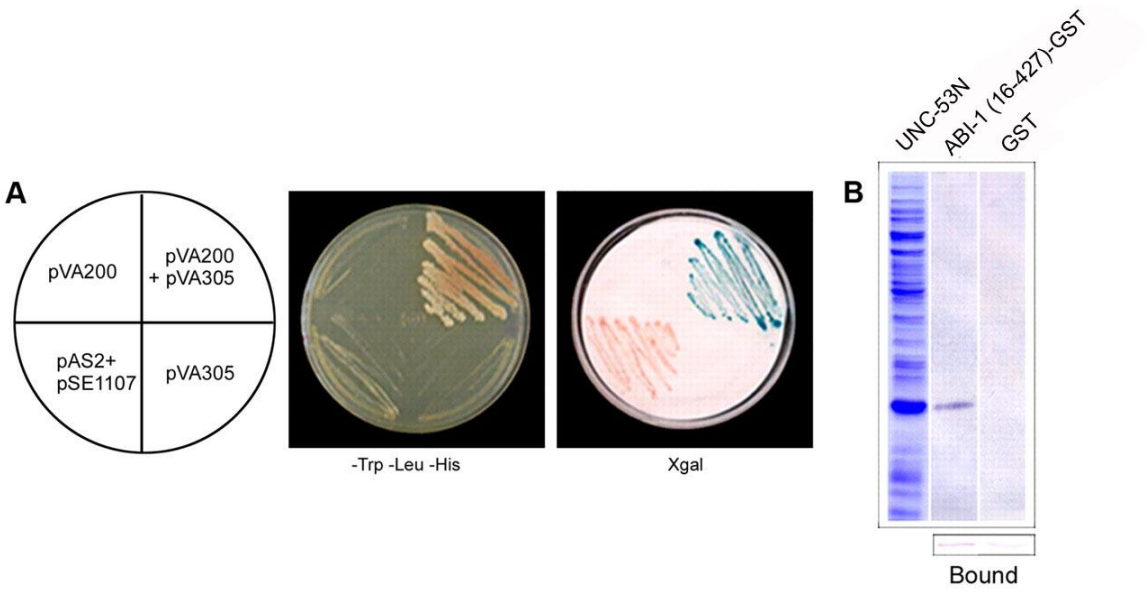

Figure 12. ABI-1 physically interacts with the N terminus of UNC-53.

(A) ABI-1::GAL4AD interacts with UNC-53N::GAL4DBD by yeast two-hybrid assay. Yeast harboring both bait (pVA200) and prey (pVA305) plasmids grow in triple drop-out media (-Trp-Leu-His, 25mM 3AT) and are positive for β-galactosidase (Xgal), in contrast to yeast transformed with empty vectors (pAS2 and pSE1107), or with either the bait (pVA200) or prey vector (pVA305) alone. (B) GST pull-down assay. Equal amounts of ABI-1(16-427)-GST and GST alone were expressed and purified from *E. coli* then bound to glutathione-conjugated beads (Bound). Soluble UNC-53N::6His lysates (left lane) were incubated with protein-bound beads and were observed to bind ABI-1(16-427)-GST (middle lane) but not GST alone (right lane), as detected by PAB-UNC-53N.

To characterize the domains of ABI-1 required for the interaction with UNC-53N, the extent that several domain deletion mutants of ABI-1 could bind UNC-53N was conducted (Figure 13). Using the yeast two-hybrid system it ws observed that a construct encoding full-length ABI-1 (ABI-1_{1-469}) binds UNC-53N, as does a construct devoid of the first 16 amino acids of the N-terminus of ABI-1 and most of the C-terminal SH3 domain (ABI-1_{16-427}), suggesting that these regions are not required for UNC-53N binding. Alternatively, a construct encoding amino acids 16-173 (ABI-1_{16-173}) did not bind UNC-53N while ABI-$1_{174-427}$ did, suggesting that the Q-SNARE and ABL-HHR regions of ABI-1 are not required for the UNC-53N-ABI-1 interaction, but that the interaction is dependent on a portion of ABI-1 that is serine-rich and contains SH3 binding domains. We further mapped the UNC-53N-ABI-1 interaction by testing two additional constructs that isolate these regions from each other (ABI-$1_{174-259}$ and ABI-$1_{260-427}$, Figure 13).

UNC-53N bound ABI-$1_{260-427}$ but not ABI-$1_{174-259}$, suggesting that UNC-53N can bind ABI-1 in the region containing amino acids 260-427 that contains the SH3 binding motifs.

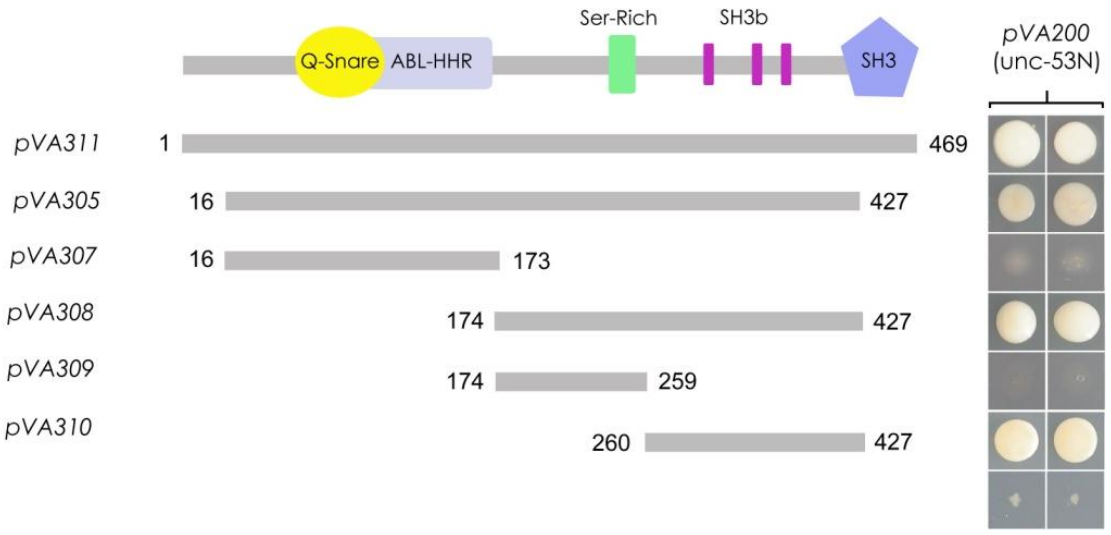

Figure 13. ABI-$1_{260-427}$ is sufficient to bind UNC-53N *in vitro.*

The domain organization of the full-length ABI-1 protein is shown on the top, with domain deletions used as indicated below. Construct names are indicated on the left. Yeast interactions shown in duplicate are given on the right. Strains containing interacting bait and prey are able to grow on minimal media (CSM-Leu-Trp-His-Ade).

2.3.3 Characterization of *abi-1 in C. elegans*

BLAST analysis revealed the presence of a single *abi-1* gene in *C. elegans*. The *abi-1* genomic locus spans 2624bp and contains 5 exons encoding a predicted polypeptide of 469 amino acids (Figure 14). *C. elegans* ABI-1 is a conserved protein that is homologous to ABI-1 of *C. briggsae* (CAE64316), *H. Sapiens* (NP_005461), *M. musculus* (Q3TJ64) and *D. melanogaster* (NP_477263). The greatest similarity resides within several recognizable protein domains suggestive of function. Near the N-terminus is a Q-SNARE motif (Echarri et al., 2004; Echarri et al., 2004; Tanos and Pendergast, 2007), which in the case of mammalian ABI-1, has been shown to be involved in growth factor receptor endocytosis and to bind Syntaxin-1 (Echarri et al., 2004). Partially overlapping with the Q-SNARE motif is an ABL-homeodomain homologous region that is similar to the DNA-binding region of homeo-domain proteins, and found exclusively in adaptor proteins that interact with Abl-family tyrosine kinases (Dai and Pendergast,

1995). Additionally, *C. elegans* ABI-1 contains a serine-rich region and multiple polyproline rich putative SH3 binding motifs. A single SH3 domain is located at the C-terminus of *C. elegans* ABI-1 and this domain has been shown to mediate ABI-1 interaction with Abelson tyrosine kinases (Shi et al., 1995), and to control ABL ability to phosphorylate downstream targets including mammalian ENABLED (Mena) (Tani et al., 2003). The *abi-1(tm494)* allele (Mitani Lab, National Bioresource Project) carries a 684 bp deletion beginning at nucleotide 1659 in exon 4 (Figure 3A) and encodes a predicted truncated product ending at proline 350 followed by TGPVRL and a premature stop codon, resulting in a 356 amino acid product (Figure 14C). The *tm494* deletion is found in a region of *abi-1* that encodes protein regions that bind UNC-53N (Figure 13). An additional allele of *abi-1* was also generated (*C. elegans* Knockout Consortium) termed *ok640*. Following several rounds of outcrossing it was observed that while *abi-1 (tm494)* animals contained a 684bp deletion as described, *abi-1 (ok640)* animals contained the expected 1110bp deletion in addition to a wild-type copy (Figure 47). The presence of a wild-type copy of *abi-1* in the background of *abi-1 (ok640)* was corroborated by others (M. Soto, personal communication) and these animals are superficially wild-type (Patel et al., 2008). As a result, further studies with this mutant were abandoned and attention was placed on *abi-1 (tm494)* and *abi-1 (rnai)*.

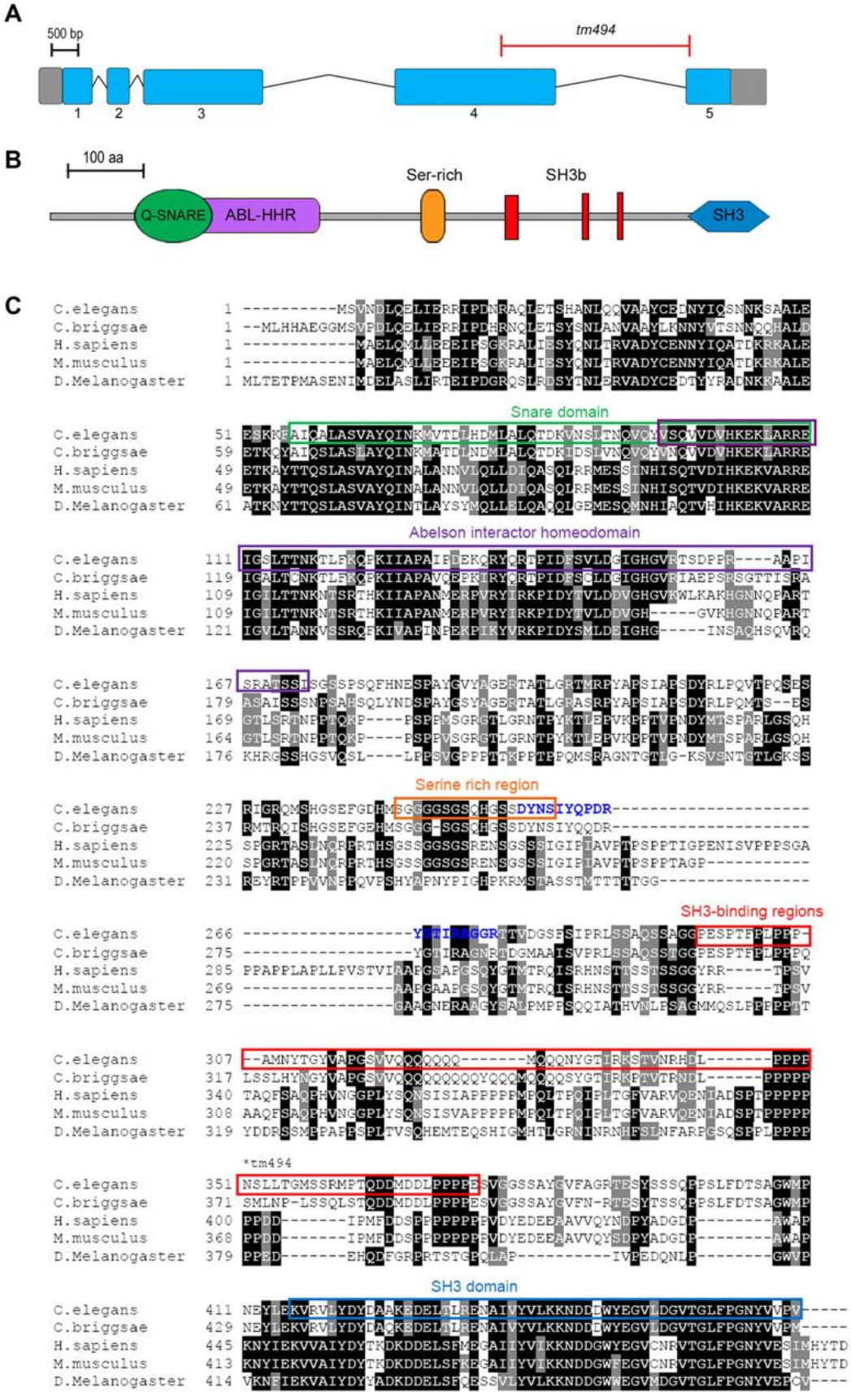
A
500 bp
tm494
1
2
3
4
5
B
100 aa
Ser-rich
SH3b
Q-SNARE
ABL-HHR
SH3
C
Snare domain
Abelson interactor homeodomain
Serine rich region
SH3-binding regions
*tm494
SH3 domain

Figure 14. Molecular organization of the *C. elegans abi-1* gene and protein.

(A) Gene structure of *abi-1*. The boundaries of introns, exons and the *abi-1(tm494)* deletion are indicated. (B) Protein structure of ABI-1. ABI-1 contains a Q-SNARE domain (Q-SNARE, green; amino acids 56-110) (Echarri et al., 2004), an Abl-interactor homeodomain homologous region (ABL-HHR, purple; 95-173), a serine-rich region (Ser-rich, orange; 243-259), three proline-rich SH3-binding motifs (SH3b, red; 296-306, 347-351 and 371-374) and an SH3 domain (SH3, blue; 416-469). ABL-HHR and SH3 domains were predicted using the Simple Modular Architecture Research Tool (SMART, http://smart.emblheidelberg.de). (C) Comparison of *C. elegans* ABI-1 with *C. briggsae*, human, mouse and *Drosophila* orthologs. Multiple alignments were performed using Clustal W 1.83 (http://align.genome.jp) with ABI-1 proteins from *C. elegans* (CE29545), *C. briggsae* (CAE64316), *H. sapiens* (NP_005461), *M. musculus* (Q3TJ64) and *D. melanogaster* (NP_477263), and were drawn using BOXSHADE (http://www.ch.embnet.org). The peptide sequence used to generate ABI-1 antibody *PAb-ABI-1* is indicated in blue and the start site of the *tm494* deletion is indicated by an asterisk.

2.3.4 *unc-53* and *abi-1* mutant phenotypes and genetic interactions

UNC-53 controls the migration of several cells and cellular processes along the anteroposterior axis in *C. elegans*, including the sex myoblasts (Chen et al., 1997), the ALN/PLN and ALM/PLM axons and the excretory canals (Stringham et al., 2002). To determine whether the observed interaction between ABI-1 and UNC-53 was relevant *in vivo*, the extent that *abi-1* and *unc-53* shared defects in migration was determined. The analysis began by examining the migration and outgrowth of both the anterior and posterior excretory canal processes using the transgenic reporter *ppgp-12*::*gfp*, which is expressed exclusively in the excretory cell from the 3-fold embryonic stage onwards (Zhao et al., 2005). The excretory cell (EC) is a large H-shaped cell in *C. elegans* and represents an excellent cell type for the study of both dorsoventral and anteroposterior migrations. During its outgrowth, two processes emerge from the EC body and migrate dorsolaterally from the ventral side of the terminal pharyngeal bulb toward the lateral hypodermis. In wild type animals, when the canals reach the lateral hypodermis they cross the hypodermal basement membrane and bifurcate, sending processes anteriorly to the head and posteriorly to the tail (Figure 15A) (Nelson et al., 1983).

By contrast, although the excretory cell body is positioned normally in *unc-53 (n166)* animals, both the anterior and posterior canals are severely truncated. The anterior processes terminated close to the excretory cell body, often not extending further than the anterior pharyngeal bulb, while the majority of posterior canals grew out approximately half way, terminating at the level of the vulva (Figure 15B). These

phenotypes were also observed by *unc-53 (rnai)* (Figure 15C, F). Notably, defects in the posterior migrations of the excretory canals in *unc-53 (n166)* animals were equally strong as in heterozygous *n166/mnDf87* worms (Figure 15F), suggesting that *unc-53 (n166)*, which removes a coiled-coil domain, an LKK motif and the AAA cassette from all isoforms, is a null allele for this phenotype. To determine the role of *abi-1* in excretory cell migration the morphology of the excretory canals in *abi-1 (tm494)* and by RNAi was assessed. Animals carrying the *abi-1 (tm494)* deletion are superficially wild-type with the exception of a mild-uncoordination defect, characterized by an increased frequency of backing. An examination of the excretory cell using *ppgp-12::gfp* showed that while the cell body in *abi-1 (tm494)* is positioned normally, a majority of the posterior excretory canals of *abi-1 (tm494)* failed to exit the gonad region (Figure 15E, F). The anterior canals extended to the same length as what is observed in N2. The position of the excretory cell body was also normal in *abi-1 (rnai)* animals, but the anterior and posterior excretory canals were severely truncated (Figure 15D, F), reminiscent of *unc-53* loss of function alleles. A number of additional defects were observed in *abi-1 (rnai)* that are not seen in *unc-53* (see Section 2.3.7). Notably, excretory canal defects were not observed to be more severe in *unc-53(n166); abi-1(tm494)* double mutants than in *unc-53(n166)* (Figure 15F). Although the deletion in *abi-1(tm494)* results in a truncated protein, the *abi-1(tm494)* allele behaves as a hypomorph as *abi-1(rnai)* exacerbates excretory canal defects in an *abi-1(tm494)* background (Table 1). As is the case for the *abi-1 (tm494); unc-53 (n166)* double mutant, *abi-1(rnai)* in an *unc-53 (n166)* background or the *abi-1 (tm494); unc-53 (n166)* background does not reduce the extension of the posterior excretory canals beyond that of *unc-53 (n166)* alone (Figure 15F). Though not definitive (because an *abi-1* null mutation is not used), this evidence suggests that these genes function within the same pathway to control outgrowth of the posterior excretory canals. Previous work suggests that *unc*-53 may function cell autonomously (Stringham et al., 2002), so given the physical interaction observed between UNC-53 and ABI-1, it was hypothesized that ABI-1 and UNC-53 may both function within the excretory canals. Consistent with this prediction, full-length *abi-1* and *unc-53* cDNA driven by the *ppgp-12* excretory cell specific promoter rescues the canal outgrowth defects of *abi-1(tm494)* and *unc-53(n152)* mutants respectively (Figure 15F).

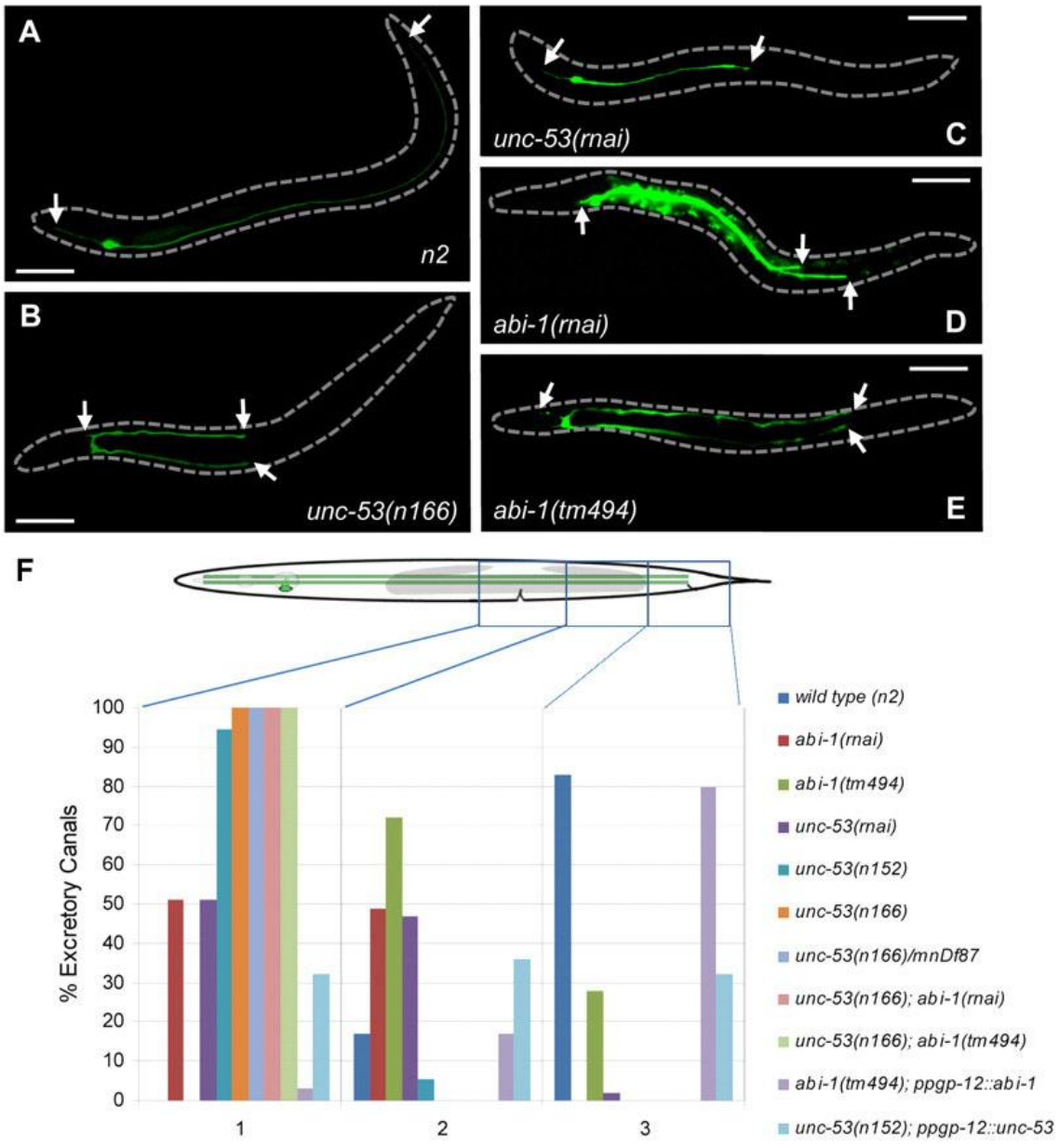

Figure 15. Excretory canal morphology in wild-type, *unc-53* and *abi-1* animals.

(A-G) Fluorescence micrographs of hermaphrodites carrying the *ppgp-12::gfp* transgene, allowing for the visualization of the excretory cell body and canals (anterior and posterior termini marked by arrows, A-E). Anterior is to the left and animals are displayed laterally with the exception of B and E, which are shown ventrally. (A) Morphology of the wild-type excretory cell body and processes. The excretory cell body is positioned on the ventral side of the posterior pharyngeal bulb and extends two canals towards the anterior of the animal to the tip of the head and two canals posteriorly to the tail. (B) *unc-53(n166).* (C) *unc-53(rnai).* (D) *abi-1(rnai).* (E) *abi-1(tm494)*. (F) Quantification of posterior excretory canal outgrowth defects. The outgrowth of the posterior canals was divided into three regions (1-3) between the vulva and the tail as shown. The stop point

of canals was determined by fluorescence microscopy for wild type (*n*=72), *abi-1(rnai)* (*n*=141), *abi-1(tm494)* (*n*=116), *unc-53(rnai)* (*n*=87), *unc-53(n152)* (*n*=37), *unc-53(n166)* (*n*=55), *unc-53(n166)/mnDf87* (*n*=107), *unc-53(n166); abi-1(rnai)* (*n*=55), *unc-53(n166); abi-1(tm494)* (*n*=55), *abi-1(tm494); ppgp-12::abi-1* (*n*=51) and *unc-53(n152); ppgp-12::unc-53L* (*n*=28). Statistically significant differences are observed between *unc-53* and *abi-1* mutant and RNAi animals compared to wild-type and between mutant *unc-53 (n152)* and *abi-1 (tm494)* with appropriated *ppgp-12* rescuing contructs (P<0.0001). Scale bars: 100 µm.

Table 1. *abi-1 (rnai)* exacerbates *abi-1 (tm494)* posterior excretory canal migration

Genetic background	*Posterior Excretory Canal Position (# animals)*			*N-value*
	1	2	3	
pPD129.36	0	7	43	50
abi-1 (rnai)	12	20	3	35†
abi-1 (tm494)	1	34	11	46†
abi-1 (rnai); abi-1 (tm494)	15	20	7	42*

†comparison to wild-type animals with empty vector (*pPD129.36)* (P<0.0001)
*comparison between *abi-1 (rnai); abi-1 (tm494)* and *abi-1 (tm494)* (P<0.0001). Chi-squared analysis is used to compared the number of worms with posterior canals scored as ‘1’ to those scored as ‘2’ and ‘3’.

To determine whether ABI-1 functions in the migration of axons the outgrowth of the mechanosensory neurons that control the touch response was examined. The cell bodies and axons of the mechanosensory neurons are reproducibly positioned in wild type animals and can be visualized using the cell specific *pmec-4::gfp* reporter. In wild-type animals, PLML/R cell bodies are positioned within lumbar ganglia of the tail where they extend a short posteriorly directed process and a long anteriorly directed axon that grows out along the lateral commisure and terminates near the cell bodies of the ALM neurons (Figure 16A). In contrast, in *unc-53(n166)* animals, both the anterior and posterior processes are shorter than wild-type as previously observed (Stringham et al., 2002). The anterior axons of the PLML/R were prematurely truncated and terminate shortly after beginning their trajectory (Figure 16B). Similar phenotypes were observed in *unc-53(rnai)* (Figure 16C). While no posterior defects were observed in *abi-1(rnai)* animals, a significant number of anteriorly directed PLM axons terminated prematurely at positions posterior to the ALML/R cell bodies (Figure 16D; Table 4). None of the PLM axons were shorter in *abi-1(rnai)* animals than in *unc-53(n166)*. In the weak *abi-*

1(tm494) allele, outgrowth of PLM was normal but misdirection of the AVM axonal projection was observed (Figure 16E,F). During wild-type development the AVM axon undergoes a short ventral migration followed by a turn and migration anteriorly along the ventral cord where it extends past the nerve ring into the tip of the head (Figure 16E). In *abi-1(tm494)* animals, the initial ventral and longitudinal anterior migrations of the AVM axons were wild-type but instead of terminating along their anterior trajectory, the AVM would occasionally reroute, turning dorsally away from the ventral cord, and then posteriorly back towards the nerve ring (Figure 16F; Table 3).

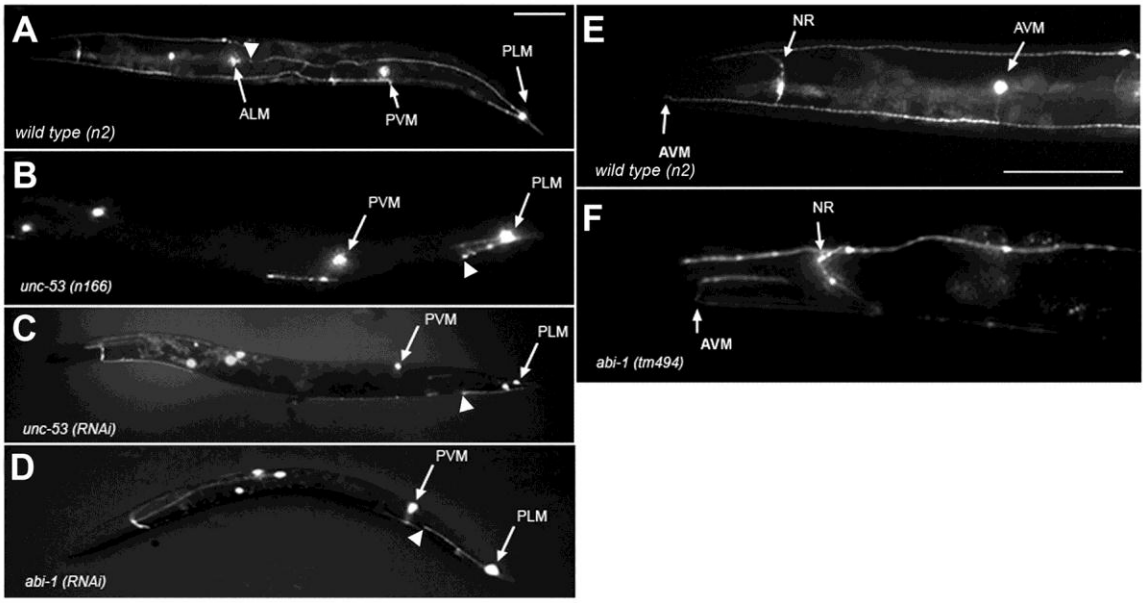

Figure 16. Mechanosensory neuron phenotype in wild-type, *unc-53* and *abi-1* animals.

(A-F) Fluorescence micrograph showing a (A) Lateral view of a wild-type hermaphrodite carrying the *pmec-4::gfp* transgene. The PLM, PVM and ALM neuronal cell bodies and axons are shown. The stop point of the PLM axon was scored with respect to the wild-type position near the ALM cell body (arrowheads indicate final position of the PLM axon). (B) *unc-53(n166)* animal with truncated PLM and PVM axons. (C) *unc-53(rnai)* animal with truncated PLM and PVM axons. (D) *abi-1(rnai)* animal showing truncated PLM axon stopping short of the PVM cell body. (E) AVM axon in a wild-type animal. AVM axons were considered wild type if they projected anteriorly past the nerve ring (NR) and terminated at the tip of the animal. (F) *abi-1(tm494)* animal showing an AVM axon misdirected dorsally (arrow), followed by an abnormal posteriorly directed migration. Scale bars: 100µm.

2.3.5 **ABI-1 and UNC-53 have overlapping expression patterns**

Given the physical interaction between UNC-53 and ABI-1, their shared phenotypes, and since UNC-53 and ABI-1 function cell-autonomously in the posterior migration of the excretory canals, it is expected that ABI-1 would be expressed in some of the same cells as UNC-53. To determine the expression pattern of ABI-1, transcriptional and translational GFP reporter fusions of *abi-1* and an affinity purified a polyclonal antibody towards a peptide corresponding to amino acids 256 to 274 were produced (Figure 14). Collectively, these approaches revealed ABI-1 expression to be concentrated to neurons. Expression in several neurons within the nerve ring and head were identified in addition to the amphid interneurons AIYL/R (Figure 17A), the RMEL/R motorneurons (Figure 17B), and ventral cord motorneurons where ABI-1 localized throughout the cell bodies and commissural axons extending to the dorsal cord (Figure 17C), similar to the tissue expression observed for UNC-53 (Figure 11C) (Stringham et al., 2002). Expression was also observed in endocytic coelomocytes (Figure 17D) similarly to UNC-53 (Figure 11C). ABI-1 expression was observed as early as the L1 larval stage through to adulthood. Expression of ABI-1 was not found in the excretory cell.

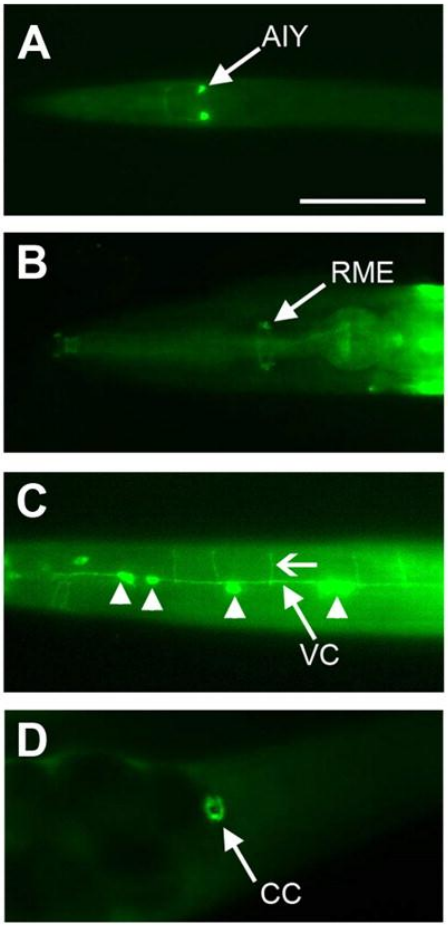

Figure 17. ABI-1 is expressed neuronally and in endocytic coelomocytes

(A-D) Expression pattern of ABI-1. (A) Head of a larva expressing *pabi-1::gfp* in the AIYL/R neurons. (B,C) Expression of ABI-1 detected by immunostaining with *PAb-ABI-1*. (B) Head of a wild-type animal showing ABI-1 expression in the nerve ring and in the cell bodies of the RMEL/R neurons (arrow). (C) Ventral surface of the midbody of an adult worm showing ABI-1 in the cell bodies of motoneurons (arrowheads), in addition to the longitudinal tracts of the ventral cord (VC) and the dorsal commissures (arrow). (D) Expression of ABI-1 in coelomocyte (CC). Scale bars: 50 µm.

2.3.6 ABI-1 and UNC-53 control dorsoventral migrations of the motorneurons

The expression of both UNC-53 and ABI-1 in motorneurons suggests that both genes may have a role in the guidance and outgrowth of these cells. Consistent with this, RNAi of *abi-1* revealed multiple defects in motorneuron guidance including the presence of ectopic branches in commissures, giving rise to disorganized neural networks (Figure 18B, C). Frequently, dorsally directed axons were unable to complete

their migration to the dorsal cord (32%, n=90, P<0.0001) and either bifurcated prematurely, extending lateral processes anteriorly and posteriorly (Figure 18C, D), or produced several knoblike structures in disoriented processes suggestive of growth cone stalling (Figure 18D). In addition to the dorsoventral defects, defasiculation of the ventral cord was also frequently observed (13%, n=90, P<0.0001) (Figure 18F). Previous reports indicate that approximately 13% of motorneuron commissures are abnormal and fail to reach the dorsal cord in *unc-53 (n152)* mutants, through defects in dorsoventral migration do not appear to be a striking feature of *unc-53* (Stringham et al., 2002). This suggests that *abi-1* and *unc-53* contribute to separate aspects of neural development.

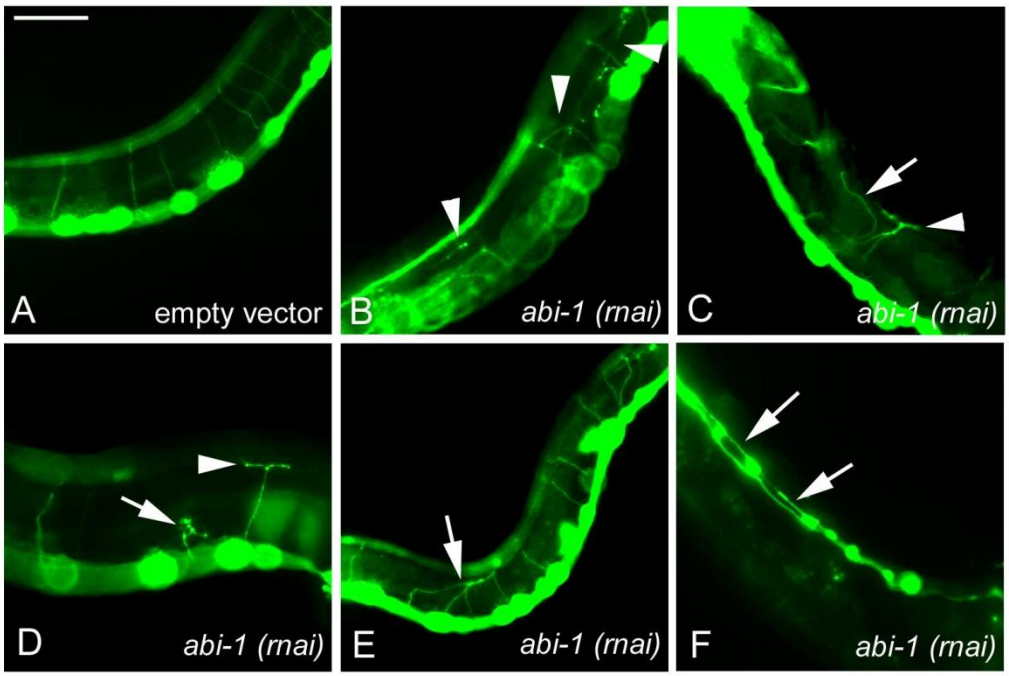

Figure 18. Dorsal migrations of ventral cord motorneurons are disrupted in *abi-1 (rnai).*

(A-F) Fluorescence micrographs showing wild-type (A) and *abi-1(rnai)* (B-F) animals. Ventral is down in all cases except F. (E) Wild-type animal with motoneuron cell bodies located ventrally and regular dorsally directed commissures extending to the dorsal cord. (B) *abi-1(rnai)* animal showing a typically disorganize neural network with axons projecting in varied directions (arrowheads) and failing to migrate to the dorsal cord. (C-D) *abi-1(rnai)* animals showing a truncated and misguided dorsal commissure (arrowhead), and truncated dorsal commissure with anterior and posterior ectopic lateral branches (arrow). (E) Misrouting and branching of dorsal commissures (arrows). (H) Ventral view of the ventral cord of an *abi-1(rnai)* animal showing marked defasciculation (arrows). Scale bar is 50 µm.

To determine if *unc-53* functions in a specific cell known to be under the control of actin regulators, the role of *unc-53* in the PDE neurons was investigated. The ventral migration of the PDE neurons have previously been shown to be defective in mutants of actin regulators including *wsp-1*, *wve-1* and the *gex* complex genes *gex-2* and *gex-3* (Lundquist, 2006; Shakir et al., 2008). The PDE neuron is born in the L2 larval stage and sends an axon directly ventrally to the VNC, where it then bifurcates and extends anteriorly and posteriorly in the VNC (Figure 19A). In *unc-53* mutant animals, rather than migrating directly to the VNC, the ventrally directed PDE axon would sometimes emerge more laterally from the cell body and can bend before proceeding to the VNC (Figure 19B). It will also sometimes meander long distances before finally reaching the VNC (Figure 19C).

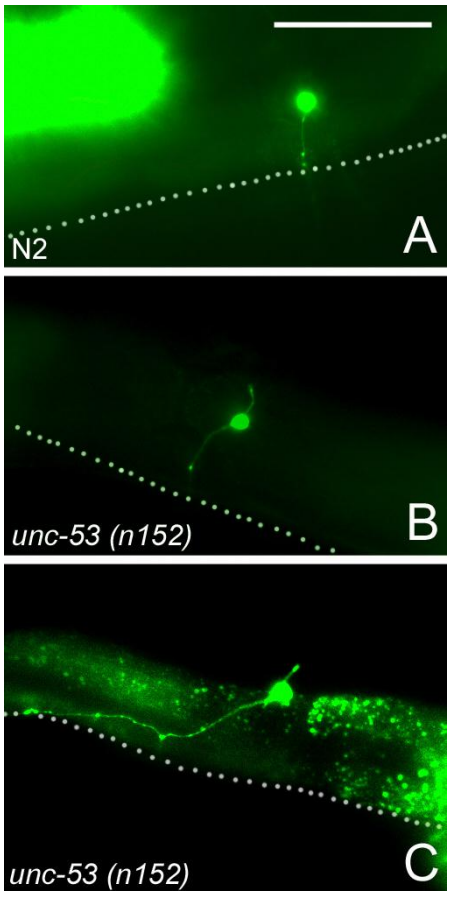

Figure 19. Defects in the ventral migration of the PDE in *unc-53 (n152)*.

Epifluorescent images of young adult animals of the indicated genotypes. Anterior is to the left and dorsal is up in all cases. The ventral nerve cord (out of focus) is indicated by

a dashed line in all the images provided. (A) Wild-type (N2) animal (0% defective, n=100) with a PDE neuron that extends ventrally to the ventral nerve cord. (B,C) *unc-53 (n152)* animals with PDE neurons that do not migrate directly to the ventral nerve cord but instead extend laterally (5% defective, $p<0.0001$, n=200). Scale bar represents 100μm.

2.3.7 ABI-1 genetic loss generates additional phenotypes not observed in *unc-53*

Genetic loss of *abi-1* by RNAi or through the use of *abi-1 (tm494)* produced longitudinal migration defects similar to those observed in *unc-53* (see Section 2.3.4), but also produced several phenotypes that are not observed in *unc-53* single null mutants, suggesting that *abi-1* controls *unc-53* independent processes (Figure 20, Table 2). We observed that *abi-1 (rnai)* animals could have anterior excretory canals that would turn and reroute posteriorly and away from the head instead of terminating normally as in wild-type (Figure 20B). These defects were reminiscent of the misdirection phenotypes observed in the anteriorly directed mechanosensory neuron axons (Figure 21, B-D). It was also possible to observe anterior canals that, instead of bifurcating normally from the cell body, would possess a single fused process exiting the cell body anteriorly rather than on the lateral sides of the animal as in wild-type (Figure 20C). In addition to these defects, defects in guidance along the midline were observed. It was common for the excretory canals in *abi-1 (rnai)* animals to meander dorsoventrally along the midline during their migration, crossing over the midline several times along their trajectory, or to have bends in the canals that direct them away from the midline (Figure 20D-F). Lastly, excretory canal cysts were found along the entire length of the canals in some animals or at seemingly random positions along the length of the canals in others (Figure 20E). The cystic phenotype may represent a canal collapse proceeding from a collapse of filaments in the internal aspects of the canal (Mattingly and Buechner, 2011). Given the role of ABI-1 as a part of the WAVE complex (Soto et al., 2002), phenotypes for *wve-1 (rnai)* animals were assessed. Some of these defects were also observed in *wve-1 (rnai)* (Table 2) and the morphology of the excretory canals in *wve-1* and *abi-1* were very similar (Figure 24).

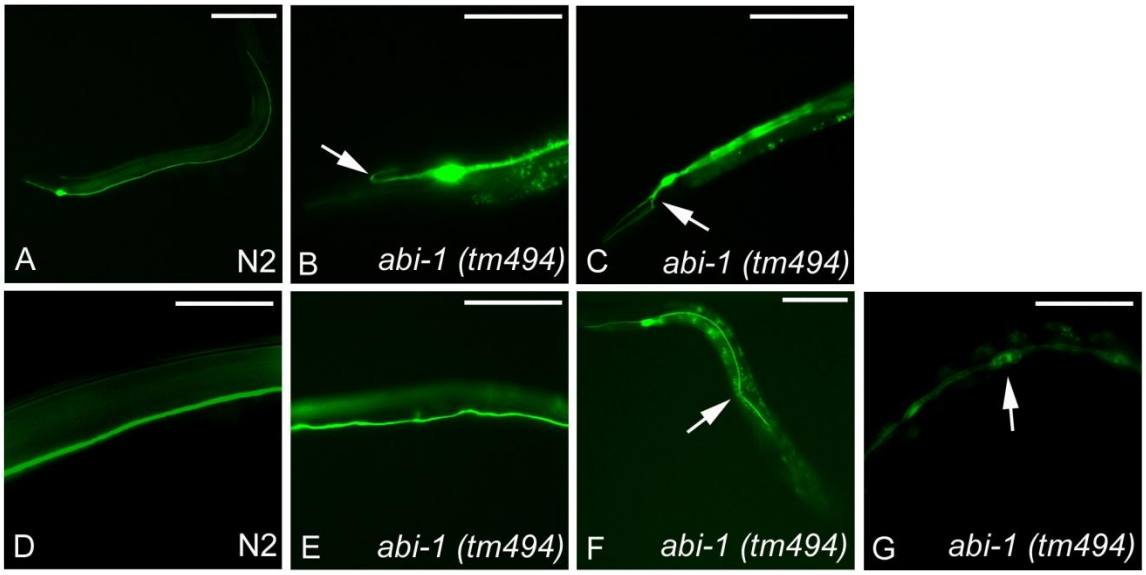

Figure 20. *unc-53* independent excretory cell defects in *abi-1 (rnai)* animals.

Epifluorescent images of animals carrying the *pgp-12::gfp* reporter expressed in excretory cell. Genetic background is indicated, and anterior is to the left with dorsal up in all cases. (A) Wild-type (N2) animal with normally extending anterior and posterior excretory canals. (B) *abi-1 (rnai)* treated animal with a defect in the anterior migration of the excretory canals, displaying a posterior rerouting (arrow). (C) *abi-1 (rnai)* showing a dorsoventral defect indicated by ventrally directed anterior canals and an abnormal ventral bifurcation (arrow). (D-F) abi-*1 (rnai)* animals have various ventral guidance defects. Rather than migrating tightly along the midline as in wild-type (D) they may often wander along the midline (E). (F) *abi-1 (rnai)* with short posterior canals and a posterior canal misdirected to the ventral part of the animal (arrow). (G) Excretory cell in a *abi-1 (rnai)* animal with several small excretory canal cysts in addition to a large cyst (arrow). Scale bars represent 100µm.

Table 2. Excretory cell defects in *abi-1 (rnai), abi-1 (tm494)*, and *wve-1 (rnai)*

Canal defect scored	*Genotype*	*% Defects*	*N-value*
ExC Canal A/P rerouting	*wild-type*	0	97
	abi-1 (rnai)	12***	133
	abi-1 (tm494)	0	75
	wvei-1 (rnai)	7**	98
ExC Midline Crossover	*wild-type*	2	100
	abi-1 (rnai)	23****	88
	abi-1 (tm494)	5	100
	wvei-1 (rnai)	9*	110
ExC Cysts	*wild-type*	0	100
	abi-1 (rnai)	14****	88
	abi-1 (tm494)	2	100
	wvei-1 (rnai)	12****	110
ExC Fusion	*wild-type*	0	100

	abi-1 (rnai)	3	88
	abi-1 (tm494)	0	100
	wvei-1 (rnai)	0	110

Pearson Chi-Squared analysis indicates significantly higher than wild-type. Lack of an asterisk indicates that the observed deviation is >95% likely due to chance. *P<0.05, **P<0.01, ***P<0.001, ****P<0.0001

In addition to scoring the longitudinal migration of the PLMs (see Section 2.3.4), *abi-1 (rnai)* animals were examined for possible defects in the morphology or migrations of the mechanosensory neurons. Six mechanosensory neurons (ALML/R, PLML/R, AVM, PVM) are present in *C. elegans* with cell bodies and axons that are found at highly reproducible positions (Figure 21A). The defects that were observed by *abi-1 (rnai)* and *abi-1 (tm494)* included anterior to posterior rerouting, defects in axon polarity, and midline guidance defects. The most striking defect was observed in the anteriorly directed axons of the ALM, AVM and PLM mechanosensory neurons that would often deviate ventrally during their anterior migration (Figure 21B-D). The rerouting of these axons appeared similar to the rerouting of the excretory canals (Figure 20B). Along with the anterior to posterior rerouting, sometimes axons that branched into two (Figure 21F), or occasionally two axons exiting from the same cell body (Figure 21G), were seen. The final phenotype that was observed regularly in *abi-1* animals was a defect in midline guidance. In these cases, the mechanosensory neuron axons would extend normally along the anteroposterior axis, but instead of migrating closely along the ventral midline they would veer along the midline and drift dorsoventrally (Figure 21H,I).

Table 3. Mechanosensory neuron defects in *abi-1 (rnai)* and *abi-1 (tm494)* animals

Axonal feature scored	*Genotype*	*% Defects*	*N-value*
Anteroposterior rerouting	*wild-type*	0	100
	abi-1 (rnai)	15****	100
	abi-1 (tm494)	6*	100
Axon branching/extra axons	*wild-type*	1	75
	abi-1 (rnai)	7	75
	abi-1 (tm494)	3	100
Midline crossover	*wild-type*	1	75
	abi-1 (rnai)	19****	75
	abi-1 (tm494)	8*	100

Pearson Chi-Squared analysis indicates significantly higher than wild-type. Lack of an asterisk indicates that the observed deviation is >95% likely due to chance. *P<0.05, **P<0.01, ***P<0.001, ****P<0.0001. Experiments conducted in *eri-1(mg366)* background.

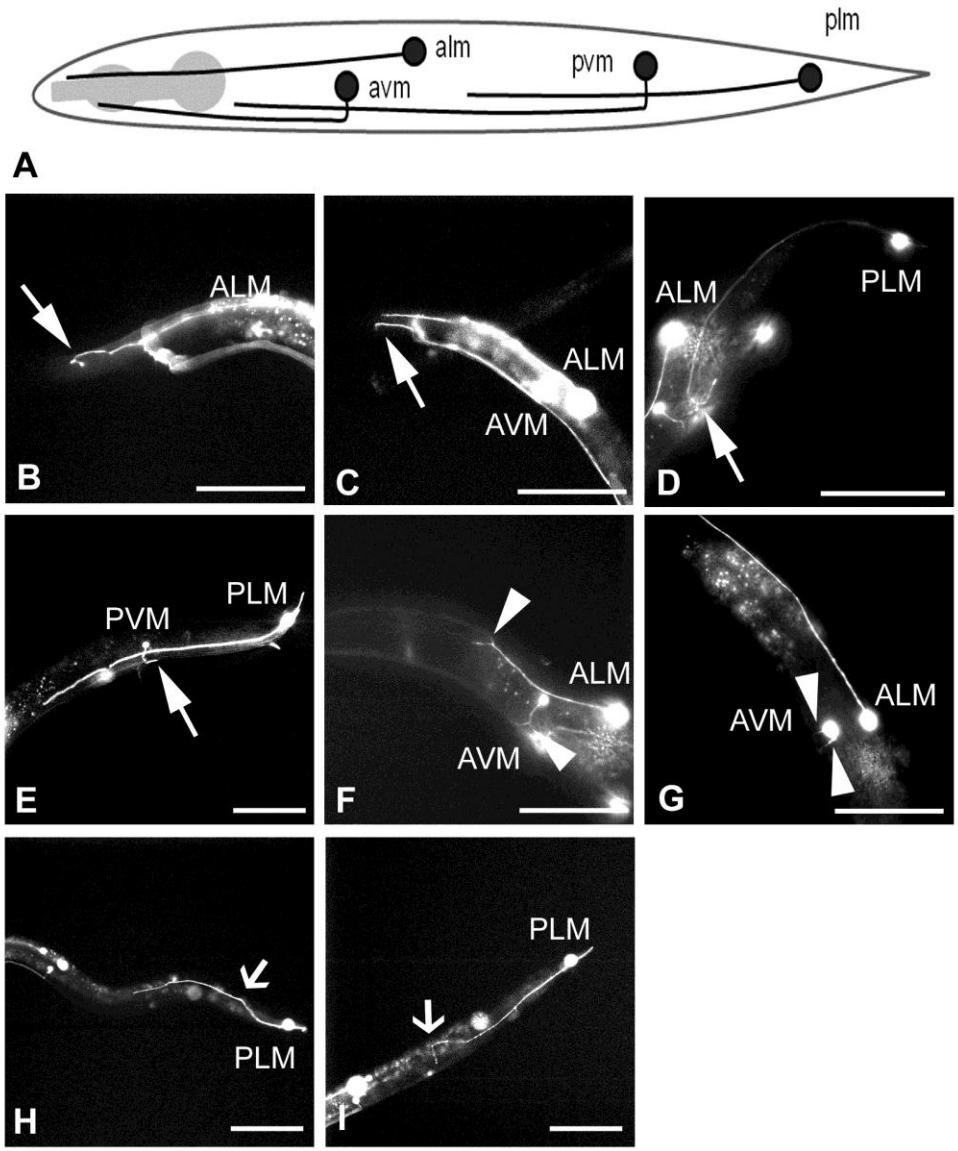

Figure 21. *abi-1* loss results in multiple *unc-53* independent defects in mechanosensory neuron morphology

(A) Drawing of a wild-type *C. elegans* showing the final wild-type positions of the cell bodies and axons of the mechanosensory neurons. ALMR and PLMR are not shown and would be positioned laterally to ALML and PLML. A photomicrograph representation of wild-type N2 animals can also be seen in Figure 16A. (B-I) Fluorescent

micrographs of *abi-1 (rnai)* treated animals showing various axonal defects of the mechanosensory neurons not observed in *unc-53* mutants. Defects include anteriorly directed axons that reroute and migrate posteriorly as observed in ALM (B), AVM (C) and PLM (D). We also observed PVM axons that undergo wild-type ventral migrations to the VNC but proceed to migrated posteriorly rather than anteriorly (E). Closed arrows show rerouting points of migrating axons. In addition to defects in longitudinal migration, axonal branching defects where axons would uncharacteristically branch during their trajectory were also found (F). We also observed cases where more than one axon would extend and migrate from mechanosensory neuronal cell bodies (G). Arrowheads show areas where axons branch or extend more than one axon. Ventral migration defects were also observed in *abi-1 (rnai)* animals (open arrowheads) where axons divert from their normal course along the lateral midline and diverge dorsally before assuming their anterior migration (H, I). Scale bars are 100µm.

2.3.8 **Disruption of UNC-53L causes defects in cell outgrowth**

While the N-terminus of UNC-53 inclusive of the CH domain and first LKK motif is sufficient to bind ABI-1 *in vitro*, this region is absent in short UNC-53 isoforms, and expression of the shorter isoforms of *unc-53* partially rescues defects in *unc-53* mutants (Stringham et al., 2002). As a result, the extent that the long isoform was required for cell migration was of interest. To determine this, RNAi directed toward exons 1-4 of UNC-53 and found that knockdown of UNC-53L moderately impairs posterior excretory canal migration when the short-isoforms are present (Figure 22A). This finding together with previous studies showing a role for the shorter isoforms in excretory cell development suggest that multiple isoforms of *unc-53* are required for excretory canal development. To test further whether the interaction between UNC-53 and ABI-1 is functionally important, the CH domain of UNC-53L was overexpressed in the excretory cell. At a low frequency, various canal defects were observed including ectopic outgrowths, cysts, and the truncation of posterior canals (Figure 22B-D), phenotypes reminiscent of *abi-1* knockdown. One interpretation is that expression of the CH domain alone may act in a dominant negative fashion to sequester endogenous ABI-1 and prevent functional interaction with wild type UNC-53 *in vivo*.

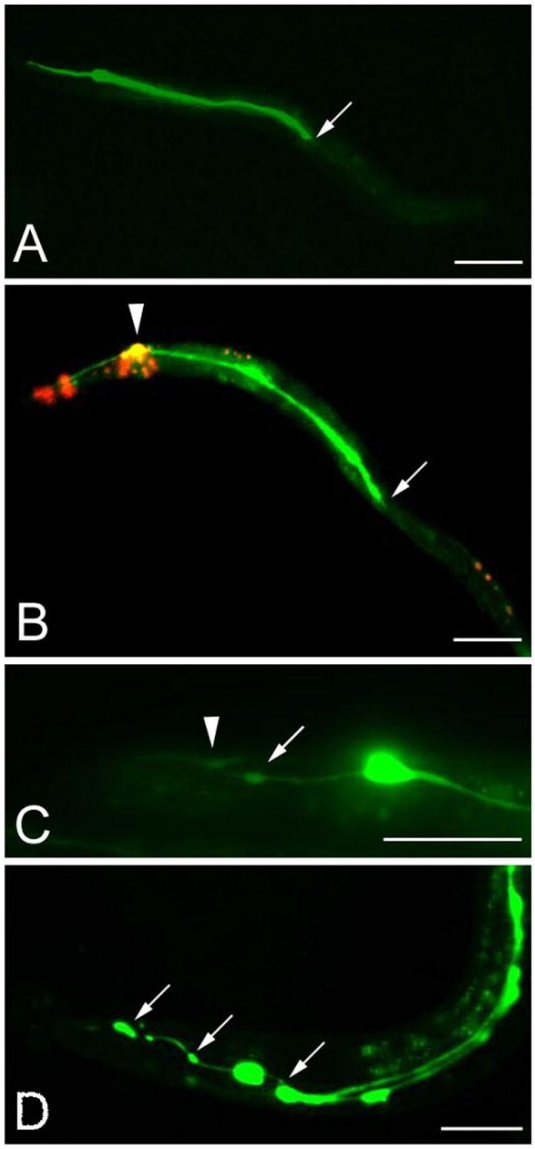

Figure 22. RNAi of the long isoform of UNC-53 and overexpression of the UNC-53 CH domain generates excretory cell defects.

(A) RNAi directed toward the long isoform of *unc-53* results in posterior canal migration, with posterior excretory canals terminating at the vulva (arrow). Three percent of animals had canals terminating at the vulva and 24% failed to exit past the posterior gonad arm (*n*=92). (B) Adult animal expressing *ppgp12::unc-53CH::gfp* in the excretory cell body, as indicated by merge (yellow, arrowhead) with dsRED co-injection marker *pDPY-30::NLS::DSRED2*, displays a posterior excretory canal truncated at the midbody position near the vulva (arrow). Seven percent of canals terminate near the vulva and 22% failed to exit the posterior gonad arm (*n*=116). (C,D) Defects of the excretory canals in adult animals expressing *ppgp-12::unc-53CH::gfp* in the excretory canal. (C) Head of an adult animal showing cysts (arrow) and ectopic anterior branches (arrowhead). (D) Adult animal showing various excretory canal cysts (arrows). Scale bars: 100 μm.

2.3.9 Mutations in actin-polymerization proteins disrupt longitudinal migration

The extension of cellular processes is mediated primarily through the extension of growth cones, highly motile ends at cell tips that are undergoing constant cytoskeletal reorganization. Evidence suggests that ABI-1 may regulate ARP2/3 through a complex with WAVE in response to Rac or by binding WASP (Stradal et al., 2004). To test if these and other proteins known to function with ABI-1 are involved in longitudinal migration in *C. elegans*, the posterior excretory canal phenotypes of mutant and RNAi treated animals that are known interactors of *abi-1* were assessed. Of the genes tested, *wve-1(rnai)*, *nck-1(ok694)* and *arx-2(rnai)* produced excretory canal migration phenotypes reminiscent of *unc-53* and *abi-1* mutants while *wsp-1* and *abl-1* did not (Figure 23). Notably, none of the genes tested had more severe phenotypes either alone or in the background of the null *unc-53* allele *(n166)*, suggesting that the initial trajectory of the posterior excretory canals to the anterior gonad arm and vulva region is unaffected by loss of *unc-53*, *abi-1* or known *abi-1* interactors. We also looked closely at the morphology of the excretory canals of *wve-1(rnai)* animals and observed that they appeared morphologically similar to *abi-1* animals, possessing excretory cell cysts and thin filaments extending from the posterior canals (Figure 24, Table 2), suggesting that they contribute to similar processes in canal outgrowth.

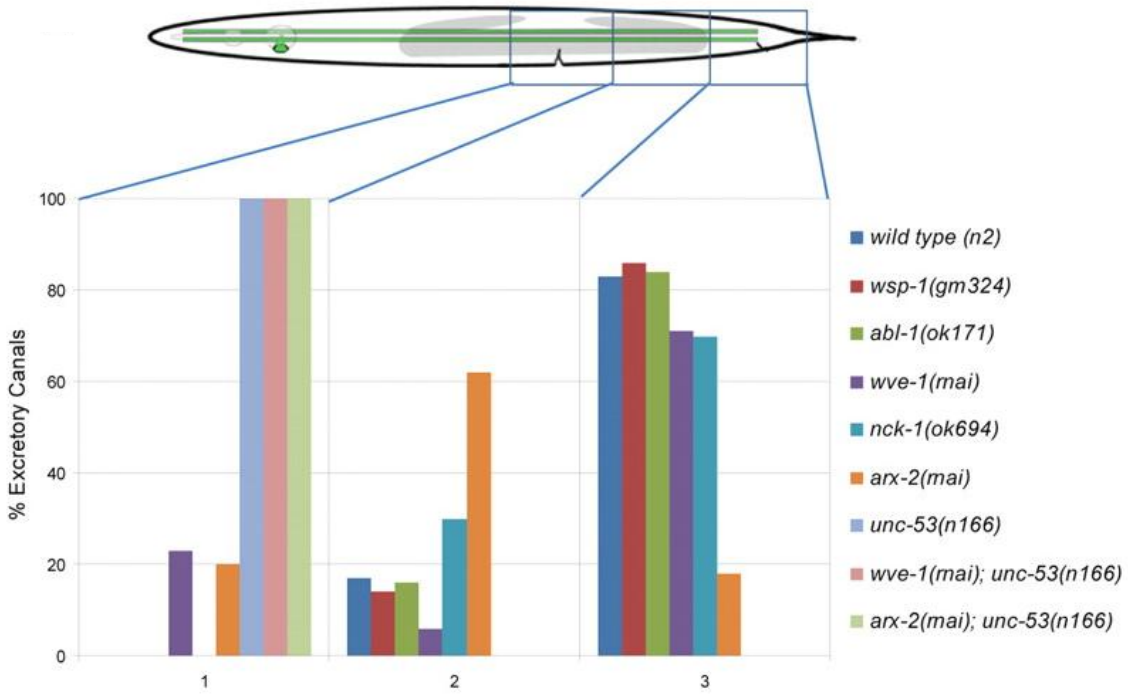

Figure 23. Excretory cell morphology in wild type*, wve-1(rnai), nck-1(ok694) and arx-2(rnai)* animals.

Quantification of posterior longitudinal migration defects. Wild type (*n*=72), *wsp-1(gm324)* (*n*=69), *abl-1(ok171)* (*n*=77), *wve-1(rnai)* (*n*=173), *nck-1(ok694)* (*n*=50), *arx-2(rnai)* (*n*=137), *unc-53(n166)* (*n*=55), *wve-1(rnai); unc-53(n166)* (*n*=90), *arx-2(rnai); unc-53(n166)* (*n*=91). Statistically significant differences are observed between *wve-1 (rnai)*, *arx-2 (rnai)*, *unc-53 (n166)* compared to wild-type (P<0.0001).

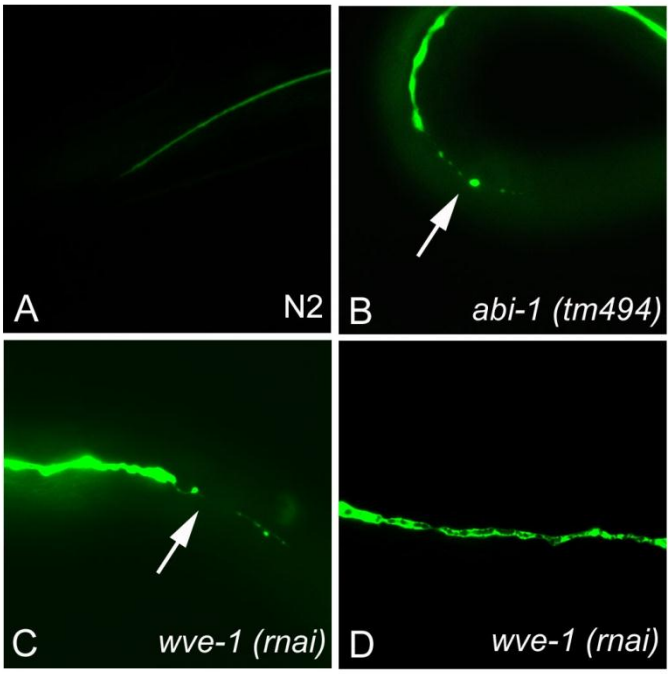

Figure 24. *wve-1* and *abi-1* have similar excretory canal morphology

(A-D) Epifluorescent micrographs showing the excretory cell morphology of *abi-1(tm494)* and *wve-1(rnai)* animals. Both *abi-1 (tm494)* (B) and *wve-1 (rnai)* animals (C) sometimes have truncated posterior canals that end with a long thin filament that extends from the canal that is not present in wild-type (A). *wve-1 (rnai)* animals (D) also have excretory canals that contain cysts along their entire length as seen in *abi-1* (Figure 20G)

In addition to the excretory cell defects observed in the actin regulators the potential role of these proteins in the migration of the PLM axons was examined. Using a RNAi enhanced strain carrying a *pmec-4::gfp* marker, modest effects on PLM outgrowth were observed (Table 4).

Table 4. Percentage of anteriorly directed PLM axons truncated in *eri-1(mg366); pmec-4::gfp*

Genotype	*Percentage of Truncated PLM axons*	*N-value*	*P-value*
Wild-type (N2)	1%	114	n/a
unc-53 (n166)	100%	114	0.0001
unc-53 (rnai)	15%	130	0.0002
abi-1 (rnai)	10%	137	0.0019
nck-1 (rnai)	4%	102	0.1374
arx-2 (rnai)	11%	104	0.0017

2.3.10 NCK-1 is expressed in the excretory cell and neurons, and has defects in cell migration

We were interested in determining the expression pattern and function of the genes known to function with *abi-1* in other systems. NCK-1 is an adaptor protein that mediates protein-protein interactions in signal transduction cascades through its Src homology 2 and 3 domains (Pawson et al., 2001). To determine the expression pattern of *nck-1* a transcriptional reporter in which the upstream 2kb promoter region fused to GFP and expected to drive the expression of *nck-1a* (Mohamed and Chin-Sang, 2011) was produced. Using this construct, expression of *nck-1a* in several cells including neurons in the head and tail (Figure 25A), the excretory cell (Figure 25A,B) and the ventral nerve cord (Figure 25C) was shown. An examination of the excretory cell in the null mutant *nck-1 (ok694)* (Mohamed and Chin-Sang, 2011) revealed a moderate posterior truncation of the excretory canals (
Figure 23) as well as a midline guidance defect (Figure 25D,E) characterized by excretory canals that meandered along the midline of the animal. This phenotype is not observed in *unc*-53 but is found in animals lacking *abi-1* (Figure 20E).

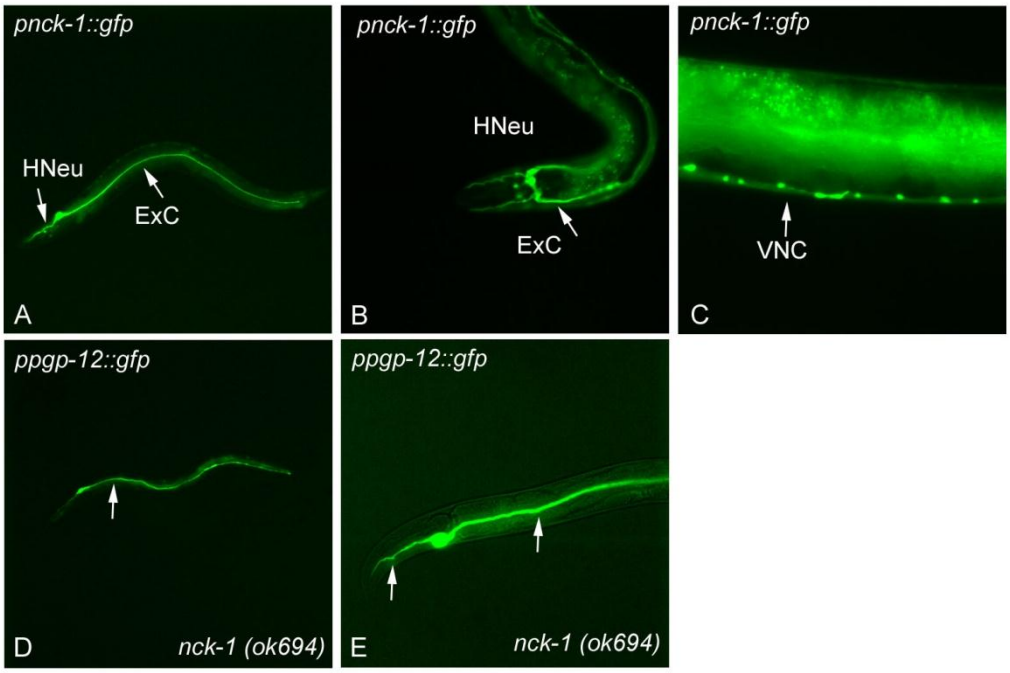

Figure 25*. nck-1* is expressed in neurons and the excretory canals, and has excretory canal defects

(A-C) Expression pattern of *nck-1* using *pnck-1::gfp*. (A,B) Adult hemaphrodites showing expression in the excretory cell (Exc) and head neurons (HNeu). (C) View of the midbody of adult hemaphrodite showing expression in several motor neurons of the ventral nerve cord (VNC). (D,E) *nck-1 (ok694)* animals carrying the *ppgp-12::gfp* excretory cell specific marker to show the excretory cell. The excretory cell in *nck-1 (ok694)* animals exhibits a ventral guidance defect with bends that occur along the midline of the animal throughout its trajectory. Notice the characteristic kinks (arrows) along the midline in these mutants. Scale bars are 50µm.

2.3.11 ABI-1 binds MIG-10A

mig-10 is the *C. elegans* homolog of Lamellipodin, and *mig-10* mutants have defects in axon guidance, neuronal cell migration, and the outgrowth of the excretory canals (Manser and Wood, 1990). To identify additional proteins that interact with MIG-10, a yeast two-hybrid screen was performed using the MIG-10A isoform as bait, isolating six *abi-1* cDNAs (McShea et al., 2012). To characterize the domains of ABI-1 required for the interaction with MIG-10A, the interactions between MIG-10A and various domain deletion mutants of ABI-1 were examined using the yeast two-hybrid system. Full-length ABI-1 and MIG-10A are shown to interact physically as observed by yeast two-hybrid, while a construct removing the C-terminus of ABI-1 lacking the SH3 domain and the first 16 amino acids (ABI-$1_{16\text{-}427}$) does not (Figure 26). This suggests that these

regions may be required for the MIG-10A interaction. However, a second construct, ABI-1_{16-173}, appeared to interact with MIG-10. This deletion construct encodes the complete SNARE and ABL-HHR domains, but is missing the first 16 amino acids of the N-terminus along with the entire C-terminus, including the SH3 domain. This result suggests that amino acids 16-173 are sufficient for a direct ABI-1-MIG-10A interaction. Numerous constructs encoding N and C-terminal truncations of ABI-1 (ABI-$1_{174-427}$, ABI-$1_{174-259}$, ABI-$1_{260-427}$) were unable to interact with MIG-10A. One way to interpret this data is that the ABI-1 SH3 domain is necessary for an interaction between ABI-1 and MIG-10A but that removal of the C-terminal portion of ABI-1 is also able to facilitate an interaction between ABI-1 and MIG-10 that is mediated through an N-terminal region of ABI-1 (16-173). The importance of the SH3 domain to the ABI-1-MIG-10A was independently verified using an insect expression vector system (McShea et al., 2012). In agreement with the yeast two-hybrid result, MIG-10A co-immunoprecipitated with wild type ABI-1:GFP, but not ABI-1_{1-426}::GFP lacking the SH3 domain or ABI-$1_{174-426}$::GFP, which lacks both the N- and C-termini of the protein. Given the finding that ABI-1 and MIG-10 are both required for the posterior migration of ExC canals, and that they interact physically, it is expected that if their interaction is relevant *in vivo* that they might both function cell-autonomously in the ExC To answer this, *mig-10a* and *mig-10b* were cloned behind the *pgp-12* promoter (pVA700) and were observed to partially rescue the ExC defects of *mig-10* cell autonomously (McShea et al., 2012) (Dr. E. Ryder, personal communication).

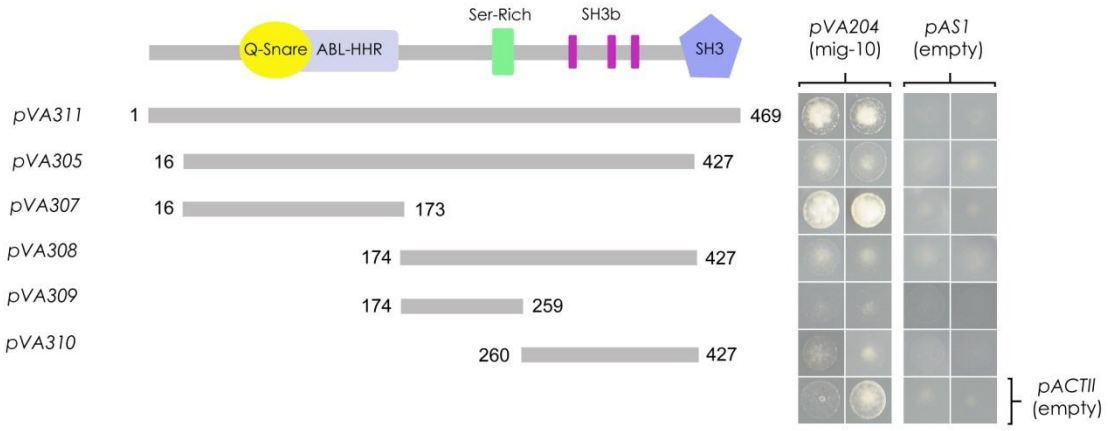

Figure 26. **ABI-1 deletion analysis showed two potential interaction regions with MIG-10.**

A schematic of the full length ABI-1 protein with predicted protein domains is shown along with the full-length and deletion constructs of ABI-1 indicated. MIG-10A and empty bait vector (pAS1) interactions at right. Strains containing interacting bait and prey will grow on complete synthetic media lacking Leu, Trp, His, and Ade (CSM-Leu-Trp-His-Ade) if a functional interaction is present.

2.3.12 UNC-53 and ABI-1 are required for endocytosis in *C. elegans*

Given the observation that UNC-53 and ABI-1 are expressed in coelomocytes (see Section 2.3.1 and 2.3.5), specialized endocytic cells in *C. elegans*, it was reasoned that *unc-53* and *abi-1* may play a role in endocytosis. Two different assays to visualize endocytosis in *C. elegans* were employed. The first was the coelomocyte uptake (CUP) assay. This assay uses the *arIs37 [pmyo-3::ssGFP]* strain, in which the first 79 amino acids from *sel-1*, along with a signal sequence, is fused to GFP under the control of the *myo-3* promoter (Fares and Greenwald, 2001). This causes signal sequence tagged GFP to be synthesized and constitutively secreted from body wall muscle into the pseudocoelom. The secreted GFP is then endocytosed and degraded by coelomocytes (Figure 27A). In wild-type *arIs37* worms this causes brightly glowing vesicles in coelomocytes and low level diffuse fluorescence in the pseudocoelom. Defects in coelomocyte endocytosis resulted in the accumulation of GFP in the pseudocoelom, with little or no GFP endocytosed by the coelomocytes (Fares and Greenwald, 2001). We observed that while wild-type *arIs37* animals had very little accumulation of GFP in the pseudocoelom, a minority of *unc-53 (e2432)* animals displayed increased pseudocoelomic GFP accumulation and very little GFP in coelomocytes (Figure 27C,

Table 5) that was similar to *cup-4 (ar494)* positive control animals. While a CUP defect in *unc-53(e2432)* was observed, a similar defect in other alleles of *unc-53* tested (*n152*, *n166*) were not. A coelomocyte uptake defect was also not found in either *abi-1 (rnai)* or *abi-1 (tm494)* animals. RNAi seems to be a relatively ineffective for coelomocytes in *C. elegans* (Fares and Greenwald, 2001). Given that neither *abi-1 (tm494)* nor *abi-1 (rnai)* treatment constitute complete genetic loss, it is possible that a more complete disruption of *abi-1* could result in a CUP phenotype.

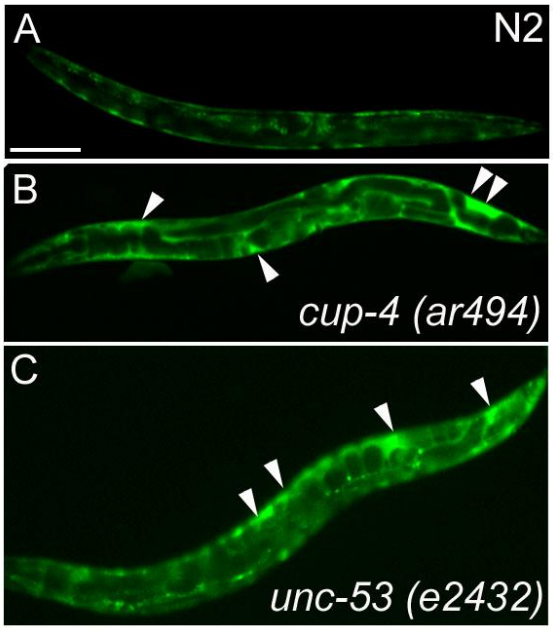

Figure 27. Coelomocyte uptake is disrupted in *unc-53 (e2432)* mutant animals

(A-C) Fluorescence images showing wild-type and mutant animals carrying the *arIs37* coelomocyte marker. Wild-type animals (A) show GFP expression in bodywall muscle and coelomocytes with little expression in the body cavity. (B) *cup-4 (ar494)* mutants are positive controls and show no coelomocyte uptake with bright diffuse GFP expression in the pseudocoelom. *unc-53* (*e2432*) animals (C) have GFP accumulation in the pseudocoelom in addition to the bodywall and very little GFP in coelomocytes. Scale bar is 100 μm.

The second assay used to investigate endocytosis in ABI-1 and UNC-53 focussed on the uptake of the yolk protein VIT-2 into developing oocytes. During the normal lifecycle of *C. elegans*, the intestine produces large amounts of proteins and lipids that are endocytosed by oocytes to provide nutrients for developing embryos (Fares and Grant, 2002; Grant and Hirsh, 1999). The yolk-uptake assay requires a

comparison of the amount of YP170::GFP (VIT-2::GFP) that undergoes clathrin-mediated endocytosis into oocytes compared to what remains in the pseudocoelmic space (Fares and Grant, 2002; Grant and Hirsh, 1999). Defective receptor mediated endocytosis results in animals with excessive pseudocoelomic YP170-GFP compared to oocyte YP170-GFP. Consistent with a role for *unc-53* and *abi-1* in receptor-mediated endocytosis, the abnormal accumulation of YP170-GFP in the pseudocoelom of both *unc-53 (n152)* and *abi-1 (rnai)* animals (Figure 28A,B,D; Table 5) was found. An observed decrease in oocyte GFP was also common in *unc-53 (n152)* and *abi-1 (rnai)* animals. As oocytes mature they progress towards the spermatheca for fertilization and naturally accumulate greater amounts of YP170 during their progression (Grant and Hirsh, 1999). When the amount of GFP in mutant worms was compared to wild-type, it was found that while GFP could be observed in proximal or primary oocytes as well as secondary oocytes in wild-type animals (Figure 28C), very little to no GFP was observed in the secondary oocytes of *unc-53 (n152)* and *abi-1 (rnai)* animals (Figure 28F,G). Furthermore, it was also possible to find *unc-53 (n152)* animals containing embryos with no YP170 accumulation (Figure 28F).

Table 5. Summary of the effects of *unc-53* and *abi-1* on endocytosis

Endocytosis Assay Used		*% worms with GFP accumulation in pseudocoelom*	*N-value*
CUP Assay (*arIs37*)	wild-type (arIs37)	0%	233
	unc-53 (e2432)	14%*	202
	unc-53 (n152)	0.1%	164
	unc-53 (n166)	0%	196
	abi-1 (rnai)	0%	156
	abi-1 (tm494)	0%	232
Yolk Assay (YP170-GFP)	wild-type†	0.6%	158
	unc-53 (n152)	18%*	193
	abi-1 (rnai)	28%*	205

CUP assays were performed in duplicate and were assessed by two different observers. N-values indicated are the sum of both experiments. †Wild-type animals were strain DH1033 treated with pPD129.36 empty vector. Similar values were observed for DH1033 animals not treated to RNAi. * P< 0.0001, compared to wild-type.

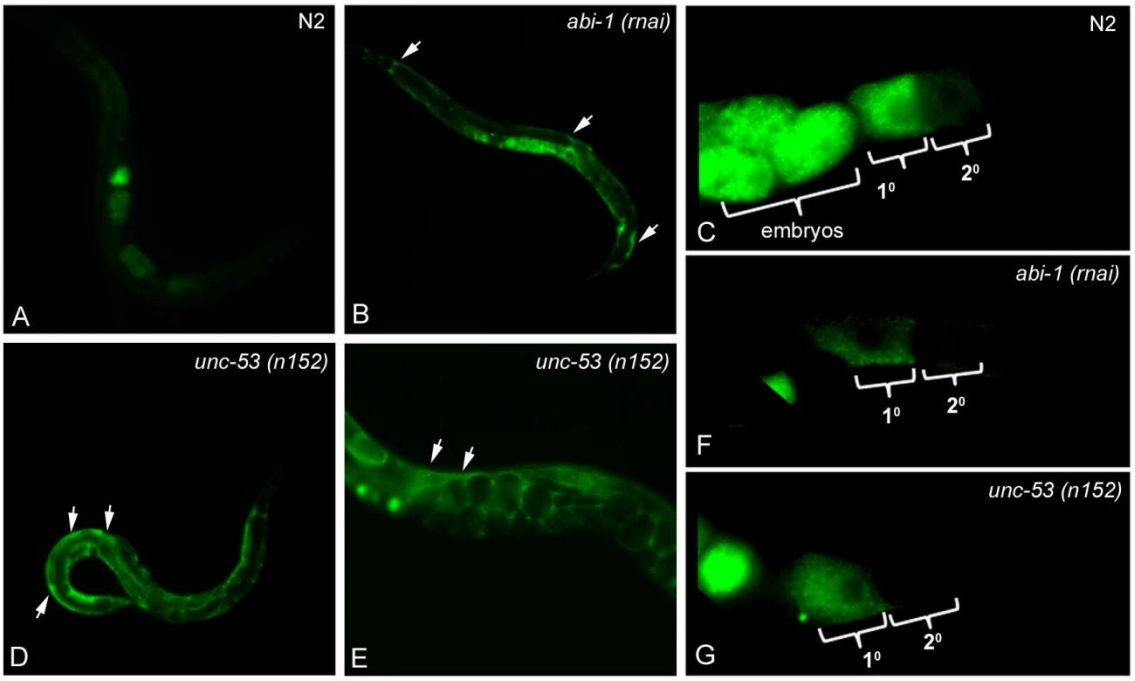

Figure 28. *unc-53* and *abi-1* are required for optimal YP170-GFP uptake

Photomicrographs showing wild-type and mutant animals with YP170-GFP (VIT-2::GFP) accumulating to various degrees in the pseudocoelom and oocytes. (A,B,D,E) Photomicrographs showing accumulation of YP170-GFP in the pseudocoelom of mutant and wild-type animals. N2 animals (A) show GFP expression in oocytes with little expression in the body cavity. *abi-1 (rnai)* (C) and (E) *unc-53 (n152)* mutants show strong diffuse GFP expression in the pseudocoelom. (E) *unc-53* (*n152*) animals have no expression of GFP in embryos. Arrows show representative areas of GFP expression in the body cavity. (C, F, G) Photomicrographs showing GFP expression in oocytes. Wild-type animals (C) have GFP expression in primary (proximal) oocytes as well as secondary oocytes while *abi-1 (rnai)* (F) and *unc-53 (n152)* (G) animals do not. Scale bar is 100 µm.

2.4 Discussion

2.4.1 The long-isoform of *unc-53* functions in cell migration and is expressed in adult animals

unc-53 and its *Nav* homologs have complex genomic loci that produce multiple isoforms expressed in tissue specific ways. The *unc-53* locus was previously shown to contain two internal promoters that drive expression of the shorter isoforms of *unc-53, punc-53SA* and *punc-53SB* (Stringham et al., 2002). The promoter *punc-53SA* with its

associated isoform (*punc-53SA::unc-53SA*) is expressed in the ExC and was able to partially rescue the posterior migration defects in *unc-53* mutants tested (Stringham et al., 1992). In this study, an antibody raised to the N-terminal portion of UNC-53 (UNC-53N) and a transcriptional promoter fusion expected to drive the expression of the longest isoform of *unc-53* to determine its expression were producted. The long-isoform of *unc-53* was expressed in embryos, larva, and adult animals where *unc-53* is thought to function, generating an expression pattern that is in some ways similar to the combined expression pattern of both smaller isoforms (Stringham et al., 2002), though with additional expression observed in endocytic coelomocytes. It is difficult to understand why a gene like *unc-53* might have multiple promoters that are expressed in such similar ways. It is estimated that roughly 2.7% of the *C. elegans* genome is regulated by a two-promoter system using an large intron coupled to an SL1, and that in most cases these internal promoters confer additional tissue specificity (Choi and Newman, 2006). *unc-53* is a unique gene in that it contains multiple large intervening introns all coupled to SL1 splice sites, leaving the question open as to how many additional promoter or enhancer elements are present within the *unc-53* gene that have so far not been accounted for. Certainly the two internal promoters driving the internal isoforms of *unc-53* confer tissue specificity as you might expect (Stringham et al., 2002). The *C. elegans* gene *nck-1* has two promoters, and while these promoters have varied expression there is substantial overlap (Mohamed and Chin-Sang, 2011). It was observed that the differences between *nck-1a* and *nck-1b* was not in their tissue specific patterns of expression but instead their subcellular localization. For example, while both *nck-1* isoforms are expressed in the CAN cells, *nck-1a* is expressed cytoplasmically while *nck-1b* is localized to the nucleus (Mohamed and Chin-Sang, 2011). Thus, it is possible that the various *unc-53* isoforms, even if expressed in the same cells, may confer varied subcellular distributions.

Isoform specific RNAi of the isoforms of *unc-53* that encodes the CH domain result in a truncation of the posterior excretory canals as does the overexpression of the CH domain cell-autonomously within the ExC, together providing evidence that the long-isoform is required for the elongation of the posterior canals. This observation is consistent with the finding that human *Nav2*, which also contains the CH domain, is able to rescue the longitudinal migration of the mechanosensory neurons in *unc-53* (Muley et

al., 2008). Previous investigations of the short isoforms show only partial rescue of the longitudinal migration defects of the ExC (Stringham et al., 2002) as does this study. One possibility is that the various isoforms of *unc-53* may function together in cooperative ways in excretory cell elongation and development. The smaller isoforms of *unc-53* more closely resemble *Nav1* in that they lack the N-terminal CH domain that is conserved between NAV2 and NAV3. Given that the smaller isoforms under control of intronic promoters produce polypeptides that lack CH domains, it is possible that their ability to interact with ABI-1 or the actin cytoskeleton could be limited, altering their subcellular localization or their potential scaffolding function, affecting the way they contribute to ExC canal development.

We observed that overexpression of the CH domain resulted in the development of canal cysts as did the knockdown of *abi-1* and *wve-1.* One way to interpret this finding is that overexpressing the CH domain acts in a dominant negative fashion, sequestering wild-type copies of ABI-1 and WVE-1 within the ExC The presence of ExC cysts could suggest that this isoform as well as *abi-1* and *wve-1* may function in the development of the tube dynamics of the ExC (Buechner, 2002), though it should be noted that the frequency of the cystic phenotype was quite low when the CH domain is overexpressed, and that cysts are not typical of *unc-53* mutants. Very little is known about how the various NAV proteins differ in their function and specificity, or whether these genes act synergistically within the cell. Also, while some of the cells and tissues where UNC-53 is expressed have been identified, the subcellular localization pattern of UNC-53 has not been determined. Further studies aimed toward understanding the relationship between the tissue specificity, domain organization, and subcellular localization of the various isoforms of UNC-53 should shed light on the function of these proteins and potentially their interrelationships.

In addition to expression during embryonic and larval stages, it was observed that *unc-53* expression persisted into adulthood. The possibility that UNC-53 could function after development is complete is perhaps not surprising given that the *Nav* homologs are also expressed in a range of adult tissues, including the brain, kidney, and cells of the immune system (Coy et al., 2002; Martinez-Lopez et al., 2005; Peeters et al., 2004). We found that UNC-53 is expressed in neurons, coelomocytes, and the excretory cell after development is completed. Our observation that *unc-53* is expressed in coelomocytes and is required for coelomocyte uptake shows that *unc-53* functions

after development and probably in a cell-autonomous way. Previous studies have found that *Nav3* mRNA localizes to synapses at neuromuscular junctions (Kishi et al., 2005) and that *Nav1* mRNA levels correlate with the mRNA levels of the presynaptic protein dysbindin in schizophrenia patients (Fung et al., 2011). Our observation that UNC-53 and ABI-1 are both expressed in neurons, and function in coelomocytes and oocytes in endocytosis (only oocytes in the case of *abi-1*), suggest that it is worth pursuing a role for *unc-53* and *abi-1* in endocytic processes at neuronal synapses. The actin cytoskeleton is implicated in several steps necessary for neurotransmission (Jockusch et al., 2004). A recent study in *C. elegans* shows that *wsp-1* negatively regulates presynaptic acetylcholine transmission at neuromuscular junctions through a Cdc42 dependent mechanism (Zhang and Kubiseski, 2010), and these authors suggest that the actin cytoskeleton may serve as a barrier for neurotransmission. Given that *wsp-1* and *wve-1* appear to act redundantly in many cellular processes in worms (Shakir et al., 2008; Withee et al., 2004), it is possible that these two APFs may also function redundantly at the synapse. Similarly, expression of *unc-53* in the excretory cell in adults may contribute to its function. The excretory cell is the *C. elegans* equivalent of the kidney and is necessary for the control of water-balance and osmotic regulation (Buechner, 2002; Nelson and Riddle, 1984). Ablation of the ExC results in results in fluid accumulation and rapid death (Nelson and Riddle, 1984) which does not occur in *unc-53* mutants. Many channels, including water-channels such as the aquaporins, which are expressed in the ExC and required for osmoregulation (Huang et al., 2007), are trafficked to their locations in the cell using actin-dependent mechanisms (Noda and Sasaki, 2008).

2.4.2 **UNC-53 and ABI-1 interact physically**

We have found that UNC-53 and ABI-1 interact physically by a yeast two-hybrid screen and that their interaction is direct as observed by a GST pulldown. The interaction observed between UNC-53 and ABI-1 was mediated by the CH domain of UNC-53 that is a feature of the long-isoforms of UNC-53, NAV2 and NAV3 and not present in the shorter isoforms of UNC-53 or NAV1. The CH domain is sufficient to bind a small region of ABI-1 containing SH3b motifs (260-427). While the CH domain of UNC-53 is sufficient to bind ABI-1, the extent that other portions of UNC-53 (that could be conserved by all isoforms) might bind ABI-1 *in vivo* or *in vitro* is not known. Attempts to bind full-length ABI-1 to full-length UNC-53 protein by yeast two-hybrid were

unsuccessful, but the ability of these contructs to express UNC-53 is not known (Adeleye, 2002). While it is not known if ABI-1 binds other portions of UNC-53, it is apparent that the CH domain of UNC-53 confers some of its function, as shown by the dominant negative effect on posterior ExC outgrowth. *In vitro* pull-down experiments with full-length UNC-53 successfully identified that SEM-5 and UNC-53 bind (Stringham et al., 2002), and could serve as a starting protein to further what is known about the interaction between UNC-53 and ABI-1. An interesting future experiment would be to overexpress the ABI-1(260-427) and to determine the extent to which this region is able to interfere with UNC-53 function *in vivo*. Overexpression of this minimal domain might be expected to abrogate UNC-53 function and to suppress the overexpression phenotype of UNC-53-CH.

2.4.3 ABI-1 functions cell-autonomously with UNC-53 in cellular process outgrowth

We would expect that if the interaction between *unc-53* and *abi-1* is relevant *in vivo* that these proteins would have similar phenotypes and be expressed in some of the same tissues. In this study *abi-1* was observed to be required for the migration of various cellular processes in *C. elegans* that also require *unc-53*. ABI-1 is the only *C. elegans* ABI, and is a member of a family of proteins that regulate WASP and WAVE to play a conserved role in ARP2/3 mediated actin-polymerization (Stradal et al., 2004). In mammals, ABI proteins are highly expressed in the developing brain where they guide nerve cell placement and axon outgrowth (Courtney et al., 2000; Grove et al., 2004). ABI-1 localizes to the motile tips of lamellipodia and filopodia, consistent with a role for ABI-1 in actin polymerization events, and distributes towards actin rich regions in response to upstream signalling including activation by Rac (Echarri et al., 2004; Stradal et al., 2001). *C. elegans* ABI-1 is required for the subcellular enrichment of actin in epidermal cells during morphogenesis through Rac-GTP, the WAVE complex and ARP2/3 (Lundquist, 2006; Patel et al., 2008; Soto et al., 2002). In this work ABI-1 is observed to be needed for the migration of cellular processes in *C. elegans*, including the anteroposterior migrations of the excretory canals, the anterior migration of the PLM neurons and dorsoventral migrations of the ventral cord motor neurons. ABI-1 expression was shown to be required for the outgrowth of the ExC canals but it was not observed to be expressed there during development or in adult animals. It is possible that endogenous levels of ABI-1 are very low or that the sequences required for

expression in these cells were absent in the reporter fusions tested. We believe that the inability to detect ABI-1 expression was due to a technical difficulty. This is likely to be the case because the cell specific expression of ABI-1 was sufficient to rescue the longitudinal migration of the posterior ExC canals, strong evidence that ABI-1 functions cell-autonomously in this migration. Also subsequent work by others has since identified that *abi-1* is ubiquitously expressed in embryos (Hurwitz et al., 2009). The cell-autonomous function of ABI-1 in the excretory cell and its expression in motorneurons where UNC-53 is expressed suggests that these two proteins function together. However, the subcellular localization of ABI-1 and UNC-53 during the migration of posterior ExC canals or migrating axons is not known. Importantly, studies subsequent to this work in mice and zebrafish have shown that vertebrate ABI and the NAVs may function together in migration (Klein et al., 2011; McNeill et al., 2010). One study from the mouse model shows that ABI and mNAV2 are coexpressed during the outgrowth of cerebellar granules which depend on mNAV2 and under the control of *atRA* (McNeill et al., 2010). Future studies in *C. elegans* should be aimed at understanding the extent to which ABI-1 and UNC-53 interact in *C. elegans* at a subcellular level in migrating neurons or the ExC, and could shed light on the nature of the interaction between these two proteins at a subcellular level.

2.4.4 UNC-53 and ABI-1 function in migration in a similar way to WVE-1 and the ARP2/3 complex

Two predominant models of ARP2/3 complex activation requiring ABI-1 have been proposed, one that relies on WAVE and another that relies on WASP (Innocenti et al., 2005). Moreover, experiments in both cell culture and model systems reveal that cell shape changes, and the extension of cellular processes are mediated through GTPases of the Rho family including Cdc42 and Rac, which induce the formation of lamellipodia and filopodia by interacting directly or indirectly with the WASP family of proteins, resulting in the activation of the ARP2/3 complex and directed actin nucleation (Kurisu and Takenawa, 2009; Spiering and Hodgson, 2011; Symons, 1996). In *C. elegans*, loss of WSP-1 or WVE-1 disrupts hypodermal cell migration and ventral enclosure during embryogenesis and axonal migration (Shakir et al., 2008; Withee et al., 2004), phenotypes also characteristic of *ced-10* mutants and ARP2/3 complex knock down (Lundquist, 2003; Lundquist, 2006; Sawa et al., 2003). ABI-1 is a member of a complex consisting of WAVE-1/WVE-1, SRA-1/GEX-2, NAP-1/GEX-3 that regulates membrane

protrusion through actin nucleation (Innocenti et al., 2004; Innocenti et al., 2005; Kurisu and Takenawa, 2009; Patel et al., 2008), and through its SH3 domain to binds to N-WASP to stimulate actin dependent vesicular transport and endocytosis (Innocenti et al., 2005). Thus ABI-1 appears to be a central figure that regulates the proportion of actin filament nucleation designated for particular processes by partitioning WASP versus WAVE activation (Innocenti et al., 2005).

In this study, it is found that *abi-1* and *unc-53* share phenotypes with actin-regulators. *wve-1*, *nck-1,* and *arx-2* function with *abi-1* in other systems and also share defects with *abi-1* and *unc-53* in this study, including the presence of truncated posterior excretory canals and defects in the outgrowth of the PLM axons. Additionally the dorsoventral migration phenotypes for *abi-1* in the motorneurons appear similarly to those of Rac mutants with respect to the formation of disorganized neural networks and ectopic branch formation (Lundquist, 2003). We also found that *unc-53* has a minor role in the ventral migration of the PDE neuron which is known to be under the genetic control of actin regulators but has not yet been examined for *abi-1* (Shakir et al., 2008). *wve-1* is needed for the migration of the PDE downstream of *ced-10*, which is under the control of the Rac-GEF *unc*-73 (Lundquist, 2003; Shakir et al., 2008). Consistent with this view, both UNC-53 and the Rac activator UNC-73 have been implicated in an EGL-17/FGF independent signaling mechanism controlling sex myoblast migration (Chen et al., 1997) and to function together in the outgrowth of the ExC (Marcus-Gueret et al., 2012), suggesting that modulation of the ARP2/3 complex may be the critical determinant of actin filament assembly in this migration as well. Determining further the genetic interactions between *unc-53*, *abi-1*, and *wsp-1, wve-1*, and the *C. elegans* Rac-genes *ced-10* and *mig-2* in the control of the PDE or the ExC could lend support to this work and could also help to place *unc-53* with respect to other actin regulators such as *unc-115* and *unc-34* (Shakir et al., 2008). Interestingly, the first part of the posteriorly directed migration of the excretory canals to the anterior gonad arm was intact for all genes tested, suggesting that another mechanism independent of the ARP2/3 complex may be driving the initial posterior outgrowth of the canals.

The observation that loss of *abi-1* and *unc-53* function disrupts the dorsal outgrowth of motorneuron commissures and the migrations of the PDE suggests these genes may participate together in dorsoventral guidance decisions. A role for the *Navs*

is also apparent in dorsoventral migrations. *mNAV1* is expressed in neurons that migrate along both the longitudinal and dorsoventral axes during rodent development, and rat pontine neuronal explants are unable to respond to the *Netrin-1* guidance cue when *mNAV1* is knocked down by RNAi (Martinez-Lopez et al., 2005). Circumferential guidance of growth cones in *C. elegans* is controlled by multiple guidance cues including UNC-6/Netrin which is expressed ventrally where it attracts UNC-40 expressing growth cones and repels those expressing both UNC-40 and UNC-5 (Wadsworth, 2002). Interestingly, UNC-34/Ena, which controls multiple aspects of cell migration and guidance (Fleming et al., 2010; Norris et al., 2009; Yu et al., 2002) can suppress ectopic UNC-5 expression (Colavita and Culotti, 1998), placing UNC-34 downstream of UNC-5 in circumferential guidance (Colavita and Culotti, 1998). Mammalian Ena function is partially dependent on ABI proteins (Tani et al., 2003), and could suggest a role for ABI-1 in circumferential guidance in worms. Importantly, while *abi-1* and *unc-53* appear to both control dorsoventral migrations, they also control migration along the anteroposterior axis. Because cell migration in the anterior-posterior and dorsal-ventral directions use different guidance cues (Killeen and Sybingco, 2008), this suggests that the mechanisms that control actin polymerization through ABI-1 are likely downstream of multiple migrate ligands.

2.4.5 ABI-1 may function independently of WSP-1 and ABL-1 in longitudinal migration

We found that *wsp-1* and *abl-1* do not share phenotypes with *abi-1*, implying that *abi-1* may function independently of these genes. In some ways it was surprising that *abi-1* functioned independently of *wsp-1* because ABI is a WASP regulator (Innocenti et al., 2005; Stradal et al., 2004). Recent studies in *C. elegans* aimed at uncovering the role of actin-based growth cone guidance in axonal migration reveal genetic redundancy between *wsp-1* and *wve-1* in the ventral migration of the PDE neuron, and that these two APFs are in parallel to *unc-115/ablim* and *unc-34/Ena* (Shakir et al., 2008). It would be interesting to examine a possible role for *wsp-1* in the posterior extension of the ExC canals in the background of *wve-1* loss because it is possible that *wve-1* may be masking a role for *wsp-1* in Exc migration. The observation that ABL-1 is not required for the migration of the excretory canals suggests that ABI-1 may function independently of ABL-1 in the posterior migration of the ExC canals. ABL-1 and ABI-1 physically interact and ABI-1 is required for the ability of ABL-1 to

phosphorylate downstream target effectors including Ena, Mena, and WAVE (Juang and Hoffmann, 1999; Leng et al., 2005; Tani et al., 2003). However, there are also examples of ABL-1 negatively regulating ABI-1 (Hurwitz et al., 2009; Sheffield et al., 2007). Subsequent to this work, Hurwitz *et al.* (2009) determined that *abi-1* is required for cell engulfment independently of known cell engulfment pathways, and that ABL-1 and ABI-1 interact physically, and that ABL-1 functions through ABI-1 to inhibit engulfment and DTC migration (Hurwitz et al., 2009). In both engulfment and DTC migration ABL-1 was only shown to be needed in these processes through its ability to suppress ABI (Hurwitz et al., 2009).

2.4.6 **NCK-1 is expressed in the ExC and has multiple defects in migration**

The adaptor NCK-1 exerts its influence in part through modulation of WVE-1, as NCK-1 and/or RAC activation is able to release SCAR-1 from an inhibitory complex containing ABI-2 to activate the ARP2/3 complex (Ibarra et al., 2005). We observed that *nck-1* was required for longitudinal migration of both the PLM axon and the ExC canals, and that NCK-1 was expressed in the ExC No attempt to establish a physical interaction between UNC-53 and NCK-1 was conducted in this study, though it is of potential interest that NCK-1 is an SH2-SH3 domain containing protein and that UNC-53 contains multiple SH3 binding domains. Additionally, the *Drosophila* homolog *Sickie* was observed to bind the fly NCK-1 homolog *Dock in vitro* (Giot et al., 2003).

In addition to the observed longitudinal migration defects of *nck-1*, *nck-1* mutants were found to have a midline guidance defect in the ExC, characterized by ExC canals that meander along the midline during their migration. Recent evidence has shown that the same allele used in this study *nck-1 (ok694)* is required for midline guidance of the HSN axons in a pathway that is parallel to *unc-40* (Mohamed and Chin-Sang, 2011), and a possible explanation is that *nck-1* functions with the *Eph/vab-1,* which is needed to prevent migration overextension (Mohamed et al., 2012). Future experiments are needed to understand the varied *nck-1* phenotypes observed here and their potential relationship to *unc-53*.

2.4.7 **ABI-1 and MIG-10A interact and function cell-autonomously in the excretory canal outgrowth**

ABI-1 was identified as a yeast two-hybrid interactor of the *C. elegans* MRL family protein MIG-10/Lpd (McShea et al., 2012), a multidomain protein required for actin polymerization that exhibits interactions with Ena, Rac and PIP_2 (Adler et al., 2006; Chang et al., 2006; Quinn et al., 2006). *mig-10* is required for many cell migrations in *C. elegans* including those of the HSN neurons, the mechanosensory neurons, and the longitudinal migration of the excretory canals (Manser and Wood, 1990). ABI-1 binds MIG-10 through an interaction that appears to be mediated by the N-terminus of ABI-1 as well as the SH3 domain of ABI-1, an observation that was corroborated by a coIP experiment in *Drosophila S2* cells (McShea et al. 2012). Importantly, MIG-10a functions cell-autonomously in the longitudinal migration of the posterior canals similarly to what is observed in *unc-53* and *abi-1* mutant and RNAi animals (McShea et al, 2012) (Dr. E. Ryder, personal communication). Only a few proteins have so far been shown to function cell-autonomously in the longitudinal migration of the ExC canals, including UNC-73, UNC-71, UNC-53, ABI-1 and now MIG-10. The observation that ABI-1 functions cell autonomously in the ExC and interacts with two proteins that are required in the longitudinal migration of the excretory canals (MIG-10 and UNC-53) is strong evidence that *abi-1* plays an important role in the development of this cell. Moreover, the observation that UNC-53 and MIG-10 both promote outgrowth (Chang et al., 2006; Stringham et al., 2002) and interact with ABI-1 suggests that ABI-1 could be central to driving the extension of cellular processes. *mig-10* functions to polarize cells for outgrowth during guided migrations (Chang et al., 2006; Fleming et al., 2010; Quinn et al., 2006). The observation that MIG-10A interacts with ABI-1, a protein so critical to the establishment of actin polymerization during outgrowth, provides a link between the asymmetric localization of MIG-10 response cues and its outgrowth promoting activity. How MIG-10 and ABI-1 might regulate each other to promote outgrowth is not known. It is possible that the asymmetric localization of MIG-10 preceeds the localization of ABI-1 and the polymerization of actin.

An interaction between ABI-1 and MIG-10 also places ABI-1 within the context of known signalling cues and Rac activation. *mig-10* functions in dorsoventral guidance through the well-studied guidance cues *slt-1* and *unc-6* (Quinn et al., 2006). In addition,

MIG-10 requires the WAVE effector CED-10 (Quinn et al., 2008), which polarizes MIG-10 and the actin cytoskeleton in response to guidance cues (Quinn and Wadsworth, 2008). Elimination of *ced-10, slt-1,* and *unc-6* eliminates MIG-10 polarization and the polarity of the actin cytoskeleton. Genetic manipulation of the *unc-6, unc-5* and *unc-40* pathway was also shown to alter F-actin accumulation as well as axonal protrusion in *C. elegans* (Norris and Lundquist, 2011), so it follows that ABI-1 could be downstream of one of these guidance cues in cell polarization and outgrowth. While the conserved dorsoventral guidance cues *unc-6* and *slt-1* play a role in longitudinal migration, other possibilities also exist. Conserved guidance cues controlling the longitudinal axis are more elusive, due possibly to genetic redundancy (Killeen and Sybingco, 2008). One relevant set of guidance molecules along the longitudinal axis are the secreted Wnts which control migration through Fz receptors (Pan et al., 2006). Fleming *et al.* (2010) investigated the signals controlling polarization of the ALM neurons and found that *mig-10* controls polarity along the anteroposterior axis, and that *mig-10; cwn-1* have a synthetic effect on polarization along the longitudinal axis (Fleming et al., 2010). Is a Wnt cue controlling longitudinal migration of the ExC through *abi-1* and *mig-10*? Does *unc-53* function alongside *mig-10* and *abi-1* in longitudinal migration? While the genetic interaction between *unc-53* and *mig-10* is not known, it is possible that there is a division of function between these genes. *unc-53* mostly controls AP migrations while MIG-10 functions in both anteroposterior and dorsoventral guidance. It is possible that ABI-1 and UNC-53 function together in anteroposterior guidance while MIG-10 and ABI-1 function together in guidance along the anteroposterior and dorsoventral axes. The observation that *abi-1* genetic loss results in phenotypes that are not shared between UNC-53 and ABI-1 suggests an additional role for ABI-1 independently of *unc-53*, possibly in cooperation with MIG-10. Additional genetic studies are needed to answer these questions.

2.4.8 **UNC-53 and ABI-1 are required for endocytosis**

Studies aimed at identifying the expression pattern of UNC-53 and ABI-1 revealed persistent expression of ABI-1 and UNC-53 in adult animals, suggesting that these proteins may work together following the completion of development. In particular, the expression of ABI-1 and UNC-53 in endocytic coelomocytes was intriguing. Consistent with a potential role for these proteins in endocytosis *unc-53* functions in both coelomocyte uptake and yolk-protein uptake while *abi-1* functions in oocyte uptake as

has been observed previously (Giuliani et al., 2009). The expression of ABI-1 in coelomocytes would suggest that they function within this cell in endocytosis also. We expect that the lack of a CUP phenotype in *abi-1 (rnai)* or *abi-1 (tm494)* animals may be due to the fact that these genetic treatments are too weak. Future studies using stronger alleles, or null alleles of *abi-1* could solve this problem. *C. elegans* ABI-1 has been identified to associate with the F-Bar domain containing protein TOCA-1 in oocyte uptake in *C. elegans* (Giuliani et al., 2009) and both *unc-53* and *abi-1* were identified in an RNAi screen for yolk-uptake by RNAi that identified numerous polarity proteins (Balklava et al., 2007). The role of *unc-53* and *abi-1* in endocytosis is not known, though an association between *abi-1* and *toca-1/2* suggests a link between actin polymerization and the bending of membranes.

Given the role of *unc-53* and *abi-1* in endocytosis, it is also possible that *unc-53* and *abi-1* function together in migration through an endocytic process. Guidance receptors are delivered to the cell surface through intracellular trafficking and genes that control trafficking affect cell migration. A particularly powerful example of the importance of receptor trafficking comes from *C. elegans*. Watari-Goshima *et al.* (2007) and Levy-Strumpf *et al.* (2007) describe how the *C. elegans* kinesin-like motor protein VAB-8L controls the localization of receptors (Levy-Strumpf and Culotti, 2007; Watari-Goshima et al., 2007). It appears that VAB-8L targets the *C. elegans Robo* homolog SAX-3 and UNC-40, which bind the worm guidance cues SLIT-1 and UNC-6 respectively, to cell membranes in a pathway involving the Rac-GEF UNC-73/TRIO and MIG-2/RHO. While *unc-53* has recently been shown to function independently of *vab-8* in the migration of the excretory cells, there is evidence to suggest that *unc-53* antagonizes *vab-8* in some cells (Wolf et al., 1998; Wolf, 1998) (Dr. G. Garriga, personal communication). One model is that that *unc-53* antagonizes *vab-8* by promoting receptor removal from membranes through an endocytic process while *vab-8* trafficks receptors to the membrane.

2.4.9 **A model for UNC-53 and ABI-1 in the outgrowth of cellular processes**

Previously, it was shown that UNC-53 interacts physically with SEM-5 (Stringham et al, 2002), a SH2SH3 adapter involved in multiple RTK pathways including the FGF/FGFR (Burdine et al., 1997; Fleming et al., 2005). At present, it is unclear whether UNC-53 is a participant in one or several signaling cascades. For example, while both

unc-53 and *egl-15* are expressed in the migrating sex myoblasts (Goodman et al., 2003; Stringham et al., 2002) *egl-15* is not expressed in axons where it regulates outgrowth but instead it exerts its effect through the underlying hypodermis on which they migrate (Bulow et al., 2004). As UNC-53 is a cytoplasmic protein that functions cell autonomously, this suggests that it does not act directly downstream of EGL-15 signaling in neuronal cell migrations, but may be recruited by a different receptor upstream of SEM-5. Moreover, UNC-53, the cell adhesion molecule UNC-71 and UNC-73, have all been implicated in a EGL-17/FGF independent signaling mechanism controlling sex myoblast migrations (Chen et al., 1997), suggesting non-FGFR signaling is involved in this pathway as well. Therefore the identity of ligands and receptors upstream of the SEM-5/UNC-53 interaction in cell migration remain elusive.

In this study, a restricted region of the N-terminus of UNC-53 containing a CH domain was sufficient to bind ABI-1 *in vitro*, and the UNC-53-ABI-1 interaction mediated by this domain was required for longitudinal cell outgrowth *in vivo*. CH domains are commonly found in proteins involved in signal transduction and actin binding and are classified by the number and position of CH domains they contain. Type 1/2 CH domains are found in proteins such as α–actinin, B-spectrin, and dystrophin which function in actin-bundling and membrane anchoring (Broderick and Winder, 2005) and contain two N-Terminal CH domains in tandem. The first Type 1 CH domain mediates actin-binding while the second Type 2 CH domain may either (i) stabilize the actin interaction of the Type I domain, (ii) localize the actin binding protein to the cytoskeleton, or (iii) act as a scaffold for signal transduction (Gimona and Mital, 1998; Gimona et al., 2002). In contrast, UNC-53 possesses a single N-terminal CH domain, and in this respect is more closely related to Type 3 CH domain containing proteins such as Vav, IQGAP, alphaPix, and SM22 (Gimona et al., 2002; Stradal et al., 1998). Type 3 CH domains function like Type 2 CH domains in that they act as scaffolds that bind proteins involved in the control of cytoskeletal change and signal transduction (Galkin et al., 2006; Gimona et al., 2002; Korenbaum and Rivero, 2002; Leinweber et al., 1999). In such a model, UNC-53 may be a scaffold that coordinates upstream signals transduced through SEM-5 or other unknown adaptors and the actin cytoskeleton (Figure 29).

A growing body of literature has implicated UNC-53 homolog NAVs as plus end microtubule binding proteins (Martinez-Lopez et al., 2005; van Haren et al., 2009).

+TIPs influence microtubule dynamics and link microtubules to other cellular structures such as actin, cortically-bound factors, and intracellular membranes (Akhmanova and Steinmetz, 2010; McNeill et al., 2010). Overexpression of NAV proteins in non-neuronal cells is able to induce neurite outgrowth (van Haren et al., 2009). It is not known to what extent the NAVs stabilize MTs or simply cause the outgrowth of membranes followed by MT stabilization. The AAA domain is needed for ectopic neurite outgrowth (van Haren et al., 2009), and these domains are known to induce conformational changes in substrate proteins (Hanson and Whiteheart, 2005). While future studies are needed to determine the extent that UNC-53 controls microtubule and actin dynamics, it is clear that UNC-53 has a role at the leading edge of cells with ABI-1. As mentioned, a recent study in mice shows mNAV2 and ABI1 coexpressed during outgrowth in cerebellar cells (McNeill et al., 2010). Of particular interest from the perspective of ABI-1 and UNC-53 was a more recent study examining the role of *Nav3* in hepatoblast migration in the vertebrate zebrafish model (Klein et al., 2011). Klein *et al.* (2011) show that a novel isoform of vertebrate *Nav3a* is required for liver organogenesis under the control of Wnt2b signalling and that in the absence of *Nav3a*, liver bud hepatoblasts failed to migrate while overexpression of *Nav3a* results in ectopic hepatocyte budding. Defects in *Nav3a* morphants were the result of a lack of actin-assembly in lamellipodia and filipodia during development, and NAV3a and ABI-1 were found to redistribute and colocalize to actin-rich leading edges in response to Cdc42 activation in migrating cells (Klein et al., 2011). Given evidence from a range of organisms including *C. elegans*, it is proposed that UNC-53 and the NAVs are +TIP proteins that mediate the outgrowth of cellular processes through the control of actin with ABI-1 (Figure 29).

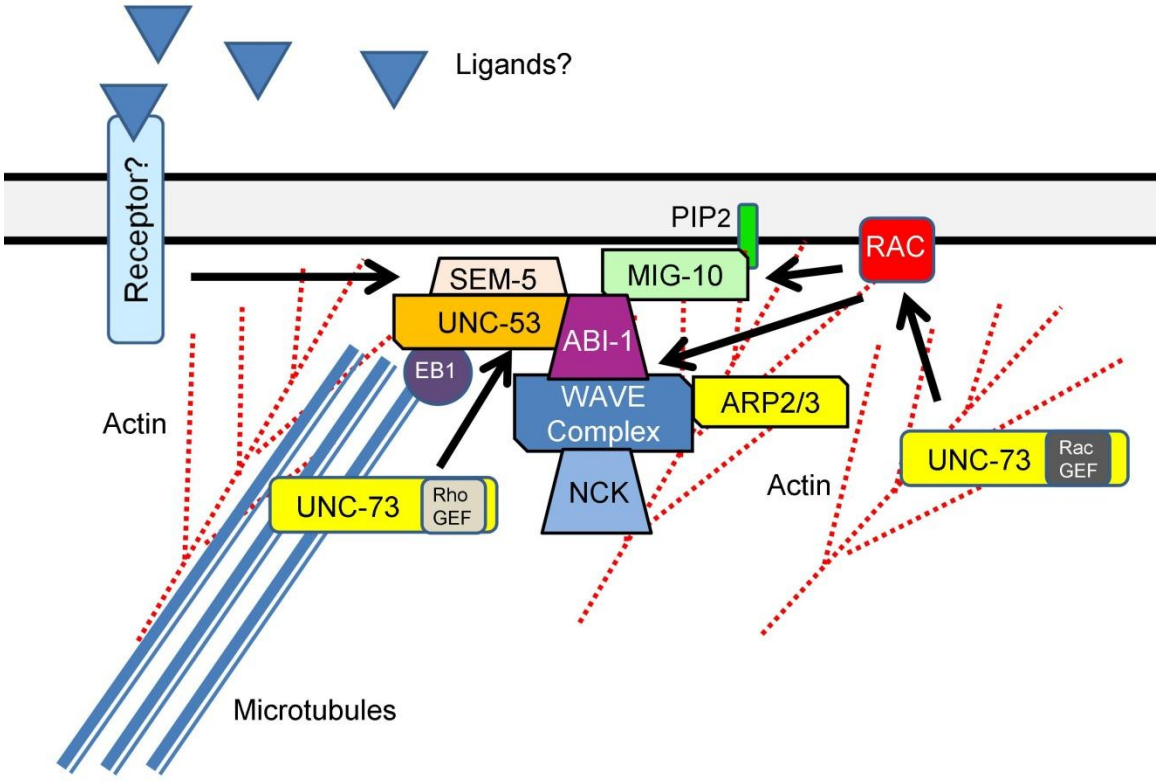

Figure 29. Model of UNC-53-ABI-1-MIG-10 function in outgrowth.

UNC-53 is +TIP protein (shown binding EB1) that also binds ABI-1, a regulator of actin filament assembly through the WAVE complex (GEXs not shown for simplicity) and ARP2/3 complex (not shown). UNC-53/NAV2 may function to link branched actin filament assembly in protrusions at the leading edge of migrating cells to the plus ends of microtubules. SEM-5 is an interactor of UNC-53 but the upstream receptor linking UNC-53 and SEM-5 is not known. ABI-1 also binds to MIG-10 which interacts with PIP_2 and Rac. UNC-73 is also known to function with UNC-53 through a RhoGEF domain (Marcus-Gueret et al., 2012) while UNC-73 also possesses a Rac-GEF domain that can interact with Rac.

2.5 Materials and Methods

2.5.1 *C. elegans* strains

C. elegans Bristol (N2) and mutant strains were maintained at 20-25ºC depending on the strain used and according to standard protocols (Brenner, 1974;

Stiernagle, 2006). Double mutant strains and strains containing transgenic reporters were constructed using standard techniques and were verified by the presence of individual phenotypes, the presence of the expected transgenic marker, or by PCR confirmation. *unc-53(n166)* mutants were placed over the *mnDf87* deficiency strain to test if the *n166* allele is null for the excretory canal phenotype. The deletion within the *mnDf87/mnC1 dpy-10(e128) unc-52(e444)* rearrangement lies on chromosome II and includes the region of *unc-53*. *+/ mIn1* males were first crossed to *mnDf87/dpy-10* balanced hermaphrodites. *mnDf87*/*mIn1* males were selected by the presence of pharyngeal GFP and crossed to homozygous *ppgp-12::gfp; unc-53(n166)* hermaphrodites. Non-*mIn1* hermaphrodites of the genotype *+/ppgp-12::gfp; unc-53(n166)/mnDf87* were selected by the presence of excretory canal GFP and the *egl* phenotype. These hermaphrodites were allowed to self-fertilize, and finally F_3 progeny hermaphrodites displaying *ppgp-12*::GFP expression, and *egl* phenotype were selected and assayed for excretory canal defects. Other strains used in this study include:

BC06288 *ppgp12::gfp (sIs10089)* (Zhao et al., 2005);
ZB171 *pmec-4::gfp (bzIs7)*;
BC12924 *pnck-1::gfp (sIs12798* [*dpy-5(e907*)/*dpy-5(e907)*; sEx12728 [rCesZK470.5::GFP + pCeh361]*)*;
BC14371 *punc-53L::gfp (sEx14371* [*dpy-5(e907)*/*dpy-5(e907)*; sEx14371 [rCesF45E10.1a::GFP + pCeh361]*)* { F45E10.1A – AGTATCCCATTTTGGCTTATTTACG; F45E10.1A*- AAAAATGCGGGGATGAGAC; F45E10.1B- AGTCGACCTGCAGGCATGCAAGCTCACCAACATTTCGTTCGATG};
BC10129 *pabi-1::gfp (sEx10129* [*dpy-5(e907)*/*dpy-5(e907)*; sEx14371 [rCesB0336.6::GFP + pCeh361]*)*;
VA97 *pabi-1::abi-1::gfp (pmEx97* [pabi-1::abi-1(1-1410)::GFP + pRF4]*)*;
VA71 *unc-53(n166); sIs10089*;
VA106 *unc-53(n152); sIs10089*;
VA72 *unc-53(n166); bzIs7*;
FX494 *abi-1(tm494)* (684bp deletion III: 5690340...5691023), outcrossed >5x;
VA74 *abi-1(tm494); sIs10089*;
VA99 *abl-1(ok171); sIs10089*;
VA100 *wsp-1(gm324); sIs10089*;
VA75 *abi-1(tm494); bzIs7*;
VA76 *nck-1(ok694)*; *sIs10089* [*nck-1(ok694)* contains a 1814bp deletion X: 4150378...4152191, outcrossed >5x];
VA77 *nck-1(ok694); bzIs7*;
VA79 *unc-53(n166); abi-1(tm494); sIs10089*;
VA91-VA92 *abi-1(tm494)*; *sIs10089*; *pmEx91-92* [ppgp12::abi-1(1-1410) + pDPY-30::NLS::DSRED2 (Cordes et al., 2006)];
VA93-VA96 *sIs10089; pmEx93-96* [ppgp12::unc-53(1-416)::GFP + pDPY-30::NLS::DSRED2 (Cordes et al., 2006)];
VA103-VA104 *unc-53(n152); sIs10089; pmEx103-104* [ppgp12::unc-53(F45E10.1a) +

pDPY-30::NLS::DSRED2 (Cordes et al., 2006)];
VH715 *nre-1(hd20); lin-15b(hd126); hdIs17; hdIs10*;
VA78 *eri-1(mg366); bzIs7*;
GS192 *arIs37* [pmyo-3::ssGFP] (Fares and Greenwald, 2001)
VA442 *unc-53 (n152); arIs37*
VA443 *unc-53 (n166); arIs37*
VA444 *unc-53 (e2432); arIs37*
VA445 *cup-4 (ar494); arIs37*
VA446 *abi-1 (tm494); arIs37*
DH1033 *sqt-1 (sc103); bIs1* [vit-2::gfp + *rol-6 (su1006)*]
VA447 *unc-53 (n152); bIs1*
LE309 *lqIs2* [osm-6::gfp]
VA448 *unc-53 (n152); lqIs2* [osm-6::gfp]

2.5.2 **Yeast two-hybrid experiments**

A *Nde*I-*Nco*I fragment of the *unc-53* cDNA (corresponding to amino acids 1 to 139 of *unc-53*) was subcloned into pAS2 (Matchmaker, Clontech Laboratories Inc.) to generate pVA200 (Adeleye, 2002). Using pVA200 as bait and a mixed stage *C. elegans* cDNA library as prey (gift of Bob Barstead, USA) candidate binding partners were identified in a yeast two-hybrid screen by assaying for growth on triple drop-out media (-Trp-Leu-His) and B-galactosidase activity of doubly transformed yeast Y190 cells as described (Adeleye, 2002; Aspenstrom, 2005). Six of the positives corresponded to the B0336.6/*abi-1* locus. pVA305 corresponds to the shortest *abi-1* cDNA isolated in the screen cloned into the pSE1107 vector and codes for amino acids 16 to 427 of ABI-1 and was used for GST pulldown. Yeast two-hybrid mapping between UNC-53N and MIG-10a with ABI-1 were performed as follows. Full-length ABI-1 and ABI-1 deletion constructs were generated by PCR cloning ABI-1 from sequenced template cDNA (gift of Yuji Kohara) (Hurwitz et al., 2009) using sequence specific primers engineered along with XhoI restriction sites to clone into the XhoI site of pACTII. The correct identity and orientation of the clones was determined by a combination of restriction analysis and PCR. Correct identity and frame usage was confirmed by sequencing (Macrogen). Bait and prey plasmids were sequentially transformed into PJ69-4A (James et al., 1996) using a LiAc/SSDNA/Peg based plasmid transformation protocol (Gietz and Schiestl, 2007). To perform the transformation, a generous loopful of yeast cells was transferred to a microcentrifuge tube along with 500µl of PLATE solution (40% PEG3350 (w/v), 100 mM lithium acetate (LiAc), 10 mM Tris, pH 7.5, 0.4 mM EDTA), 10µl of single-stranded sonicated salmon sperm DNA (10mg/ml) and 1-2µg of the plasmid to be transformed, and were left at room temperature for 24-48hrs. Cells were then centrifuged at 16,000g

for 30 seconds, the supernatant was removed, and the cells were resuspended in 200µl of sterile water followed by plating on selective media. Positive interactions were identified by streaking individual doubly transformed colonies onto quadruple dropout media (-Trp-Leu-His-Ade) (Sunrise Yeast Source) in the presence of 25mM 3AT for yeast containing ABI-1 and UNC-53 plasmids, or 100mM 3AT for those yeast containing ABI-1 and MIG-10A plasmids. Interactions were also corroborated dropping 5µl volumes of doubly transformed liquid cultures onto selective plates. Experiments were performed in duplicate.

2.5.3 *In vitro* binding assays

ABI-1::GST and UNC-53N::6XHIS protein were purified from *E. coli* BL21(DE3) harboring pVA600 and pVA63 respectively. pVA63 was generated previously (Adeleye, 2002) and pVA600 was made by subcloning a 1.3kb XhoI fragment from pVA305 (see Section 2.5.2) into pGEX4T2 (Invitrogen) followed by sequencing (UBC Sequencing Service). UNC-53-6XHIS was expressed and purified under denaturing conditions and using a Ni^{+2} based ProBond column according to manufacturer's protocols (Amersham Pharmacia) (Adeleye, 2002). Recombinant proteins ABI-1::GST or GST were expressed and purified according to manufacturer's instructions (Invitrogen) with modifications (Frangioni and Neel, 1993). To express ABI-1-GST and GST, overnight cultures were grown for a maximum of 15hrs in LB-AMP (75µg/ml). The following day, 1:100 dilutions were produced in LB-AMP media, followed by growth at 37ºC shaking at 200rpm to bring the culture to mid-log growth (OD 0.4-0.5). IPTG was added to a final concentration of 1mM and cultures were grown for 3hrs at 37ºC at 200rpm. GST containing cells were purified according to manufacturer's instructions (Invitrogen) and were dialyzed in GST binding buffer along with the use of a protease inhibitor cocktail (Roche #11836153001). ABI-1-GST containing cells were centrifuged (6,000rpm, 4ºC), washed one time in 1xPBS and were resuspended in 1xPBS with a protease inhibitor cocktail. Samples were sonicated on ice along with 1% N-lauryl sarcosine followed by dialysis in GST binding buffer. Protein concentrations were determined using Bradford Assays and Microassays (BioRad). 10µg of ABI-1::GST or GST were applied to glutathione resin for pulldown experiments. 25µg of total UNC-53N::6XHis lysates were applied to ABI-1::GST or GST glutathione resin and incubated at 4°C for 3hr. Following incubation, beads were washed four times with 20mM Tris pH 7.4, 0.1mM EDTA, 300mM NaCl and 0.1% Triton X-100. Bound proteins were extracted according to

manufacturer's instructions and were analyzed by SDS-PAGE and Western blotting (1:10,000 primary PAB-UNC-53N).

2.5.4 **RNA interference and mutant analysis**

RNAi experiments were performed by feeding essentially as described (Kamath et al., 2001) using RNAi clones obtained from Geneservice Ltd. with the exception of the *unc-53L* RNAi clone pVA504, generated by cloning a 0.3 kb *Xho*I-*Nco*I PCR fragment corresponding to nucleotides 1 to 280 (exons 1-4) of the *unc-53* cDNA from pTB113 in tandem into pPD129.36. RNAi clone identity was confirmed by its similarity to loss of function mutants, restriction analysis, and PCR size confirmation. RNAi experiments were typically scored using F_2 animals whose parents had fed on dsRNA containing bacteria for at least 24hrs. RNAi feeding experiments were performed as follows. A colony from each desired bacterial strain was grown for 12 hours in 5 ml LB AMP (50µg/ml) at 37ºC, 200 rpm. Cultures were concentrated 5-fold by centrifugation and removing a portion of the supernatant. These cultures were then seeded to NGM IPTG/carbenicillin plates which were allowed to induce overnight at room temperature. The following day, 1-3 young adult hermaphrodites were transferred onto each P_o plate of the appropriate strain and left for 24 hours at room temperature for the adults to lay. F_1 progeny were transferred onto freshly seeded plates 24 hours later, and scanned for visible phenotypes. F_1 worms were allowed to lay and L3-L4 progeny were transferred to freshly seeded plates every 24 hours. The F_2 generation was scored at the L4 to young adult stage. Each experiment was repeated three times to confirm phenotypic results.

Animals carrying the *ppgp-12::gfp* reporter were scored for excretory canal outgrowth with respect to the position of the gonad arms, the vulva and the anus. Chi-squared analysis was used to establish statistical significance between mutants using Graphpad Prism 5 unless stated otherwise. In cases where single mutants were compared to wild-type N2 animals, posterior canal extension was scored as described, and statistical comparisons were made between groups by comparing the number of animals exhibiting normal canal extension (scored as 3) and reduced canal extension (scored <3). In cases where double null mutant alleles were examined, the worse of the two null alleles was set as the baseline for comparison. Additional excretory cell morphology defects are described in the Results and statistical comparisons were made

between the number of animals exhibiting a defect in mutant or RNAi treated animals compared to wild-type using Chi-squared analysis (Graphpad Prism 5).

Neuronal RNAi was carried out using either the RNAi enhanced strain *eri-1(mg366); pmec-4::gfp* for mechanosensory neurons (Kennedy et al., 2004), or *nre-1(hd20); lin15b(hd126)* for motorneurons. The anterior process of the PLM neuron was scored as abnormal if the stop point was posterior to the wild-type position at the mid-body. Ventral cord motorneuron commissures were determined to have defects if two or more axons exhibited ectopic lateral branching or stalling and were unable to reach the dorsal cord. The PDE axons were visualized with a *posm-6::gfp* (LE309) strain (Struckhoff and Lundquist, 2003) as previously described (Shakir et al., 2008). PDE axons were considered to have defective guidance if the axon failed to reach the ventral nerve cord or approached the ventral cord at angles greater than 30 degrees. Percentages of defective PDE axon guidance in each strain were determined. Statistical analysis of neuronal migration defects was achieved by comparing mutant and RNAi treated animals to controls by Chi-squared analysis with a significance value of $P<0.05$.

2.5.5 Preparation of UNC-53 and ABI-1 polyclonal antisera

unc-53 cDNA that corresponding to amino acids 1 to 139 was subcloned into the expression vector pRSET (Amersham Pharmacia) to generate pVA63 (Adeleye, 2002), expressed in *E. coli* BL21 cells according to manufacturer's protocols (Invitrogen). Purified protein was emulsified in Titre Max^{TM} Gold and injected into a female New Zealand white rabbit (SFU Animal Care Facility). The antisera collected was active at titers of 1:30,000 on western blots of recombinant fusion protein. The specificity of *PAb-UNC-53N* was confirmed by staining animals that ectopically express UNC-53 in the intestine under control of the *hsp-16* promoter (Stringham et al., 1992). Whereas no staining was observed in control animals, strong staining in the cytoplasm of intestinal cells was observed after heat shock (Adeleye, 2002). For the generation of ABI-1 polyclonal antibody (*PAb-ABI-1*), a synthesized peptide (DYNSIYQPDRYGTIRAGGR) containing amino acids 256 to 274 from ABI-1 was coupled to keyhole limpet (KLH) and used to immunize guinea pigs. Anti-sera was affinity purified towards the ABI-1 peptide (Open Biosystems Inc) and was active at 1:10,000 on Western blots of recombinant protein (show blot in appendix).

2.5.6 **Expression pattern of UNC-53L and ABI-1**

To detect UNC-53 *in vivo* by immunostaining, embryos, staged larvae and adults were fixed and permeabilized using freeze-cracking and the methods of Ruvkun and Finney (Bettinger et al., 1996; Duerr, 2006). Nematodes were harvested using 0.14 M NaCl or M9 Buffer, washed several times, and were hypochlorite treated to obtain eggs. The freeze-crack method was used to permeabilize eggs while the Ruvkun fixation method was used to permeabilize whole animals. UNC-53 was detected using PAB-UNC-53N. Fixed specimens were incubated overnight (4°C) in primary antibody solution (AbA [1X PBS, 1% bovine serum albumin, 0.5% Triton, 0.05% sodium azide, 1 mM EDTA]) (1:100 dilution of PAB-UNC-53N), washed in AbB buffer (AbA + 0.1% BSA) with several changes of the buffer over a 15 minutes period and incubated overnight (4°C) with the secondary antibody solution (1:30 dilution of Cy3-conjugated sheep anti-rabbit; Sigma). The nematodes were washed again in AbB buffer, mounted in a commercially available mounting medium (Vectashield, Vector Laboratories) and viewed with a Zeiss compound microscope with rhodamine filters. GFP was viewed with a Leica compound microscope with GFP filters. PAB-ABI-1 antibody was used at 1:100 with secondary anti-Rabbit IgG (Invitrogen Molecular Probes) and anti-Guinea Pig IgG (Open Biosystems Inc.) used at 1:500 and 1:400 respectively. Detection of ABI-1 expression in transgenic lines carrying *pabi-1::abi-1::gfp* was performed using anti-GFP immunostaining with a chick anti-GFP primary at 1:100 with secondary rabbit anti-Chick IgG at 1:400 (Millipore, USA). Several *pabi-1::abi-1::gfp* strains carrying extrachromosomal arrays generated by co-injecting 1ng/µl of the *pabi-1::abi-1::gfp* containing 0.5kb upstream of *abi-1* and the entire *abi-1* locus fused to GFP with the pRF4 coinjection marker at 100ng/µl and showed expression similar to using PAB-ABI-1. Expression of *abi-1* and *unc-53* were also determined using promoter GFP transcriptional fusions. *pabi-1::gfp* fusion (BC10129) included 275bp upstream of *abi-1* fused to GFP while 2.9kb upstream of *unc-53* was fused to GFP to generate BC14371 (McKay et al., 2003). Specimens were viewed with an Olympus IX81 or Leica DMLB fluorescence microscopes using appropriate filter sets.

2.5.7 **Cell autonomy and overexpression experiments**

Rescue of the *abi-1(tm494)* posterior canal defects was achieved by co-injecting 10ng/µl of the PCR fusion *ppgp12::abi-1* containing the *pgp-12* promoter (Zhao et al.,

2005) fused to full length *abi-1* with 100ng/µl of the plasmid pDPY-30::NLS::DSRED2 (Cordes et al., 2006) into the strain VA74 to create *vaEx91* and *vaEx92*. *unc-53(n152)* posterior canal defects were rescued by coinjecting the PCR fusion *ppgp12::unc-53L* (100ng) with pDPY-30::NLS::DSRED2 into *unc-53 (n152)/mIn1* animals followed by scoring transgenic *unc-53(n152)* animals as described. UNC-53CH expressing arrays *vaEx93-vaEx96* were generated by coinjecting *ppgp-12::unc-53CH::gfp* containing the *pgp-12* promoter fused to the first 422 nucleotides of unc-53 cDNA from pVA63 and GFP at 100ng/µl along with 100ng/µl of the plasmid pDPY-30::NLS::DSRED2 (Cordes et al., 2006) into the strain BC06288. Excretory canal morphology was scored in young adult animals coexpressing GFP and dsRED from all lines for general defects and for posterior canal migration position as described above. Cell autonomous rescue of the ExC defects in *mig-10* mutants was performed by first cloning *Hin*dIII/*Pst*I PCR amplified genomic fragment containing the *ppgp-12* promoter to the GFP-coding cassette pPD95.77 to create pVA700. This was subsequently used in experiments expressing *mig-10a* and *mig-10b* cell autonomously in the excretory cell by cloning the PCR-amplified coding sequence for either *mig-10a* or *mig-10b* into the pVA700 vector using the KpnI and PstI sites (McShea et al., 2012) (Dr. E.Ryder, personal communication).

2.5.8 Coelomocyte and yolk-uptake experiments measuring endocytosis

Coelomocyte uptake was measured by observing adult young wild-type, mutant and RNAi treated animals carrying the transgenic coelomocyte uptake reporter *arIs37* (see Section 2.5.1). RNAi treatment was performed as described (see Section 2.5.4) and mutant animals and RNAi treated animals were assessed for CUP defects by comparing the GFP accumulation pattern to *cup-4 (ar494)* positive controls, focussing specifically on the amount of GFP in the pseudocoelom. Worms were quantified using a Leica DMLB fluorescence dissecting microscope and the data was expressed as the percentage of worms with a CUP phenotype. Worms were mounted on 2% agarose pads and anesthetized with 20mM sodium azide for imaging, captured using an Olympus IX2 with InVivo software. Measures of yolk-uptake were performed as described (Grant and Hirsh, 1999) with the strain DH1033 (see Section 2.5.1) using synchronized animals and assaying for GFP accumulation in the pseudocoelom. Animals were imaged by mounting on 2% agarose pads in 20mM sodium azide, and using an Olympus IX2 with Metamorph software. All image acquisition settings were identical between strains. Statistical significance for both the CUP assay and yolk-

uptake assay was established by comparing treatment and control groups using a two-tailed Pearson Chi-squared analysis (http://in-silico.net/statistics/chi2test/2x2).

2.6 Acknowledgements

I would like to thank L. Ramsay, E. Kreiter, W. Bronec, T. Martens and S. Grainger for technical assistance; the *Caenorhabitis* Genetics Centre, Dr. M. Driscoll, Dr. S. Mitani and Dr. H. Hutter for nematode strains; Dr. B Barstead for the *C. elegans* yeast two-hybrid library. I am grateful to Dr. N. Hawkins, Dr. *C.* Beh, Dr. N. Harden, Dr. M. Soto, and Dr. M. Hurwitz for helpful discussions.

3: THE NEURON NAVIGATOR HOMOLOG UNC-53/NAV-2 FUNCTIONS IN INNATE IMMUNITY

3.1 Abstract

Innate immunity in *Caenorhabditis elegans* depends on several conserved and independent signalling pathways, including the PMK-1, DBL-1-TGF-B and insulin-like DAF-2-DAF-16 pathways. Here the cell migration molecule UNC-53/NAV2, a cytoskeletal binding protein that controls cell migration, is shown to have a novel post-developmental role in *C. elegans* innate immunity. *unc-53* mutant animals are highly susceptible to *Pseudomonas aeruginosa* PA14, a phenotype that is at least partially independent of its role in development. *unc-53* expression persists in a range of adult tissues, including the intestine and neurons, two tissues crucial to immune function. Measures of Aldicarb sensitivity reveal that *unc-53* mutants have defective synaptic transmission. RNA levels of the neuronally secreted DAF-2 agonist *ins-7* are increased in *unc-53* mutants, suggesting that *unc-53* may partially exert its effect through the regulation of immune effectors. Consistent with a role for *unc-53* in insulin-like signalling, *unc-53* animals have decreased nuclear DAF-16 following recovery from heat-stress. A strong loss of function allele of *daf-2* and a null allele of *ins-7* only partially suppress *unc-53*, suggesting a *daf-16* independent function for *unc-53.* Additionally, a *pmk-1* null mutant does not exacerbate *unc-53*, consistent with a potential insulin-independent function for *unc-53* in innate immunity through a PMK-1 pathway. This data together with an analysis of the relevant tissues requiring *unc-53* suggests that multiple isoforms, tissues, and genetic pathways could be needed for *unc-53* function in innate immunity

3.2 Introduction

3.1 Innate Immunity

Given that metazoans encounter thousands of pathogenic threats throughout their lifetime, defense responses represent some of the most sophisticated, ancient and evolutionarily conserved biological processes in existence. Immunity is generally

categorized as either ‘cell-mediated’, found exclusively in vertebrates, or ‘innate’, which is conserved in both vertebrates and invertebrates (Hoebe et al., 2004). Cell-mediated immunity relies on the extensive production of a diverse repertoire of host-defense proteins (e.g. antibodies), formed through somatic recombination, in addition to an array of multiple cell and tissue responses, culminating in the specific detection of pathogens and the subsequent development of antigenic memory. While highly-specific, cell-mediated immunity is slower-acting, requires threat detection, and depends on a cell-mediated immune education. Innate immunity, by contrast, is immediate in its onset, through comparatively non-specific (Gravato-Nobre and Hodgkin, 2005; Hoebe et al., 2004). Innate immunity includes general physical barriers such as the epithelial membranes that prevent pathogen invasion, the activation of phagocytic cells, as well as more sophisticated systems such as the complement system (Partridge et al., 2010). It also involves the constitutive and inducible production of antimicrobial defense proteins. At a molecular level, these immune responses occur by PAMPs (pathogen associated molecular patterns) binding to PRRs (pathogen recognition receptors) (Vance et al., 2009), activating intracellular signalling cascades and the controlled production and secretion of numerous conserved immunomodulatory and antimicrobial compounds (Janeway and Medzhitov, 2002; Tross et al., 2009). PAMPs include a diverse assortment of molecules such as lipopolysaccharide (LPS), peptidoglycan, licholeic acid, virus-associated nucleic acid variants, and host-derived products of pathogen damage (Tan and Shapira, 2011). These PAMPs are detected by pathogen recognition receptors (PRRs), resulting in the initiation of intracellular signalling pathways. These signalling pathways direct the expression of precise sets of defense genes, limiting the infection or destroying the invading threat.

Some of the key molecular pathways that have been discovered across species include the Toll (TLR/Rel/NF-kB) and IMD signalling pathways extensively studied in *Drosophila* (Wang and Ligoxygakis, 2006), the p38 and JNK MAPK pathways (Tross et al., 2009), and the DBL-1-TGF-B (Delaney and Mlodzik, 2006; Partridge et al., 2010) and FOXO (Becker et al., 2010; Salminen et al., 2008) pathways. Genetic disruption of innate immunity has a profound effect on numerous biological processes, including, aging and lifespan (DeVeale et al., 2004; Salminen et al., 2008), as well as oxidative stress and hypoxia (Kawli et al., 2010; Nizet and Johnson, 2009). Innate immunity is also required for the delayed antigen-specific adaptive immune response in vertebrates

(Hoebe et al., 2004), and several human diseases such as sepsis, asthma and atherosclerosis are partially rooted in innate immune dysfunction (Cook et al., 2004)

3.2 *C. elegans* as a model for host-pathogen interactions

Since its inception as a model organism by pioneer Sydney Brenner (Brenner, 1974), *C. elegans* has contributed to many fields of study. However, it is only comparatively recently that worms have been used alongside powerful model organisms such as mice and flies to study the complexities of the innate immune system. Worms are soil-dwelling, free-living microbivores, that spend the majority of their existence in constant contact with potential pathogens, including bacteria and fungus (Gravato-Nobre and Hodgkin, 2005). As a result, *C. elegans* has evolved mechanisms to protect themselves from potential pathogenic infections. As an invertebrate, these mechanisms are limited to innate immunity, and include non-specific as well as specific defences. Some of the non-specific aspects of worms that contribute to their ability to resist pathogens are their tough polysaccharide cuticle as well as their grinder (Gravato-Nobre and Hodgkin, 2005). *C. elegans* also has three sets of coelomocytes that in other organisms are shown to be involved in general phagocytosis, but in *C. elegans* these cells have not been shown to to contribute to an immune response (Fares and Greenwald, 2001). Given these external obstacles to pathogen attack, worms are usually only sensitive to pathogenesis through openings including the intestine as well as the vulva and anus (Partridge et al., 2010). Infections in *C. elegans*, when they do arise, usually result from an overgrowth of bacteria through the intestine followed by gut engorgement and numerous cytopathological changes in intestinal cells that culminate in host death (Irazoqui et al., 2010a). For this reason, worms are often used as a model system to investigate the interactions between pathogen and host across an epidermal boundary (Irazoqui et al., 2010b). Also of interest is that because *C. elegans* are nematodes, understanding their immune system is of particular importance from the perspective that significant morbidity and mortality in developing nations occurs occurs from neglected diseases including nematode infections (Hotez et al., 2012).

The laboratory use of *C. elegans* in pathogen responses is relatively easy, given that these animals feed on bacteria. The standard laboratory feeding strain for *C. elegans* is *E. coli* OP50 that is only slightly pathogenic, as evidenced by the observation that animals grown on heat-killed *E. coli* survive longer than when grown on live bacteria

(Garsin et al., 2003; Haskins et al., 2008). When conducting immunity assays, all that is required is for the standard *E. coli* strain to be substituted with pathogenic bacteria (Shapira and Tan, 2008). Several pathogenic changes occur in *C. elegans* following an infection, so several different outputs can be measured as indicators of pathogenicity. Some of the measurements that can be made include viability, the degree of gut engorgement through the use of GFP-tagged pathogen strains, as well as changes in reporter gene expression (Shapira and Tan, 2008). While there are many benefits to using *C. elegans* in studies of innate immunity, there are some drawbacks. In particular, it can be difficult to eliminate the potentially spurious observations from what is considered to be bonafied pathogen death. Also, it is observed that worms are somewhat divergent from mammals and insect from an innate immune perspective, and lack some commonly observed innate immunity pathways and components (e.g. NF-kB) (Pujol et al., 2001).

Several pathogens are used to examine the role of innate immunity in worms and phenotypes are generated in a pathogen-dependent way. One of the most well-characterized is the Gram-negative pathogen *Pseudomonas aeruginosa* (Kim et al., 2002). *P. aeruginosa* is a gram-negative soil microbe that encounters *C. elegans* in its natural habitats (Gravato-Nobre and Hodgkin, 2005) and is classified as a multi-host opportunistic pathogen that is a problem in immunocompromised individuals, burn victims, and is a common source of vaginal infections. *C. elegans* infections by *P. aeruginosa* PA14 occur by way of either a 'slow-killing' or 'fast-killing' (toxin-mediated) process depending on the culture conditions used (Kim et al., 2002). A third mechanism of killing by *P. aeruginosa* occurs in the strain PAO1 which mediates its effect through cyanide poisoning and a resultant muscle paralysis (Gallagher and Manoil, 2001). One gene known to function in PAO1 killing is *egl*-9 which encodes a dioxygenase that adds hydroxyl residues to HIF-1 in the presence of oxygen, leading to HIF-1 destruction by the proteosome (Shao et al., 2009; Shao et al., 2010). The absence of *egl-9* or an oxygen-depleted environment results in HIF-1 persistance and the expression of HIF-1 dependent genes that confer protection in times of oxygen stress (Shao et al., 2009). *egl-9* loss of function mutants are resistant to PAO1 infections, suggesting that cyanide mediated paralysis is mediated through EGL-9 (Budde and Roth, 2011; Gallagher and Manoil, 2001; Shao et al., 2010). The N-terminus of UNC-53 inclusive of the CH domain and LKK motif was originally shown to interact with ELG-9 (Adeleye, 2002), through the

nature of the interaction between UNC-53 and EGL-9 has not been pursued. Despite these diverse forms of pathogen-mediated death, it appears that many of the *P. aeruginosa* virulence factors important to pathogenicity in *C. elegans* are relevant in other organisms (Kim, 2008).

3.3 Innate immunity pathways in *C. elegans*

Several conserved signal transduction pathways controlling innate immunity have been discovered in *C. elegans* (for detailed reviews see (Ewbank and Zugasti, 2011; Gravato-Nobre and Hodgkin, 2005; Irazoqui et al., 2010b; Partridge et al., 2010)). These signalling cascades contribute to worm survival through different mechanisms, usually by preventing host damage through the expression of antimicrobial proteins (AMPs), or by limiting deleterious processes (e.g. unfolded protein response, UPR; programmed cell death, PCD) (Irazoqui et al., 2010b). The conserved pathways that have been explored in worms include: Toll-like and IMD signalling pathways, MAP Kinase pathways, DAF-2/DAF-16 insulin-like signalling pathway, programmed cell death (PCD) pathway, and the SMA/TGF-B pathway (Figure 30) which are described in the following sections (see Sections 3.3.1-3.3.5). The degree of conservation of each of these pathways to those in other organisms varies, and there appears to be a strong relationship between the signal transduction cascade employed during an infection and the specific pathogen, pathogenic mechanism, and tissue involved (Irazoqui et al., 2010b). Additionally, many of these cascades show multiple tissue involvement, requiring the coordinated function of multiple cell-types for a successful immune-response (Kawli and Tan, 2008; Shivers et al., 2009; Zugasti and Ewbank, 2009). It is fascinating that all of these signalling pathways have additional well-described roles in developmental processes and appear to have been co-opted to function in innate immunity (Partridge et al., 2010).

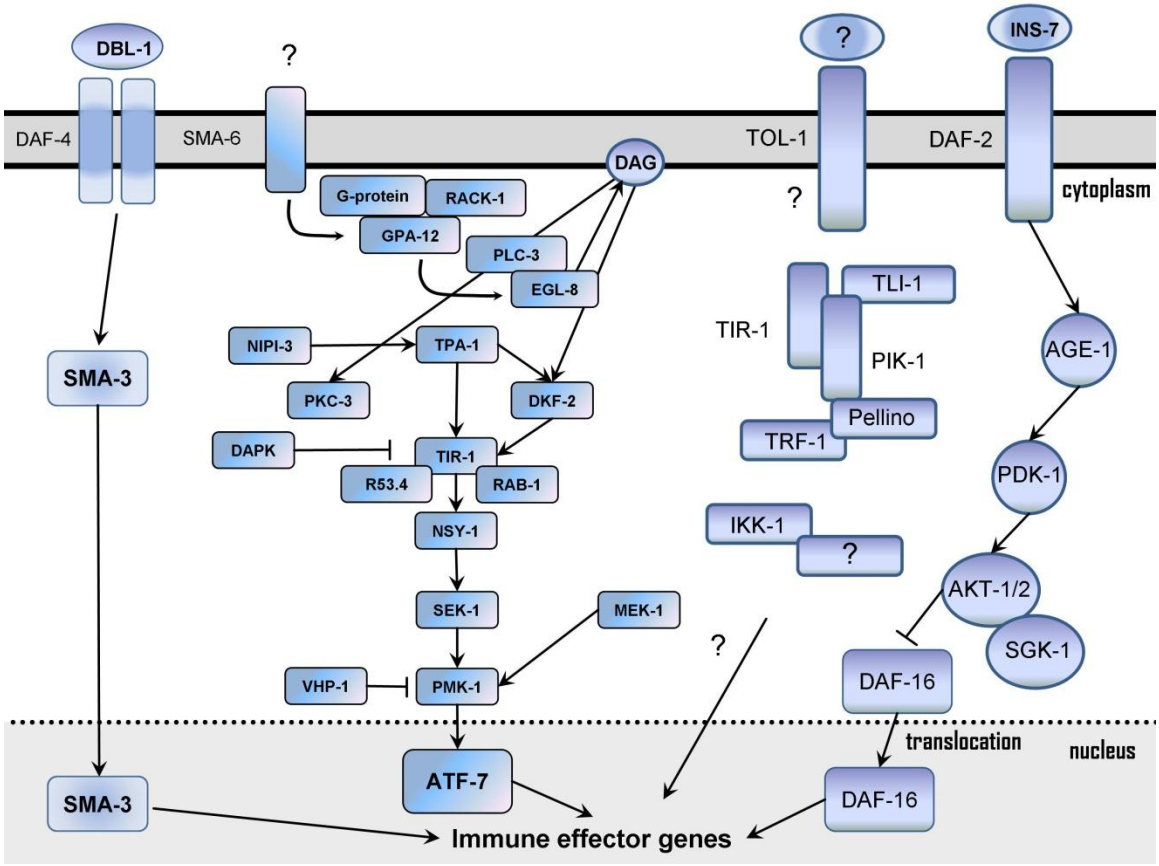

Figure 30. Conserved innate immunity pathways in *C. elegans*

The main parallel signalling pathways identified in *C. elegans* are outlined in order, including: the TGF-B/DBL-1 pathway, the p38 MAPK pathway and relevant upstream signals represented from combined studies in *P. aeruginosa* and *D. Coniospora*, the conserved components of the Toll pathway, and the INS-7-DAF-2-DAF-16 pathway. Specific details of these pathways are provided in the associated text. In brief the TGF-B homolog DBL-1 signals to SMA-3 in the epidermis through a DAF-4-SMA-6 heteromeric receptor during a *D. Coniospora* infection to regulate the expression of immune effector genes (e.g. canaecins, not shown). Unknown signals induced the transcription of immune response genes (e.g. NLPs, not shown) in a cascade involving G-protein subunits GPA-12 and RACK-1, the phospholipase C protein PLC-3, EGL-8 and the PMK-1 pathway in a *D. Coniospora* infection (see text). During wounding, DAPK-1 negatively regulates the PMK-1 pathway upstream of PMK-1 but its location is not known. TPA-1 and DKF-2 activate PMK-1 during a *P. aeruginosa* infection in the intestine while MEK-1 and VHP-1 also regulated the PMK-1 cassette as shown. The Toll pathway does not have a clear role in immune signalling in *C. elegans* though some elements are conserved. In the case of Toll signalling TOL-1 may trigger signalling through TIR-1and the worm IRAK protein, PIK-1. TRF-1 would propagate the signal, leading to release of an unknown transcription factor by the IκB homolog IKK-1 (Gravato-Nobre and Hodgkin, 2005). The DAF-2 agonist INS-7 signals to prevent the nuclear translocation of DAF-16 through a conserved signalling cascade (see text). Adapted from (Irazoqui et al., 2010b) and (Partridge et al., 2010).

3.3.1 Toll and IMD signalling pathways

Studies of the Toll and IMD pathways from *Drosophila* show that they converge on signalling through TFs similar to NF-κB which are family of transcription factors that control both developmental and immune functions across species (Akira et al., 2006; Kawai and Akira, 2007). Both pathways have been extensively studied in *Drosophila* and are also strongly conserved in mammals. Only some elements of the Toll pathway are conserved in *C. elegans* (Figure 30) (Gravato-Nobre and Hodgkin, 2005). Given that these pathways converge on NF-κB, and the apparent lack of a worm NF-κB homolog, their significance in worms is not known (Pujol et al., 2001; Tenor and Aballay, 2008). The Toll pathway was first described to control embryonic patterning and specification in the fly dorsoventral axis (Morisato and Anderson, 1995), and was later found to play pivotal roles in innate immune defences to Gram-positive bacteria and fungus (Ferrandon et al., 2007). The Toll-pathway is similar to the mammalian Toll-like receptor (TLR)/IL-1R signalling pathways (Kawai and Akira, 2007), encoding numerous receptors (TLR1-11) that differ in the PAMPs that they detect (Kumar et al., 2009). TLR4 is the TLR that recognizes bacterial LPS. It signals through MyD88 and TRIF to activate NF-kB, IRF3, and the MAPKs p38, ERK, and JNK (Kawai and Akira, 2011; Kumar et al., 2011). The fly IMD pathway is necessary for responses to Gram-negative bacterial pathogens and is more closely related to the mammalian TNFR/RIP1 (Hetru and Hoffmann, 2009).

Drosophila have three NF-kB transcription factors (Dorsal, Dif, and Relish*)* that all contain associated Rel domains, though Relish also has multiple Ankyrin repeats (Hetru and Hoffmann, 2009). These transcription factors control tissue patterning and also function in immunity in flies. In the Toll pathway *Dorsal* and *Dif* are maintained in the cytoplasm through the IκB homolog *Cactus* and the proteolytic cleavage of *Cactus* results in the release of *Dorsal/Dif* inhibition followed by their translocation to the nucleus to turn on the expression of antimicrobial *Defensins*. In this pathway, the Spatzle ligand (processed from PAMPs upstream) binds to Toll to allow for its dimerization and the recruitment of the adaptor protein MyD88 by intracellular TIR domains (Kumar et al., 2009), recruiting Tube and the kinase Pelle (an IRAK family protein) to MyD88 to form a death-domain mediated complex (Horng and Medzhitov, 2001; Sun et al., 2002; Tauszig-Delamasure et al., 2002). The formation of this complex results in the

phosphorylation of *Cactus* followed by its K48-ubiquitination and degradation, allowing for Dorsal/Dif nuclear translocation (Hetru and Hoffmann, 2009).

The IMD pathway is stimulated by direct binding via PAMPs to the PGRP-LC receptor to generate multimers and clustering followed by a complex signalling cascade (Kaneko and Silverman, 2005). Binding of the PGRP-LC receptor recruits the death domain containing protein IMD homologous to RIP1 (Lemaitre et al., 1995). This interaction induces a complex that contains the *Drosophila* Fas-associated DD (dFadd) and death-related ced-3/NEDD2-like protein (Dredd) (Kaneko and Silverman, 2005). Dredd cleaves IMD to generate an exposed N-terminal A31 that binds the E3 ligase DIAP2 via its BIR2/3 domains. In conjuction with the E2-ubiquitin conjugating enzymes UEV1a, Bendless (Ubc13) and Effete (Ubc5), IMD and DIAP2 are K63-polyubiquitinated (Paquette et al., 2010). This K63 polyubiquitination induce the activation of downstream dTak1, a MAPKKK; dTak1 then activates via phosphorylation an IKK complex containing Ird5 and Kenny, IKK homologs. This activated IKK complex then phosphorylates Relish, which is also cleaved by Dredd (Reichhart et al., 1993; Rutschmann et al., 2000). dTAK also stimulates a second branch of the pathway that activates the JNK signalling cascade by targeting JNKK and JNK to signal to AP1 for the expression of downstream targets involved in wound repair and apoptosis (Kaneko and Silverman, 2005). To better understand the IMD pathway, Foley *et al*. (2004) conducted a genome wide RNAi screen in *Drosophila S2* cells, examining the expression of *Diptericin* in response to LPS stimulation (Foley and O'Farrell, 2004). In this screen the novel *Nav* homolog *Sickie* was identified to be necessary for the expression of *Dipt* in response to LPS, implicating *Sickie* in the IMD pathway. Subsequent experiments revealed that *Sickie* was required along with Dredd and PGRP-LC for the nuclear-translocation of GFP-Relish, and epistasis experiments showed that *Sickie* was needed for induction of *Dipt* by Dredd and IMD, upstream or in parallel to the *Drosophila* WAVE homolog *Scar* (Foley and O'Farrell, 2004).

Given the importance of the Toll pathway, Pujol *et al.* (2001) took a reverse genetics approach in worms and generated mutants for all of the known genes that could be involved in a Toll-like pathway in *C. elegans*, including: *tol-1*, *pik-1*, *trf-1* and *Ikk-1* (Pujol et al., 2001). Using these strains they determined that *tol-1* is required for successful development but not in pathogen resistance directly. However, *tol-1* partial

loss of function mutant was found that is defective in avoidance to *Serratia marcesens* and *tol-1* was expressed in neurons as would be expected for a putative avoidance role. Subsequent studies identified that *S. marcesens* produced a lipodepsipentapeptide serrawettin W2 that mediates this lawn avoidance phenotype through a G-protein coupled signalling process in AWB neurons (Pradel et al., 2007). The observation that *tol-1* is involved in pathogen avoidance but not susceptibility per se, along with the observation that worms lack NF-κB, suggests that *C. elegans* may not use the same Tol pathway as found in other organism for pathogen susceptibility. It is also possible that some other NF-κB–like protein could be involved as many members of the Toll-like pathways other than NF-κB are present (Alper et al., 2008; Pujol et al., 2001). While Pujol *et al.* (2001), show that *tol-1* is not involved in immunity, Denor *et al* (2008), show that a Toll pathway influences the defense response to *S. enterica* mediated infection. In particular, TOL-1 prevents pharyngeal colonization by *S. enterica* and that it is required for upregulation of the defensin like gene *abf-2*, and the heat-shock gene *hsp-16* (Tenor and Aballay, 2008).

3.3.2 MAP Kinase pathways

MAP Kinase pathways have well-defined roles in innate immunity across organisms, including plants, insects and animals where they contribute to both developmental and stress-mediated processes (for reviews see (Gravato-Nobre and Hodgkin, 2005; Symons et al., 2006; Zhang and Dong, 2005)). *C. elegans* has three collections of conserved MAP Kinases: extracellular signal-regulated protein kinases (ERKs), the c-Jun N-terminal kinases (JNKs) and the p38 MAP kinases (PMKs). ERK and JNK signalling is less understood with respect to its role in innate immunity in worms compared to the PMK-1 pathway. ERK signalling appears to be involved in pathogen specific responses to the pathogen *Microbacterium nematophilum* and *Staphylococcus aureus* (Partridge et al., 2010) and JNK signalling, which is well studied in stress responses (Mizuno et al., 2004; Mizuno et al., 2008), contributes to p38 MAPK signalling in the immune response. The most well described MAP kinase pathway in *C. elegans* immunity is the p38 MAPK/PMK-1 pathway, which is required for resistance to several pathogenic organisms including several species of bacteria and fungus (Irazoqui et al., 2010b).

The *C. elegans* p38 MAP Kinase pathway was identified through a genetic screen for Esp (enhanced susceptibility to pathogens) mutants that were subjected to *P. aeruginosa* PA14 (Kim et al., 2002). This screen identified *nsy-1*/ASK (Neuronal Symmetry-1) and *sek-1*/MKK3/6 (SAPK/ERK Kinase) mutants as Esp and later identified *pmk-1*/p38MAPK as necessary for pathogen resistance and the downstream target of NSY-1 and SEK-1 in a phosphorylation cascade. Previous studies identified *nsy-1* and *sek-1* as downstream of the Ca+2/Calmodulin-dependent kinase UNC-43 in the control of the asymmetric expression of the odorant receptor STR-2 in AWC neurons (Sagasti et al., 2001; Tanaka-Hino et al., 2002). UNC-43 does not function in pathogen resistance (Kim et al., 2002), however, and PMK-1 has no known role in neuronal symmetry decisions in *C. elegans* (Sakaguchi et al., 2004), implying a division of function with respect to some aspects of this signalling cassette. Following the identification of the PMK-1 pathway, Kim *et al.* (2004) show a significant degree of cross-talk and signal integration between the p38 pathway and c-Jun N-terminal kinase signalling in innate immunity (Kim et al., 2004). Null mutant *mek-1*/MKK7 animals that signal through JNK in heavy metal stress (Mizuno et al., 2004) are required for the full activation of PMK-1 along with SEK-1, and the JNK homolog *kgb-1*/JNK2 has an Esp phenotype (Kim et al., 2004). Additionally, it is observed that mutants of the worm homolog of the MKP7 phosphatase VHP-1 suppress *mek-1* null alleles and cause an increase in PMK-1 and KGB-1 phosphorylation, resulting in increased pathogen resistance (Kim et al., 2004).

Several other components of the core *C. elegans* p38MAPK pathway have been identified since the original Esp screens. p38MAPK pathways are known to function downstream of Toll-like receptor signalling (Irazoqui et al., 2010b; Valanne et al., 2011; Zhang and Ghosh, 2001). Worms encode a single Toll-like receptor (TOL-1) (Liberati et al., 2004; Pujol et al., 2001), though the worm genome includes two genes (*tol-1* and *tir-1*) encoding proteins with TIR (Toll/IL-1 resistance/SARM) domains that are required for Toll signalling and allow Toll receptors and their adaptors to interact and induce downstream signalling (Valanne et al., 2011). A reverse genetics approach using RNAi identified *tir-1* as required for resistance to both *P. aeruginosa* and *E. faecalis*, and that TIR-1 is essential for PMK-1 phosphorylation and activation (Liberati et al., 2004). *tir-1 (rnai)* animals are also susceptible to the fungal pathogen *Drechmeria coniospora* and the expression of the bioactive antimicrobials *nlp-29* and *nlp-31* is dependent on *tir-1* (Couillault et al., 2004). *rab-1* and the *C. elegans* gene R53.4 (ATP synthase f subunit)

are similarly required for *nlp-29* and *nlp-31* expression as well *D. Coniospora* resistance, and are interactors of TIR-1 as determined by a yeast two-hybrid assay, implicating them in a TIR-1 pathway (Couillault et al., 2004). Interestingly, the TOL-1 receptor does not function with TIR-1 in pathogen resistance (Couillault et al., 2004; Pujol et al., 2001), and as such, the upstream receptor(s) that function as a part of the PMK-1 signalling pathway remain unknown. Other studies of anti-fungal epidermal responses to *D. Coniospora* have elaborated the PMK-1 pathway (Figure 30). In a genetic screen for mutants defective in *nlp-29* expression, the Tribbles homolog NIPI-3 was identified as required for survival from a *D. Coniospora* infection and *nlp-29* inducibility upstream of *sek-1*, and independent of epidermal wounding (Pujol et al., 2008). Similar criteria using this screen identified new alleles of the *C. elegans* PKCδ (Protein Kinase C) homolog *tpa-1* (Ziegler et al., 2009), and by analogy also identified the paralog *pkc-3* which plays a non-redundant role with *tpa-1* in *D. Coniospora* resistance. It is interesting that administration of the phorbol ester PMA, which mimics DAG (diacyglycerol), successfully induced *nlp-29* expression through its activation of TPA-1, and that *tpa-1* mutants blocked this effect, implying direct activation through TPA-1 by DAG (presumably through its DAG binding domain). PMA activation of *nlp-29* is blocked in *tir-1* mutants, placing *tpa-1* upstream of *tir-1*. Further, this study identified that the PLC paralogs EGL-8 and PLC-3, as well as the heterotrimeric G protein subunits GPA-12 and RACK-1 signal upstream of TPA-1 and PMK-1 (Ziegler et al., 2009). Studies using *P. aeruginosa* as a model to study TPA-1 activity in immunity reveal that TPA-1 regulates the activity of the PKD (Protein kinase D) DKF-2, and that DKF-2 signalling is controlled by p38 MAPK dependent and independent signalling (Ren et al., 2009).

Several transcription factors are implicated in downstream signalling from PMK-1. One relevant TF is ATF-7, a member of the CREB/activating transcription factor (ATF) family of basic-region leucine zipper (bZIP) transcription factors and an ortholog of mammalian ATF2/ATF7. ATF-7 is expressed in the intestine where PMK-1 is known to function, and an analysis of loss of function and gain of function *atf-7* mutants reveals that ATF-7 normally functions as a repressor of PMK-1 signalling but is altered to an activating form through PMK-1 phosphorylation (Shivers et al., 2010). More recent evidence has implicated the TF SKN-1 as downstream of PMK-1 during pathogen infection (Hoeven et al., 2011) in addition to its already well-known role with PMK-1 in oxidative stress (Inoue et al., 2005). SKN-1 localizes to intestinal nuclei in the presence

of pathogens, *skn-1* mutants are pathogen susceptible like *pmk-1* animals, and overexpressing SKN-1 results in pathogen resistance (Hoeven et al., 2011). In the context of a pathogen infection with either *P. aeruginosa* or *S. enterica* it appears that reactive oxygen-species (ROS) generated through the dual oxidase Ce-Duox1/BLI-3 activates SKN-1 through PMK-1, suggestive of an indirect induction of this TF. A third transcription factor, STA-2, is shown to function downstream of MAPK signalling in the context of *D. Coniospora* infection (Dierking et al., 2011).

While the p38 MAPK signalling pathway functions cell-autonomously at the site of the infection (Shivers et al., 2009), there is also a cell non-autonomous neuronal contribution to pathogen resistance from some elements of this pathway. For example, while the TIR-1-NSY-1-SEK-1 cassette is required intestinally for *P. aeruginosa* resistance as expected, it also functions in neurons to control aversive behaviour to *P. aeruginosa* (Shivers et al., 2009). The neuronal role of this cassette is independent of PMK-1 and is only apparent when animals are grown on small lawns that allow for 'nutritional choice' and the discrimination of aversion phenotypes. The pathogen avoidance effect for TIR-1-NSY-1-SEK-1 is serotonin-dependent and appears to function through chemosensory neurons, as the chemosensory neuron specific promoter for *osm-5* can rescue the avoidance defect of *sek-1* null mutants. Additionally, NRP-1, a G-protein coupled receptor (GPCR) that functions in sensory neurons to regulate response to environmental stimuli, and most specifically oxygen concentration (Aballay, 2009; Styer et al., 2008), exhibits enhanced pathogen susceptibility independently or its role in oxygen. NPR-1 appears to inhibit the activity of AQR, PQR, URX amongst others that suppress innate immunity function, and that GCY-35, TAX-2, and TAX-4 are required for the activation of AQR, PQR and URX neurons (Styer et al., 2008). Additionally, microarray experiments with *npr-1* mutants show an enrichment in p38 MAPK target AMP genes, suggesting that GPCRs may integrate pathogen presence to immune activation (Aballay, 2009).

Lastly, while p38 MAPK pathways specifically contributes to innate immunity, there is a strong association between innate immune responses and lifespan. Genetic loss of the *C. elegans* insulin-receptor DAF-2 increases lifespan by allowing for DAF-16 nuclear translocation and the expression of genes controlling lifespan, stress and immunity (Troemel et al., 2006). Lifespan extension in *daf-2* mutants is partially dependent on an intact PMK-1 pathway, even though DAF-16 and PMK-1 control the

expression of different subsets of immune-regulated genes (Troemel et al., 2006). Similarly, a decline in PMK-1 activity is observed as worms age, resulting in bacterial engorgement and death, suggesting a major role for PMK-1 in immunosenescence (Youngman et al., 2011).

3.3.3 DAF-2/DAF-16 Insulin-like signalling pathway

The DAF-2/DAF-16 insulin-like signalling pathway is conserved and controls a diverse repertoire of biological processes, representing one of the most well-studied and important signalling cascades in *C. elegans* (White and Kahn, 1994). This pathway has contributed significantly to what is known about the genetic factors controlling development, metabolism, lifespan, stress resistance, and now host defence (Irazoqui et al., 2010b). Activation of the DAF-2/DAF-16 pathway requires the binding of an agonist insulin-like molecule to the *C. elegans* homolog of the vertebrate insulin-receptor, DAF-2. Activation of DAF-2 signals the activation of AGE-1/PI3K which catalyzes the conversion of PIP_2 to PIP_3 and the activation of PDK and the AKT-1/AKT-2 complex and SGK-1, followed by the phosphorylation and inhibition of the Forkhead transcription factor DAF-16/FOXO, retaining it in the cytoplasm and preventing nuclear translocation and the expression of genes controlling stress-response, lifespan and immunity (Ewbank, 2006; Irazoqui et al., 2010b). DAF-16 nuclear translocation is also influenced by JNK signalling which can directly phosphorylate DAF-16, retaining it in the cytoplasm (Oh et al., 2005; Wolf et al., 2008). The translocation of DAF-16 to the nucleus protects *C. elegans* from pathogens but an overabundance of nuclear DAF-16 can also render animals susceptible to pathogens (Singh and Aballay, 2009). Decreased DAF-2 signalling (for example through the binding of a DAF-2 antagonist insulin, or decreased availability of an agonist insulin), leads to a dephosphorylated form of DAF-16 and its entry into the nucleus followed by the transcription of target genes (Figure 30). Loss of function mutants in *daf-2* and *age-1* are resistant to a wide-range of Gram-positive and Gram-negative pathogens (Garigan et al., 2002; Garsin et al., 2001; Garsin et al., 2003; Irazoqui et al., 2010b). *daf-2* mutants also show an increase in the expression of antimicrobial genes, suggesting that *daf-2* function in immunity is not only a consequence of a DAF-2 effect on lifespan (Troemel et al., 2006). As is the case with the enhanced longevity of *daf-2* mutants, the enhanced pathogen resistance of these animals is dependent on functional DAF-16, so *daf-2; daf-16* double loss-of-function mutants resemble wild-type (Troemel et al., 2006). It has been suggested that because

daf-16 animals do not alter AMP expression independently of DAF-2, and that *daf-16* null mutants are not Esp, that the DAF-2-DAF-16 insulin-like signalling pathway does not contribute to pathogen resistance directly but may work indirectly through the effects of this pathway in other processes (e.g. stress response) (Irazoqui et al., 2010b). It is becoming clear that DAF-2-DAF-16 function in lifespan and immunity are separable. While previous studies show no phenotype for lone *daf-16* mutants, more recent intestinal specific RNAi approaches directed towards *daf-16* do result in an Esp phenotype, suggesting that whole worm decreases in *daf-16* are less important than specific knockdown of *daf-16* in the intestine where it is known to function (Evans et al., 2008a). Evidence for a separation between lifespan and immunity in this pathway also comes from the observation, that while *daf-2* mutants extend lifespan in relatively non-pathogenic organisms (~2-fold), that in some pathogenic organisms that this lifespan extension can be much greater (~5-fold) (Irazoqui et al., 2010b). Also, it has been shown that the phenotypes of pathogen resistance and lifespan can be separated genetically (Evans et al., 2008a). DAF-2 and AGE-1 signal to numerous downstream effector proteins including PDK-1, AKT1/2 and SGK-1 (Figure 30). Evans et al., (2008) show that SGK-1 contributes only to lifespan while AKT1/2 contribute to both longevity and immunity, as SGK-1 had comparable gut engorgement to wild-type and unaltered antimicrobial expression changes compared to DAF-2 and AKT-1/2 . Further to this, more recent studies directed toward understanding the role of pore-forming toxins (e.g. Cry5) on innate immunity, show that cellular defenses to PFTs are achieved through a DAF-2 pathway dependent on WWP-1 that functions in parallel to DAF-16 implying that the DAF-2 and DAF-16 are separable depending on the cellular context (Chen et al., 2010).

While the DAF-2-DAF-16 pathway works in the intestine for pathogen resistance it is clear that upstream neuronally derived cues are important. One neuronally derived insulin-like peptide important to this pathway is *ins-7* (Figure 30) (Kawli and Tan, 2008). INS-7 expression is pathogen-induced and used by *P. aeruginosa* to circumvent *C. elegans* host-immunity (Evans et al., 2008b; Kawli and Tan, 2008). Given that INS-7 is a DAF-2 agonist, the expression of INS-7 results in DAF-2 activation, promoting the retention of DAF-16 in the cytoplasm, decreasing AMP production downstream of DAF-16 (Kawli and Tan, 2008). Since INS-7 is expressed in neurons (Murphy et al., 2007), it follows that genes regulating neurosecretion could influence DAF-2-DAF-16 signalling. It

is observed that genes controlling neurosecretion contribute to longevity (Shen et al., 2007) and immunity (Kawli and Tan, 2008). For example, the *C. elegans* genes *unc-64*/*syntaxin* and *snb-1/synaptobrevin* that form part of the core machinery required for dense-core vesicle fusion are pathogen resistant owing to the fact that these mutants have decrease neuronal exocytosis of INS-7 (Kawli and Tan, 2008). Similarly, loss of function mutations in genes that negatively regulate neurosecretion exhibit sustained hypersecretion, as is observed in the case of mutants like *dgk-1* or *goa-1* (Miller et al., 1999) that do not live as long on *P. aeruginosa* as wild-type, and have decreased antimicrobial expression, and increased pathogen engorgement in the intestine (Kawli and Tan, 2008).

Interestingly, while overexpression of DAF-16 promotes pathogen resistance the chronic overexpression of DAF-16 is deleterious for *C. elegans*. While *daf-2* mutants show increased translocation of DAF-16 into the nucleus, resulting in pathogen resistance, the same mutants in the background of a DAF-16 overexpressing strain are more susceptible to *P. aeruginosa* than *daf-2* (Singh and Aballay, 2009). Similar results are found when heat-shock stress situates DAF-16 into the nucleus while DAF-16 is overexpressed. Therefore, it seems as though the export of DAF-16 is as important as DAF-16 nuclear import in pathogen resistance. Heat-shock factor-1 (HSF-1) appears to be required for DAF-16 nuclear export, and increased nuclear DAF-16 results in the overexpression of the water-channel AQP-1, connecting HSF-1, DAF-16 and water homeostasis (Singh and Aballay, 2009).

DAF-2 is also relevant in the pathogenesis of the intracellular bacterium *S. typhimurium*, independently of the PCD pathway and apparently through the control of autophagy (Jia et al., 2009). Inactivation of autophagy results in the intracellular bacterial accumulation of *S. typhimurium*. Also *daf-2* loss of function or DAF-16 overexpression results in increased resistance to *Salmonella typhimurium,* a phenotype that is dependent on autophagy genes as knockdown of *bec-1* or *lgg-1* by RNAi abrogates this resistance and decreases DAF-2 mediated autophagosome formation (Jia et al., 2009).

3.3.4 **PCD pathway**

The identification of the programmed cell death (PCD) pathway in innate immune responses in *C. elegans* was established when it was determined that intestinal colonization of *C. elegans* by *S. typhimurium* (but not *P. aeruginosa*) induced an increase in PCD in the *C. elegans* germline during infection(Aballay and Ausubel, 2001)(Aballay and Ausubel, 2001) and that mutants in *ced-3, ced-4*, and *ced-9* along with *egl-1*, are susceptible to *S. typhimurium* (Aballay and Ausubel, 2001). *S. typhimurium* colonization appears to generate increased cell-death in the gonad and the induction of the PCD pathway serves a protective role by promoting the formation of cell corpses. Furthermore, activation of the PCD pathway in response to *S. typhimurium* is dependent on PMK-1, as *pmk-1 (rnai)* inhibits the formation of gonad cell-corpses in response to pathogen-stress and *pmk-1 (rnai)* animals are susceptible to *S. typhimurium*, implying a link between p38 MAPK pathway and the PCD pathway (Aballay et al., 2003). In this pathway CED-9 is downstream of PMK-1 as *ced-9* loss of function mutants promote cell-corpse persistence when *pmk-1* is removed genetically. This study also excluded *C. elegans* Toll signaling proteins (*tol-1*, *trf-1*, *pik-1*) from a role in the PMK-1-dependent CED pathway. In addition to the CED-3-CED-4-CED-9 pathway, an additional CED pathway involving the EGF-repeat containing phagocytic receptor CED-1 controls immunity, as *ced-1* mutants are susceptible to *S. typhimurium* (Haskins et al., 2008). CED-1 appears to activate the expression of the *pqn/abu* family of prion-like glutamine/asparagines (Q/N-rich domain proteins that are activated by ER stress and aid in the unfolded-protein response (UPR) (Viswanathan et al., 2005) that are required for successful pathogen clearance and survival, coupling CED-1 to the UPR response. It has been suggested that CED-1 activation of the UPR may be activated by pore-forming toxins (Irazoqui et al., 2010b) as studies using the pathogen *B. Thuringiensis* show that Cry5B toxins initiate a survival dependent UPR response in worms (Bischof et al., 2008), though the extent that these two pathogen specific UPR responses overlap is not known.

3.3.5 **SMA/TGF-B pathway**

The SMA/TGF-B pathway is well-recognized for its developmental role in controlling male tail development and body size (Soete et al., 2007). In this signalling pathway the diffusible cue DBL-1 engages the heteromeric receptor DAF-4/SMA-6.

Activated SMA-6 signals through the SMAD complex (SMA-2/SMA-3/SMA-4) to elicit expression of many genes including AMPs (Figure 30) (Ewbank, 2006; Irazoqui et al., 2010b). DAF-4 and SMA-6 are expressed in the intestine and epidermis where they control the expression of several antimicrobial proteins and are found to be susceptible to *P. aeruginosa* and *S. marcescens* (Ewbank, 2006). The DBL-1/TGF-B pathway was first recognized in innate immunity by Mallo *et al.* (2002) who identified significant overlap between their *S. marcescens* induced genes and those previously identified through screens targeting the SMA/TGF-B pathway in another study (Mallo et al., 2002). Subsequent work identified that *dbl-1* genetic loss renders animals susceptible to pathogenic *S. marcescens* as well as *E. coli* OP50 (Tenor and Aballay, 2008). Of particular interest is that infections with *D. Coniospora*, which are controlled by a *pmk-1* pathway (see Section 3.3.2), separately induce the SMA/TGF-B pathway, resulting in the expression of *caenacin-2*. This latter induction functions in a cell non-autonomous way, being established by neuronally expressed DBL-1 cue that signal in a neuroendocrine fashion (Zugasti and Ewbank, 2009).

3.4 Results

3.4.1 Pathogen resistance requires *unc-53* in adult tissue

unc-53 and the *Navs* have described roles in cell migration and cytoskeletal dynamics during development (Schmidt et al., 2009; Stringham et al., 2002; Stringham and Schmidt, 2009). However, very little is known about the role of *unc-53* or the NAVs in adult tissue after development is complete (see Sections 1.1 and 1.2). A previously conducted RNAi screen identified *unc-53* as required for the expression of a *C. elegans* C-type lectin (*clec-85*) (Alper et al., 2008), a putative antimicrobial protein that is expressed in response to pathogens and under the control of multiple genetic pathways in innate immunity (Alper et al., 2007), implicating *unc-53* in the *C. elegans* immune response.

To determine whether *unc-53* functions in *C. elegans* innate immunity, the extent that *unc-53* mutant and *unc-53 (rnai)* treated animals could survive exposure to the Gram negative human and nematode pathogen *P. aeruginosa* PA14 was assessed, as rapid death in the presence of *P. aeruginosa* is observed in animals mutant at loci for *C. elegans* genes with a conserved role in innate immunity, including those found in PMK-1, DBL-1/TGF-B and DAF-2-DAF-16 signalling pathways (Gravato-Nobre and Hodgkin,

2005). Consistent with a role for *unc*-53 in innate immune function, *unc-53* mutant animals and animals treated with *unc-53 (rnai)* as embryos died significantly faster than corresponding wild-type control animals when exposed to *P. aeruginosa* (Figure 31A,C; Appendix 1, Table 11). The mutants *unc-53 (n152)* and *unc-53 (n166)* died slightly faster than *unc-53 (e2432)* and *unc-53 (e404)*, and *unc-53 (rnai)*. *unc-53 (n152)* susceptibility to *P. aeruginosa* was rescued by the fosmid WRM0628aD12 (II:11054597..11095584) containing the entire *unc-53* locus complete with the upstream and internal regulatory regions that are expected to drive the expression of all the *unc-53* isoforms as well as the gene *rpl-42* (Figure 31A, Appendix 1, Table 11).

Premature death on *P. aeruginosa* was independent of the internal hatching due to the Egl defect in *unc-53* animals because animals tested were treated with FUDR (Fluorodeoxyuridine) throughout the course of the assays to induce sterility. Similarly, *unc-53* animals treated with sterilizing *lin-60/cdc-25.1 (rnai)*, a gene required for germline proliferation (Ashcroft and Golden, 2002; Kim et al., 2009), are more susceptible to *P. aeruginosa* than *lin-60/cdc-25.1 (rnai)* controls (Appendix 1, Table 11). *unc-53 (n152); him-8 (e1489)* males are more susceptible to *P. aeruginosa* compared to *him-8 (e1489)* control males (Figure 31E; Appendix 1, Table 11), making it unlikely that the pathogen susceptibility of *unc-53* is due to a matricidal effect. In addition to being sensitive to *P. aeruginosa*, *unc-53 (n152)* and *unc-53 (n166)* mutants also exhibited a short lifespan when grown on the relatively non-pathogenic laboratory strain *E. coli* OP50-1 (Figure 31B, Table 12), consistent with the observation that *E. coli* can colonize and kill immunocompromised animals depending on the culture conditions used (Garigan et al., 2002; Garsin et al., 2001; Hahm et al., 2011; Haskins et al., 2008). However, it was also observed that *unc-53 (n152)* lifespan was slightly decreased compared to wild-type N2 animals when exposed to heat-killed *P. aeruginosa* PA14 (Figure 31F, Appendix 1, Table 11), suggesting that these mutants may have decreased general fitness or longevity in addition to increased pathogen susceptibility. Importantly, *unc-53 (e404)*, *unc-53 (e2432)* and *unc-53 (rnai)* treated animals were not significantly different from wild-type on *E. coli* (Figure 31B,D, Appendix 1, Table 12) despite having an enhanced sensitivity to *P. aeruginosa*, revealing that *unc-53* is specifically required for pathogen resistance and that the observed death is not exclusively the result of a general

decrease in fitness or longevity in the case of *unc-53 (e404)*, *unc-53 (e2432)* and *unc-53 (rnai)*.

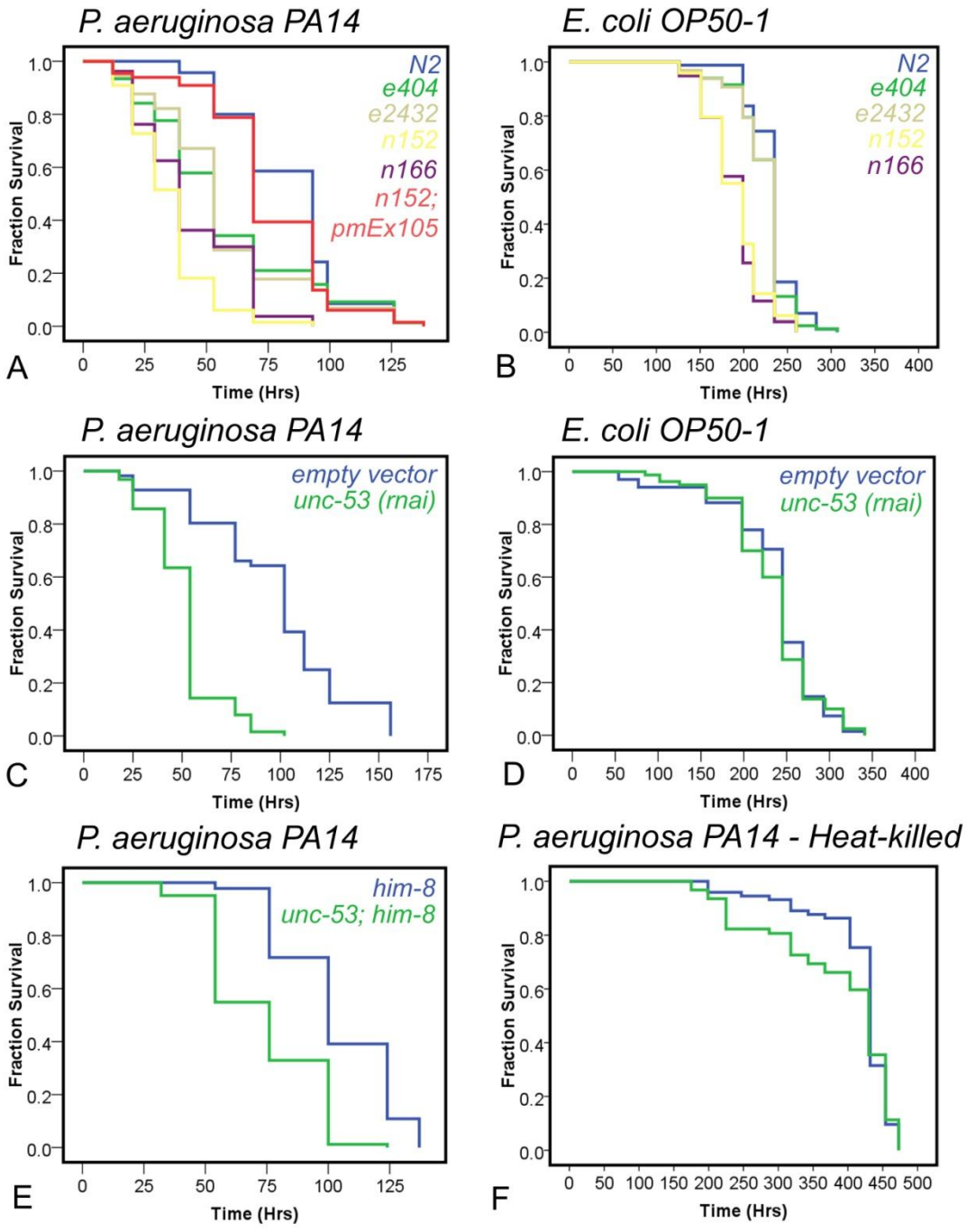

Figure 31. *unc-53* is required for resistance to *P. aeruginosa PA14* in *C. elegans.*

(A-F) Kaplan-Meier plots showing the survival of *unc-53* mutant or *unc-53 (rnai)* treated animals compared to control animals when exposed to indicated bacteria. (A) Survival of *unc-53 (e404)* (n=76), *unc-53 (e2432)* (n=73), *unc-53 (n152)* (n=77), *unc-53 (n166)* (n=66) and *unc-53 (n152)*; *pmEx105* {WRM0628aD12 (II:11054597..11095584)} (VA541) (n=65) was compared to wild-type N2 animals (n=70). (B) Survival of *unc-53 (e404)* (n=83), *unc-53 (e2432)* (n=97), *unc-53 (n152)* (n=78), *unc-53 (n166)* (n=49) was compared to wild-type N2 (n=86). (C) Survival of *unc-53 (rnai)* (n=53) was compared to empty vector controls (*pPD129.36*, n=63). (D) Survival of *unc-53 (rnai)* treated animals (n=68) compared to empty vector controls (n=77). (E) Survival of *unc-53 (n152); him-8 (e1489)* (n=68) males were compared to *him-8 (e1489)* males (n=73). (F) Survival of *unc-53 (n152)* (n=66) animals were compared to wild-type N2 animals (n=48). Statistics were carried out as described (see Section 3.6.2) and are shown for all replicates in Appendix 1 Table 11 and Table 12. Representative experiment is shown. A minimum of two replicates were performed. All treatments were performed in the presence of FUDR with the exception of male animals carrying the *him-8 (e1489)* mutation.

Given the observation that *unc-53* controls the migration of numerous cells and cellular processes including neurons in *C. elegans* (Schmidt et al., 2009; Stringham et al., 2002; Stringham and Schmidt, 2009), and reports showing a strong neuronal basis for innate immunity in both evasive behaviour (Shivers et al., 2009) and as sources of endocrine cues (Kawli and Tan, 2008; Zugasti and Ewbank, 2009), the extent that the defects in innate immunity were secondary to the role of *unc-53* during embryonic and larval stages was of interest. To answer this question, L4 staged animals were treated with *unc-53 (rnai)* by the feeding method and were found to be more susceptible to *P. aeruginosa* compared to negative control animals (Figure 32), albeit less than *unc-53* mutants or *unc-53 (rnai)* animals exposed to *unc-53* dsRNA as embryos. The observation that treating adult animals to *unc-53* dsRNA does not render them as susceptible to *P. aeruginosa* as *unc-53* mutants could also be interepreted to suggest that some defects occurring before adulthood contribute to pathogen susceptibility in *C. elegans*.

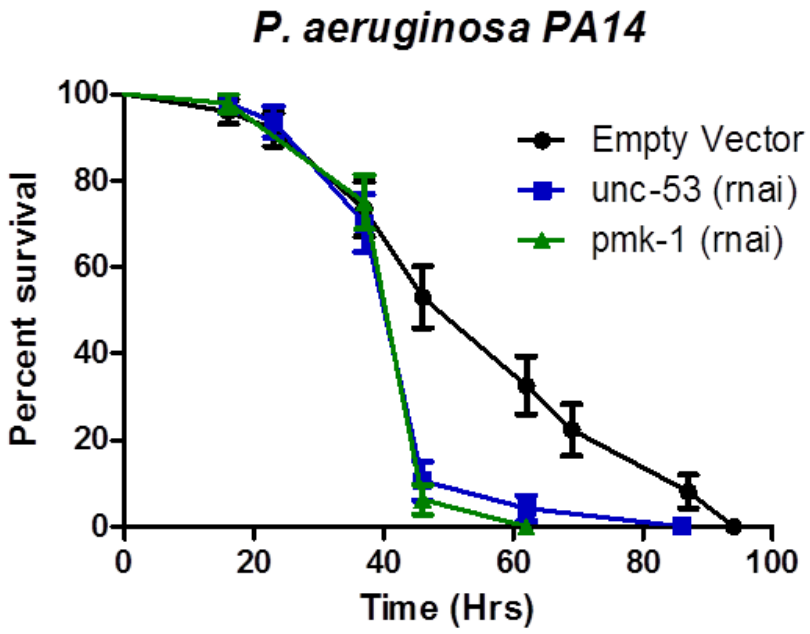

Figure 32. *unc-53 (rnai)* animals treated as adults are susceptible to *P. aeruginosa* PA14

unc-53 (rnai) animals treated as adults (n=47) and *pmk-1 (rnai)* animals (n=49) and empty vector (*pPD129.36*) controls (n=49) are compared and statistically significant differences (P<0.05) are observed. Statistics were carried out as described (see Section 3.6.2) and are shown for all replicates in Appendix 1 Table 13. Representative experiment is shown. A minimum of two replicates were performed. Treatments were performed in the absence of FUDR.

3.4.2 UNC-53 expression is maintained in adult tissue

UNC-53 is expressed in a number of cells and tissues during embryonic and larval stages where it has been shown to function cell-autonomously in cell migration and outgrowth (Schmidt et al., 2009; Stringham et al., 2002). Given the observation that *unc-53 (rnai)* treatment of adult animals confers some susceptibility to *P. aeruginosa*, the expression pattern generated by the promoter upstream of *unc-53* (see Section 2.3.1) was reexamined. *punc-53L::gfp* animals expressed GFP in several cells in adults including the excretory cell (Figure 11A), neurons in the head and tail ganglia and neurons along the ventral nerve cord (Figure 11B-D), as well as the uterine and vulval muscle cells forming the adult vulva (Figure 11E) as previously discussed (see Section 2.3.1). In addition to this expression pattern, expression was found in the intestine of

larval and adult animals (Figure 33). No expression was observed in the cells of the hypodermis.

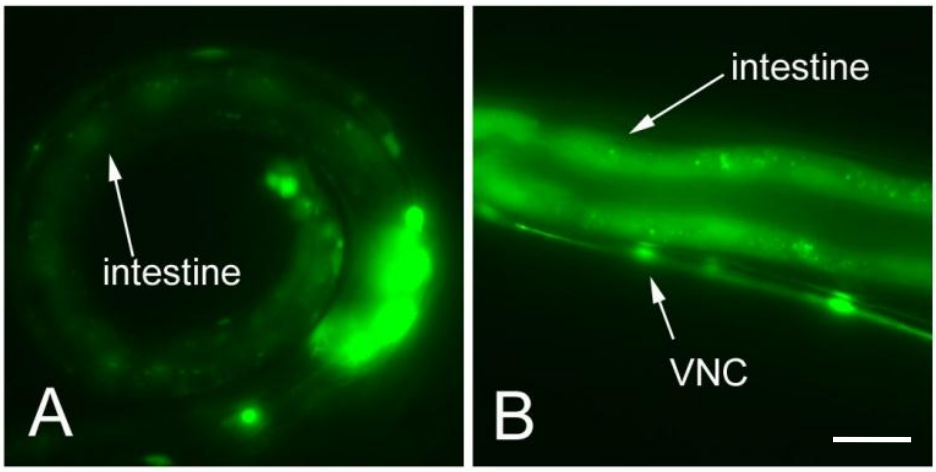

Figure 33. *unc-53* is expressed in the intestine in both larval and adult animals in *C. elegans*

(A,B) Expression of *unc-53* as shown by the *punc-53L::gfp* reporter (strain BC14371) reveals the intestinal expression of *unc-53* in both larva (A) and adult animals (B). Expression is also shown in cells of the ventral nerve cord (VNC) and the head and tail ganglia (not labelled). Scale bar is 100 µm.

3.4.3 Multiple tissues and isoforms may require *unc-53* for an immune response

C. elegans responds to bacterial infections through the coordinated response of several tissues, and animals mutant for genes controlling innate immunity can be rescued using heterologous promoters (Kawli et al., 2010; Shivers et al., 2009). Given the finding that *unc-53* is expressed in neurons and the intestine, two tissues required for an innate immune response, it was predicted that one or both of these tissues may be the site of *unc-53* function during a *P. aeruginosa* infection. To assess whether the intestine or neurons contribute to *unc-53* function, several strains carrying the *unc-53 (n152)* mutation and transgenes expressing the *unc-53L* isoform of *unc-53* cDNA under the control of the intestinal specific promoter *ges-1* (Kennedy et al., 1993), the pan-neuronal promoter for *rab-3* (Nonet et al., 1997), and both *ges-1* and *rab-3* to drive *unc-53* simultaneously in both tissues, were generated. The *unc-53L* cDNA is equivalent to

the F45E10.1a isoform and contains all of the exons of *unc-53* with the exception of the alternatively spliced exon 18. Portions of this cDNA have been used to rescue the posterior migration of the ExC, the Egl defect, and the mechanosensory neuron migration defect (Schmidt et al., 2009; Stringham et al., 2002). Rescue of the pathogen susceptibility phenotype of *unc-53 (n152)* was not observed when *unc-53* was expressed using *pges-1::unc-53L* or *prab-3::unc-53L* alone, or in transgenic lines carrying both *pges-1::unc-53L* and *prab-3::unc-53L* in *unc-53 (n152)* (Figure 34). The functionality of the *prab-3::unc-53L* constructs was established by rescuing the PLM mechanosensory neuron migration defect (Appendix 1 Table 15). To test if *unc-53* F45E10.1a cDNA could be successfully expressed under the control of the *ges-1* promoter, a UNC-53-GFP tagged construct (*pges-1::unc-53L::gfp)* was produced and was observed to be expressed throughout the intestine (Appendix 1 Figure 48), but was unable to rescue the innate immunity defect (Appendix 1 Table 14).

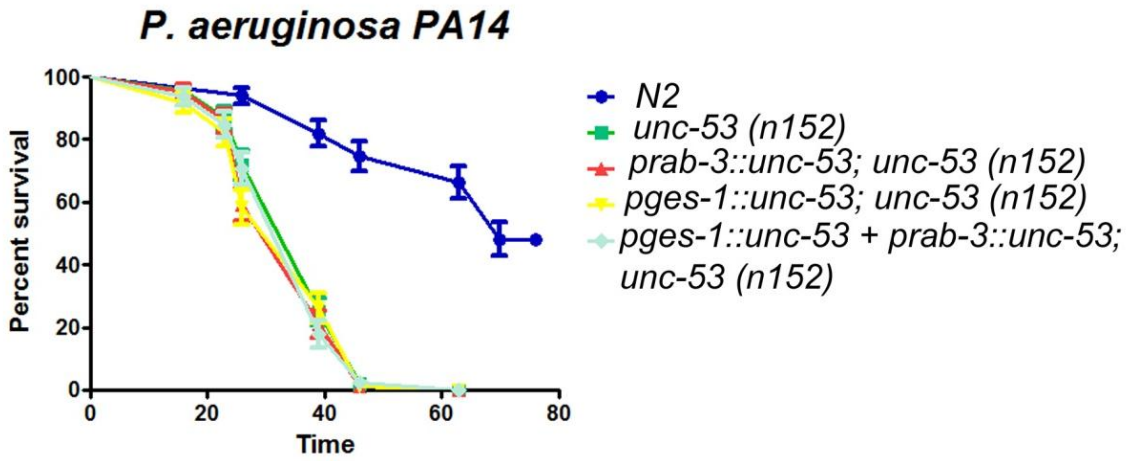

Figure 34. Pan-neuronal and intestinal tissue specific expression fails to rescue *P. aeruginosa* susceptibility of *unc-53 (n152)*

unc-53 (n152) animals expressing of *unc-53L* cDNA under the control of the *rab-3* promoter (VA381, n=86), the *ges-1* promoter (VA378, n=84), or both (VA375, n=78) are not significantly different from *unc-53 (n152)* (n=93). N2 (n=42). Statistics were carried out as described (see Section 3.6.2) and are shown for all replicates in Appendix 1 Table 14. Representative experiment is shown. A minimum of two replicates were performed with a minimum of two transgenic lines. All treatments were performed in the presence of FUDR.

Because the pathogen susceptibility phenotype of *unc-53 (n152)* can be rescued with the fosmid WRM0628aD12 (Figure 31A), which expresses every exon of *unc-53*, the extent that the lack of rescue by the neuronal and intestinal specific constructs might be due to the fact that the *unc-53L* cDNA corresponding to F45E10.1a lacks exon 18, and that perhaps exon 18 was required for rescue of the innate immunity phenotype, was assessed. This is not likely to be the case because the short-isoforms of *unc-53* that also lack exon 18 are able to rescue pathogen susceptibility in *unc-53 (n152)* when expressed by their endogenous promoters. To rescue the pathogen susceptibility of *unc-53 (n152)* using the smaller isoforms, the small isoforms containing the same 3' end of the F45E10.1a cDNA and also lack exon 18 (Stringham et al., 2002) were expressed. The constructs used were driven by the *punc-53SA*, *punc-53SB*, and *punc-53SAB* promoters fused to the corresponding cDNA isoforms and crossed into *unc-53 (n152)* (Stringham et al., 2002). *punc-53SA::unc-53SA*, *punc-53SB::unc-53SB*, and *punc-53SAB:unc-53SAB* promoter constructs showed partial rescue of the *unc-53 (n152) P. aeruginosa* susceptibility (Figure 35). These experiments suggest that the alternative exon 18 is somewhat dispensible for immune function, and that the lack of rescue using the pan-neuronal and intestine specific contructs could be attributed to the fact that *unc-53* cDNA used in those constructs contains a different N-terminus or that the differences in the promoters lend themselves to varying abilities to rescue the *unc-53* immunity phenotype. The *punc-53SA* and *punc-53SB* promoters are expressed in a wide range of cells and tissues including neurons, muscles, distal tip cells and the excretory cell (Stringham et al., 2002). It is noteworthy that all of the constructs show some degree of rescue, suggesting that each isoforms contributes to pathogen resistance in some way, and that pathogen resistance does not seem to be attributable to any one small isoform so far tested. Also, an additive effect between *punc-53SA* and *punc-53SB* using the *punc-53SAB* construct was not observed, so it is not possible to conclude that individual isoforms combine to promote pathogen resistance.

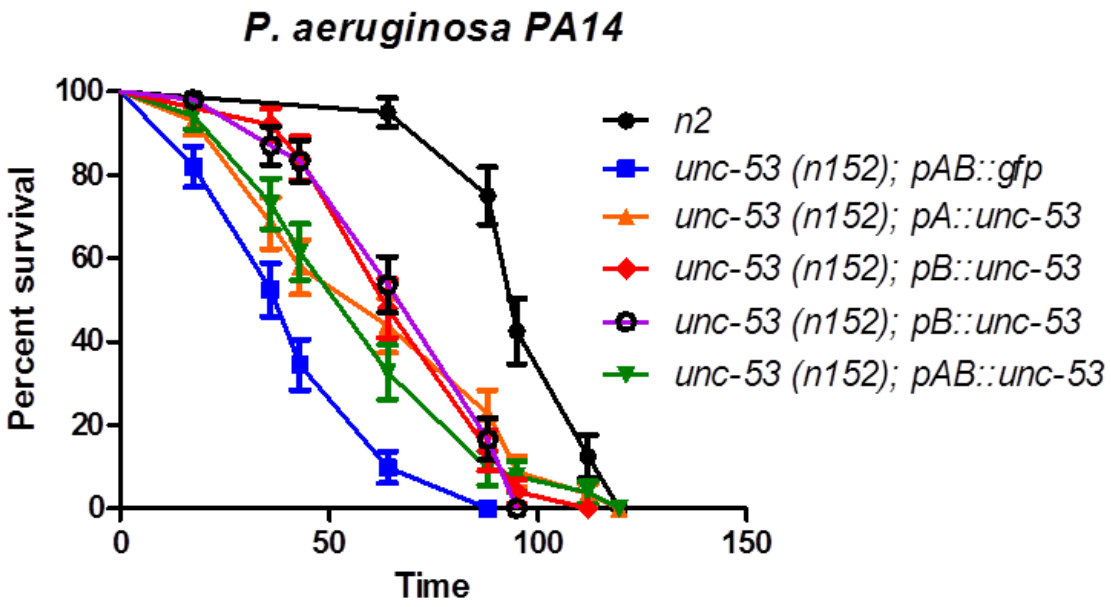

Figure 35. Small isoforms of *unc-53* partially rescue the *P. aeruginosa* susceptibility of *unc-53 (n152)*.

Statistically significant rescue (P<0.0001) is observed when *unc-53 (n152)* mutants subjected to *P. aeruginosa* expressing *punc-53SA::unc-53SA* (UG62, n=57), *punc-53SB::unc-53SB* (UG188, orange, n=50; UG189, purple, n=56) and *punc-53SAB::unc-53SAB* (UG176, n=52) compared to those expressing *punc-53SAB::gfp* (UG17, blue, n=61) (Stringham et al., 2002). Statistics were carried out as described (see Section 3.6.2). All treatments were performed in the presence of FUDR

To complement these rescue experiments, a series of tissue-specific RNAi experiments were conducted. These experiments take advantage of the observation that *unc-53 (rnai)* renders animals susceptible to *P. aeruginosa* (Figure 31C). Previously generated strains (strain name in brackets) that allow for tissue-specific RNAi in the intestine (OLB11), muscle (NR350), and hypodermis (NR222) were subjected to *unc-53 (rnai)* using a clone that is expected to knockdown all of the isoforms of *unc-53*. OLB11, NR350, NR222 strains carry the mutation *rde-1 (ne219)* that makes animals RNAi resistant (Tabara et al., 1999) except in the tissues where the gene is rescued in a tissue-specific way (Pilipiuk et al., 2009; Qadota et al., 2007). Using these strains it was observed that tissue-specific knockdown of *unc-53* in the intestine, muscle or hypodermis was insufficient to render animals susceptible to *P. aeruginosa* (Figure 36). Notably, muscle-specific RNAi resulted in animals that were Egl, but it did not render animals significantly susceptible to *P. aeruginosa,* suggesting that the sex myoblast

defects in *unc-53* do not contribute substantially to pathogen susceptibility. Given the observation that knockdown of all of the isoforms of *unc-53* in muscle, hypodermis or intestine, has no effect on pathogen susceptibility, perhaps *unc-53* may function in some other tissue not tested, or a combination of the tested tissues. This is consistent with the rescue using the fosmid WRM0628aD12, which expresses all of the isoforms of *unc-53* in several tissues.

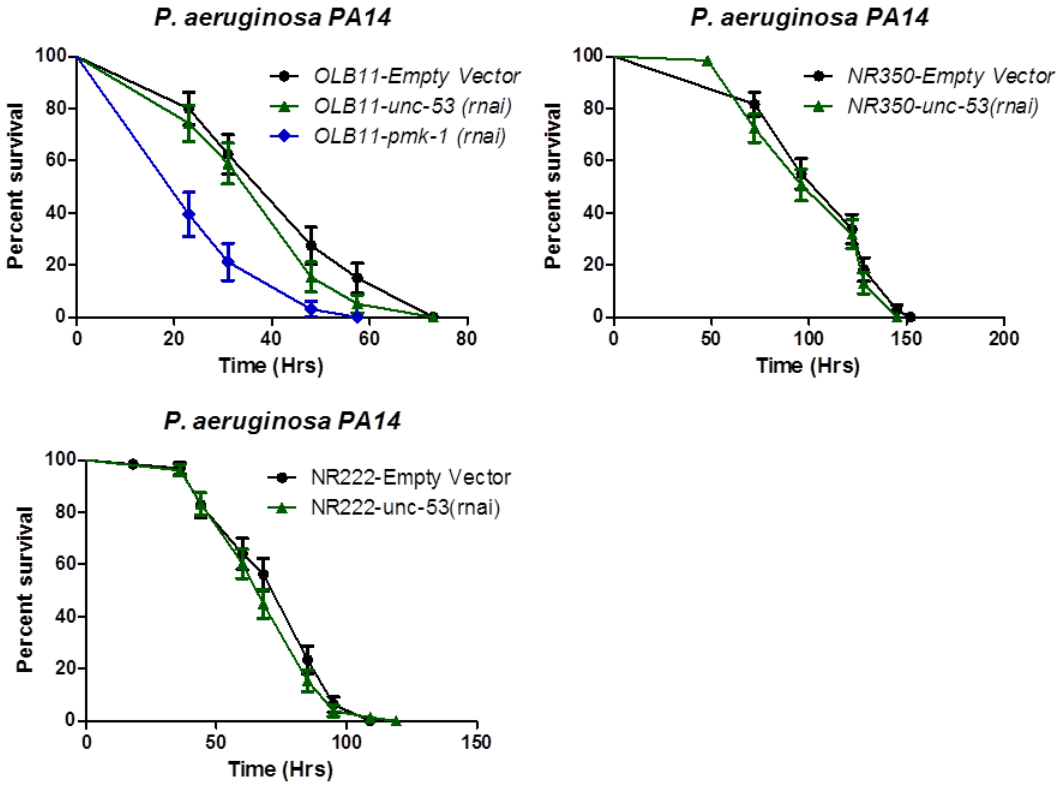

Figure 36. Tissue specific *unc-53 (rnai)* in the instestine, muscle, and hypodermis does not render animals susceptible to *P. aeruginosa* PA14.

(A-C) Survival plots shown for tissue specific RNAi experiments conducted towards *unc-53* and negative control empty vector (*pPD129.*26) as shown in the intestine (OLB11) (A), muscle (NR350) (B), and hypodermis (NR222) (C). Statistically significant differences were not observed between *unc-53 (rnai)* and empty vector RNAi for any of the strains tested. (A) OLB11 (*unc-53* = 65*, pmk-1* =47*,* empty vector = 63). (B) NR350 (*unc-53*; n=69*;* empty vector, n=71). (C) NR222 (*unc-53* = 78*,* empty vector = 64). Statistics were carried out as described (see Section 3.6.2) and are shown for all replicates in Appendix 1 Table 16. Representative experiment is shown. A minimum of two replicates were performed. All treatments were performed in the presence of FUDR.

3.4.4 UNC-53 is required for synaptic transmission, and negatively regulates *ins-7*

C. elegans innate immunity is controlled in part through the secretion of immunomodulatory proteins that exert their effects on distant tissues in an endocrine fashion (Evans et al., 2008b; Kawli and Tan, 2008; Kawli et al., 2010; Shivers et al., 2009). Given the observation that *unc-53* is expressed in numerous neurons after development is complete, the extent that *unc-53* might contribute to immunity by regulating synaptic transmission was determined. Previous work has implicated *unc-53* in endocytosis (see Section 2.3.11), and evidence from vertebrates shows *Nav1* mRNA localization at neuromuscular junctions (NMJs) (Kishi et al., 2005), suggesting that *unc-53* may function to control synaptic transmission. To test for a defect in synaptic transmission in *unc-53*, animals were subjected to the acetylcholinesterase inhibitor Aldicarb, which causes acute paralysis through the accumulation of acetylcholine (ACh) at NMJs (Mahoney et al., 2006). Hypersensitivity to aldicarb-induced paralysis occurs in mutants that increase ACh signalling at synapses by either increased secretion, decreased degradation, or increased ACh responsiveness (Mahoney et al., 2006). Additionally, alterations in ACh secretion is also representative of dense-core vesicle transmission as many of the core structural components are conserved between the two processes (Charlie et al., 2006; Sieburth et al., 2007). Following 1hr exposure to 1mM Aldicarb, significantly more *unc-53 (n152)* animals were paralyzed compared to wild-type (Figure 37), indicating that *unc-53* is normally required to limit acetylcholine synaptic transmission. Importantly, Aldicarb hypersensitivity is independent of the role of *unc-53* during development as adult *unc-53 (rnai)* treated animals were similarly hypersensitive compared to controls (Figure 37).

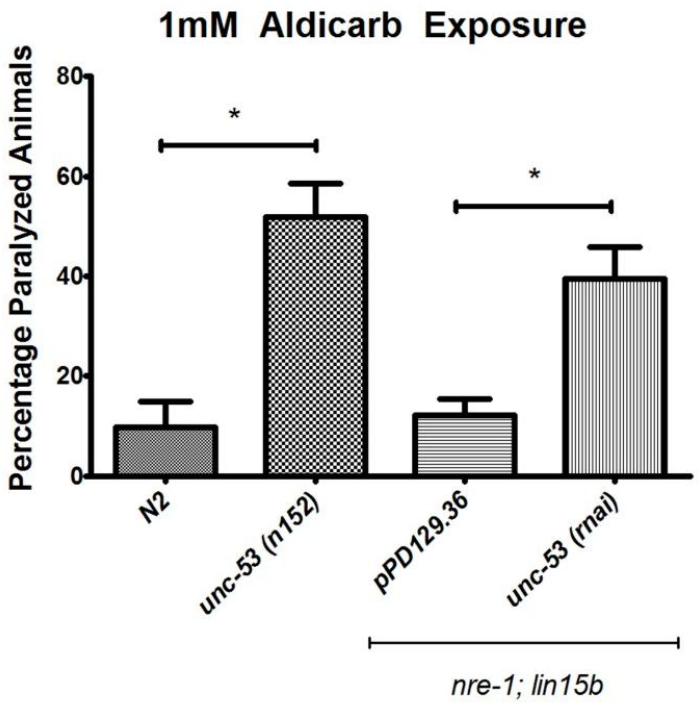

Figure 37. *unc-53* animals are hypersensitive to the acetylcholinesterase inhibitor Aldicarb.

Significantly more *unc-53 (n152)* (n=150) mutants were paralyzed following a 1hour treatment with 1mM Aldicarb than wild-type N2 animals (n=140) ($P<0.001$). Similarly, a significantly greater percentage of animals treated with *unc-53 (rnai)* as adults (n=170) were paralyzed in 1mM Aldicarb compared to empty vector (pPD129.36) RNAi treated animals (n=162) ($P<0.05$). Adult RNAi experiments were conducted in the enhanced RNAi strain *nre-1 (hd20); lin15b (hd126)* strain. Data represents the mean of two experiments with a 95% confidence interval shown (Graphpad Prism 5).

Given the finding suggesting that *unc-53* negatively regulates synaptic transmission (Figure 37) and positively regulates pathogen resistance (see Section 3.4.1), it was hypothesized that *unc-53* may function to downregulate the production and/or secretion of negative regulators of innate immunity. *C. elegans* immunity is partially regulated by insulin-like DAF-2–DAF-16 signalling (Evans et al., 2008b; Garsin et al., 2003; Gravato-Nobre and Hodgkin, 2005; Kawli and Tan, 2008). *daf-2* and *daf-16* mutants have altered antimicrobial signatures (Troemel et al., 2006), and worms mutant for the insulin-like receptor DAF-2 are pathogen-resistant, a phenotype that is dependent on DAF-16 (Garsin et al., 2003; Troemel et al., 2006). While DAF-2–DAF-16 signalling functions locally in the intestine in immunity (Evans et al., 2008a) it is also regulated

through the expression and secretion of neuronally secreted cues (Evans et al., 2008b; Kawli and Tan, 2008). One important negative regulator of immunity is *ins-7*, a neuronally expressed insulin-like peptide that is an agonist of DAF-2. During the course of an infection, *P. aeruginosa* partially subverts host defence by inducing the increased neuronal expression and secretion of INS-7 (Kawli and Tan, 2008), resulting in DAF-16 inhibition and a further increases in INS-7 through a positive-feedback mechanism (Murphy et al., 2003; Murphy et al., 2007). Structural proteins required for neurosecretion (e.g. *snb-1*/synaptobrevin, *unc-64*/syntaxin), are required for INS-7 secretion and are pathogen resistant, while negative regulators of neurosecretion (e.g. DGK-1/diacylglycerol kinase, GOA-1/Go alpha subunit) are pathogen-susceptible and have decreased levels of *ins-7* (Kawli and Tan, 2008). To test if *unc-53* affects *ins-7* production, qPCR was used to measure the *ins-7* transcript levels in *unc-53 (n152)* in the presence of *E. coli* and *P. aeruginosa*. *unc-53 (n152)* animals had increased *ins-7* RNA levels in non-pathogenic *E. coli* and pathogenic *P. aeruginosa* PA14 compared to wild-type (Figure 38A), evidence that *unc-53* negatively regulates *ins-7* at the RNA level.

To confirm an antagonistic role for *unc-53* on DAF-2 signalling genetically, double mutants were constructed between *unc-53 (n152)* and the strong loss of function mutant *daf-2 (e1370)* and the null mutant *ins-7 (ok1573)* and were subjected to *P. aeruginosa*. It was expected that if the function of *unc-53* is to limit DAF-2 signalling through INS-7, that double mutants with either *daf-2* or *ins-7* would completely suppress *unc-53*. Both *daf-2 (e1370)* and *ins-7 (ok1573)* suppressed the innate immunity defect of *unc-53 (n152)* (Figure 38B,C) but not to the level of either *ins-7* or *daf-2* alone. This could be interpreted to suggest that *unc-53* functions independently of DAF-2-DAF-16 signalling in innate immunity.

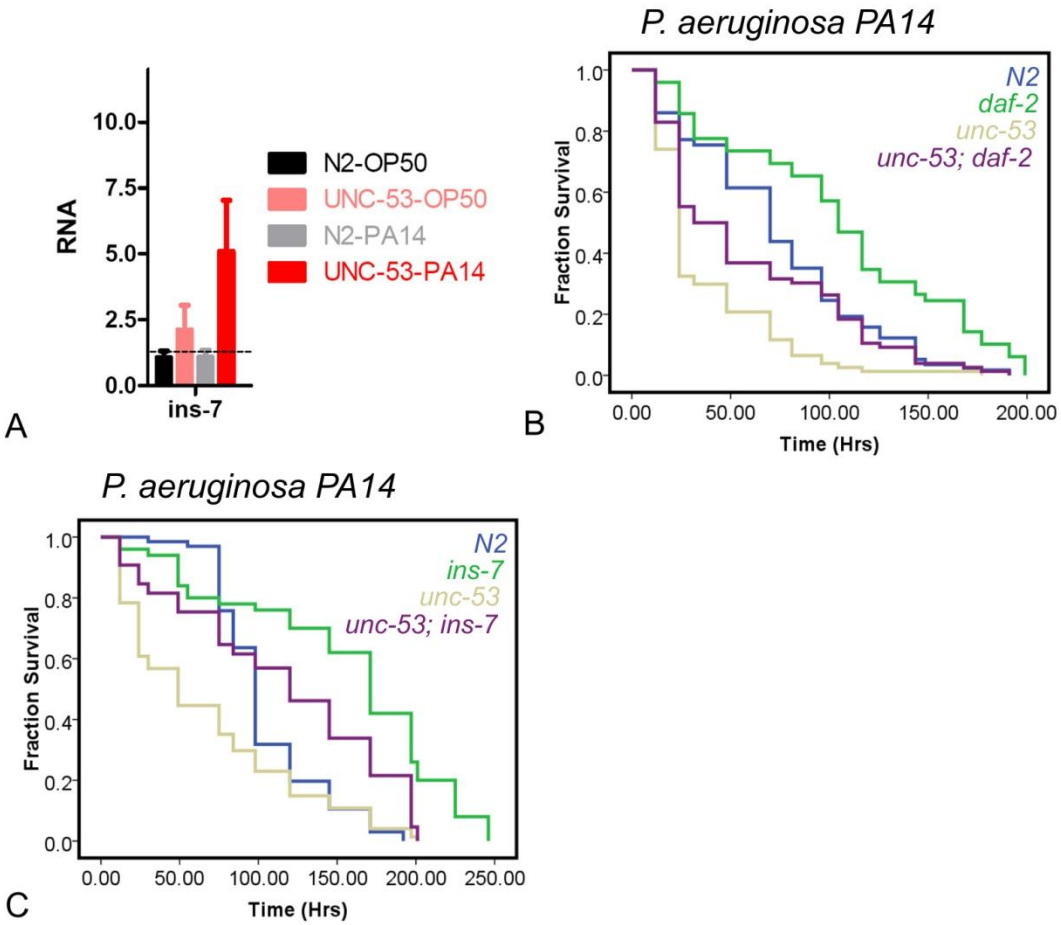

Figure 38. *unc-53* antagonizes DAF-2-DAF-16 signalling by limiting *ins-7* levels.

(A) qPCR was performed to measure levels of *ins-7* RNA. *unc-53 (n152)* and wild-type strains were grown in parallel on *E. coli* OP50 and were then treated to *E. coli* OP50 or *P. aeruginosa* PA14 for 12hrs as described (Kawli and Tan, 2008) (see Section 3.6.6). Expression was compared between *unc-53 (n152)* and wild-type which was grown in parallel. Depicted on the graph is the fold-change of RNA (y-axis labelled "RNA") in *unc-53 (n152)* compared to N2 animals exposed to *E. coli* OP50 which is normalized to "1". The fold changes represent the mean of three independent experiments using *mlc-1* to normalize RNA concentration (see Section 3.6.6). The fold changes represent the mean of three independent experiments. Expression levels of *ins-7* were significantly increased in *unc-53 (n152)* compared to wild type ($P<0.05$, one-tailed t-test). (B,C) Kaplan-Meier plots showing survival of *unc-53 (n152)* and wild-type animals compared to *unc-53 (n152); daf-2 (e1370)* (B) or *unc-53 (n152); ins-7 (ok1573)* (C). (B) *unc-53 (n152); daf-2 (e1370)* (n=103) animals live significantly longer than *unc-53 (n152)* (n=112) animals ($P<0.0001$) but not as long as *daf-2 (e1370)* (n=81), N2 (n=76). (C) *unc-53 (n152); ins-7 (ok1573)* (n=97) animals live significantly longer than *unc-53 (n152)* (n=82) animals ($P<0.0001$) but not as long as *ins-7 (ok1573)* (n=102), *N2* (n=68). These experiments were carried out in duplicate using *lin-60/cdc-25.1 (rnai)* for sterilization and

the combined data is shown. Statistics were carried out as described (see Section 3.6.2).

3.4.5 Recovery of cytoplasmic DAF-16 following heat-stress depends on *unc-53*

The expression of DAF-16 target genes is controlled through the translocation of cytoplasmic DAF-16 to the nucleus in response to upstream signalling cascades including DAF-2 (Garsin et al., 2003;Murphy et al., 2003) (see Figure 30). In normal growth conditions, the DAF-2 pathway is active and DAF-16 is phosphorylated and evenly distributed between the cytoplasm and nucleus throughout every tissue in the worm (Lin et al., 2001). Under conditions of decreased DAF-2 signalling or increased cellular stress (e.g. heat-stress), DAF-16 translocates to the nucleus. Following recovery from stress, or increased DAF-2 signalling, DAF-16 redistributes to the cytoplasm (Lin et al., 2001). Since *unc-53* decreases *ins-7* transcript levels *in vivo* and antagonizes *daf-2* and *ins-7*, it is expected that DAF-16 might relocalize to the cytoplasm more rapidly in *unc-53 (n152)* animals compared to wild-type following its nuclear localization from heat-stress. To examine the subcellular localization of DAF-16 the transgenic reporter strain TJ356 (*pdaf-16::daf-16::gfp)* expressing DAF-16::GFP was crossed into *unc-53 (n152)*. DAF-16-GFP is localized to the nucleus and cytoplasm in wild-type and *unc-53 (n152)* animals under normal growth conditions (Figure 39A,D) and localized to the nucleus following a brief heat-shock in both *unc-53 (n152)* and N2 (Figure 39B,E), showing that *unc-53* does not affect DAF-16 nuclear import in response to heat-stress. Following heat-shock the relocalization of DAF-16 to the cytoplasm was monitored over time (Figure 39C,F-G), and observed that DAF-16::GFP relocated to the cytoplasm in a majority of *unc-53* animals by 8hrs, whereas DAF-16-GFP was still primarily nuclear in wild-type worms (Figure 39G). The altered subcellular localization could not be rescued by expressing the F45E10.1a cDNA of *unc-53* under the control of the pan-neuronal promoter (*prab-3::unc-53*) (Figure 39G). These results suggest that while the maintenance of DAF-16-GFP in the nucleus following heat-stress is dependent on *unc-53*, this effect is not mediated by *unc-53* through its activity in neurons, or some other isoform or combination of isoforms is required neuronally to rescue this defect in *unc-53 (n152)*.

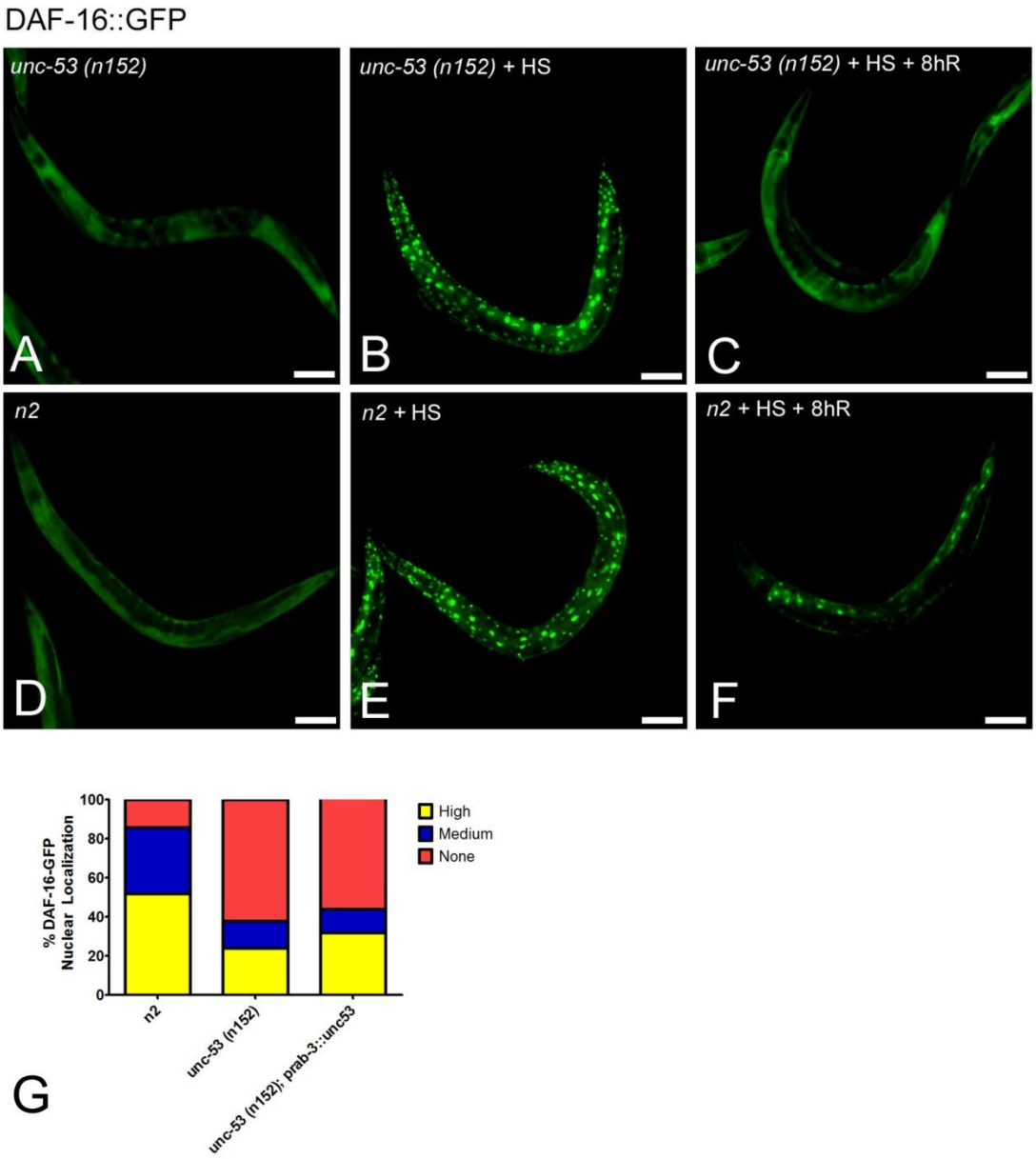

Figure 39. DAF-16-GFP is mislocalized following heat-stress in *unc-53 (n152)* mutants.

(A-F) *unc-53 (n152)* and wild-type (N2) animals carrying the *pdaf-16::daf-16::gfp* transgene grown (A,D), following heat-stress (B,E), and after 8hrs of recovery (C,F). DAF-16-GFP is found to be cytoplasmic in N2 and *unc-53 (n152)* in non-stress conditions (A,D) and exclusively nuclear immediately following heat-stress (B, E). After eight hours of recovery following heat-shock, DAF-16-GFP is primarily cytoplasmic in *unc-53 (n152)* (C) and high/medium in N2 (F). Scale bar is 100 μm. (G) Quantitation of the DAF-16-GFP nuclear localization in *unc-53 (n152)* and *N2* (n=100 worms per strain), and *unc-53 (n152); prab-3::unc-53* (n=102). Worms were classified as none, medium or

high with respect to their nuclear DAF-16-GFP localization as previously described (Kawli and Tan, 2008).

3.4.6 *unc-53 (n152)* does not enhance *pmk-1 (km25)*

The strong loss of function mutation *daf-2 (e1370)* and the null mutant *ins-7 (ok1573)* fail to completely suppress *unc-53 (n152)* (Figure 38), suggesting that *unc*-53 may function independently of *daf-2* and *ins-7*. The DAF-2-DAF-16 and PMK-1 pathways function independently (Troemel et al., 2006) so it is predicted that if *unc-53* functions exclusively in a DAF-16 pathway that it might enhance null mutants from the PMK-1 pathway. To test this hypothesis, double mutants between *unc-53 (n152)* and *pmk-1 (km25)* were constructed. The allele *pmk-1 (km25)* was chosen because it is a null allele and highly sensitive to *P. aeruginosa* (Kim et al., 2002). Double mutant *unc-53 (n152); pmk-1 (km25)* animals did not display enhanced *P. aeruginosa* susceptibility compared to *unc-53 (n152)* or *pmk-1 (km25)* alone. Several interpretations of this result are possible and further experiments are required to explain this finding. One possibility is that *unc-53* functions in both *daf-16* and *pmk-1* pathways.

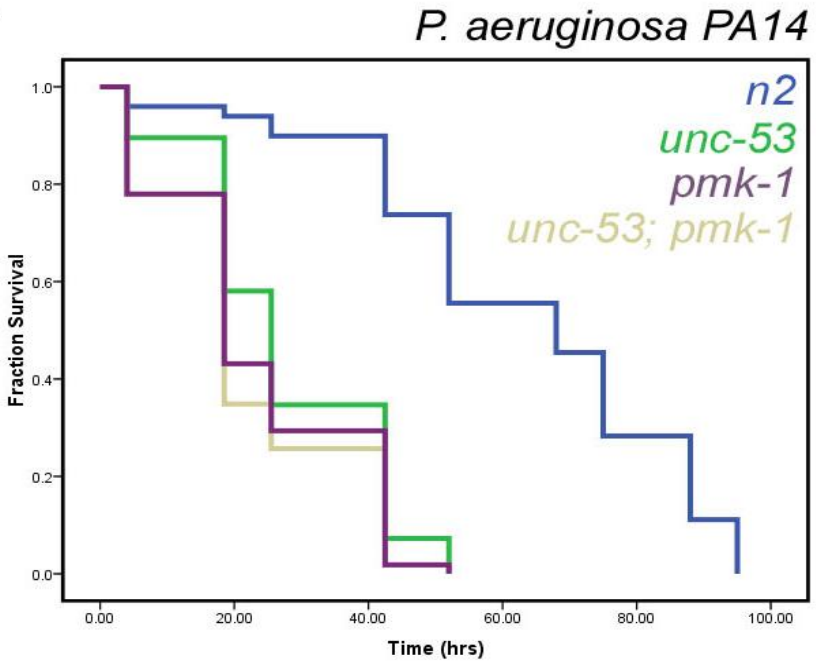

Figure 40. *unc-53 (n152)* does not enhance *pmk-1 (km25)*.

Indicated mutant and wild-type animals were exposed to *P.* aeruginosa. Statistically significant differences were observed between *unc-53 (n152)* (n=50)*, pmk-1 (km25)* (n=49) and *unc-53 (n152); pmk-1 (km25)* (n=45) compared to N2 (n=35) (P<0.0001), but *unc-53 (n152); pmk-1 (km25)* was not statistically different from *unc-53 (n152)* or *pmk-1 (km25)*. Representative experiment is shown. A minimum of two replicates were performed. All treatments were performed in the presence of FUDR (See Appendix 1 Table 11).

3.4.7 UNC-53 does not substantially influence the basal or inducible expression of a subset of antimicrobials from known immunity pathways

C. elegans mounts a response to pathogens through the constitutive and inducible expression of antimicrobial genes in tissues found in direct contact with invading pathogens: intestine, hypodermis, pharyngeal and rectal tissue, and numerous sensory neurons (Alper et al., 2007; Couillault et al., 2004; Shivers et al., 2009; Troemel et al., 2006). Microarray and quantitative PCR (qPCR) studies have shown that expression of a given antimicrobial may be under the control of either distinct or overlapping genetic pathways (Alper et al., 2007; Troemel et al., 2006). Given the observation that *unc-53* is required for a successful immune response to *P. aeruginosa*, the extent that *unc-53* altered antimicrobial expression was tested. Changes in

antimicrobial expression in *unc-53 (n152)* and *unc-53 (e404)* animals using qPCR to examine the relative expression of a small subset of six antimicrobials (*lys-1, lys-7, lys-8, clec-85, dod-22,* and *F55G11.7*) known to be under the control of the PMK-1, DBL-1/TGF-B, and DAF-2-DAF-16 pathways (Table 6 and Figure 41A) (Alper et al., 2007). Under the culture conditions used (see Section 3.6.6) *unc-53 (n152)* and *unc-53 (e404)* animals did not have significantly decreased expression of any of the tested antimicrobials in the presence of *E. coli* as a measure of basal antimicrobial expression in a non-pathogenic state or when exposed to *P. aeruginosa* (Figure 41B,C). The one exception was a significant increase in the expression of F55G11.7 in both *unc-53 (n152)* and *unc-53 (e404)* animals compared to wild-type when exposed to *E. coli* OP50-1 and *P. aeruginosa* PA14 (Figure 41C).

Table 6. Description of antimicrobial genes assayed on *E. coli* OP50 and *P. aeruginosa* in *unc-53* mutants.

Class	*Genes*	*Function*	*Selected Targets*
Lysozymes	*lys-1 – lys-10*	Cleavage of bacterial cell wall peptidoglycan	*lys-1*, *lys-7* and *lys-8*
CUB-like domain	~108 members	CUB-like domain, a domain found in diverse proteins, including the C1s and C1r complement peptidases	F55G11.7, *dod-22*
C-type Lectins	~278 members CTLD protein	Pathogen recognition	*clec-85*

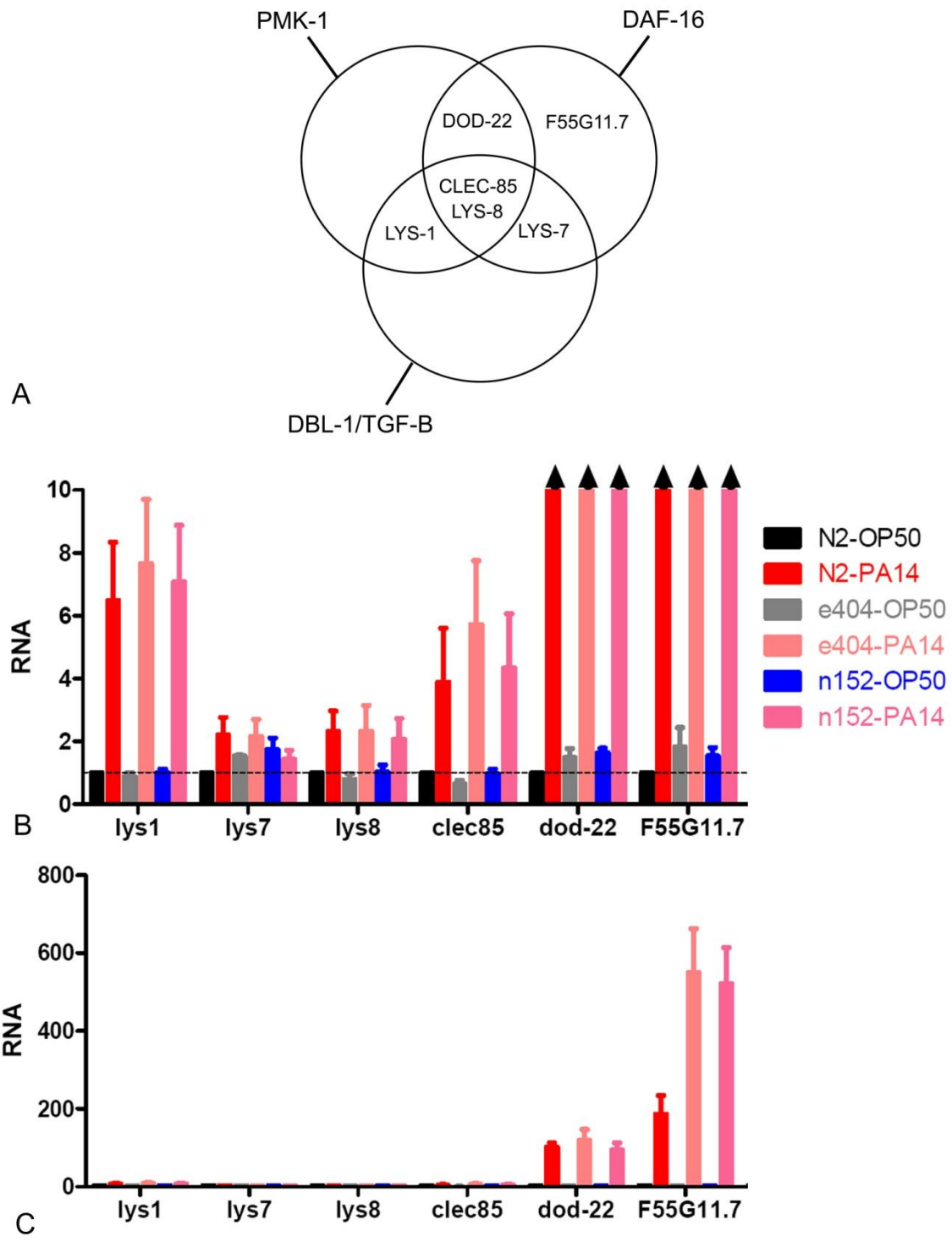

Figure 41. *unc-53* does not affect the basal or inducible expression of a subset of known antimicrobial genes.

(A) Venn diagram showing the antimicrobial genes assayed by qPCR in this study, as well as the genetic pathway(s) that control their expression (Alper et al., 2007). (B,C)

qPCR analysis of *unc-53 (n152)* and *unc-53 (e404)* mutant nematodes compared to wild-type N2 when exposed to *E. coli* OP50 or *P. aeruginosa* PA14 as indicated (see Section 3.6.6). Depicted on the graph is the fold-change of RNA (y-axis labelled "RNA") in *unc-53* compared to N2 animals exposed to *E. coli* OP50 which is normalized to "1". The fold changes represent the mean of three independent experiments using *mlc-1* to normalize RNA concentration (see Section 3.6.6). For each treatment, worms were prepared and treated as described and RNA was purified from each strain (see Section 3.6.6). Expression levels were not significantly different between mutant and wild type except for F55G11.7 when mutant *unc-53* animals were grown on *E. coli* OP50 or *P. aeruginosa* PA14 ($P<0.05$).

3.4.8 **UNC-53 microarray analysis**

To determine the underlying mechanism of *unc-53* function in innate immunity, transcriptional profiling (Genomics and Microarray Core, University of Colorado, Denver) using full genome oligonucleotide microarrays (Agilent) was performed to examine the genes upregulated and downregulated in *unc-53 (n152)* and wild-type (N2) animals in the presence of *E. coli OP50-1* and *P. aeruginosa PA14*. For each treatment, animals were grown from a synchronized egg population to the late-L4/young adult stage on *E. coli OP50-1* for 48hrs at 20°C and were transferred to either fresh *E. coli OP50-1* or *P. aeruginosa PA14* for 12hrs followed by harvesting for total RNA. Two day old adults were chosen to match previous experiments examining changes in *ins-7* RNA levels (Kawli and Tan, 2008). N2 animals treated to *P. aeruginosa PA14* had 352 transcripts altered compared to *E. coli OP50-1* treated N2 animals at a 5% FDR (False Discovery Rate) (see Appendix 2 Table 17 for a full list of transcripts). Of these transcripts, 138 were upregulated > 2-fold in the presence of *P. aeruginosa* and 144 were downregulated > 2-fold, indicating that a substantial number of genes are induced and suppressed in the context of a *P. aeruginosa PA14* infection in *C. elegans*. A statistically significant overlap in the genes altered in the presence of *P. aeruginosa* PA14 in this study to a previous microarray study examining transcriptional changes in the presence of *P. aeruginosa* PA14 in adult N2 animals at 8hrs (477 altered transcripts total, 49/477 overlap (see Table 19 for a list of the overlapping genes) vs. 7/477 in a random control-set, $p<0.0001$) (Troemel et al., 2006). This suggests that the data generated from the microarray experiments should serve as an appropriate tool to investigate pathogen-induced changes. It should be noted that while the overlap between this study and Troemel *et al.* (2006) is statistically significant, that only a small number of genes overlap between the two studies (49/352, ~14%). Other studies aimed at investigating *P. aeruginosa* also note limited numbers of overlapping genes (<20%) (Shapira and Tan,

2008; Troemel et al., 2006). This may be an indication of differences in experimental setup including factors such as induction times and culture conditions, the microarray platforms used, and inherent limitations in microarray technology (Jordan, 2004; Larkin et al., 2005; Wong et al., 2007).

3.4.9 Pseudomonas aeruginosa PA14 downregulated genes in *unc-53 (n152)*:

154 genes were exclusively altered in *unc-53 (n152)* mutants compared to N2 in the presence of *P. aeruginosa PA14* and in the absence of a fold-change restriction (Figure 42; see Appendix 2 Table 18 for a full list of the genes). Of this group, nineteen were downregulated > 2-fold (Table 7). Several of these genes (36.8%, 7/19) were previously identified as having altered expression in the presence of a pathogen (Mallo et al., 2002; O'Rourke et al., 2006; Pujol et al., 2008; Shapira et al., 2006; Wong et al., 2007) and 26.3% (5/19) were osmotically regulated (Rohlfing et al., 2010). Four of the osmotically regulated genes were also pathogen regulated, suggesting a concordance between the transcription of relevant pathogen-sensitive and osmosensitive genes for *unc-53* as previously described in innate immunity generally (Rohlfing et al., 2010). None of these pathogen-altered genes were previously identified as being under the control of either the *pmk-1* or *daf-16* (Troemel et al., 2006). We grouped the 19 genes into several categories based on their wormbase annotations (WS190), Interpro GO Mapping (Biological Processes, Molecular function) annotations, domain structure (http://genome.sfu.ca/gexplore), BLASTP homology matches, and published *C. elegans* function. A majority of the genes (7/19, 36.8%) were categorized as 'Unknown' because they had no known function or clear homology, and were previously uncharacterized. The other broadly defined groups that were found, in order of frequency, were (i) Transporters (5/19, 26.3%), (ii) Cell signalling (4/19, 21.1%), (iii) Metabolism (2/19, 10.5%) and (iv) Secreted (1/19, 5.3%).

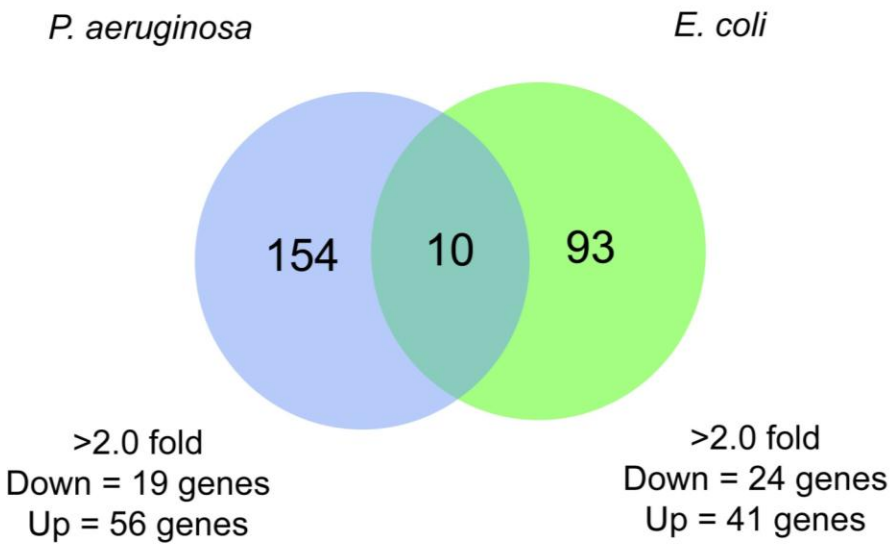

Figure 42. Venn diagram summarizing number of genes with altered expression in *unc-53 (n152)* grown on *P. aeruginosa* PA14 and *E. coli* OP50-1

unc-53 (n152) and N2 animals were exposed to *P. aeruginosa* PA14 and *E. coli* OP50-1 and total RNA was collected and examined for gene expression changes by microarray as described (see Section 3.6.7). The number of genes with expression changes in the absence of a fold-change restriction in *unc-53 (n152)* compared to N2 exposed to either *P. aeruginosa* PA14 (blue) or *E. coli* OP50-1 (green) as well as overlapping genes (centre of the Venn diagram) is indicated. The number of genes upregulated and downregulated >2-fold in these groups is given below.

Transporters: Of the several transporters identified in this study (Table 7), only *hmit-1.1* and *aqp-8* have been investigated in *C. elegans*. *hmit-1.1* is one of three *C. elegans* homologs (along with *hmit-1.2* and *hmit-1.3*) of the HMIT family of myo-inositol osmolyte transporters (Kage-Nakadai et al., 2011), and exhibited the largest fold-change in expression in *unc-53 (n152)* (14.9 fold). The expression of *hmit-1.1* has been previously observed to be dowregulated in the presence of *P. aeruginosa* PA14 compared to non-pathogenic bacteria (*E. coli OP50* or *P. aeruginosa gacA* mutants) (Troemel et al., 2006), and *hmit-1.1* expression is also altered under conditions of osmotic stress where it functions in adaptation to hyperosmotic environments (Kage-Nakadai et al., 2011). The *hmit* genes have an expression pattern that is similar to *unc-53*. *hmit-1.1* is expressed exclusively in the intestine where it localizes to the lumenal

membrane, while *hmit-1.2* and *hmit-1.3* are expressed in the excretory cell (Kage-Nakadai et al., 2011).

The other described transporter downregulated in *unc-53 (n152)* was the channel protein *aqp-8*, one member of the aquaglyceroporin family of genes (*aqp-1, aqp-2, aqp-3, aqp-7*) that transports water and glycerol across membranes (Huang et al., 2007). *aqp-8* is also pathogen and osmotically-regulated (Rohlfing et al., 2010) and is required along with the other aquaglyceroporins for recovery from osmotic stress (Huang et al., 2007). Of particular interest is that *aqp-8* is expressed exclusively in the excretory cell and that its expression through development is mediated by the POU homeodomain transcription factor CEH-6 (Mah et al., 2007; Mah et al., 2010) which controls the expression of many excretory cell expressed genes (Burglin and Ruvkun, 2001). Given that *unc-53* functions cell-autonomously in the excretory cell (Schmidt et al., 2009; Stringham et al., 2002), and *aqp-8* is only expressed there, it is expected that *unc-53* may affect *aqp-8* expression through its effects within the excretory cell. *aqp-8* is also predicted to interact with the gene R11F4.1/glycerol kinase, which is upregulated (1.56-fold) in *unc-53 (n152)* mutants in the presence of *P. aeruginosa* PA14.

Cell signalling: This group includes several genes encoding Serpentine-type seven-pass transmembrane receptor G-protein coupled receptors, including two members from class-G (*srg-19* and *srg-40*) as well as *srh-268* that is a member of the class-H. Their shared homology to the larger family of chemoreceptors suggests that they play a conserved role in chemosensation and may be relevant in controlling *C. elegans* response to environmental stimuli including pathogen responses (Robertson and Thomas, 2006; Thomas and Robertson, 2008). The other member of this group was *arrd-3*, which encodes a protein predicted to belong to the Arrestin family, a group of multifunctional adaptor proteins that regulate signal transduction and have been most well described in their role in the silencing of GPCR signalling (Shukla et al., 2011). The *arrd-3* paralog *arr-1* regulates chemotactic signalling with subsequent defects in olfaction and chemosensation in *C. elegans*. *arr-1* positively regulates *daf-2* signalling, and *arr-1* mutant animals have increased longevity together with increased DAF-16 nuclear localization (Palmitessa and Benovic, 2010).

Metabolism: Two genes were downregulated in *unc-53 (n152)* that are predicted to be involved in metabolic processes. This group consists of F45E1.4 which is a haloacid dehalogenase-like hydrolase and *fmo-2/fmo-12* which encodes a flavin-containing monoxygenase that is osmotically-regulated and was previously found to be upregulated in the presence of *E. faecalis* and *S. aureus* (Irazoqui et al., 2010a; Wong et al., 2007). *fmo-2* expression in *S. aureus* is dependent on *bar-1* and *egl-5*, and functions independently of *pmk-1* and *daf-16* (Irazoqui et al., 2008). *In vivo* expression of *fmo-2* is found in intestinal cells along with additional expression in unidentified cells near the excretory gland (Petalcorin et al., 2005). Of potential interest is that the expression of *fmo-2* is regulated by hypoxia under the direct-control of the hypoxia-inducible factor *hif-1* (Shen et al., 2005). HIF-1 is regulated by EGL-9, an interactor of the N-terminus of UNC-53 (Adeleye, 2002). *tbx-33* is another gene under the control of *hif-1* (Shen et al., 2005) that is slightly downregulated by *unc-53 (n152)* (-1.87 fold).

Secreted: Only a single gene known to encode a secreted protein (*clec-167*) was observed to be downregulated greater than 2-fold in *unc-53 (n512)* in the presence of *P. aeruginosa* PA14. *clec-167* contains a C-type lectin domain and has been observed to be upregulated in *S. marcescens* (Wong et al., 2007), and may function similarly to the other known C-lectins in pathogen recognition or binding as previously described (Schulenburg et al., 2008).

Table 7 . Genes downregulated >2 fold in *unc-53 (n152)* mutants compared to N2 exposed to *P. aeruginosa PA14*

Systematic Name	*Basic Description*	*Group/Class*	*p-value*	*Fold-Change*	*Pathogen Regulated?‡*	*Osmotically Regulated?£*
Y51A2D.4†	hmit-1.1, H(+) Myo-Inositol Cotransporter	Transport	0.000401639	-14.9274	Yes	Yes
F45E1.4†	Haloacid dehalogenase-like hydrolase	Metabolism	0.000649957	-6.46482		Yes
K08C7.5	fmo-2/fmo-12, Flavin-containing monooxygenase	Metabolism	0.000101609	-4.83386	Yes	Yes
C04H5.9	Unknown	Unknown	0.000538223	-4.26948		
K02G10.7b	aqp-8, Aquaglyceroporin	Transport	0.000910824	-3.67548	Yes	Yes
W05E10.1	Predicted transporter/transmembrane protein	Transport	0.000741447	-3.43857	Yes	
H03G16.3	Unknown	Unknown	0.000424573	-2.90386		
F59A6.11	Unknown	Unknown	0.00081436	-2.83856		
T19C4.4	srg-40, Serpentine receptor, class G	Signalling	0.000884343	-2.55397		
M176.1	arrd-3, Arrestin domain containing protein	Signalling	0.000664266	-2.51724		
C46F2.1	Unknown	Unknown	3.93E-05	-2.44153	Yes	Yes
C54F6.1	srh-268, Serpentine receptor, class H	Signalling	0.000915937	-2.44049		
F38A1.4	clec-167, C-type Lectin	Secreted	0.000957943	-2.38218	Yes	
Y57G11*C*.44	Sodium channel protein	Transport	0.000268582	-2.34844		
Y105C5A.11	srg-19, Serpentine receptor, class G	Signalling	0.000720201	-2.28509		
K10C2.6	Unknown	Unknown	0.000461374	-2.25945		
T15B7.7	Unknown	Unknown	2.06E-05	-2.11393	Yes	
F32H5.4	Synaptic vesicle transporter (SVOP)	Transport	0.000406292	-2.09703		
C50A2.2	Unknown	Unknown	0.000412256	-2.00452		

†Indicates that the gene was tested for an altered pathogen response by RNAi. ‡Indicates that the gene was previous identified to be pathogen regulated and a blank indicates that no reference was found (Mallo et al., 2002; O'Rourke et al., 2006; Pujol et al., 2008; Shapira et al., 2006; Wong et al., 2007) with details available at www.wormbase.org. £ Indicates osmotic regulation (Rohlfing et al., 2010)

3.4.10 *Pseudomonas aeruginosa* PA14 upregulated genes in *unc-53 (n152)*:

Fifty six genes were upregulated > 2-fold in the presence of *P. aeruginosa PA14* in *unc-53 (n152)* mutants compared to N2 animals (Table 8). Similarly to the genes observed to be downregulated in *unc-53 (n152)* in the presence of *P. aeruginosa*, the largest group of upregulated genes could be classified as 'Unknown' (23/56, 39.3%).

Cell signalling: This is the largest category of genes upregulated in *unc-53 (n152)* compared to N2 when subjected to *P. aeruginosa PA14* (15/56, 26.8%), and several of the identified genes have potential or defined roles in innate immunity. The majority of the genes identified were serpentine-type seven transmembrane receptors, and three of these genes (*str-196*, *srh-72*, *srh-10*) have predicted 7TM olfactory type-receptors (Robertson and Thomas, 2006; Thomas and Robertson, 2008). By homology, this group is expected to control the perception of chemical stimuli and responses to environmental stimuli including potentially pathogens. Two nuclear hormone receptors were also identified (*nhr-258* and *nhr-141*). *nhr-258* was previously identified to function downstream of *let-60/Ras* (Romagnolo et al., 2002), and *unc-53* has been previously implicated in *let-60* signalling (Chen et al., 1997). The sole *C. elegans* TRAF homolog *trf-1* is upregulated in *unc-53 (n152)* compared to N2 (2.4 fold) on *P.aeruginosa*. TRAF proteins function downstream of mammalian TLR signalling to NF-κB (Kawai and Akira, 2007). An additional cell-signalling molecule identified in the microarray was *shc-1.* SHC-1 is an adaptor protein containing a PTB and an SH2 domain that is required for aging and various forms of cellular stress (Neumann-Haefelin et al., 2008). SHC-1 binds MEK-1 and acts a scaffold for JNK-1 MAPK signalling (Neumann-Haefelin et al., 2008). At the same time it also binds DAF-2 and promotes DAF-16 nuclear localization (Mizuno et al., 2008), so it appears that SHC-1 functions in both insuling signalling and JNK pathways, upstream of DAF-2 and MEK-1 respectively (Mizuno et al., 2008; Neumann-Haefelin et al., 2008). Two other proteins identified as being upregulated in *unc-53 (n152)* were the genes *abu-7* and *pqn-5*. Interestingly these proteins were idenfied as upregulated in the context of a blocked unfolded protein response (UPR) in the ER, and ABU-7 and PQN-5 may helped to protect the organism from improperly folded proteins (Viswanathan et al., 2005). Both of these genes are under the control of the transcription factor CED-1, and lack of either protein results in increase susceptibility to

pathogens (Haskins et al., 2008). The increased expression of these genes in *unc-53 (n152)* could be interpreted to suggest that *unc-53* is involved in the UPR response as a negative regulator, or that increased damage due to *unc-53* activity could result in increased UPR activation as a secondary consequence.

Metabolism: Several metabolic genes were identified in these microarray experiment that were upregulated in *unc-53 (n152)* compared to N2 in the presence of PA14 (7/56, 12.5%). A majority of these genes (5/7, 71.4%) were previously identified as pathogen-altered (Mallo et al., 2002; O'Rourke et al., 2006; Pujol et al., 2008; Shapira et al., 2006; Wong et al., 2007). One gene of interest, *gln-3,* is a glutamine sythetase which catalyzes the formation of glutamine through the condensation of glutamate and ammonia. *gln-3* that interacts with *ugt-3* (ref), an interactor of *swan-1*. SWAN-1 interacts with EGL-9 (Shao et al., 2010), an UNC-53 interacting protein (Adeleye, 2002). Another interesting interactor is the threonine/serine dyhydratase K01C8.1 that interact with *klp-11* which is a kinesin-like protein that is required for intraflagellar transport and functions in the IFTB pathway (Khan et al., 2000).

Secreted: Six genes were upregulated that could be described as secreted proteins (6/56, 10.7%), and several are expected to function in innate immunity. Two genes were identified that belong to the C-lectin family (*clec-76* and *clec-181*). The more strongly upregulated of the two was *clec-76,* and both *clec-76* and *clec-181* have not been described so far in *C. elegans*, but by homology may function in pathogen detection or clearance (Schulenburg et al., 2008). A second gene upregulated in these experiments was *nlp-27*, a neuropeptide-like protein that is part of a larger family that makes up a conserved syntenic cluster referred to as the *nlp-29* cluster that is upregulated in the presence of the fungus *D. Coniospora* as well as wounding, and is expressed independently of *pmk-1* (Pujol et al., 2008). Another gene observed to be upregulated in this study in *unc-53 (n152) was* cnc-*5 a canaecin* protein that by homology with other canaecins may possess antimicrobial properties. Two other secreted genes observed in this study include an uncharacterized secreted protein rich in cysteines (R11D1.3), and a nematode specific peptide of the E family (*nspe-1*).

Transporters: Unlike the down-regulated gene group, only a few genes that could be classified as transporters that were upregulated in *unc-53 (n152)* in the

presence of *P. aeruginosa* PA14 (3/56, 5.3%). One of these genes was *amt-4* which is an ammonium ion transporters that was previously shown to be downregulated in *P. aeruginosa* PA14 but in this study was upregulated by *unc-53 (n152)* in the presence of *P. aeruginosa.* This gene is osmotically regulated (Rohlfing et al., 2010) as observed for some other transporters, and *amt-4* was identified as a suppressor of the *unc-53* interacting protein EGL-9 . Another transporter observed in this study was the inhibitory GABA-type ligand-gated ion channel *lgc-35* (Jorgensen, 2005).

Structural: Two structural genes were also identified in the microarray studies: a collagen molecule *col-10* and a mucin/alpha-tectorin protein (R09E10.5).

Table 8. Genes upregulated >2 fold in *unc-53 (n152)* mutants compared to N2 exposed to *P. aeruginosa PA14*

Systematic Name	Basic Description	Group/Class	p-value	Fold-Change	Pathogen Regulated ?	Osmotically Regulated ?
C45B2.3†	Unknown	Unknown	0.000735293	26.2228		
C26B2.4†	nhr-258, Nuclear hormone receptor family	Cell signalling	0.000132614	5.7644		
F59C6.7	che-13, IFT57/Hippi homolog	Cell signalling	0.000576771	5.28407	Yes	
Y46C8AR.1	clec-76, C-type lectin	Secreted	0.000157289	5.18117	Yes	
F46F2.5	Unknown	Unknown	1.38E-05	4.81268		
M195.2	Unknown	Unknown	7.70E-06	4.6379		
F59A1.6	Unknown	Unknown	0.000496737	4.62832	Yes	
B0213.2	nlp-27, Neuropeptide-like protein	Secreted	0.000572301	4.33961	Yes	
T07C12.5	srj-34, Serpentine receptor, class J	Cell signalling	7.06E-06	3.93719		
F54A5.3c	shc-1, Src Homology Ortholog	Cell signalling	0.000568278	3.92416		
R09B5.10	cnc-5, Caenacin peptide	Secreted	0.000479612	3.76533	Yes	
C37H5.11	cwp-2, Co-expressed with polycystins	Cell signalling	0.000983243	3.75213		
T19B10.2	Unknown	Unknown	0.000384331	3.70378	Yes	Yes
K01C8.1	Threonine/serine dehydratases	Metabolic	0.000983347	3.64681	Yes	Yes
R11D1.3	Secreted protein with conserved cysteines	Secreted	0.000252767	3.56282	Yes	
C36C9.6	Unknown	Unknown	0.000201862	3.53192		
T01G6.3	str-196, Serpentine receptor, class T	Cell signalling	0.00027226	3.4988	Yes	
Y38C1AA.1b	Predicted phosphate acyltransferases	Metabolic	0.000246903	3.46198		
T08G5.8	Unknown	Unknown	0.000311096	3.40684		
F29F11.5a	ceh-22, NK-2 family homeodomain factor	Trans- factor	0.000145401	3.3994		
ZC204.5	srh-72, Serpentine receptor, class H	Cell signalling	0.000645266	3.30247		
Y46G5A.26	lgc-35, Ligand-gated channel, GABA receptor	Transporter	0.000802351	3.24845		

W05B10.3	Unknown	Unknown	0.000182296	3.19486		
H19N07.3	Unknown	Unknown	0.000348684	3.12676		
F25E5.6b	nhr-141, Nuclear hormone receptor family	Cell signalling	0.000465895	3.04493		
Y18D10A.2	Unknown	Unknown	0.000113034	3.04417	Yes	
Y7A5A.3	Predicted IFN-y induced thiol reductase	Metabolic	0.000113083	3.03502	Yes	
Y105C5B.28	gln-3, Glutamine synthase	Metabolic	4.49E-06	2.85341	Yes	
F08C6.5	Oxoacid dehydrogenase	Metabolic	0.000118531	2.82111	Yes	
C09E9.1	Unknown	Unknown	0.000688365	2.80404		
C08A9.3a	Unknown	Unknown	0.000148419	2.76977	Yes	
Y38E10A.13	nspe-1, Nematode specific peptide family, E	Secreted	0.000164495	2.75884		
C05E11.5	amt-4, Ammonium transporter homolog	Transporter	3.30E-05	2.6813	Yes	Yes
Y59H11AR.5	clec-181, C-type lectin	Secreted	0.000404315	2.67641		
Y38A10A.3	srh-10, Serpentine receptor, class H	Cell signalling	0.00044363	2.63881		
C55C3.7	Unknown	Unknown	0.000637795	2.61855		
R04B5.5	Sorbitol dehydrogenase	Metabolic	0.000940211	2.5619		
T27E4.5	Unknown	Unknown	0.000904227	2.52347		Yes
Y41C4A.13	Unknown	Unknown	0.000371164	2.51889		Yes
F45G2.6	trf-1, TRAF homologous protein	Cell signalling	0.000878618	2.44108	Yes	
F18E3.9	srw-78, Serpentine receptor, class W	Cell signalling	0.000744675	2.43772		
C03A7.8	abu-7, Activated in Blocked UPR	Cell signalling	6.01E-05	2.37264		Yes
R09E10.5	Mucin/alpha-tectorin	Structural	0.000113249	2.34388		
Y105C5A.17	Unknown	Unknown	7.46E-05	2.30158		
Y55F3C.8	srt-24, Serpentine receptor, class T	Cell signalling	0.000331249	2.29345		
Y38H6C.21	Unknown	Unknown	0.000107989	2.27101	Yes	
B0222.8	col-10, collagen	Structural	0.0006114	2.2557		Yes
Y102A5C.10	fbxa-204, F-box containing protein	Unknown	7.74E-05	2.24131		
C17H1.10	Unknown	Unknown	0.000223938	2.20715		
T19A6.4	Unknown	Unknown	0.000496829	2.2063		

Y7A9C.4	srz-39, Serpentine receptor, class Z	Cell signalling	0.000336474	2.15328		
C03A7.4	pqn-5, Prion-like-(Q/N-rich)-domain	Cell signalling	4.76E-05	2.11369		Yes
K10D11.2	Unknown	Unknown	0.000198915	2.09067	Yes	
R10F2.5	Organic solute carrier protein	Transporter	0.00045402	2.08642		
Y64G10A.2	Unknown	Unknown	0.000423566	2.02761		
T26C5.5	Unknown	Unknown	4.09E-05	2.02174		

†Indicates that the gene was tested for an altered pathogen response by RNAi. ‡Indicates that the gene was previous identified to be pathogen regulated and a blank indicates that no reference was found (Mallo et al., 2002; O'Rourke et al., 2006; Pujol et al., 2008; Shapira et al., 2006; Wong et al., 2007) with details available at www.wormbase.org. £ Indicates osmotic regulation (Rohlfing et al., 2010).

3.4.11 Genes commonly altered in *unc-53 (n152)* mutants subjected to *P. aeruginosa PA14* or *E. coli OP50*

The expression of a small subset of genes was altered in *unc-53 (152)* mutants independently of whether they were grown in the presence of *E. coli OP50-1* or *P. aeruginosa PA14*. Of the ten genes identified, four were downregulated and 6 were upregulated, and the direction of the altered expression was the same between both bacteria used. The most strongly downregulated gene (Y111B2A.9, -28.8 fold in PA14 and -21.3 fold in OP50-1) has not yet been examined in *C. elegans* and lacks clear homologs in other organisms. The three other downregulated genes (*her-1*, *pdr-1, tpk-1*) have been previously studied. *her-1* encodes a small cysteine rich secreted gene that is nematode-specific and is required for sex-determination in wild-type male XO animals (Perry et al., 1993). *tpk-1* was also downregulated, and is a *C. elegans* thiamine pyrophosphate kinase that converts thiamine (Vitamin B1) to TPP (Thiamine pyrophosphate). *tpk-1* was originally isolated in a screen for mutants with decreased development and slowed aging (de Jong et al., 2004). One gene of interest that was identified in this microarray study was *pdr-1*, the worm homolog of human PARKIN (PARK2) that is the causative gene of the autosomal recessive juvenile forms of Parkinson's disease (Springer et al., 2005). *pdr-1* is an E3 ubiquitin ligase that functions in the ubiquitin-proteosome system for the removal of unwanted proteins and was isolated in a screen for mutants unable to clear alpha-synuclein, a hallmark feature of many neurodegenerative diseases like Alzheimer's and Parkinson's disease (Springer et al., 2005; Vartiainen et al., 2006).

Of the six genes upregulated in both bacteria, two were classified as unknown, three were classified as metabolic, and one gene was a transporter (Table 9). The transporter gene identified here as upregulated in *unc-53 (n152)* in both *E. coli* and *P. aeruginosa* was T28F2.7, one of 23 degenerin family genes that exists in *C. elegans*. T28F2.7 was the most upregulated of all the genes examined in the microarray (277.3 fold in *P. aeruginosa* PA14, 371.8 fold in *E. coli* OP50). Degenerins are members of an ion channel subunit superfamily that encode amiloride-sensitive sodium ion channels that are important in many diverse processes ranging from sensory perception to water balance and homeostasis (Kellenberger and Schild, 2002). The three metabolic genes

isolated in this microarray as downregulated in *unc-53 (n152)* include an Asparaginase (C27A7.5c), a Fructose-6-phosphate kinase (Y110A7A.6b.1), and a Serine-Proteinase Inhibitor (Y49G5A.1), none of which have been studied in *C. elegans.*

Table 9. Genes altered >2 fold in *unc-53 (n152)* mutants compared to N2 exposed to *P. aeruginosa PA14* and *E. coli OP50*

Systematic Name	*Basic Description*	*p-value (unc-53 mut Pseudomonas vs. wild type Pseudomonas)*	*Fold-Change (unc-53 mut Pseudomonas vs. wild type Pseudomonas)*	*p-value (unc-53 mutant E. coli vs. wild type E. Coli)*	*Fold-Change (unc-53 mutant E. coli vs. wild type E. Coli)*
Y111B2A.9a‡	Unknown	1.41E-06	-28.876	0.000253539	-21.3355
ZK287.8b‡	her-1, Small secreted cyteine rich	0.000963004	-3.85058	0.000194816	-3.94555
K08E3.7.2	pdr-1, Parkinson's disease related	0.000868464	-1.81877	0.000502037	-2.15174
ZK637.9b	tpk-1, Thiamine phosphokinase	0.000919628	-1.46765	0.000822776	-1.48923
C27A7.5c	Asparaginase	0.000456583	1.97452	0.000543349	1.76447
F31F6.8	Unknown	1.88E-05	2.28208	0.000432105	2.87739
Y110A7A.6b.1	Fructose-6-phosphate 2-kinase	0.000672285	3.84282	3.94E-05	4.66766
F26A1.8	Unknown	0.000218727	7.8084	0.000381564	9.18129
Y49G5A.1†	Serine proteinase inhibitor	2.48E-05	15.3456	0.000692682	19.2554
T28F2.7†	Degenerin	0.000218393	277.329	5.06E-05	371.841

†Indicates that it was tested for an altered pathogen response by RNAi. ‡Indicates that the RNAi clone was not available.

3.4.12 **Ingenuity Pathway Analysis of microarray candidate genes**

As a way to determine the relevance of the candidates obtained from the microarray experiments, the mammalian orthologs from the various *C. elegans* datasets were analyzed using Ingenuity Pathways Analysis (IPA, Ingenuity Systems). In the IPA networks application, a data set containing candidate gene identifiers and corresponding expression values is uploaded into the IPA application, and each identifier is mapped to a corresponding object in the Ingenuity Knowledge Database. Entered gene candidates are then superimposed onto a large-scale network of molecules developed from information contained in the IPA knowledge base, and interacting networks are generated using algorithms that determine interactions between candidate genes and among database genes based on their connectivity, and a statistical significance score is given. Graphical molecular network representations are then generated that depict genes or their products as nodes, and the biological relationship between two nodes is represented as an edge (line) (Ingenuity Systems Inc.) (Figure 43).

The top-ranking network (Score 24, p-value=1.0 x 10^{-24}) comparing *unc-53 (n152)* to N2 on *P. aeruginosa* is presented , and was comprised of 11 focus molecules from the empirically derived data combined with 35 molecules from the IPA database (Figure 43). The top functions derived from the IPA networks were “Hematological System Development and Function”, and “Cell Death”. Several of the genes identified in this network (Network ID#1, Table 10) were previously determined to function in innate immunity in other systems. Central to the IPA derived network are the NF-κB complex, TRAF6, TNF-alpha receptors, RIP1. The *Drosophila* homolog *Sickie* was previously observed to function in the IMD pathway that is homologous to the TNF-α/RIP1 signalling cascade (Foley and O'Farrell, 2004).

Table 10. UNC-53 Network #1 Candidate Genes Isolated by IPA analysis

ID	*Molecules in Network*	*Score*	*Focus Molecules*
1	Act1, AHCY, ARRB1, BCL2, BRAF, CD27, CTNNB1, DAK, IFNB1, IFT57, LTBR, Macf1, NFATC2IP, NFkB (complex), NFkB (family), PARK2, PFKFB3, RBM5, RIPK4,	24	11

	RS1, SARM1, STAP2, TMEM68, TNFRSF4, TNFRSF8, TNFRSF9, TNFRSF17, TNFRSF18, TNFRSF19, TNFRSF13B, TRAF5, TRAF6, TRAF5/6, TRAIP, ZFP36

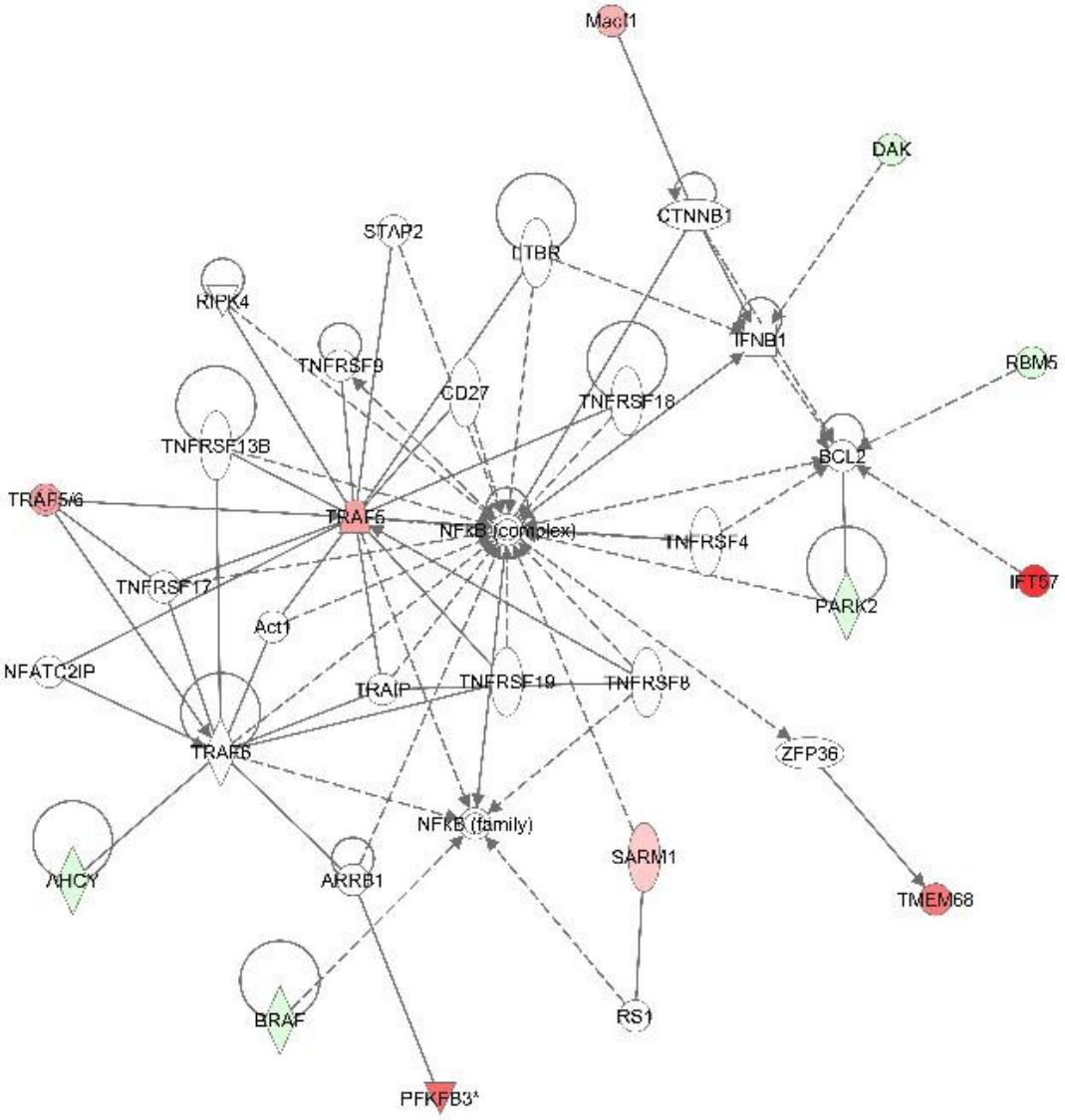

Figure 43. UNC-53 Network #1 derived from IPA analysis comparing the *P. aeruginosa* PA14 altered genes between *unc-53 (n152)* and N2.

IPA analysis was conducted using gene candidates derived from the *unc-53 (n152)* microarray comparing mutants to N2 when exposed to *P. aeruginosa*. The candidate gene mammalian homologs are shown. Colored symbols are genes that were isolated from the microarray experiment (Red is downregulated and green is upregulated) and additional proteins were derived from the IPA database. Solid lines imply direct

relationships between proteins; dashed lines imply indirect interactions (Ingenuity Systems Inc.)

3.4.13 **Immunity assays of candidate genes**

It is predicted that relevant candidate genes isolated from the microarray experiments comparing *unc-53* mutant to wild-type animals exposed to *P. aeruginosa* and *E. coli* may exhibit altered pathogen susceptibility. As a result a small number of candidates that were most altered in their expression in *unc-53 (n152)* mutants compared to wild-type when exposed to *E. coli* and *P. aeruginosa* or both bacteria (top two from each category) were tested. RNAi clones were not available for Y111B2A.9a or *her-1* but the other candidate genes (*hmit-1.1*, F45E1.4, C45B2.3, *nhr-258*, Y49G5A.1, and T28F2.7) (Table 7, Table 8, Table 9) were analyzed. RNAi feeding did not reveal a pathogen susceptibility phenotype (Figure 44) for any of the genes tested, though for some of these genes (e.g. *hmit-1.1*) functional redundancy may account for the lack of an effect (Kage-Nakadai et al., 2011). We also decided to test the *unc-53* interacting gene *abi-1* by RNAi and found that it was pathogen sensitive (Figure 45).

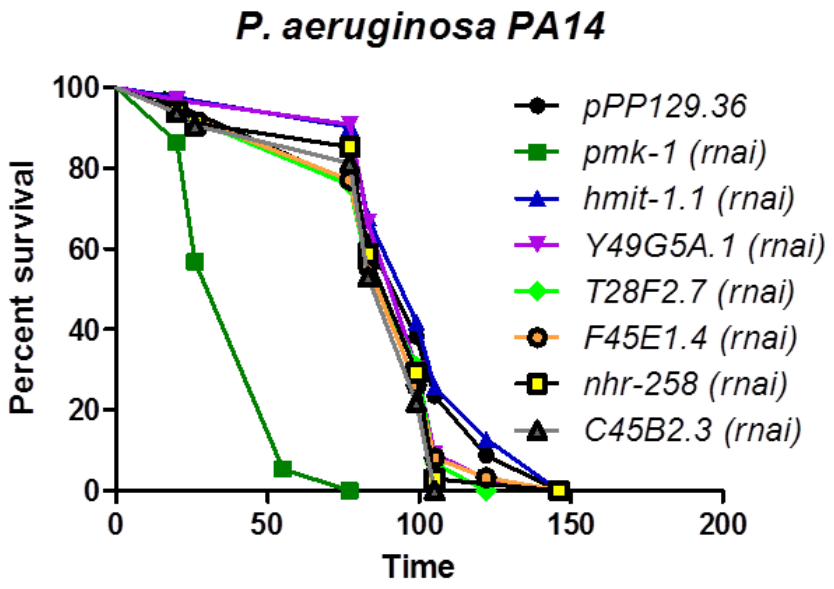

Figure 44. Microarray candidate genes are not susceptible to *P. aeruginosa*

Indicated microarray candidate genes were compared to empty vector controls and a positive control *pmk-1 (rnai)* are indicated. Significant differences were not observed

between any of the microarray candidates tested and the empty vector (*pPD129.*36). Tested constructs include (*hmit-1.1*, n=31; F45E1.4, n=61; C45B2.3, n=32; *nhr-258*, n=34; Y49G5A.1, n=33; T28F2.7, n=29; *pPD129.36*, n=34; *pmk-1*, n=37). Only one experiment was performed.

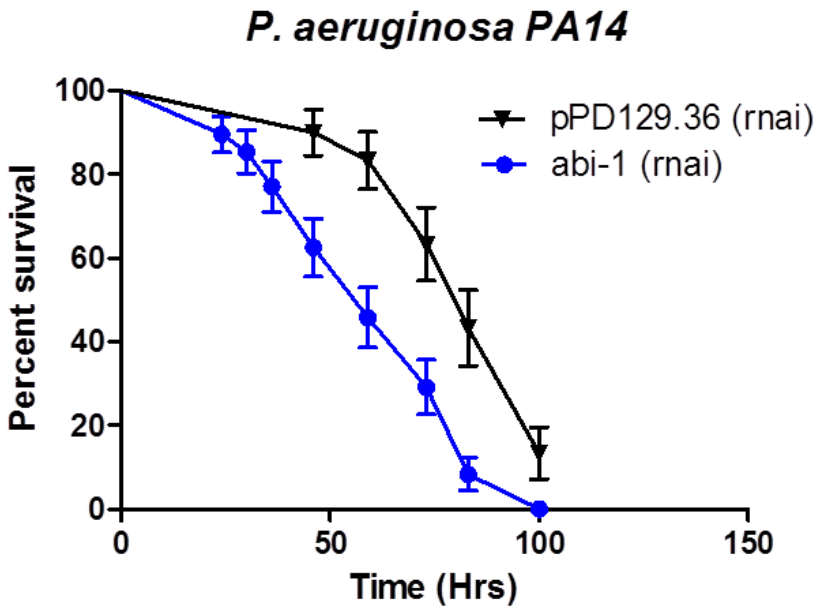

Figure 45. *abi-1 (rnai)* is susceptible to *P. aeruginosa*

abi-1 (rnai) and empty vector controls were treated to *P. aeruginosa* and *abi-1 (rnai)* animals (n=48) died significantly faster than empty vector controls (n=26) (P<0.0001). Statistics performed using Log Rank (Mantel Cox), Graphpad Prism 5. Only one experiment was performed.

3.5 Discussion

3.5.1 UNC-53 contributes to *P. aeruginosa* resistance

UNC-53 has described roles in the cell-autonomous control of the migration of cells and cellular processes during development in *C. elegans* (Schmidt et al., 2009; Stringham et al., 2002) and is needed to integrate upstream guidance cues to changes in the cytoskeleton (Martinez-Lopez et al., 2005; Schmidt et al., 2009; van Haren et al., 2009). Studies from the *Navs* suggest a possible role for this family of proteins in immune responses (Foley and O'Farrell, 2004; Maliniemi et al., 2011), and a previously

conducted RNAi screen in *C. elegans* identified *unc-53* as required for the expression of *clec-85::gfp* (Alper et al., 2008), a putative antimicrobial under the expression of numerous genetic pathways (Alper et al., 2007). In addition, a previously conducted yeast two-hybrid screen identified that UNC-53 interacts with the *C. elegans* homolog of P62/sequestome (T12G3.1) (Adeleye, 2002). p62 interacts with the p38 MAPK and it is required for the nuclear translocation of P38 in response to MAP Kinase signalling (Kawai et al., 2008; Sudo et al., 2000). T12G3.1 is expressed in the intestine where PMK-1 is expressed (Adeleye, 2002), and T12G3.1 is upregulated in response to pathogens (Wong et al., 2007), and is itself expressed in response to *P. aeruginosa* in a way that is dependent on *sek-1* (Troemel et al., 2006). Given the physical interaction between UNC-53 and T12G3.1 (Adeleye, 2002), a potential role for *unc-53* in innate immunity was tested. Evidence from this study shows that several *unc-53* alleles as well as *unc-53 (rnai)* treatment causes susceptibility to the Gram-negative multi-host pathogen *P. aeruginosa* and that this phenotype can be rescued using a fosmid covering *unc-53,* implicating *unc-53* in *P. aeruginosa* resistance.

Pathogen susceptibility can arise from non-specific decreases in general fitness, and changes in longevity or lifespan can be reflected in changes in pathogen susceptibility (Evans et al., 2008a; Garigan et al., 2002; Garsin et al., 2003). *unc-53 (n152)* animals are susceptible to the relatively non-pathogenic lab strain *E. coli* OP50. This is not surprising given that *E. coli* is observed to be slightly pathogenic to immunocompromised animals ((Garsin et al., 2003; Hahm et al., 2011; Haskins et al., 2008)) and that *E. coli* OP50 elicits an immune response in *C. elegans* that is mediated by insulin signalling (Hahm et al., 2011). However, *unc-53 (n152)* animals die slightly faster than wild-type on heat-killed bacteria, which can be interpreted to suggest that susceptibility to *P. aeruginosa* may be due to a decrease in general fitness. Of interest is that the relative degree of death between *unc-53 (n152)* and N2 on heat-killed *P. aeruginosa* is much lower than what is observed on live *P. aeruginosa*, and comparable to what is found for other known immune-response genes exposed to heat-killed bacteria (Tenor and Aballay, 2008). Importantly, *unc-53 (e404)*, *unc-53 (e2432)*, and *unc-53 (rnai)* animals die with kinetics similar to wild-type when subjected to *E. coli* but die much quicker than wild-type when exposed to *P. aeruginosa.* Therefore, while a strong allele such as *unc-53 (n152)* is pathogen susceptible but may also exhibit a

general decrease in fitness, weaker alleles and RNAi treated animals die only when exposed to a pathogen.

The observation that *unc-53 (n152)* has a decreased lifespan is consistent with the finding that *unc-53 (n152)* affects the subcellular localization of DAF-16-GFP in the presence of heat-stress independently of a pathogen-threat, and has increased *ins-7* transcript levels compared to wild-type when exposed to both *P. aeruginosa* and *E. coli*. Decreasing *ins-7* results in lifespan extension, and overexpressing *ins-7* results in a decrease in lifespan (Murphy et al., 2007). *unc-53 (n152)* animals have increased *ins-7* transcript levels which might therefore be reflected in a decreased lifespan in addition to pathogen susceptibility. The question of the extent that lifespan and pathogen resistance are genetically separable in *unc-53* is a relevant one. The subcellular localization of DAF-16 is under the control of several upstream kinases including four Ser Thr kinases (PDK-1, AKT1/2, SGK-1) that have been examined in both aging and immunity (Evans et al., 2008a). *pdk-1* and *sgk-1*, show wildtype resistance to pathogens while *akt-1/2* have modest effects on lifespan, but show enhanced resistance to pathogens along with changes in intestinal engorgement and antimicrobial expression (Evans et al., 2008a). Further experiments are needed to determine the role of *unc-53* in both lifespan and immunity. Examining the effect of *unc-53 (e404)* or *unc-53 (rnai)* on DAF-16-GFP localization would be informative because they do not appear to affect longevity or general fitness. Also, so far the only meaningful readout tested is the ability of *unc-53* animals to survive a *P. aeruginosa* infection. Other measures of innate immune function are needed. One possibility is to examine the alterations in the expression of antimicrobials which has been done here. Another is to examine the degree of gut engorgement using GFP-tagged *P. aeruginosa*. Testing these parameters could shed light on the specific nature of this observed pathogen susceptibility.

3.5.2 UNC-53 contributes to *P. aeruginosa* resistance in adult tissue

Given the strong developmental role of *unc-53* it was important to determine the extent that *unc-53* is required in adult animals for pathogen resistance. A role for *unc-53* in pathogen resistance in adults is evidenced by the fact that *unc-53 (rnai)* performed on adults confers sensitivity to *P. aeruginosa*. The finding that *unc-53* has independent roles in development and in adult tissues is interesting. In this way, UNC-53 is similar to

the other innate immunity pathway genes described in worms (Partridge et al., 2010). PMK-1 pathway mutants *sek-1* and *nsy-1* have additional developmental roles in assigning neuronal asymmetry (Sagasti et al., 2001; Sagasti et al., 2001; Tanaka-Hino et al., 2002), and the DBL-1 pathway has been extensively described in body size regulation and male tail development (Maduzia et al., 2002; Savage-Dunn et al., 2003). Similarly, DAF-2-DAF-16 signalling contributes to development (Larsen et al., 1995).

While a post-developmental role for *unc-53* exists, adult-treated *unc-53 (rnai)* animals are substantially less susceptible to *P. aeruginosa* than *unc-53* mutants or *unc-53 (rnai)* animals exposed to dsRNA as embryos. A number of possibilities can explain these discrepancies. First, RNAi treatment can have variable effects and is less penetrant in adults when performed by feeding (Kamath et al., 2001; Simmer et al., 2003). Alternatively, the decreased effect of adult RNAi in *unc-53* could suggest an additional developmental contribution. Given the known roles for *unc-53* during development, several possibilities exist. The simplest explanation could be that *unc-53* animals are uncoordinated and are simply unable to avoid bacteria in the context of a pathogen assay. While *unc-53* animals are uncoordinated, rnai treated animals are not particularly Unc. Also, there are many Uncoordinated mutants that have no effect on innate immunity such as *unc-22,* and others such as *unc-64* that are pathogen-resistant (Kawli and Tan, 2008), so this argument is not favoured. Another important consideration is that *unc-53* may affect neural development in a way that disrupts pathogen resistance resulting in an inability to mediate the secretion of endocrine cues or pathogen avoidance (Kawli and Tan, 2008; Shivers et al., 2009; Styer et al., 2008). The pathogen avoidance response to *P. aeruginosa* is partially mediated by sensory neurons and involves learning (Aballay, 2009; Chang et al., 2011; Reddy et al., 2009; Styer et al., 2008). *unc-53* expression in the nervous system is widespread, so it is possible that the developmental function of *unc-53* could contribute to either or both of these processes is some undefined way. While this is a very plausible, it is found that the pan-neuronal expression of *unc-53L* rescues the PLM defect, and animals remain susceptible to *P. aeruginosa*, making a neural development contribution less likely.

It is also possible that *unc-53* may function in the development of non-neuronal tissues to affect the ability of *unc-53* animals to resist a pathogen. Pathogens mediate

entry into *C. elegans* through openings in the animal including tissues such as the vulva and the anus (Gravato-Nobre and Hodgkin, 2005). Given the important role for *unc-53* in vulval morphogenesis (Chen et al., 1997; Stringham et al., 2002) it seemed possible that an Egl defect or underlying vulval instability due to the vulva and uterine muscle cell attachment defects (Stringham et al., 2002) may generate the observed pathogen susceptibility. Several lines of evidence suggest that the vulva is not an appreciable factor in the pathogen response: (1) sterilization by FUDR or *lin-60/cdc-25.1 (rnai)* removes the Egl defect but leaves animals susceptible to *P. aeruginosa*, (2) *unc-53* males are susceptible to *P. aeruginosa*, (3) muscle-specific RNAi generates a Egl defect but renders animals resistant to *P. aeruginosa* resistant animals, (4) the *punc-53SA::unc-53SA* construct does not rescue the Egl defect (Stringham et al., 2002) but partially rescues *P. aeruginosa* susceptibility.

unc-53 is expressed in both the anal muscles and the stomato-intestinal-muscle (Adeleye, 2002; Stringham et al., 2002) which are required for defecation and digestion (Avery and Thomas, 1997; McGhee, 2007), so it is again possible that these tissues may contribute to the observed pathogen defect. However, the inability to generate a phenotype solely by muscle specific RNAi makes it unlikely that an insular defect in muscle is the cause of the *unc-53* susceptibility. Another possibility is that *unc-53* may have a developmental role in the intestine. *unc-53* is intestinally expressed in larva, and ABI-1 is shown to work with the Arp2/3 complex in the maturation of apical junctions in intestinal cells in developing embryos, and the depletion of the Arp2/3 complex in adult tissue results in a mislocalization of apical junction proteins (Bernadskaya et al., 2011). *abi-1* animals are pathogen sensitive similarly to *unc-53* so it is possible that these genes function together in the intestine during development and otherwise. Again, however, no measurable contribution to *P. aeruginosa* is observed for *unc-53* from the intestine alone. Therefore, if non-specific developmental defects are expected to be contributing to pathogen sensitivity it is expected to be the result of a combination of defects.

Further experiments are necessary to prove that *unc-53* is required in adult tissue. One possibility is to rescue *unc-53* using a heat-shock promoter to time expression in adults. *unc-53* expression under the control of the heat-shock promoter

causes widespread expression (Adeleye, 2002) and the heat shock expression and rescue of *unc-53* in adult mutant animals would provide conclusive evidence that *unc-53* is required in adults. The caveat is that heat-shock induction renders animals pathogen-resistant (Singh and Aballay, 2006), potentially eliminating meaningful explanation. A better experiment would be to conditionally express *unc-53* using the *mec-8* dependent splicing system to allow embryonic expression of *unc-53* followed by adult removal in response to a switch in physiological temperature (Calixto et al., 2010b).

3.5.3 Multiple tissues and isoforms may require *unc-53* for pathogen resistance

unc-53 and the *Navs* have complex genomic loci with multiple-promoters and alternative splicing that confers varied tissue and isoform expression (Maes et al., 2002; Schmidt et al., 2009; Stringham et al., 2002). Innate immune responses even in a relatively simple organism like *C. elegans* are incredibly complex and involve coordinated responses from multiple tissues, producing numerous behavioral and host-effector responses (Chang et al., 2011; Kawli and Tan, 2008; Shivers et al., 2009; Styer et al., 2008; Troemel et al., 2006).

Several experiments in this study were conducted to try to understand the tissue and isoform combinations needed for *unc-53* immune function. Through a combination of tissue-specific RNAi, tissue-specific rescue experiments using pan-neuronal and intestinal promoters, and the use of promoter mini-gene constructs expressing the shorter isoforms of *unc-53* (Stringham et al., 2002), some conclusions can be made. Partial rescue of *unc-53 (n152)* pathogen sensitivity was achieved using the fosmid that covers the *unc-53* locus as well the mini-gene contructs driving *unc-53* cDNA corresponding to the short isoforms (Stringham et al., 2002). At the same time expressing the long-isoform of *unc-53* cDNA using a neuronal *rab-3* promoter was unable to rescue the pathogen sensitivity defect even though this construct was observed to be functional, as evidenced by its ability to rescue the PLM migration defect. Similarly, *unc-53* cDNA expressed under the control of the *ges-1* promoter was unable to rescue the pathogen defect even when its expression was confirmed through GFP-tagging. Similarly, intestinal specific RNAi directed towards *unc-53* was unable to render animals susceptible to *P. aeruginosa*. One interpretation is that *unc-53* might be

required together in neurons and the intestine to allow for the rescue of the *unc-53 (n152)* pathogen sensitivity. To test a model for *unc-53* being needed simultaneously in both tissues, contructs in which *unc-53* cDNA was expressed simultaneously under the control of both the *rab-3* and the *ges-1* promoters were produced. These constructs also did not rescue. One explanation for the lack of rescue with these constructs is that they may not be functional. Although they rescue the PLM defect their activity in the intestine is not known. Another option is that *unc-53* may not function in either of these tissues. To test this possibility tissue specific RNAi experiments towards *unc-53* specifically in muscle where *unc-53* is expressed (Schmidt et al., 2009; Stringham et al., 2002) and the hypodermis were carried out. Removing *unc-53* in these two tissues individually also did not render animals susceptible to *P. aeruginosa*. Therefore, the balance of the evidence suggests that if *unc-53* is needed in either the muscle, hypodermis, or intestine, it does not function in any of these tissues in isolation. One tissue of interest that expresses UNC-53 in adults that has not been examined is the excretory cell.

Expressing the long-isoform of *unc*-53 in the neurons and intestine alone or in combination does not rescue the *unc-53 (n152)* phenotype. One interpretation is that *unc-53* may function in these tissues but that it does not do so in isolation from some other undefined tissue. Another possibility is that because these constructs express the long-isoform of *unc-53* but do not rescue the *P. aeruginosa* resistance, it may be that the long-isoforms do not contribute to innate immunity. The CH domain is unique to the long-isoform of *unc-53*, and it is possible that the possessing a CH domain excludes it from functioning at the necessary times and/or locations to rescue the observed immunity defect. The inability of a functional *prab-3::unc-53L* construct to rescue the DAF-16 mislocalization phenotype, which is controlled through a neuronal mechanism (Kawli and Tan, 2008; Kawli et al., 2010), supports this possibility. Isoform specific differences between gene products affect gene function and subcellular localization (Hu et al., 2011; Mohamed and Chin-Sang, 2011; Steven et al., 2005). We observed rescue of the *unc-53 (n152)* pathogen susceptibility phenotype using small isoform mini-gene constructs that are similar to the long-isoform of *unc-53* at their C-terminus but differ in their N-terminus (Stringham et al., 2002), which could lend support to a model where the short isoforms of *unc-53* are needed for pathogen resistance. Also, the rescuing mini-genes were driven under the expression of endogenous promoters, so the timed

expression of *unc-53*, may be more appropriate than expressing *unc-53* with *rab-3* and *ges-1* promoters. The *punc-53SA* and *punc-53SB* promoters can express *unc-53* in a range of tissue at a given time, including several different neurons, muscle cells, socket cells, and the ExC It is possible that the coordinated expression of *unc-53* in several of these tissues at one time is what is needed for *unc-53 (n152)* rescue. The endogenous promoters also drive *unc-53* expression in tissues not covered by *rab-3* and *ges-1*. In particular, the excretory cell has not been tested by excretory cell specific-rnai or using the *pgp-12::unc-53L* construct, and represents a possible candidate tissue. However, while the excretory cell might be involved in pathogen resistance, it also seems unlikely that it is involved in isolation from other tissues because expressing *punc-53SB::unc-53SB* that does not express *unc-53* in the ExC partially rescues the phenotype.

Future experiments are necessary to understand the tissues and isoforms requiring *unc-53* in innate immunity. Also, all of the rescue experiments were performed in *unc-53 (n152)*, which may possess a decrease in overall general fitness that is not observed in weaker alleles or by RNAI. Performing rescue experiments using a weaker allele like *unc-53 (e404)* may avoid any confounding effects created by *unc-53 (n152)*. In addition, given that the short isoform cDNA appears to rescue the immune defect it would be helpful to determine if the cDNA of the shorter isoforms might rescue *unc-53* alleles in a tissue specific way. Alternatively, it would be useful to determine whether full-length cDNA expressed under the promoter for the long isoform is able to rescue the observe pathogen defect. A potentially more difficult question from an experimental perspective would be determining the extent to which a combination of isoforms of *unc-53* may contribute to innate immune function. Determining a complex contribution from several tissues and isoforms may involve the need to perform multiple isoform rescuing experiments, perhaps along with examining an allelic series.

3.5.4 UNC-53 does not substantially affect antimicrobial production at the RNA level

Pathogen susceptibility can be assessed by assaying for death in the presence of a pathogen or by measuring alterations in the expression of antimicrobials (Alper et al., 2007; Irazoqui et al., 2010b; Troemel et al., 2006). Mutations in genes from the major known immunity pathways in *C. elegans* cause alteration in antimicrobial

expression (Alper et al., 2007). To determine if antimicrobial expression was affected by *unc-53*, a small subset of pathogen induced genes known to be under the control of overlapping and independent genetic pathways in *C. elegans* (Alper et al., 2007) were assayed by qPCR. Of this set, no change in the expression of any antimicrobials at the RNA level was observed in *unc-53 (e404)* or *unc-53 (n152)* mutants grown in *E. coli* OP50 representing a basal uninfected state or in the presence of *P. aeruginosa* representing an induced and infected state. All of the genes showed increased expression in the presence of *P. aeruginosa* in N2 as expected but no observed differences were found between *unc-53* and N2. The one exception was a significant increase in the expression of F55G11.7 in both *unc-53 (n152)* and *unc-53 (e404)* animals compared to wild-type when exposed *P. aeruginosa* PA14 (Figure 41C). F55G11.7 is a DAF-16 target gene (Murphy et al., 2003) that is expressed in the intestine, rectal gland cells, head neurons including one amphid neuron, and a phasmid neuron (Alper et al., 2007). F55G11.7 is strongly induced by Gram-negative pathogens, and is decreased in *daf-16* loss of function mutants (Murphy et al., 2003), but was observed to be increased in mutants from the *tir-1* and *dbl-1* pathways (Alper et al., 2007). F55G11.7 contains a CUB domain though its physiological role in innate immunity is not known. UNC-53 is not likely a negative regulator of DAF-16 considering the finding that *unc-53* limits *ins-7* RNA levels and that DAF-16 localizes to the cytoplasm preferentially compared to N2 following heat stress (see Sections 3.4.4 and 3.4.5) in *unc-53 (n152)*. Another possibility is that *unc-53* regulates a pathway that is parallel to *daf-16* that causes a compensatory response in increased DAF-16 induction.

Given the small subset of genes tested by qPCR that only represented immunity candidates from known genetic pathways, a whole-genome microarray to search for additional antimicrobial candidate genes altered in *unc-53 (n152)* in the presence of *P. aeruginosa* was conducted. While the microarray analysis must be verified, large-scale changes in the expression of known antimicrobials at the transcriptional level did not materialize in *unc-53 (n152)* animals when compared to N2 animals in the presence of *E. coli* or *P. aeruginosa*. Instead, there are a few candidate genes that can be explored. *clec-167* was found to be significantly reduced in *unc-53* compared to N2 in the presence of *P. aeruginosa* and is a putative antimicrobial protein (Schulenburg et al., 2008). Of interest as well is the observation that the microarray identified several putative secreted proteins that were upregulated in *unc-53 (n152)* mutants, surprising

from the perspective that AMPs promote pathogen resistance. It should be noted, however, that the physiological roles of some of these particular AMPs is not known and some antimicrobials can positively and negatively regulate pathogen resistance depending on the particular AMP and involved pathogen (Marsh et al., 2011). The role of these putative AMPs in *unc-53* immunity needs to be explored in an individualized way.

Of particular interest is that the qPCR analysis did not identify alterations in the expression of *clec-85,* which originally identified *unc-53* as a putative innate immune gene through an RNAi screen (Alper et al., 2008). A few important differences exist between that study and this one. Firstly, the RNAi screen employed a *clec-85::gfp* strain that was analyzed by a COPAS biosorter (Alper et al., 2008), and may therefore have provided for a sensitized background when monitoring AMP alterations compared to direct quantitation by qPCR as done here. Secondly, and probably more importantly, the previous study identifying *clec-85::gfp* changes in *unc-53* was conducted under different culture conditions then those performed here (Alper et al., 2008). Alper *et al*. (2008) conducted their RNAi screen at 25ºC rather than 20ºC, and worms were exposed to bacteria grown on normal NGM plates rather than peptone rich plates. These different culture conditions may also explain why no changes in antimicrobial expression are observed in this study while *unc-53 (e404)* when subjected to *E. coli* OP50 at 25ºC on normal NGM media as conducted previously (Alper et al., 2007) was observed to have decreases in several antimicrobials by qPCR including *clec-85*, *dod-22*, *lys-8* and K08D8.5 (Dr. S. Alper, personal communication). Culture conditions can have profound effects on pathogen behavior and host susceptibility (Alper et al., 2010; Kim et al., 2002). Addressing these apparent differences in *unc-53* mediated AMP expression changes is necessary to understanding the mechanism of function of *unc-53* in *P. aeruginosa* susceptibility.

3.5.5 Synaptic transmission, *ins-7* RNA levels, and DAF-16-GFP recovery following heat shock are dependent on *unc-53*

Central to the thesis is the observation that in addition to being susceptible to *P. aeruginosa*, *unc-53* mutants have increased transcript levels of the DAF-2 agonist *ins-7*,

exhibit delocalized DAF-16-GFP compared to N2 following heat-shock, and show decreased synaptic transmission as measured by Aldicarb hypersensitivity.

unc-53 mutants are hypersensitive to Aldicarb. Aldicarb is an acetylcholinesterase inhibitor and in this capacity is able to provide one measure of synaptic transmission in a comparatively easy way compared to other techniques (Mahoney et al., 2006). Importantly, hypersensitivity to Aldicarb is not restricted to *unc-53* mutants but can be reproduced by treating RNAi sensitive animals to *unc-53 (rnai)* as adults. The penetrance of the RNAi treatment was similar to that observed in *unc-53* mutants, so while there is the possibility that an *unc-53* developmental role could contribute to Aldicarb hypersensitivity it is seems more plausible that a post-developmental function for *unc-53* accounts for this observation. Acetylcholine is the major neurotransmitter used at neuromuscular junctions in *C. elegans* and many acetylcholine receptors and signalling molecules needed for acetylcholine transmission have been identified (Rand, 2007). While acetylcholine is expressed in neurons, acetylcholine receptors are expressed in both neurons and muscle (Rand, 2007). Examples of mutants that result in increased hypersensitivity to Aldicarb include loss of function mutants of negative regulators of synaptic transmission including GOA-1 and the DAG kinase DGK-1 (Miller et al., 1999). It is possible that *unc-53* could have an effect on acetylcholine transmission through a role in either neurons (negatively regulating signalling controlling acetylcholine release) or in muscle (negatively regulating acetylcholine responsiveness). Given the alterations in *ins-7* transcript levels and an already existing model explaining *ins-7* production and DAF-16 localization through host responses in neurons (Kawli and Tan, 2008), the former is the priority model. However, while a neuronal role is favored, a role for *unc-53* in Aldicarb hypersensitivity through a muscle mediated mechanism cannot be ruled out. The effectiveness of the Aldicarb treatment on conferring hypersensitivity by *unc-53 (rnai)* treatment as adults was surprising given the refractory nature of neurons to RNAi treatment, though an RNAi sensitive strain was used (Schmitz et al., 2007); additionally, rescue of the DAF-16-GFP mislocalization was not observed by expressing *unc-53L* by the pan-neuronal promoter even though this construct is functional as evidenced by its ability to rescue the PLM defect. A priority is to test the *prab-3::unc-53* constructs for its ability to rescue Aldicarb hypersensitivity in *unc-53* mutants and to test for a role for *unc-53* in hypersensitivity to

Aldicarb through muscle using muscle-specific RNAi. Additionally, it would be interesting to perform epistasis experiments with genes known to control the neurosecretion of INS-7 (Kawli and Tan, 2008) alongside studies aimed to identify the subcellular localization of UNC-53 within neurons as performed previously (Zhang and Kubiseski, 2010).

Trafficking at neuronal synapses plays an important role in signalling in both the aging and immune responses of *C. elegans*. Some of the proteins controlling *ins-7* levels and DAF-16 activity include the SNARE domain containing proteins UNC-64/syntaxin and SNB-1/synaptobrevin that function in varied aspects of synaptic transmission including vesicle tethering, docking, priming, and fusion (Hosono and Kamiya, 1991; Iwasaki et al., 1997; Saifee et al., 1998). Loss of function *goa-1* and *dgk-1* mutants that negatively regulate synaptic vesicle release have increased levels of *ins-7*, are pathogen sensitive, and are quick to allow for the relocalization of DAF-16::GFP following a heat-shock. We find that *unc-53* function similarly to negative regulators like *goa-1* and *dgk-1*. While rescue of these defects using a pan-neuronal promoter expressing *unc-53L* does not rescue these defects as would be predicted, a simple model can be proposed (Figure 46). In this model an infection with *P. aeruginosa* induces the release of INS-7 from hormone containing dense-core vesicles as a way to subvert host immunity (Kawli and Tan, 2008). INS-7 acts in an endocrine way to signal to DAF-2 in the intestine, preventing the nuclear localization of DAF-16, and protecting the pathogen from DAF-16 mediated host-effectors (Kawli and Tan, 2008). At the same time host factors employ the neurosecretory machinery to limit INS-7 release, promoting DAF-16 nuclear localization. The results in this study are in keeping with a model where UNC-53 could normally function as a part of the host cell machinery to limit INS-7 release and DAF-2 signaling in the context of a *P. aeruginosa* infection.

Assuming a neuronal role, how might *unc-53* negatively regulate vesicle release at the synapse? One possible model extends from a previously observed interaction between UNC-53 and ABI-1 (Schmidt et al., 2009), a conserved protein that regulates the ARP2/3 actin-polymerizing machinery through its interaction with either WASP or WAVE (Echarri et al., 2004; Innocenti et al., 2004; Innocenti et al., 2005; Leng et al., 2005; Steffen et al., 2004). ABI-1 has a conserved SNARE domain and binds the UNC-64 and SNB-1 homologs in mammalian cell culture (Echarri et al., 2004) as well as

synaptojanin and dynamin (So et al., 2000), which function in neuronal trafficking in *C. elegans* (Clark et al., 1997; Harris et al., 2000; Schuske et al., 2003). *unc-53* is needed for endocytosis as measured by the coelomocytes uptake assay and oocyte uptake assay and *abi-1* is required for *abi-1* oocyte uptake (see Section 2.3.12) (Giuliani et al., 2009). Also, both proteins are expressed in neurons in adult animals (see Section 2.3.1 and 2.3.5). These observations make it plausible that *unc-53* and *abi-1* may function together in synaptic transmission. This possibility is especially intriguing given the finding that *abi-1* is required for resistance to *P. aeruginosa*. The *unc-53* alleles examined in this study lack the C-terminal AAA ATPase domain found in UNC-53 and the AAA ATPase domain is critical to *unc-53* function in other processes like for example the induction of neurite outgrowth (van Haren et al., 2009). AAA ATPases are protein domains that couple ATP hydrolysis to changes in the conformational states of target substrates (Hanson and Whiteheart, 2005). Although AAA ATPase domains assign function depending on their targets and their other associated domains, one of the most well described AAA domain containing protein is NSF-1 which catalyzes the release of SNARE proteins in response to membrane fusion (Hanson and Whiteheart, 2005). One possibility is that AAA ATPase of UNC-53 may similarly influence the SNARE domain of ABI-1. Another possibility is that UNC-53 and ABI-1 control actin dynamics at the synapse to negatively regulate synaptic secretion. Recently, the *C. elegans wsp-1* homolog, like *unc-53* observed here, was found to negatively regulate synaptic vesicle trafficking (Zhang and Kubiseski, 2010). Interestingly, *wsp-1* and *wve-1* which both interact with ABI-1 and regulate ARP2/3, function in parallel in neuronal migration and tissue morphogenesis in *C. elegans* (Shakir et al., 2008; Withee et al., 2004). Therefore, it is plausible that UNC-53 functions with ABI-1 and WVE-1 to control actin dynamics at synapses like WSP-1.

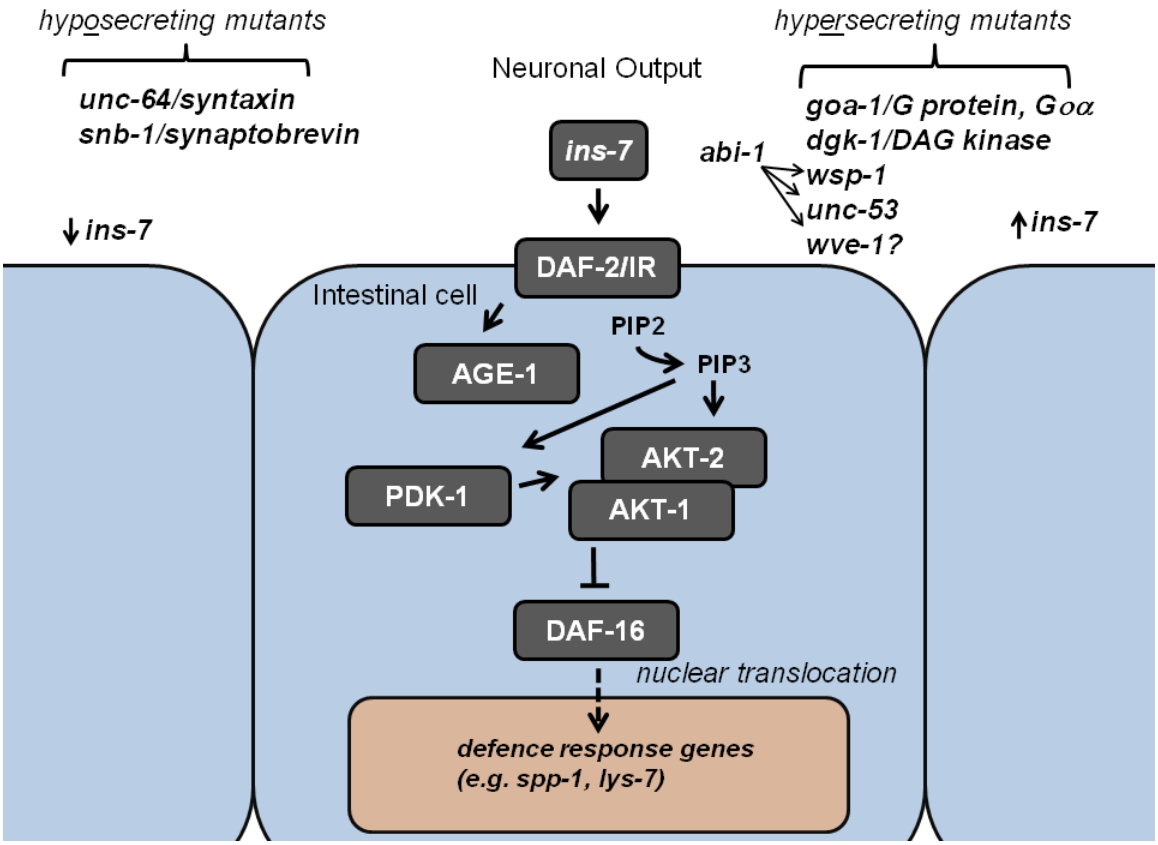

Figure 46. Model for *unc-53* function in DAF-16 mediated immunity

In the presence of *P. aeruginosa* PA14 infection, DAF-16 immunity is circumvented by an increase in the neuronally secreted DAF-2 agonist INS-7, activating the DAF-2 receptor which in turn activates AGE-1/PI3K, converting PIP_2 into PIP_3. PIP_3 binds to AKT1/2 and AKT-1 phosphorylates the transcription factor DAF-16, retaining it in the cytoplasm, preventing the production of defence response genes such as SPP-1 and LYS-7 (Gravato-Nobre and Hodgkin, 2005). INS-7 levels are under the control of proteins required for synaptic vesicle release such as UNC-64 and SNB-1, and those that limit neurosecretion such as GOA-1, DGK-1 (Kawli and Tan, 2008), and possibly UNC-53. WSP-1 has been found to negatively regulate neurosecretion (Zhang and Kubiseski, 2010), though its role in INS-7 production is unknown. UNC-53 interacts with ABI-1 (Schmidt et al., 2009), a protein involved in WVE-1 mediate actin-mediated cellular events (Kurisu and Takenawa, 2009) and a known physical interactor of the UNC-64 and SNB-1 homologs (So et al., 2000). ABI-1 interacts with WSP-1 and WVE-1, two proteins that act in parallel in many processes in *C. elegans* (Shakir et al., 2008; Withee et al., 2004). It is possible that UNC-53 may limit neurosecretion through its interactions with ABI-1 through WVE-1, UNC-64 or SNB-1.

3.5.6 **UNC-53 may function in more than one genetic pathway**

The finding that the *unc-53* innate immunity phenotype is not completely suppressed by null alleles of either *ins-7* or *daf-2* suggests that *unc-53* has an *ins-7* and *daf-2* independent function in innate immunity. In this respect, UNC-53 may be functioning through either neuronal or non-neuronal mechanisms. Mutants in DCV exocytosis such as *unc-64* and *unc-31* are more resistant to *P. aeruginosa* PA14 than *ins-7* mutants (Kawli and Tan, 2008), which could suggest that that DCVs are carrying other insulins or neuropeptides affecting innate immunity. The finding that *daf-2* does not completely suppress *unc-53* suggests that if *unc-53* regulates the neurosecretion of additional peptides that they must be *daf-2* independent. Both the *dbl-1* and *pmk-1* pathways are under neuronal control (Shivers et al., 2009; Zugasti and Ewbank, 2009). The neuroimmune function of the *dbl-1* pathway has only been described in fungal infections (Zugasti and Ewbank, 2009) and not *P. aeruginosa* which is the focus of this work. The observation that *unc-53; pmk-1* double mutants do not enhance either single mutation could suggest an additional role for *unc-53* through a *pmk-1* pathway. While a neuronal function for *pmk-1* pathway mutants has been found, *pmk-1* itself does not function neuronally (Shivers et al., 2009), and the role of *sek-1* and *nsy-1* appears to be in controlling the *C. elegans* aversive response to bacteria (Shivers et al., 2009). An aversive role for *unc-53* has not been tested. From a *pmk-1* perspective, a more likely candidate tissue is the intestine, the primary site of *pmk-1* activity (Shivers et al., 2009), though so far an individual role for *unc-53* in the intestine is not shown.

The observation that *unc-53* is expressed in many tissues in adults and that rescue has only been observed when using *unc-53* endogenous promoters that are expressed in multiple tissues, suggests the potential for multiple tissue involvement in *unc-53* mediated pathogen resistance. As previously discussed, *unc-53* is expressed in neurons, vulval cells, intestine, and the excretory cell. While expression of *unc-53* in the vulva is observed, and the vulva is a source of neuropeptides (Li and Kim, 2008), the finding that *unc-53* males are susceptible to pathogenic bacteria makes the vulva an unlikely candidate tissue for *unc*-53 immune activity. The excretory cell represents an interesting candidate from the perspective that its tissue-specific involvement has not been examined. Recent microarray studies show that the physiological activation of osmosentive gene expression mimics pathogen infection transcriptional signatures, which suggests that these two forms of environmental stress may share conserved

regulatory networks (Rohlfing et al., 2010). The microarray studies conducted in this work identified multiple candidate genes with a putative role in osmoregulation including some that are expressed in the excretory cell. So far the candidates tested from the microarray experiments did not display altered pathogen resistance, and the microarray has so far not been verified. Future studies aimed towards verifying the microarray data and testing candidate genes may offer insight into the function of *unc-53* in *C. elegans* immunity to *P. aeruginosa*.

In a genome-wide RNAi screen in *Drosophila*, the *unc-53* homolog *Sickie* was identified as an activator of the *caspase-8* homolog *Dredd*, upstream of the NF-κB homolog *Rel*, and required for *Rel* translocation to the nucleus (Foley and O'Farrell, 2004). The closest homolog to *Dredd* in *C. elegans* is *ced-3* which functions in engulfment. Given the role of *abi-1* in engulfment (Hurwitz et al., 2009) and here in innate immunity, a model involving *abi-1* and *unc-53* with *ced-3* is worth testing. *ced-3* is necessary for protection from *S. typhimurium* along with other engulfment genes, however, it does not so far appear that *ced-3* offers protection from *P. aeruginosa* (Aballay and Ausubel, 2001). Of particular interest with respect to *Sickie* and *Dredd* is that these genes function in the IMD pathway, the *Drosophila* equivalent of the mammalian TNF-α/RIP1 pathway (Foley and O'Farrell, 2004). Ingenuity pathway analysis identified a genetic network including several members of the TNF-α/RIP1 pathway, and the microarray identified two genes altered in *unc-53 (n152)* that are homologous to genes from from the Toll pathway (*trf-1*, +2.44 fold, P<0.001*; tir-1*, +1.33 fold, P<0.001). Worms do not appear to have a homolog with sequence similarity to NF-κB (Pujol et al., 2001) but have conserved members of NF-κB signalling including *tol-1*, *tir-1*, *trf-1*, *pik-1*, and *ikb-1* (Pujol et al., 2001; Tenor and Aballay, 2008), and several putative NF-κB regulators have been identified in a screen for *C. elegans* immunity genes (Alper et al., 2008) which could suggest the presence of a TF that acts similarly to NF-κB in *C. elegans*. Several TFs are known to control the immune response and include the GATA transcription factor ELT-2 (Kerry et al., 2006), the bZIP transcription factor ATF-7 (Shivers et al., 2010), and the TF STA-2 (Dierking et al., 2011). Without a clear NF-κB in *C. elegans* the identification of the relevant TF functioning with UNC-53 might remain elusive. For this reason, future studies using experimental platforms other than *C. elegans* may be more helpful in elucidating the role of *unc-53* and the *Navs* in innate immunity. Along these lines, current studies using bone marrow derived

macrophages from *Nav2* knockout mice show a dimished response to PAMP challenge (Dr. S. Alper, personal communication).

3.6 Materials and Methods

3.6.1 Strains and genetics

C. elegans strains were grown under standard conditions (Brenner, 1974; Stiernagle, 2006) at 20°C or 25°C depending on individual strains, and were fed either *E. coli* OP50 or OP50-1. Double mutants were constructed using standard genetic techniques and were confirmed by the presence of individual phenotypes or by PCR in the case of deletion alleles. Individual alleles used were as follows: wild-type (N2), *unc-53 (n152)*, *unc-53 (n166)*, *unc-53 (e404)*, *unc-53 (e2432)*, *him-8 (e1489), rrf-3 (pk1426), pmk-1 (km25)*, *sek-1 (km4)*, *daf-2 (e1370)*, *ins-7 (ok1573)*, *nre-1 (hd20); lin15b (hd126)*. Strains used included: ZB171 *pmec-4::gfp (bzIs7)*, BC14371 {*sEx14371 [punc-53::gfp;* pCEH361*], dpy-5(e907)/dpy-5(e907)*} (Schmidt et al., 2009), VA541 {[WRM0628aD12 (II:11054597..11095584); pmyo-2::gfp] ; *unc-53 (n152)*}, VA381/VA382 {*vaEx528/ vaEx529* [*prab-3::unc-53(F45E10.1a); pmyo-2::gfp*]; *unc-53 (n152)*}, VA378/VA379 {*vaEx530/vaEx531* [*pges-1::unc-53(F45E10.1a); pmyo-2::gfp*]; *unc-53 (n152)*}, VA375/VA376 {*vaEx547/vaEx548* [*prab-3::unc-53(F45E10.1a); pges-1::unc-53(F45E10.1a); pmyo-2::gfp*]; *unc-53 (n152)*}, VA508 {*vaEx548* [*pges-1::unc-53(F45E10.1a)::gfp; pmyo-2::gfp*]; *unc-53 (n152)*} OLB11 {*pges-1::rde-1; rde-1 (ne219)*} (Hoffmann et al., 2010; McGhee et al., 2009), NR350 {*kzIs20*[pKK1253(*hlh-1::rde-1*), pTG96(*sur-5p::nls::gfp)*]; *rde-1(ne219)*} (Qadota et al., 2007), NR222 {*kzIs9*[pKK1260(*lin-26p::nls::gfp*), pKK1253(*lin-26p::rde-1*), pRF4(*rol-6* marker)]; *rde-1(ne219)*} (Qadota et al., 2007), TU3401 {*uIs69* [*pCFJ90(myo-2p::mCherry)* + *unc-119p::sid-1]; sid-1(pk3321)*} (Calixto et al., 2010a), TJ356 {*zIs356 [pdaf-16::daf-16::gfp; rol-6]*} (Henderson and Johnson, 2001), UG17 {*unc-53(n152);bgEx3* [pNP3;pRF4]}, UG62 {*unc-53(n152);bgEx20* [pNP9;pNP10;pRF4]}, UG176 {*unc-53(n152);bgEx26* [pNP3;pNP8;pRF4]}, UG188 {*unc-53(n152);bgEx36* [pNP24;pNP21;pRF4]}, UG189 {*unc-53(n152);bgEx37* [pNP24;pNP21;pRF4]} (Stringham et al., 2002). The fosmid containing *unc-53 (n152)* strain VA541 was produced by injecting the fosmid WRM0628aD12 at 10ng/µl along with the coinjection marker *pmyo-2::gfp* (*pPD118.33*) at 75ng/µl into wild-type animals, which was then crossed to *unc-53 (n152)*. PCR fusion techniques (Hobert, 2002) were used to generate *unc-53(F45E10.1a)* containing

rescuing constructs. In each case, wild-type animals were injected with 50ng/µl of either the PCR fusion *prab-3::unc-53* containing the *rab-3* promoter (Nonet et al., 1997) or *pges-1::unc-53* containing the *ges-1* promoter (Kennedy et al., 1993) fused to *unc-53* cDNA (F45E10.1A from pTB115, sequenced to confirm identity, Macrogen Inc.) (Stringham et al., 2002) along with 75ng/µl of *pPD118.33* containing the *pmyo-2::gfp* pharyngeal muscle marker. These injections created transgenic lines carrying the construcs *vaEx528/vaEx529* and *vaEx530/vaEx531* which were crossed to *unc-53 (n152)* to generate VA381/VA382 and VA378/VA379 to be used in rescue experiments. The double rescuing strains VA375/VA376 were similarly constructed by injecting *prab-3::unc-53(F45E10.1a)* and *pges-1::unc-53(F45E10.1a)* coinjected at 50ng/µl each with 75ng/µl of the *pmyo-2::gfp* coinjection marker to wild-type to get transgenic lines carrying *vaEx547/vaEx548* which were crossed to *unc-53 (n152)*. VA508 was constructed by PCR fusion, fusing a 3' gfp coding region (and the *unc-54 3'UTR*) coding region (from pPD95.77) to a purified *pges-1::unc-53* PCR product to create *pges-1::unc-53::gfp* which was injected (50ng/µl) along with pCEH361 (75ng/µl) into wild-type animals to generate transgenic lines with intestinal fluorescence. One of these lines was crossed to *unc-53 (n152)* to generate VA508 which was examined for rescue. Note that several other lines with different construct concentrations (1ng/µl – 100ng/µl) and coinjection markers (pRF4[*rol-6*], 100ng/µl) that were generated and equally unsuccessful at rescuing the pathogen defect (data not shown).

3.6.2 Immunity and lifespan assays

Survival on *P. aeruginosa* PA14 was assessed at 20°C or 25°C given the particular growth conditions necessary for the nematode strains used, and making some modifications to standard procedures (Shapira and Tan, 2008). Strains carrying the gene *daf-2 (e1370)* are temperature-sensitive and were grown to L2-L3 before being shifted to 25°C by L4 to avoid dauer formation. All assays were carried out at matched temperatures between strains. *P. aeruginosa* PA14 cultures (obtained from the Hancock Lab, UBC) were thawed from glycerol stocks on a regular basis to ensure continuity (2 weeks to 1 month). Immunity assays were conducted as follows. For each assay, *P. aeruginosa* was grown overnight from a single colony in 5mls of Luria Broth at 37°C shaking at 200rpm for no more than 15hrs. 15µl of the culture was seeded dropwise and streaked onto small (6cm) peptone-rich NGM plates (Stiernagle, 2006) (2.5% peptone). Plates were incubated unsealed for 24hrs at 37°C, and then were allowed to cool to

assay temperature (20°C or 25°C) for 8-24hrs (24 hrs more typical). To avoid premature death from the egg-laying defects of *unc-53*, hermaphrodites were rendered sterile by treatment with FUDR (fluorodeoxyuridine) (VWR Inc.) which was added directly to the pathogen containing plates (50 µg/ml dissolved in 95% ethanol) prior to microbial growth or by pretreating embryos by feeding RNAi of *lin-60/cdc25.1 (rnai)* (from the Ahringer RNAi library) (Shapira and Tan, 2008), a gene required for embryonic viability and germline proliferation (Ashcroft and Golden, 2002), prior to exposing the nematodes to *P. aeruginosa*. When *lin-60/cdc-25.1 (rnai)* was used, embryos from a hypochlorite treatment were put onto preinduced RNAi plates (NGM with 1mM IPTG) and were allowed to grow to the L4 stage (Evans et al., 2008a) prior to being placed on pathogen plates. When FUDR was used, approximately 40-75 L4 animals were picted to a pathogen plate. When *lin-60/cdc-25.1 (rnai)* was used, animals were picked to individual plates in groups of ten (with 50-80 animals used per treatment group) and the *P. aeruginosa* was not streaked following the dropwise addition prior to incubation. Death was assessed by the absence of a response following a gentle tap by a platinum wire. FUDR and pretreated *lin-60/cdc-25.1 (rnai)* animals were usually counted in 8-12 hr intervals. For FUDR treated animals, worms were counted and removed only when they were dead, while both live and dead animals were tracked (with dead animals removed) along the course of the assays in *lin-60/cdc25.1 (rnai)* treated animals. Worms that crawled off the plates or appeared damaged during the experiments were not included in the analysis.

Lifespan assays were carried out similarly to the *P. aeruginosa* immunity assays except that *E. coli* OP50-1 or heat-killed *P. aeruginosa* PA14 was used instead of *P. aeruginosa*. Heat-killed *P. aeruginosa* was generated by autoclaving overnight cultures produced as described above. Following autoclaving, cultures were centrifuged at 3,500 rpm for 5 minutes and were concentrated 10-fold. 100µl of the heat-killed cultures were spread onto peptone-rich FUDR containing NGM plates. Confirmation of the heat-kill was performed by observing no growth under the high magnification on the dissecting mircroscope on separate LB plates streaked with an aliquot of heat-killed bacteria for 24hrs at 37°*C.* Due to the large number of worms that are lost in these assays, approximately 100 worms were added to the plates. To avoid carry over contamination of *E. coli*, worms were first washed in M9 buffer (Stiernagle, 2006) or 0.14M NaCl prior to addition to heat-killed bacteria. Worms on heat-killed *P. aeruginosa* were assayed in

approximately 24hr intervals through the course of the experiment, counting and removing dead nematodes as described above.

Survival plots were generated for each treatment group and the data was analyzed for statistical significance by LOG Rank (Mantel-Cox) test using Graphpad Prism 5 software (statistical significance $P<0.01$ or $P<0.0001$ as described) except Figure 38 which was determined using SPSS software. Significance was determined from the data collected from all the biological replicates (minimum of two experiments performed). Median death was also calculated using Graphpad Prism 5 software for inclusion in those Tables found in Appendix 1.

3.6.3 **RNAi treatments for immunity assays**

RNAi treatments were done by feeding essentially as described (Kamath et al., 2001) at 20°C or 25°C depending on the strain used. When RNAi treatments were performed prior to immunity and lifespan assays (described above), progeny were used whose parents had fed on dsRNA containing bacteria (*E. coli* HT115) for at least 24hrs and were brought to the L4 stage prior to analysis. RNAi cultures were generated from overnight cultures of RNAi clones (Geneservice Ltd.) that were maintained on LB AMP (75µg/ml) Tet (15µg/ml) plates and grown overnight in 5mls of LB AMP (75µg/ml) media for no more than 15hrs. Cultures were centrifuged at 3,500rpm for 5min and were concentrated 5-fold. 15µl aliquots were spread onto small plates (6cm) containing 1mM IPTG and were induced for approximately 24hrs. L4 animals from NGM/OP50-1 plates (Stiernagle, 2006) were set to feed on the dsRNA bacteria for 24hrs and were subsequently transferred to fresh RNAi plates to feed for 5-12hrs to generate a synchronous population. L4 progeny from these plates were used in subsequent immunity and lifespan assays. RNAi clones were obtained from Geneservice Ltd. and the Fire Lab (pPD129.36). Identity was confirmed by its similarity to loss of function mutants, restriction analysis, and/or by PCR size confirmation, except those clones assayed in Section 3.4.13, which were not confirmed for correct clone identity (with the exception of the *abi-1 (rnai)* clone, see Section 2.5.4). Adult RNAi plates were induced as described above. For these experiments L4 RNAi sensitive *rrf-3 (pk1426)* animals fed on dsRNA at 20°C for 36-40hrs prior to subjecting them to *P. aeruginosa*.

3.6.4 **Aldicarb assays**

To examine synaptic transmission, *unc-53 (n152)* and adult *unc-53 (rnai)* animals and controls were subjected to the acetylcholinesterase inhibitor Aldicarb as described (Mahoney et al., 2006). For the mutant treatments, 10 young adult animals were placed onto individual plates at timed-intervals, preseeded with a 15µl drop of *E. coli* OP50 (incubated at room temperature for 4hrs) and containing 1mM Aldicarb (Chemservice Inc.) added to the NGM media during preparation. Prior to the aldicarb assays, plates were stored in the fridge (4°C) and were warmed to room-temperature (22°C, assay temperature) for several hours prior to use. Plates used in individual experiments were produced in the same batch. Following their addition to Aldicarb containing media, nematodes were scored for paralysis every 15-20 minutes and were considered paralyzed if they showed absolutely no movement following three gentle taps with a platinum wire. The total number of animals paralyzed was summed over the 1hr. Adult *unc-53 (rnai)* treated animals were similarly assessed but were first treated with *unc-53 (rnai)* by feeding for 36-40hrs starting at the L4 stage using the RNAi sensitive strain *nre-1 (hd20); lin15b (hd126)*. Two experiments were performed employing three replicates (with ~50 animals per replicate) each. Resultant means of the number of paralyzed animals were compared using a two-tailed t-test with Graphpad Prism 5 software.

3.6.5 **Heat-shock treatment of DAF-16::GFP**

Assessing the localization of DAF-16-GFP following recovery from heat-shock was preformed as described ((Kawli and Tan, 2008)) except that recovery was monitored over an 8hr time interval. *unc-53 (n152)* and wild-type animals carrying the *pdaf-16::daf-16::gfp* transgene (TJ356) were first synchronized by a hypochlorite treatment of gravid animals followed by placing them on fresh plates containing *E. coli* OP50 where they were allowed to grow into young adults for 48hrs at 20°*C.* Animals were then heat shocked by being parafilmed and immersed in a 37°C waterbath for 30 minutes, followed by recovery at 25°*C.* Nematodes were monitored during the recovery period and after 8hrs of recovery, similarly aged healthy and active (crawling) worms were scored for their DAF-16 nuclear localization using a Leica DMLB fluorescence microscope as follows: high (completely nuclear), moderate (nuclear with some cytosolic expression) or none (completely cytosolic) as previously described (Kawli and Tan, 2008).

3.6.6 Quantitative PCR of mutant nematodes

qPCR of *unc-53 (n152), unc-53(e404)* and N2 nematodes was performed as previously described (Alper et al., 2007). In each case, strains were first synchronized by hypochlorite treatment of gravid animals. Eggs were then placed on *E. coli* OP50 for 48hrs at 20°C, after which they were transferred to *E. coli* OP50 or *P. aeruginosa* PA14 for 12hrs. *E. coli* and *P. aeruginosa* plates were prepared similarly to those used in the immunity assays described above except that cultures were inoculated onto large peptone-rich NGM plates (10cm) with 100µl of an overnight culture spread evenly across the surface prior to incubation. Additionally, these nematodes were not treated with FUDR or *lin-60/cdc25.1 (RNAi)* as done previously. Following incubation in the presence of pathogenic or control bacteria, nematodes were harvested using M9 buffer and were centrifuged at 3,500 rpm for 5 minutes. Three subsequent washes were conducted with M9 buffer. Following the final wash, the M9 buffer was removed and the nematodes were snap-frozen in liquid nitrogen and stored at -80°C for future use. Total RNA was isolated using Trizol reagent (Invitrogen Inc), and qPCR was performed on an ABI 7900 instrument using the Quantitect real-time RT-PCR kit (Qiagen Inc.) according to the manufacturer's instructions. Primers used for the qPCR are previously described (Alper et al., 2007; Kawli and Tan, 2008), and the total RNA concentration was normalized using *mlc-1* (myosin light chain) expression (Alper et al., 2007). Strains were analyzed in triplicate and were compared by using Graphpad Prism 5 software.

3.6.7 Microarray experiments

RNA collected for the microarray analysis was done as described above and was purified using Qiagen column purification. Total RNA was labeled with Cy3 using the QuickAmp labeling kit and was hybridized on whole genomes arrays using Agilent protocols. Gene expression analysis was done by using the *C. elegans* (V2) 44K Gene Expression Microarray (Agilent) Arrays scanned using an Agilent microarray scanner. Intensities were extracted from array images using Agilent Feature Extraction Software and data were normalized and scaled using robust multiarray analysis. Fold changes in RNA expression were calculated by comparing *unc-53* mutant nematodes to wild type nematodes grown on either OP50 or PA14 and differentially expressed genes were identified using two-factor ANOVA in MultiExperiment Viewer (http://www.tm4.org).

Genes with Bonferroni corrected p values < 0.05 (corresponding to raw $p < 1.0 \times 10^{-6}$) were considered statistically significant.

3.7 Acknowledgements

I would like to thank E. Kreiter, *C.* Grypma and D. Tu for technical assistance with this project; *C. elegans* Genetics Centre and Dr. N. Pujol for strains. I am grateful to Dr. N. Hawkins, Dr. C Beh, and Dr. N. Harden from Simon Fraser University and to Dr. V Singh and Dr. A. Aballay from Duke University for helpful discussions.

4: CONCLUSIONS

The migration of cells and the extension of cellular processes such as axons is crucial to the development of both invertebrates and vertebrates, and requires a precisely regulated interplay between upstream guidance cues and their receptors, intermediate signalling molecules, and changes in the cytoskeleton (Lowery and Van Vactor, 2009). Previous research into *unc-53* in *C. elegans* (Stringham et al., 2002) has already offered considerable insight into the function of the *Nav* gene family, and this study, as well recent cell biological and genetics research into the *Nav* homologs in vertebrates (Klein et al., 2011; Maes et al., 2002; Martinez-Lopez et al., 2005; McNeill et al., 2010; Muley et al., 2008; van Haren et al., 2009) has expanded what is known about the *Navs* even further. *unc-53* and the *Navs* have emerged as a family of conserved signal transduction and cytoskeletal binding proteins that link upstream guidance cues to changes in the cytoskeleton, with putative roles in cancer (Carlsson et al., 2012; Karenko et al., 2005; Maliniemi et al., 2011), neuropathologies (Fung et al., 2011; Shioya et al., 2010), and immune dysfunction (Foley and O'Farrell, 2004; Maliniemi et al., 2011). The aim of this project was to expand on what is known about the role of *unc-53* both during and after development in *C. elegans*. To accomplish this, an interaction between UNC-53 and ABI-1, a protein with conserved roles in actin polymerization through the ARP2/3 complex (Echarri et al., 2004; Innocenti et al., 2004; Innocenti et al., 2005; Leng et al., 2005; Steffen et al., 2004) was identified and characterized, leading to the discovery that UNC-53 and ABI-1 function together in cell migration and endocytosis, showing that UNC-53 function is mediated at least partly by its involvement in the control of actin dynamics. A role for *unc-53* in innate immunity was also explored, and it was found that *unc-53* was needed for resistance to *P. aeruginosa*, and that *unc-53* mutants have impaired synaptic transmission together with increased transcript levels of *ins-7* and altered DAF-16 localization. Experiments aimed towards understanding the tissue requirements of *unc-53* suggest a possible involvement from multiple tissues or isoforms in pathogen resistance. Taken together, this work offers insight into varied roles for UNC-53 in *C. elegans*, and offers future directions for studies into *unc-53* and the broader *Nav* family.

4.1 Role for UNC-53L in cell migration through ABI-1

unc-53 and the *Navs* possess complex genomic loci, containing numerous promoters that direct tissue and isoform specificity (Maes et al., 2002; Stringham et al., 2002). Previous work with *unc-53* suggested that the long-isoform of *unc-53* may not be necessary for longitudinal migration because its expression did not appear to correlate with the known phenotypes of *unc-53* and because a construct devoid of the long-isoform was sufficient to rescue *unc-53* mutant phenotypes (Stringham et al., 2002). To test a model showing a requirement for the long isoform, an antibody was raised to the portion of UNC-53 contained within the first 5 exons and a transcriptional reporter to the predicted long-isoform was produced. It was found that the long-isoform of *unc-53* was expressed in many cells requiring UNC-53 and that UNC-53 expression persists in many cells and tissues following development including the intestine, neurons, coelomocytes, and the excretory cell. The observed expression of *unc-53* suggests a model where the long-isoform of *unc-53* is needed during and after development. Long-isoform specific RNAi and the overexpression of the CH domain moderately abrogated the migration of the posterior excretory canals, suggesting that the long-isoform of *unc-53* is required for excretory cell development. Also, a yeast two-hybrid screen using the CH domain as bait identified ABI-1 as an UNC-53 interacting protein, suggesting that this isoform may function in actin dynamics with ABI-1.

Given the role of ABI-1 in the control of actin polymerization through WAVE and the ARP2/3 complex (Kurisu and Takenawa, 2009) the hypothesis that ABI-1 might function with UNC-53 in cell migration in a conserved process controlling actin dynamics was pursued. Consistent with a model involving UNC-53 and ABI-1 in the control of migration through an actin-mediated process it was found that UNC-53 and ABI-1 shared many of the same migration phenotypes including the anterior and posterior extension of the excretory canals, the anterior migration of the PLMs, and the dorsoventral migration of the motorneurons. The potential for a migration defect in the ventral projection of the PDE neuron in an *unc-53* mutant was assessed and a mild defect was observed, an interesting observation given that the migration of the PDE is under the control of actin regulators (Shakir et al., 2008). To ensure that UNC-53 and ABI-1 functioned together in these processes it was shown that they interact genetically and that they are expressed in some of the same cells including neurons and coelomocytes, and that ABI-1 functions cell autonomously in the excretory cell.

Consistent with a potential role for UNC-53 in actin-mediated migration it was also observed that *arx-2*, *nck-1*, and *wve-1* function in the migration of the ExC.

Unresolved questions:

While the role of *unc-53* after development has become more clear, several questions remain. One question is the relative contribution of each of the isoforms of unc-53. Three putative promoters have now been identified for *unc-53* and so far it appears that all of the isoforms are necessary for migration in *C. elegans*. It is important to understand the full contribution of all the isoforms from this complex locus because it could have implications for the *Navs* generally. Each *Nav* gene resembles a specific isoform to some degree. One possibility is that the isoforms contribute to different aspects of migration given their subcellular location as well as their varied tissue expression. Techniques currently exist that allow for the isoform specific GFP tagging of large genomic loci like *unc-53* (Dolphin and Hope, 2006) that could be used to answer some of these questions.

Another question concerns the nature of the interaction between UNC-53 and ABI-1. While it is known that they are involved in similar processes and function together genetically and cell-autonomously, the way that UNC-53 and ABI-1 might regulate each other is unknown. ABI-1 and NAV3 colocalize in response to GTPase activation in zebrafish hepatoblasts (Klein et al., 2011). While it is known that UNC-53 and ABI-1 are expressed in some of the same cells, the nature of their subcellular localization and the extent that their localization depends on each other is not known. Future studies should be pursued that would give insight into the subcellular expression pattern of these genes. A model was suggested whereby UNC-53 binds the plus ends of microtubules and functions as a scaffold protein to localize ABI-1 to the actin-cytoskeleton. Subcellular localization studies with ABI-1 and UNC-53 together with the various components of the cytoskeleton including actin and microtubules would be very informative to this end.

4.2 UNC-53 and ABI-1 function in trafficking

Given the co-expression of UNC-53 and ABI-1 in the coelomocytes and the role of actin in trafficking the possibility that these genes may function in endocytosis was examined. While a role for *unc-53* in coelomocytes uptake was observed, a role for *abi-*

1 was not. However, both *abi-1* and *unc-53* are involved in the receptor mediated uptake of yolk-protein in oocytes, favouring a model where both of these proteins could function together in endocytosis or trafficking. Two ambiguities arose in the trafficking studies. The first is that *abi-1* did not appear to be necessary for coelomocyte uptake despite being expressed in coelomocytes. This may be due to a number of reasons including the use of RNAi and a hypomorphic allele. Future studies could address this using enhanced RNAi strains and sensitized genetic backgrounds. Given that *abi-1* appears to function in oocyte uptake (Giuliani et al., 2009) suggests that pursuing *abi-1* in an endocytic role is worthwhile. Secondly, while *unc-53* functions in both coelomocyte uptake and oocyte uptake, only *unc-53 (e2432)* animals displayed a CUP defect. *unc-53 (n152)* was tested for a role in oocyte uptake. Given the complex nature of the *unc-53* locus it is possible that allelic differences such as this might arise. Many alleles of *unc-53* exist that are uncharacterized, so examining other alleles for this phenotype would be a good first step. *unc-53 (e2432)* does differ from *unc-53 (n152)* in some respects (Siddiqui and Culotti, 1991) including enhanced posterior versus anterior muscle vulva muscle attachment defects (Dr. E. Stringham, personal communication).

Another important question related to *abi-1* and *unc-53* with respect to endocytosis concerns specificity. *abi-1* has been shown to function in the uptake of YP170-GFP in a process that involves TOCA-1/2, which functions through WASP and WAVE (Giuliani et al., 2009) and this study suggest a role for *abi-1* with the WAVE complex in migration. Given the finding that UNC-53 functions with ABI and WAVE and ARP2/3, one model would suggest that UNC-53 may be functioning with ABI-1 and the WAVE complex in oocytes. The TOCA1/2 study, and this one, do not provide any information about the precise role that ABI-1 or UNC-53 are playing in oocytes. While the expectation might be that ABI-1 and UNC-53 function to control actin in endocytosis, this is not necessarily the case. Grant *et al.* (1999) show that mutations affecting YP170-GFP uptake are not specific to endocytosis. Defects are observed in mutants targeting the early steps of CME (e.g. clathrin, AP2) as well as endosomal sorting *Rabs*, and even the conserved secretion pathways that traffic the RME-2 receptor to the membrane (Grant and Hirsh, 1999). Understanding the localization of ABI-1 and UNC-53 in the oocytes and coelomocytes using *Rab* specific markers as well as examining some the potential secretory defects in these cells would assist in understanding the potential role of UNC-53 and ABI-1 in trafficking.

Of potential importance given the observation that *unc-53* and *abi-1* function in both endocytosis and migration is the extent to which endocytic defects might contribute to other defects observed in these mutants. One possibility is that endocytic defects in *unc-53* and *abi-1* might contribute to the migration defects observed in these mutants. The kinesin-like protein VAB-8 trafficks guidance receptors to the plasma membrane (Levy-Strumpf and Culotti, 2007; Watari-Goshima et al., 2007), and UNC-53 antagonizes VAB-8 function in some cells (Wolf et al., 1998; Wolf, 1998)(Dr. G. Garriga, personal communication). One possibility is that UNC-53 may antagonize VAB-8 by countering receptor traffic to the membrane through endocytosis. Another phenotype observed in *abi-1* but not so far observed in *unc-53* is a defect in cell corpse engulfment (Hurwitz et al., 2009). *abi-1*, *wve-1 and gex-2/3* are shown to be involved in engulfment (Dr. M. Hurwitz, personal communication), a phagocytic process that is Rac-dependent (Lundquist et al., 2001). It would be interesting to examine a potential role for *unc-53* in engulfment in *C. elegans*. The *Drosophila* homolog *Sickie* was observed to interact with *Drosophila Reaper* and *Pallbearer* through a yeast two-hybrid screen (Giot et al., 2003) and *Sickie* regulates *Dredd*, whose closest *C. elegans* homolog is *ced-3*. While these are interesting connections, the extent to which these engulfment pathways are conserved between flies and worms is not known.

4.3 Post-developmental role for UNC-53 in innate immunity

Previous work through an RNAi screen identified that *unc-53* is needed for the expression of *clec-85::gfp* (Alper et al., 2008). *clec-85* expression is increased in response to *P. aeruginosa* (Alper et al., 2007), so a potential role for *unc-53* in resistance to *P. aeruginosa* was assessed. Consistent with this model, it was found that *unc-53* mutants are highly susceptible to *P. aeruginosa* and that this defect was at least partially unrelated to the role of *unc-53* during development or a general decrease in fitness. We also observed that *unc-53* was expressed in several tissues in adult animals including neurons and the intestine, two tissues with described roles in innate immunity. We tested these two tissues for a potential role in immunity and observed that at least the long-isoform of *unc-53* was not sufficient to rescue these defects. This finding disproves a model that *unc-53L* is needed in these two tissues alone or in combination for pathogen resistance. Subsequently, a combination of tissue-specific RNAi experiments and isoform-specific rescuing experiments yielded data that is consistent

with a model where *unc-53* may be required in a tissue that has not yet been tested or that a combination of tissues and isoforms may be required.

A second tested hypothesis was that *unc-53* influences the DAF-2-DAF-16 pathway to mediate pathogen-resistance. Consistent with this hypothesis it was found that *unc-53* is hypersensitive to Aldicarb, had increased *ins-7* RNA levels, and affected DAF-16 localization. Taken together, this is strong evidence that *unc-53* influences DAF-16 through a neuronal mechanism. To further test this model genetically, double mutants between *unc-53 (n152)* and *daf-2* and *ins-7* were constructed, and it was found that they did not completely suppress *unc-53 (n152)* which could be interpreted to suggest that *unc-53* functions independently of *daf-2* and *ins-7*, though it does not preclude an additional role for *unc-53 (n152)* in the DAF-2-DAF-16 pathway. RNA was also collected to test for alterations in transcript levels of DAF-16 target genes (Kawli and Tan, 2008) but marked decreases in the DAF-16 target antimicrobials tested was not found.

Unresolved questions

An important question that has arisen from this work is one of tissue specificity. Given the complex nature of *unc-53* it is possible that a precise isoform or combinations of isoforms in a specific subset of tissues is necessary for innate immunity in *C. elegans*. Again, this suggests that an inquiry into the relative contributions of the various isoforms of *unc-53* for all of these processes, and especially innate immunity, is worth investigating. Another complex gene with multiple tissue involvement and varied isoform specific phenotypes is *unc-73* (Steven et al., 1998; Steven et al., 2005). Solutions to the isoform specific differences in *unc-73* were solved by using a combination of isoform specific expression contructs and alleles (Marcus-Gueret et al., 2012; Steven et al., 1998; Steven et al., 2005). A similar approach could be applied to *unc-53*.

A difficult point to resolve in this study is the apparent lack of antimicrobial changes in *unc-53* on either *E. coli* in a basal state or in an induced pathogen-exposed state in the presence of *P. aeruginosa*. One possibility is the culture conditions. Under different culture conditions (bacteria grown on standard NGM media and pathogen exposures performed at 25ºC), expression of numerous antimicrobial genes were decreased in an *unc-53 (e404)* mutant background (assayed by qPCR) (Dr. S. Alper, personal communication). Culture conditions can have profound effects on pathogen

behavior and host susceptibility (Alper et al., 2007; Kim et al., 2002). We did not observe antimicrobial changes in peptone-rich media at 20ºC by either qPCR or in the microarray, though some possible candidate genes from the microarray may given clues to *unc-53* function in immunity. It is possible that altering the culture conditions could reveal antimicrobial expression changes, clarifying a role for *unc-53* in immunity, and shedding light on the genetic pathways needing *unc-53*, given that antimicrobial signatures between genetic pathways vary (Alper et al., 2007; Troemel et al., 2006). While changing the culture conditions may yield measurable anti-microbial changes, it is interesting that the culture conditions used to collect RNA for the qPCR and microarray studies are the same culture conditions that lead to death for *unc-53* mutant and RNAi treated animals. It is possible that the pertinent antimicrobials were not assayed. Some of the antimicrobial previously shown to be under the control of INS-7 and DAF-16 have not been tested (Kawli and Tan, 2008). Another possibility is that *unc-53* does not regulate anti-microbial expression at the RNA level.

Another question concerns a possible relationship between the observed trafficking defects for *unc-53* and *abi-1* and their innate immunity defects. A role for trafficking in innate immunity has been slow to develop in both *C. elegans* and mammals. For example, only a few of the over 60 RABs and 40 RAB-GAPs in mammals have been tested for a role in immunity. They include RAB10, required for the transport of the LPS receptor TLR4 to the cell surface, RAB7b, required for TLR4 trafficking to the lysosome for destruction, and the RAB-GAP *tbc-1*/Tbc1d23, which regulates innate immunity in *C. elegans* and mice (De Arras et al., 2012; Wang et al., 2006; Wang et al., 2007). Recent studies in *C. elegans* describe a central role for endocytosis in *C. elegans* immunity. Dunbar *et al.* (2012) show that a *P. aeruginosa* infection inhibits mRNA translation in the intestine via the endocytosed translation inhibitor Exotoxin A (Dunbar et al., 2012), and Los *et al.* (2012) show that RAB-5 and RAB-11 provide host-protection from pore-forming toxins and restore membrane integrity following pathogen attack (Los et al., 2011). Additionally, dyn-1 affects the transcriptional response to infection of SNF-12 in an association with endocytic vesicles (Dierking et al., 2011). These studies provide excellent examples of the complex nature of the immune responses and the importance of trafficking pathways to innate immunity. Given the evidence that *unc-53* and *abi-1* are involved in immunity and trafficking, and given especially previous studies showing a role for mammalian ABI-1 in binding

relevant trafficking proteins (e.g. synaptojanin, syntaxin, SNAP-25, dynamin) (Echarri et al., 2004; So et al., 2000), certainly a role for these proteins in a trafficking process in *C. elegans* immunity is worth pursuing.

4.4 Multiple or overlapping roles for *unc-53/Nav2*?

In this work multiple and seemingly independent roles for *unc-53* in cell migration, trafficking and innate immunity were uncovered. The observation that UNC-53 is involved in these varied processes is worth consideration.

The multiple roles for *unc-53* could suggest that this gene plays such a pivotal role in the cell that it is needed for multiple independent processes. The observation that evolution has devised ways for individual proteins and even entire signal transduction cascades to be assigned to different functions at different times is common. A classic example is the observation that Toll signalling controls pattern specification along the dorsoventral axis in *Drosophila* but also has a role in innate immunity (Silverman et al., 2009). Many of the proteins known to control innate immunity in *C. elegans* have additional roles in cell migration. DBL-1/TGF-B has clear roles in both innate immunity and axonal guidance in *C. elegans* (Savage-Dunn, 2005). The p38 MAPK signalling cascade is conserved across kingdoms and has conserved roles in cell growth, migration, proliferation. Genetic silencing of MAPK signalling results in profound developmental defects in vertebrates (Krens et al., 2006). Similarly, DAF-16 negatively regulates muscle arm extension during *C. elegans* development (Dixon et al., 2008), and the mammalian FOXO transcription factor is needed for T-cell proliferation and for the expression of homing molecules essential for T-cell trafficking in the body (Carrette et al., 2009). Of particular importance to this study is the observation that *abi-1*, which was observed to function in both innate immunity and cell migration here, has also been shown to be involved in cell migration and innate immunity elsewhere. A role for ABI-1 in migration is well-documented (Kurisu and Takenawa, 2009), while a role for ABI-1 in immunity has only recently been developed. The WAVE complex is observed to control actin dynamics in immune cells (Park et al., 2010), and ABI has been shown to be required along with WASP and Ena for *Listeria* invasion through the Met receptor (Bierne et al., 2005). The *abi-1* interactor *abl-1* is needed for *Shigella flexneri* pathogenesis (Burton et al., 2006). Also, a relatively recent study by Marsh *et al.* (2011) in *C. elegans* showed that *abi-1* and *abl-1* are necessary for a 'balanced immunity

phenotype' and that loss of *abi-1* or *abl-1* function results in a susceptibility to the fungal pathogen *C. neoformans* (Marsh, 2010; Marsh et al., 2011).

The multiplicity of function observed for *unc-53* also seems to be a feature of the *Navs* more generally. *Sickie* was identified as a novel molecular player of the IMD pathway in *Drosophila* but is also expressed in the *Drosophila* nervous system during development and is required for mushroom body formation (Dr. T. Tabata, personal communication). In this respect, it is interesting that the same screen that identified *Sickie* as required for *Rel* nuclear translocation and the expression of *Dipt* also found that the *Drosophila* actin regulator *Scar/Wave* functioned in parallel to or downstream of *Sickie* (Foley and O'Farrell, 2004). Studies into the *Navs* which have known roles in migration (Martinez-Lopez et al., 2005; McNeill et al., 2010; van Haren et al., 2009) are being shown to have potential roles in immunity (Carlsson et al., 2012). Similarly, there are indications that the Navs may function at synapses, as *Nav3* mRNA is enriched at neuromuscular junctions (Kishi et al., 2005). Studies of *unc-53* have already been of considerably useful to investigations into the *Navs*, so it is expected that uncovering these new roles for *unc-53* will similarly shed light on the role of the Navigators.

4.5 Implications for the Neuron Navigator family

Recent studies of the *Navs* have focused on a role for these proteins as microtubule +TIPs that couple ATPase activity to outgrowth (van Haren et al., 2009). Considerable efforts have shown that *Navs* are key downstream effectors of *atRA* signalling and are absolutely required for neural development (McNeill et al., 2010; Muley et al., 2008). In this study UNC-53 is found to bind ABI-1 through the CH domain, which is conserved in NAV2 and NAV3. Expression of *Nav2* rescues neuronal outgrowth defects in *C. elegans* (Muley et al., 2008), showing that these proteins can function similarly across species. As a result, inquiries into the role of mammalian ABI proteins with the NAVs are warranted. *atRA* signalling is needed for cerebellar development, and both mNAV2 and ABI are expressed in outgrowing cerebellar granule cells (McNeill et al., 2010). Similarly, a link between ABI and NAV3 in zebrafish is observed (Klein et al., 2011). Given the observation that the NAVs bind EB1 and are +TIPs, it is possible that NAVs control the integration of signalling from microtubules to the actin cytoskeleton like other +TIP proteins (Akhmanova and Steinmetz, 2010). So the question of the exact nature of UNC-53 function at the plus ends of microtubules at

cortical actin is a relevant one, and this study suggest that considering a role for the *Navs* in ARP2/3 mediated actin polymerization at these sites may be worthwhile. Also, while the function of the AAA ATPase of UNC-53 was not investigated in this study(Akhmanova and Steinmetz, 2010), AAA ATPases are known to mediate the activity of SNARE domain containing proteins (e.g. NSF-1), and to promote conformational changes in target substrates (Hanson and Whiteheart, 2005). Given that ABI-1 is a SNARE domain containing protein and that both of these genes are involved in trafficking, it is possible that the NAVs may regulate some aspect of trafficking along microtubules or at endocytic sites at the plasma membrane to mediate outgrowth.

These studies may also be informative to studies of the *Navs* in cancer. *Nav3* is emerging as a relevant tumor suppressor (Shi et al., 1995)(Shi et al., 1995) (Karenko et al., 2005; Maliniemi et al., 2011) and roles for ABI proteins in tumor suppression are also shown {{23 Shi,Y. 1995}}. We found that UNC-53 and ABI-1 function with the ARP2/3 complex in migration and endocytosis. Branched actin nucleation has a central role in promoting tumor cell invasiveness and in controlling cancer signalling through the endocytosis of receptors (Kurisu and Takenawa, 2010; Nurnberg et al., 2011). It is possible that NAV3 and ABI1/2 function in tumor biology in one or both of these ways. Of additional interest to the study of tumor biology from the perspective of the *Navs* is a recent study linking *Nav3* to tissue inflammation in colon cancer (Carlsson et al., 2012). The most striking association between innate immunity and cancer is observed in cases of chronic inflammation, a hallmark of excessive innate immune signalling; estimates suggest that ~15% of cancers are attributed to bacterial and viral infections (Karin et al., 2006). Polymorphisms in the Toll-like receptors (Piccinini and Midwood, 2010; Sato et al., 2009), are overly represented in numerous cancers, including: gastric cancer, colorectoral cancer, and nasopharyngeal carcinomas (Balistreri et al., 2009; El-Omar et al., 2008). Aberrations in TLR signalling also exert profound effects on the microenvironment of tumours and result in accelerated tumour proliferation and size, decreased apoptosis, as well as increased tumour angiogenesis, aggressiveness and metastasis (Castro et al., 2011; Fukata et al., 2009; Paone et al., 2010; Sato et al., 2009). Preliminary studies in the *Nav2* mouse model show altered cytokine responses to multiple PAMPs (Dr. S. Alper, personal communication), further suggesting that the *Navs* could function in immunity, inflammation, and cancer.

5: APPENDIX 1

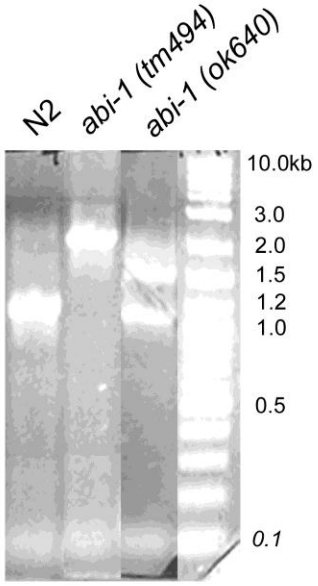

Figure 47. *abi-1 (ok640)* deletion mutants carry a wild-type copy of *abi-1.*

Representative amplification products from genomic DNA isolated from N2, *abi-1 (tm494)* and *abi-1 (ok640)* animals. Deletion strains were outcrossed greater than five times to wild-type (N2) and were amplified using flanking primers and a diagnostic primer internal to the expected deletion regions as indicated (see Section 2.5.1). Amplification of *abi-1 (tm494)* reveals a single amplification product consistent with the expected deletion (~2.0kb) while PCR of *abi-1 (ok640)* animals gives rise to an amplification product similar to N2 (~1.1kb) as well as a deletion product (~1.6kb).

Table 11. Summary of survival analysis of *unc-53* mutant and *unc-53 (rnai)* animals exposed to *P. aeruginosa PA14.*

Bacterial challenge	*Genetic background*	*Median Survival (Hrs)*	*N*	*P-value*
P. aeruginosa PA14	N2	69.9	203	-
	unc-53 (e404)	59.3	233	<0.0001
	unc-53 (e2432)	58.0	231	<0.0001
	unc-53 (n152)	34.5	233	<0.0001
	unc-53 (n166)	25.1	230	<0.0001
	unc-53 (n152);	63.4	144	<0.0001

	WRM0628aD12			
	pmk-1 (km25)	41.2	218	<0.0001
	pPD129.36 (rnai)	92.2	92	-
	unc-53 (rnai)	47.0	99	<0.0001
	pmk-1 (rnai)	59.8	95	<0.0001
	him-8 (e1489)	85.8	177	-
	unc-53 (n152); him-8 (e1489)	64.5	206	<0.0001
	lin-60/cdc-25.1 (rnai)	84.6	166	-
	unc-53 (n152); lin-60/cdc-25.1 (rnai)	47.7	150	<0.0001
	N2	60	117	-
	unc-53(n152)	45	149	<0.0001
	pmk-1 (km25)	45	143	<0.0001
	unc-53(n152); pmk-1 (km25)	46	129	P=0.8426
P. aeruginosa PA14 *(heat-killed)*	N2	481.4	238	-
	unc-53 (n152)	418.1	276	<0.0001

P-values compare the survival curves using the Log Rank (Mantel-Cox) statistic. All P-values are compared to wild-type controls or empty vector (pPD129.36) except *unc-53 (n152);* WRM0628aD12 which was compared to *unc-53 (n152)* and *unc-53 (n152); pmk-1 (km25)* which was compared to *unc-53 (n152)*. Median values were calculated using Linear Regression Analysis (SPSS) except for the epistasis experiments involving *unc-53 (n152)* and *pmk-1 (km25)* which were determined using Graphpad, Prism 5).

Table 12. Summary of survival analysis of *unc-53* mutant and *unc-53 (rnai)* animals exposed to *E. coli OP50-1.*

Bacterial challenge	*Genetic background*	*Median Survival (Hrs)*	*N*	*P-value*
E. coli OP50-1	N2	222.9	150	-
	unc-53 (e404)	212.2	150	0.1536
	unc-53 (e2432)	199.2	174	0.1123
	unc-53 (n152)	180.7	144	<0.05
	unc-53 (n166)	181.2	124	<0.01
	pPD129.36 (rnai)	199.1	125	-
	unc-53 (rnai)	196.3	138	0.6759
	pmk-1 (rnai)	193.3	117	0.7646

P-values compare the survival curves using the Log Rank (Mantel-Cox) statistic. All P-values are compared to wild-type controls or empty vector (pPD129.36). Median values were calculated using Linear Regression Analysis (SPSS).

Table 13. Summary of survival analysis of *unc-53 (rnai)* adult treated animals exposed to *P. aeruginosa PA14.*

Bacterial challenge	Genetic background	Median Survival (Hrs)	N	P-value
P. aeruginosa PA14	*pPD129.36*	65	181	-
	unc-53 (rnai)	51	206	P<0.001
	pmk-1 (rnai)	45	115	P<0.001

P-values compare the survival curves using the Log Rank (Mantel-Cox) statistic. All P-values are compared to wild-type controls or empty vector (pPD129.36).

Table 14. Details of the rescue of *unc-53 (n152) P. aeruginosa* PA14 susceptibility using *prab-3::unc-53, pges-1::unc-53,* and *pges-1::unc-53::gfp* constructs.

Bacterial challenge	*Genetic background*	*Median Survival*	*N*	*P-value*
P. aeruginosa PA14	*N2*	70	101	-
	unc-53 (n152)	35	129	P<0.0001
	VA381	33	108	P=0.9845
	VA382	39	97	P=0.7658
	N2	70	101	-
	unc-53 (n152)	35	129	P<0.0001
	VA378	39	126	P=0.9584
	VA379	33	97	P=0.7441
	N2	69	45	
	unc-53 (n152)	41	98	P<0.0001
	VA375	38	111	P=0.5801
	VA376	35	96	P=0.8593
	N2	66	75	-
	unc-53 (n152)	38	120	P<0.0001
	VA508	38	117	P=0.9142

P-values compare the survival curves using the Log Rank (Mantel-Cox) statistic. *unc-53 (n152)* is compared to wild-type (N2) and VA strains are compared to *unc-53 (n152)*. P-values are compared to *unc-53 (n152)*.

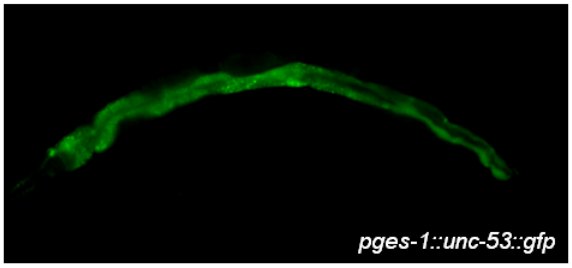

Figure 48. *pges-1::unc-53::gfp* expressed GFP in the intestine

Strain VA508 is shown to express GFP in the intestine. Strain construction details are found in Section 3.6.1.

Table 15. Rescue of the *unc-53 (n152)* PLM defects by pan-neuronal expression of *unc-53* using prab-3::*unc-53)*, and the fosmid WRM0628aD12.

Construct used	Percentage of animals with wild-type length	N
*vaEx528 (VA381)**	~98%	>100
vaEx529 (VA382)	~98%	~50
vaEx547 (VA375)	~95%	~50
vaEx548 (VA376)	~98%	~50
WRM0628aD12 (VA541)	~95%	>100

PLM defects assessed using *pmec-4::gfp (bzIs7)* marker. In each case the strain was crossed to *unc-53 (n152); pmec-4::gfp* and the PLM defect was examined as described (see Section 2.5.4). The strain carrying the given array is indicated in brackets. *unc-53 (n152)* is a null allele and has a 100% penetrant PLM defect similar to the null allele *unc-53 (n166)* (Table 4). *Used in attempt to rescue of DAF-16::GFP mislocalization following recovery from heat shock (Figure 39).

Table 16. Details of the tissue-specific RNAi experiments targeting *unc-53* in the intestine, muscle, and hypodermis.

Bacterial challenge	*Genetic background*	*Median Survival*	*N*	*P-value*
P. aeruginosa PA14	*OLB11-pPD129.36*	70	177	-
	OLB11-unc-53 (rnai)	70	154	P=0.1720
	NR350-pPD129.36	95	124	-
	NR350-unc-53 (rnai)	85	106	P=0.2720
	NR222-pPD129.36	68	123	-
	NR222-unc-53 (rnai)	85	144	P=0.1980

P-values compare the survival curves using the Log Rank (Mantel-Cox) statistic. All P-values are compared to wild-type controls or empty vector (pPD129.36). Median values were calculated by comparing growth curves (Graphpad Prism 5)

6: APPENDIX 2

Table 17. Significantly upregulated and downregulated genes in N2 animals exposed to *P. aeruginosa* PA14 compared to *E. coli* OP50-1

Probeset ID	*GeneName*	*p-value (N2 PA14 vs N2 OP50-1)*	*Fold-Change (N2 PA14 vs N2 OP50-1)*
A_12_P118441	F49H6.13	1.61E-05	340.442
A_12_P137520	clec-174	1.71E-05	189.923
A_12_P111832	F55G11.2	0.00019971	94.6069
A_12_P102790	clec-240	0.000139408	89.3567
A_12_P100863	F53E10.4	9.53E-05	85.336
A_12_P108474	H02F09.3	5.67E-05	79.8588
A_12_P107716	oac-32	9.25E-05	77.6873
A_12_P117478	C32H11.4	0.000303196	69.0441
A_12_P103959	F55G11.5b	0.000223143	61.7193
A_12_P102673	clec-3	0.000315715	54.9332
A_12_P118504	dod-24	0.000121877	53.846
A_12_P100733	K10D11.2	0.000360665	49.7478
A_12_P177219	clec-3	0.000184559	48.9775
A_12_P162744	F55G11.3	0.000384963	43.9255
A_12_P112501	clec-163	8.44E-05	43.6981
A_12_P116848	T05F1.9	0.000152855	42.8405
A_12_P113632	K11H12.4	0.000144761	42.7821

A_12_P112033	fbxa-128	0.000306844	41.19
A_12_P104832	F55G11.7	0.000103144	35.5709
A_12_P110312	F46B3.1	0.000180445	35.5148
A_12_P118215	clec-17	0.000302669	34.6965
A_12_P108650	F25A2.1	3.20E-05	32.9847
A_12_P119355	pgp-7	0.000227756	31.809
A_12_P177064	clec-163	0.00032694	31.7554
A_12_P178396	A_12_P178396	0.000402246	28.6965
A_12_P111543	srw-85	0.000392203	24.7658
A_12_P155595	T14E8.1	0.000172662	21.6178
A_12_P108012	pgp-7	0.000237483	21.0827
A_12_P111213	crn-2	7.57E-05	20.6667
A_12_P115833	clec-71	0.000171766	19.0956
A_12_P104919	sri-74	0.000283787	18.6833
A_12_P101591	F01D5.5	0.000179798	17.9371
A_12_P114446	F35E12.8a	0.000205089	15.6982
A_12_P113527	ugt-16	7.39E-05	15.5722
A_12_P132224	H43E16.1	1.17E-05	15.1985
A_12_P115336	F46B3.2	0.000383549	14.3404
A_12_P107692	UDP-glu-transferase	0.000202938	14.3218
A_12_P173568	T16G1.6	0.000211895	13.0946
A_12_P114420	ift-74	8.14E-05	13.0605
A_12_P107203	C56A3.7b	3.00E-05	12.2781
A_12_P109519	T16G1.6	0.000152101	12.2751
A_12_P140353	E04F6.16	0.000272786	11.8828
A_12_P102843	clec-64	0.000287165	11.7968
A_12_P112659	ZK896.5	0.000215306	11.707
A_12_P173567	T16G1.6	0.000169185	11.6314

A_12_P155046	Y43F8B.3	6.20E-05	11.0788
A_12_P119881	Y39A3A.2	0.000285556	10.9421
A_12_P107428	F35E12.5	8.36E-05	10.7314
A_12_P110335	C30G4.2	2.14E-05	10.4548
A_12_P173990	A_12_P173990	9.00E-06	9.7668
A_12_P118430	C38H2.2	0.000109557	9.21764
A_12_P104902	F09A5.2	0.000153229	8.85824
A_12_P110751	K10D11.3	0.000293322	8.24595
A_12_P115076	haf-7	0.000171793	8.24508
A_12_P163157	scl-14	4.33E-05	7.97057
A_12_P103141	Y43F8B.3	7.63E-05	7.88791
A_12_P103549	T28B4.4	3.75E-06	7.83317
A_12_P138295	C54D10.12	0.000356153	7.50655
A_12_P108886	H43E16.1	0.000124879	7.50429
A_12_P173991	A_12_P173991	0.0003825	7.01695
A_12_P113118	pgp-12	0.000292721	6.8968
A_12_P106363	amylase	9.34E-05	6.84555
A_12_P142002	C15B12.9	0.000376449	6.26035
A_12_P135950	F22B8.2	0.000115864	6.25116
A_12_P107425	clec-84	1.28E-05	6.18163
A_12_P157855	Y14H12A.2	0.000389701	6.16154
A_12_P107855	nob-1	0.000337922	6.10917
A_12_P116882	T19D12.1	0.000368592	6.00654
A_12_P111688	ocr-3	3.82E-05	5.99261
A_12_P144346	Y14H12A.2	0.000337085	5.97222
A_12_P170252	Y14H12A.2	0.000271469	5.59258
A_12_P167683	C45B11.6	0.000252782	5.58808
A_12_P113080	K10D11.6	0.000142456	5.38271

A_12_P157858	Y14H12A.2	0.000394182	5.29012
A_12_P148250	F21H12.7	0.000227648	5.23604
A_12_P105371	C12D12.1	0.00036231	5.22343
A_12_P155045	Y43F8B.3	0.000296585	5.20382
A_12_P152124	T04C12.1	0.000251865	5.17639
A_12_P170255	Y14H12A.2	0.000381553	4.94682
A_12_P164208	D73093	1.96E-05	4.92992
A_12_P113150	srsx-34	5.97E-05	4.85494
A_12_P137634	C49G7.6	0.000251754	4.76499
A_12_P170253	Y14H12A.2	2.87E-05	4.74059
A_12_P104413	clec-167	3.51E-05	4.69556
A_12_P174738	A_12_P174738	0.000362197	4.49109
A_12_P106198	W01C8.1	0.000125939	4.36633
A_12_P114203	Y34B4A.10	5.81E-05	4.36567
A_12_P131960	cgp-1	0.000391842	4.36253
A_12_P141800	C12D12.1	0.000328831	4.3221
A_12_P115674	F42C5.10	0.000393294	4.2992
A_12_P101773	ncx-6	5.31E-05	4.28411
A_12_P142751	asc-1	0.000361895	4.22837
A_12_P143440	F52E1.5	0.000242228	4.19782
A_12_P134350	pme-5	8.51E-05	3.93883
A_12_P119401	K08B5.1	5.18E-05	3.89568
A_12_P101457	pme-5	0.000288962	3.8454
A_12_P105855	F10G7.5	0.000390509	3.71441
A_12_P100695	F19B2.4	1.83E-05	3.6173
A_12_P101404	Y15E3A.4.1	0.000101252	3.53604
A_12_P110002	sma-1	0.000398677	3.52177
A_12_P100188	fbxa-166	2.17E-06	3.50187

A_12_P139840	T19D12.1	0.000230287	3.49672
A_12_P111135	rop-1	0.00036289	3.4368
A_12_P162494	E02H9.1	0.000305714	3.43252
A_12_P139861	clec-36	0.000260484	3.38489
A_12_P177155	TC170897	3.11E-05	3.37815
A_12_P177157	TC170897	0.000180737	3.37725
A_12_P177156	TC170897	0.000143381	3.37353
A_12_P118724	fibrulin-1D	0.000322726	3.3676
A_12_P105935	obr-3	1.12E-05	3.35553
A_12_P177158	TC170897	0.00023654	3.34624
A_12_P117871	NP177013	9.27E-05	3.25246
A_12_P111226	K06H7.3	0.000158084	3.08906
A_12_P177154	TC170897	4.70E-05	3.02985
A_12_P134195	crt-1	0.000365334	2.96713
A_12_P165863	obr-3	0.00024778	2.95739
A_12_P147105	eps-8	4.53E-05	2.92218
A_12_P134196	crt-1	0.00035667	2.90378
A_12_P165862	obr-3	4.22E-05	2.78756
A_12_P105110	Y41E3.3	0.000105477	2.70547
A_12_P134197	crt-1	0.000310923	2.66475
A_12_P108702	atg-2	0.000364201	2.54955
A_12_P150390	F49E2.5	0.000109636	2.54218
A_12_P176009	A_12_P176009	0.000182767	2.54013
A_12_P176013	F49E2.5	0.000191781	2.5376
A_12_P163333	eps-8	0.000108039	2.46764
A_12_P176010	F49E2.5	0.000399302	2.46639
A_12_P176012	F49E2.5	8.36E-05	2.42839
A_12_P101643	W09D10.5	0.000256061	2.41831

A_12_P176011	F49E2.5	0.000389494	2.40249
A_12_P150391	F49E2.5	8.48E-05	2.38993
A_12_P104499	mbf-1	0.000237642	2.38001
A_12_P172357	R04A9.3	0.000311961	2.32571
A_12_P149640	F13H6.1b.1	0.00025064	2.31822
A_12_P138190	fbxa-172	0.000160701	2.18029
A_12_P175084	rgs-7	0.000200776	2.07168
A_12_P175082	rgs-7	9.79E-05	2.01992
A_12_P175083	rgs-7	8.84E-05	2.00537
A_12_P102863	rgs-7	0.000307696	1.92726
A_12_P143277	F14F9.8	0.000183234	1.91174
A_12_P113425	Y46G5A.34	3.40E-05	1.88278
A_12_P154580	cutl-24	8.34E-05	1.82176
A_12_P117505	F10D7.2	0.000248441	1.80191
A_12_P110759	K09F6.4	9.47E-07	1.73374
A_12_P107837	sra-33	0.000209419	1.71405
A_12_P103668	crt-1	4.11E-05	1.66782
A_12_P108769	F40F4.7	0.000217445	1.5852
A_12_P171791	cmd-1	7.56E-05	1.57113
A_12_P115253	F53A10.2	0.000248668	1.56368
A_12_P171788	cmd-1	0.000267076	1.55326
A_12_P113817	mml-1	0.000349695	1.52548
A_12_P171789	cmd-1	6.19E-05	1.5095
A_12_P159685	T03F6.4	0.000105483	1.49768
A_12_P171787	cmd-1	0.000290352	1.47257
A_12_P117715	F59A3.5	0.000263469	-1.166
A_12_P110959	C34C6.4	0.000213949	-1.31966
A_12_P154925	ZC434.7	0.000157875	-1.32232

A_12_P167182	A_12_P167182	0.000183415	-1.32959
A_12_P112745	F28B3.6	0.000181482	-1.33121
A_12_P154929	ZC434.7	0.000224206	-1.33139
A_12_P152725	Y54G2A.50	0.000318819	-1.33765
A_12_P156672	dys-1	7.60E-05	-1.34633
A_12_P154928	ZC434.7	0.00014192	-1.35163
A_12_P104487	F56B3.8	0.000108874	-1.43194
A_12_P176922	F28B3.6	6.56E-05	-1.44657
A_12_P107815	set-18	0.000119108	-1.46714
A_12_P154926	ZC434.7	0.000230584	-1.46995
A_12_P108115	B0238.10.2	3.26E-05	-1.48445
A_12_P130522	Y18D10A.20.2	0.000198815	-1.4872
A_12_P130523	Y18D10A.20.2	0.000312039	-1.48923
A_12_P154927	ZC434.7	0.00028638	-1.49
A_12_P130525	Y18D10A.20.2	8.65E-05	-1.50045
A_12_P130521	Y18D10A.20.2	0.00011454	-1.50309
A_12_P173087	F56F11.2	0.000140221	-1.50311
A_12_P104731	B0261.8	0.000206798	-1.50866
A_12_P106453	C26B2.7	0.000305138	-1.50904
A_12_P103369	T05E11.8	8.96E-06	-1.51232
A_12_P119276	F58H1.8	0.0001181	-1.51852
A_12_P176921	F28B3.6	0.000328725	-1.52983
A_12_P168677	Y18D10A.16	0.000271295	-1.5825
A_12_P112812	dkf-1	5.15E-05	-1.59991
A_12_P108245	Y73F8A.26	3.99E-05	-1.60488
A_12_P110840	Y92H12BL.5	0.000270349	-1.6251
A_12_P163023	inx-5	0.000157058	-1.6277
A_12_P114046	sdha-1	0.000333952	-1.63086

A_12_P116001	inx-5	4.66E-05	-1.66161
A_12_P108982	fkb-2	0.000215979	-1.67164
A_12_P115747	D2023.1	0.000172559	-1.70893
A_12_P113279	Y63D3A.7	0.000356437	-1.71761
A_12_P115413	Y71H2AM.11	0.000130143	-1.71951
A_12_P112144	F13E6.3	0.000127294	-1.75876
A_12_P159160	F57G12.1	0.000185739	-1.76501
A_12_P151662	har-1	0.000389702	-1.77338
A_12_P155767	Y56A3A.19	0.000132366	-1.77461
A_12_P152422	T01D1.8.1	0.000391219	-1.77602
A_12_P116261	F30A10.1	4.61E-05	-1.78237
A_12_P159592	T21G5.5d	0.000288461	-1.80813
A_12_P143400	acr-16	0.000232323	-1.81977
A_12_P116871	moc-1	0.000270021	-1.82201
A_12_P108201	F56A8.9	0.00019254	-1.83289
A_12_P138216	D2023.1d	5.16E-05	-1.83788
A_12_P174182	lfi-1	0.000168027	-1.83994
A_12_P107310	Y69A2AR.3	0.000134992	-1.8408
A_12_P112717	Y55F3*C*.3	7.95E-05	-1.89701
A_12_P150420	F26D2.8	5.35E-05	-1.92908
A_12_P117457	F40G9.2	0.000140167	-1.95459
A_12_P151430	nas-7	0.000285871	-1.96929
A_12_P101141	T02C1.1	0.000361739	-1.9893
A_12_P160893	F35F10.1	0.000222809	-2.04705
A_12_P133971	VB0395L.1	0.000336487	-2.05576
A_12_P118810	F59B8.1	0.000348001	-2.06469
A_12_P116237	dhs-27	0.000107308	-2.09473
A_12_P105596	Y67A10A.8	0.000313114	-2.13386

A_12_P133970	VB0395L.1	0.000100275	-2.13804
A_12_P118831	B0432.4.2	0.000272393	-2.26247
A_12_P176284	BJ155310	0.000217885	-2.27162
A_12_P111596	let-268	0.000342824	-2.30957
A_12_P103805	F40F4.8	4.11E-05	-2.33282
A_12_P179449	lin-45	0.000218557	-2.37629
A_12_P102105	ZK1320.9	0.000267551	-2.38281
A_12_P114394	R151.2	0.000299691	-2.39837
A_12_P106455	B0222.5	0.000193886	-2.46235
A_12_P113711	C14F11.4	0.000230185	-2.50388
A_12_P110954	T22E7.1	0.000395843	-2.5527
A_12_P113738	R02F2.8	3.00E-06	-2.57639
A_12_P107664	fkb-5	0.000154881	-2.6145
A_12_P138012	D2030.5.2	0.000292824	-2.62838
A_12_P171464	A_12_P171464	0.000314776	-2.66511
A_12_P102258	R11D1.7	8.05E-05	-2.77471
A_12_P171642	gei-16	0.000381966	-2.79393
A_12_P110869	nhr-74	9.72E-05	-2.80397
A_12_P108549	twk-16	7.76E-05	-2.84357
A_12_P100247	folt-1	0.000268034	-2.90162
A_12_P142140	C14F11.4	0.000135749	-2.97768
A_12_P106709	F54F7.2	0.000291206	-3.02374
A_12_P131865	Y6G8.9	0.000103751	-3.12744
A_12_P109681	tsr-1	0.000250805	-3.21165
A_12_P114912	Y51A2D.18	0.000292856	-3.24526
A_12_P114850	C05C9.2	0.000117524	-3.33639
A_12_P107017	F54D5.12	0.00037983	-3.33889
A_12_P133175	D2023.8	0.000370392	-3.36568

A_12_P107925	Y37A1B.5b	0.000281814	-3.4103
A_12_P151381	C08E8.2	0.000210189	-3.45609
A_12_P105188	kat-1	0.000146871	-3.53342
A_12_P113133	T02G5.4	6.58E-05	-3.57886
A_12_P107091	F13D12.2.1	2.17E-05	-3.60509
A_12_P100620	T05B11.4	7.76E-05	-3.6376
A_12_P102289	F46F5.7	0.00024839	-3.66118
A_12_P110566	srh-258	8.80E-05	-3.73021
A_12_P146780	Y49E10.29	2.90E-05	-3.97105
A_12_P115686	ZC196.4	0.000374303	-3.98975
A_12_P108300	ZC412.4	0.000167662	-4.06716
A_12_P113427	C46F2.1	0.000109082	-4.1185
A_12_P101648	F42G8.8	0.000318746	-4.17468
A_12_P156740	F42G8.8	9.74E-05	-4.35992
A_12_P119573	K02E10.4	0.000274166	-4.4175
A_12_P180794	Y43C5A.3	0.000258038	-4.46088
A_12_P106005	Y19D10B.1	8.19E-05	-4.56061
A_12_P118071	gly-8	0.00029005	-4.72971
A_12_P162620	Y37E11B.7	0.000118983	-4.73006
A_12_P115324	C53A3.1	0.000327199	-4.87011
A_12_P153110	str-168	0.000366245	-4.90396
A_12_P104363	ZC196.2	0.000237228	-4.96257
A_12_P119849	str-168	0.000291164	-5.03048
A_12_P102819	F53F1.2.2	0.000246111	-5.18308
A_12_P131711	spp-23	0.000355123	-5.30922
A_12_P131713	spp-23	0.000279585	-5.38309
A_12_P168932	A_12_P168932	0.000166535	-5.39541
A_12_P131712	spp-23	0.000347519	-5.47769

A_12_P107743	F43E2.5	0.000376502	-5.48212
A_12_P168933	A_12_P168933	0.000215728	-5.70103
A_12_P103131	kin-15	0.000144873	-5.75091
A_12_P164850	BJ817524	0.000257318	-5.76319
A_12_P168930	A_12_P168930	0.000343249	-5.83243
A_12_P161759	F56A4.3	3.78E-06	-6.17974
A_12_P135946	F32D8.12	0.000141754	-6.23584
A_12_P110295	dhs-25	0.000163935	-6.35518
A_12_P155655	ech-6	0.000322196	-6.43066
A_12_P108765	transporter	0.00024565	-6.4405
A_12_P107171	F09F7.4	0.000190289	-6.54775
A_12_P111032	R03E9.2	8.17E-05	-6.60641
A_12_P164849	BJ817524	0.00012288	-6.64577
A_12_P117133	F32D8.12	0.000102672	-6.71948
A_12_P159861	Y37A1A.2	0.000281745	-6.95669
A_12_P113686	C31H2.4	3.91E-05	-7.19129
A_12_P117234	F44G3.2	0.000207053	-7.64267
A_12_P117303	vit-1	0.000291583	-7.73303
A_12_P117691	F21C10.9	0.000144739	-7.84955
A_12_P176856	TC175669	0.00040251	-8.02171
A_12_P170104	F58G6.9	3.93E-05	-8.05203
A_12_P152644	TC175669	0.000397328	-8.2577
A_12_P155656	ech-6	9.31E-05	-8.36655
A_12_P174012	ech-6	0.000247926	-8.49826
A_12_P104123	ech-6	1.97E-05	-8.63642
A_12_P174013	ech-6	0.000208525	-9.079
A_12_P119403	gln-3	9.89E-05	-9.15208
A_12_P143850	sams-1	7.20E-05	-9.32993

A_12_P112711	Y51H7*C*.1	0.00023397	-9.61775
A_12_P109013	col-70	0.00029275	-9.84444
A_12_P135153	C04E12.5	0.000265997	-10.1052
A_12_P137981	C49F5.9	0.000195979	-10.2956
A_12_P180434	F48C1.3	0.000130927	-10.4803
A_12_P110513	fbxa-72	2.86E-05	-10.5236
A_12_P100066	ugt-6	0.000248506	-10.7962
A_12_P114905	nhr-114	4.11E-05	-11.4908
A_12_P143086	F18E3.12	9.73E-05	-11.9645
A_12_P110839	nhr-235	9.47E-05	-13.1062
A_12_P100742	gpdh-1	0.000224468	-13.5388
A_12_P153046	Y38F1A.6	6.49E-05	-13.7504
A_12_P153045	Y38F1A.6	3.88E-06	-13.8797
A_12_P114194	peptidase	0.000333052	-14.4107
A_12_P134301	ZK1290.15	0.000178037	-14.4577
A_12_P149485	F58G6.9	0.000169361	-14.5231
A_12_P105125	F58G6.9	0.000342731	-14.6168
A_12_P105959	cyp-14A1	8.27E-05	-14.7831
A_12_P143085	F18E3.12	7.57E-06	-14.9183
A_12_P105699	Y38F1A.6	6.02E-06	-14.9399
A_12_P165251	C49F5.9	0.000258512	-15.113
A_12_P116771	F46F2.5	6.81E-05	-16.1131
A_12_P113431	R05H10.7	0.000173574	-16.4164
A_12_P165253	C49F5.9	0.000273441	-16.7296
A_12_P165252	C49F5.9	0.000182282	-16.9053
A_12_P104412	ilys-5	6.75E-05	-16.9217
A_12_P168105	C35A5.3	0.000332338	-18.7785
A_12_P179340	C26B2.8	0.000301157	-19.6002

A_12_P174042	A_12_P174042	8.95E-05	-19.7284
A_12_P118367	cyp-14A2	7.16E-05	-20.9804
A_12_P174498	BJ781362	0.000114498	-21.2947
A_12_P113225	C52D10.1	0.000310741	-21.5617
A_12_P106740	cutl-18	0.000178612	-21.7492
A_12_P118633	ilys-2	0.000106077	-22.651
A_12_P165634	F46F2.5	5.53E-05	-25.2074
A_12_P137980	C49F5.9	6.93E-05	-25.733
A_12_P115897	C30G12.2	2.45E-05	-26.8189
A_12_P100536	folt-2	4.37E-05	-31.199
A_12_P109534	pmp-5	3.24E-07	-34.2548
A_12_P168834	folt-2	0.000173835	-34.6994
A_12_P139305	pmp-5	5.29E-06	-35.0255
A_12_P168836	folt-2	0.000293637	-38.0576
A_12_P168835	folt-2	0.000185539	-38.6531
A_12_P168837	folt-2	0.000234478	-40.4007
A_12_P104529	C09B8.4	0.000344378	-42.6399
A_12_P119528	lips-14	0.000372203	-44.345
A_12_P115386	amt-1	2.44E-05	-46.6659
A_12_P115369	Y38H6*C*.21	0.000304907	-61.4041
A_12_P113053	NP012779	2.54E-05	-72.3978
A_12_P155625	T13F3.6	4.02E-05	-72.6147
A_12_P161873	acdh-1	0.000355603	-101.343
A_12_P158961	C17C3.12a.2	5.13E-06	-179.176
A_12_P115889	C17C3.12a.2	7.15E-05	-197.537
A_12_P157152	C17C3.12a.2	1.48E-05	-238.196
A_12_P158960	C17C3.12a.2	1.95E-05	-270.517

Genes identified as altered in the presence of *P. aeruginosa* PA14 is based on a 5% FDR (false-discovery rate). This table includes duplicate genes identified in the microarray that are attributed to different probesets.

Table 18. Significantly upregulated and downregulated genes in *unc-53 (n152)* animals exposed to *P. aeruginosa* PA14 compared to N2

Probeset ID	*Gene Name*	*p-value(unc-53 mut Pseudomonas vs. wild type Pseudomonas)*	*Fold-Change(unc-53 mut Pseudomonas vs. wild type Pseudomonas)*
A_12_P119147	C45B2.3	0.000735293	26.2228
A_12_P100265	nhr-258	0.000132614	5.7644
A_12_P165467	che-13	0.000576771	5.28407
A_12_P100915	clec-76	0.000157289	5.18117
A_12_P165634	F46F2.5	1.38E-05	4.81268
A_12_P101782	M195.2	7.70E-06	4.6379
A_12_P110062	F59A1.6	0.000496737	4.62832
A_12_P102154	nlp-27	0.000572301	4.33961
A_12_P152300	T07C12.5	7.06E-06	3.93719
A_12_P150251	shc-1	0.000568278	3.92416
A_12_P102580	cnc-5	0.000479612	3.76533
A_12_P113003	cwp-2	0.000983243	3.75213
A_12_P109778	T19B10.2.2	0.000384331	3.70378
A_12_P118923	K01C8.1	0.000983347	3.64681
A_12_P107058	R11D1.3	0.000252767	3.56282
A_12_P140512	C36C9.6	0.000201862	3.53192
A_12_P105863	str-196	0.00027226	3.4988
A_12_P144365	Y38C1AA.1	0.000246903	3.46198
A_12_P141155	T08G5.8	0.000311096	3.40684
A_12_P135635	ceh-22	0.000145401	3.3994

A_12_P109945	srh-72	0.000645266	3.30247
A_12_P114488	lgc-35	0.000802351	3.24845
A_12_P170841	W05B10.3	0.000182296	3.19486
A_12_P104350	H19N07.3	0.000348684	3.12676
A_12_P111747	nhr-141	0.000465895	3.04493
A_12_P110080	Y18D10A.2	0.000113034	3.04417
A_12_P173858	Y7A5A.3	0.000113083	3.03502
A_12_P181495	gln-3	4.49E-06	2.85341
A_12_P116618	F08C6.5	0.000118531	2.82111
A_12_P171437	C09E9.1	0.000688365	2.80404
A_12_P178386	C08A9.3a	0.000148419	2.76977
A_12_P168322	Y38E10A.13	0.000164495	2.75884
A_12_P103175	amt-4	3.30E-05	2.6813
A_12_P137346	clec-181	0.000404315	2.67641
A_12_P113256	srh-10	0.00044363	2.63881
A_12_P138435	C55C3.7	0.000637795	2.61855
A_12_P100208	R04B5.5	0.000940211	2.5619
A_12_P133636	T27E4.5	0.000904227	2.52347
A_12_P180756	Y41C4A.13	0.000371164	2.51889
A_12_P103058	trf-1	0.000878618	2.44108
A_12_P161430	F18E3.9	0.000744675	2.43772
A_12_P145360	abu-7	6.01E-05	2.37264
A_12_P110454	R09E10.5	0.000113249	2.34388
A_12_P111452	NP280922	7.46E-05	2.30158
A_12_P134400	srt-24	0.000331249	2.29345
A_12_P115369	Y38H6*C*.21	0.000107989	2.27101
A_12_P111190	col-10	0.0006114	2.2557
A_12_P100813	Y102A5*C*.10	7.74E-05	2.24131

A_12_P151700	C17H1.10.2	0.000223938	2.20715
A_12_P115965	T19A6.4	0.000496829	2.2063
A_12_P152708	Y7A9*C*.4	0.000336474	2.15328
A_12_P135005	pqn-5	4.76E-05	2.11369
A_12_P173062	K10D11.2	0.000198915	2.09067
A_12_P101240	R10F2.5	0.00045402	2.08642
A_12_P111035	Y64G10A.2	0.000423566	2.02761
A_12_P153805	T26C5.5	4.09E-05	2.02174
A_12_P113830	T02B11.3	0.000504581	1.98133
A_12_P107996	vab-10	0.000159911	1.97968
A_12_P104448	C34B4.5	0.000346476	1.97061
A_12_P109661	T22E5.1	0.0006798	1.94046
A_12_P141251	W08F4.10	0.000648379	1.92468
A_12_P135644	F41D3.13	0.000180197	1.9229
A_12_P107555	T06C12.9	0.000198904	1.9188
A_12_P107425	clec-84	0.000935475	1.90088
A_12_P109619	Y69E1A.5	0.000878009	1.87692
A_12_P146932	Y65B4BL.6	0.000624176	1.87346
A_12_P179229	srtx-1	0.000659873	1.86327
A_12_P115701	K08F8.1	0.000307577	1.83642
A_12_P115970	T19C4.1	0.000818626	1.82072
A_12_P140658	nab-1	5.46E-05	1.81205
A_12_P114693	F55F1.3	0.000456011	1.79879
A_12_P115633	F42A6.2	0.000408384	1.79634
A_12_P137611	C45B11.7	0.000311872	1.78625
A_12_P105881	srt-56	0.000455665	1.78572
A_12_P154150	F42D1.4	0.000344261	1.77961
A_12_P137345	clec-181	0.000771099	1.76305

A_12_P139266	T05A12.2	0.000270475	1.75123
A_12_P114259	T05A12.2	0.000574611	1.72011
A_12_P108095	C07C7.1.2	0.000182248	1.70914
A_12_P139265	T05A12.2	0.000835964	1.69968
A_12_P146116	sup-10	0.000251724	1.69872
A_12_P100185	C43F9.7	0.00068835	1.68019
A_12_P154378	F28H1.4	0.000516053	1.6668
A_12_P103109	sup-10	0.000893163	1.64955
A_12_P153701	M163.10	0.000115408	1.63829
A_12_P146115	sup-10	0.00037759	1.63399
A_12_P140555	CD4.11	0.000885265	1.61927
A_12_P110706	T25D10.4	0.000798706	1.60807
A_12_P112847	C32D5.6	1.84E-05	1.60344
A_12_P111078	Y110A2AM.1	0.000438252	1.58938
A_12_P116212	F28H7.8	0.000727641	1.58786
A_12_P105592	C38C5.1	0.000376949	1.58765
A_12_P103555	Y71H2AM.16	0.000135573	1.58129
A_12_P117584	R11F4.1	0.000770199	1.56652
A_12_P110850	str-263	0.000365904	1.52813
A_12_P173283	sri-19	1.78E-05	1.50336
A_12_P116016	W09B7.1	0.000948086	1.49998
A_12_P105706	clec-78	0.000366207	1.47994
A_12_P116186	tax-4	0.000294428	1.46832
A_12_P115758	nhr-6	0.000622998	1.46706
A_12_P100726	ZC204.6	0.000158635	1.45478
A_12_P102876	ifta-1	9.96E-05	1.39126
A_12_P112451	qua-1	0.000690698	1.38144
A_12_P100851	unc-9	0.000332137	1.35733

A_12_P133970	VB0395L.1	0.000813377	1.33737
A_12_P157851	tir-1	0.00024081	1.33047
A_12_P136373	TC176241	0.000105504	1.31716
A_12_P139075	srsx-39	0.000960514	1.26322
A_12_P132660	F31E3.2	0.000824185	-1.0093
A_12_P148014	F55C9.11	0.00033475	-1.0095
A_12_P105658	F15E6.5	0.000597791	-1.01022
A_12_P154990	Y26D4A.14	0.000691621	-1.01031
A_12_P155690	T26A8.5	0.000838987	-1.01048
A_12_P163143	Y55B1BL.1	0.000849448	-1.01196
A_12_P119137	srt-28	0.000938974	-1.01241
A_12_P119486	srh-303	0.000790371	-1.01298
A_12_P106494	F53E10.3	0.000919247	-1.01368
A_12_P141641	C01A2.9	0.000948437	-1.01462
A_12_P136804	C02F12.1	0.000610423	-1.01465
A_12_P148226	F26C11.4	0.000831547	-1.01587
A_12_P116260	R07H5.8	0.000524636	-1.16716
A_12_P112654	K08F4.9.1	0.000652578	-1.20578
A_12_P148016	F13H10.9	0.00085066	-1.2326
A_12_P178519	F59E11.4	0.00025881	-1.26288
A_12_P175019	T08B2.5	0.000650598	-1.28783
A_12_P108967	C46A5.8	0.000645003	-1.29969
A_12_P101456	C32E8.9	0.000106301	-1.302
A_12_P179452	lin-45	0.00097981	-1.31011
A_12_P138010	D2030.5.2	0.000610644	-1.33265
A_12_P102258	R11D1.7	0.000141398	-1.38567
A_12_P105767	T17H7.7	0.000267517	-1.39504
A_12_P168549	C04G6.10	0.000827966	-1.3957

A_12_P103130	srab-4	0.000168226	-1.41808
A_12_P107927	K02F2.2	0.000741659	-1.43333
A_12_P107800	Y113G7A.12	0.000169235	-1.44096
A_12_P110086	F16B4.6	0.000486249	-1.44911
A_12_P131267	afd-1	0.000857859	-1.51064
A_12_P167885	sinh-1	0.000144929	-1.52964
A_12_P120043	tag-10	0.000453493	-1.66767
A_12_P111708	W02H5.8	0.000871775	-1.71953
A_12_P150937	F49H6.12	4.90E-05	-1.72981
A_12_P102684	nhr-199	4.00E-06	-1.76936
A_12_P114045	tbx-33	0.00011838	-1.8701
A_12_P110317	C50A2.2	0.000412256	-2.00452
A_12_P177015	F32H5.4	0.000406292	-2.09703
A_12_P106873	T15B7.7	2.06E-05	-2.11393
A_12_P146475	K10C2.6	0.000461374	-2.25945
A_12_P105277	srg-19	0.000720201	-2.28509
A_12_P102702	Y57G11*C*.44	0.000268582	-2.34844
A_12_P104413	clec-167	0.000957943	-2.38218
A_12_P101437	srh-268	0.000915937	-2.44049
A_12_P113427	C46F2.1	3.93E-05	-2.44153
A_12_P100337	arrd-3	0.000664266	-2.51724
A_12_P111072	srg-40	0.000884343	-2.55397
A_12_P148031	F59A6.11	0.00081436	-2.83856
A_12_P132320	H03G16.3	0.000424573	-2.90386
A_12_P112126	W05E10.1	0.000741447	-3.43857
A_12_P120370	aqp-8	0.000910824	-3.67548
A_12_P134885	C04H5.9	0.000538223	-4.26948
A_12_P101376	fmo-2	0.000101609	-4.83386

A_12_P112999	F45E1.4	0.000649957	-6.46482
A_12_P103609	hmit-1.1	0.000401639	-14.9274

Genes in this table have expression levels that are significantly altered in *unc-53 (n152)* animals compared to wild-type. Duplicate genes have been removed from this series when identified by more than one probeset. The largest-fold change was selected for each duplicate gene identified.

Table 19. Forty-nine genes altered in the presence of *P. aeruginosa* PA14 compared to *E. coli* OP50-1 that overlap with (Troemel et al., 2006)**.**

Comparison	*Genes*
N2 animals grown on *E. coli* OP50-1 compared to *P. aeruginosa* PA14 for 12hrs	C05E11.4, C25E10.3, C30G12.2, C32H11.12, C32H11.4, C35A5.3, C38H2.2, C41H7.7, C46F2.1, C49F5.1, C52D10.1, C55B7.4, CD4.2, F01D5.5, F09E10.3, F22A3.6, F25A2.1, F31F4.15, F35E12.5, F37B4.7, F42C5.10, F43E2.5, F46B3.1, F47G4.3, F49H6.13, F53E10.4, F55G11.2, F55G11.3, H02F09.3, H17B01.3, H43E16.1, K09F5.2, K10D11.6, K11H12.4, T05F1.9, T10H9.5, T13F3.6, Y105C5B.28, Y34D9A.11, Y38F1A.6, Y43C5A.3, Y45G5AM.1, Y46C8AL.2, Y46C8AL.4, Y47D3A.2, Y50E8A.16, ZC443.6, ZC455.4, ZK896.5

Comparison is made to the genes found altered in N2 between PA14 and OP50-1 in this study (12hr exposure) to those of Troemel *et al* (2006) (8hr exposure).

7: REFERENCE LIST

Aballay, A. (2009). Neural Regulation of Immunity: Role of NPR-1 in Pathogen Avoidance and Regulation of Innate Immunity. *Cell. Cycle* **8,** 966-969.

Aballay, A. and Ausubel, F. M. (2001). Programmed Cell Death Mediated by Ced-3 and Ced-4 Protects *Caenorhabditis elegans* from Salmonella Typhimurium-Mediated Killing. *Proc. Natl. Acad. Sci. U. S. A.* **98,** 2735-2739.

Aballay, A., Drenkard, E., Hilbun, L. R. and Ausubel, F. M. (2003). *Caenorhabditis elegans* Innate Immune Response Triggered by Salmonella Enterica Requires Intact LPS and is Mediated by a MAPK Signaling Pathway. *Curr. Biol.* **13,** 47-52.

Adeleye, A. (2002). The N-Terminus of UNC-53 Interacts with Regulators of the Actin Cytoskeleton. *M. Sc. Thesis Simon Fraser University*.

Adler, *C.* E., Fetter, R. D. and Bargmann, *C.* I. (2006). UNC-6/Netrin Induces Neuronal Asymmetry and Defines the Site of Axon Formation. *Nat. Neurosci.* **9,** 511-518.

Akhmanova, A. and Steinmetz, M. O. (2010). Microtubule +TIPs at a Glance. *J. Cell. Sci.* **123,** 3415-3419.

Akira, S., Uematsu, S. and Takeuchi, O. (2006). Pathogen Recognition and Innate Immunity. *Cell* **124,** 783-801.

Alper, S., Laws, R., Lackford, B., Boyd, W. A., Dunlap, P., Freedman, J. H. and Schwartz, D. A. (2008). Identification of Innate Immunity Genes and Pathways using a Comparative Genomics Approach. *Proc. Natl. Acad. Sci. U. S. A.* **105,** 7016-7021.

Alper, S., McBride, S. J., Lackford, B., Freedman, J. H. and Schwartz, D. A. (2007). Specificity and Complexity of the *Caenorhabditis elegans* Innate Immune Response. *Mol. Cell. Biol.* **27,** 5544-5553.

Alper, S., McElwee, M. K., Apfeld, J., Lackford, B., Freedman, J. H. and Schwartz, D. A. (2010). The *Caenorhabditis elegans* Germ Line Regulates Distinct Signaling Pathways to Control Lifespan and Innate Immunity. *J. Biol. Chem.* **285,** 1822-1828.

Ashcroft, N. and Golden, A. (2002). CDC-25.1 Regulates Germline Proliferation in *Caenorhabditis elegans*. *Genesis* **33,** 1-7.

Aspenstrom, P. (2005). The Verprolin Family of Proteins: Regulators of Cell Morphogenesis and Endocytosis. *FEBS Lett.* **579,** 5253-5259.

Avery, L. and Thomas, J. H. (1997). Feeding and Defecation. In *C. elegans II* (ed. D. L. Riddle, T. Blumenthal, B. J. Meyer and J. R. Priess). Cold Spring Harbor (NY).

Balistreri, *C.* R., Colonna-Romano, G., Lio, D., Candore, G. and Caruso, *C.* (2009). TLR4 Polymorphisms and Ageing: Implications for the Pathophysiology of Age-Related Diseases. *J. Clin. Immunol.* **29,** 406-415.

Balklava, Z., Pant, S., Fares, H. and Grant, B. D. (2007). Genome-Wide Analysis Identifies a General Requirement for Polarity Proteins in Endocytic Traffic. *Nat. Cell Biol.* **9,** 1066-1073.

Bashaw, G. J. and Klein, R. (2010). Signaling from Axon Guidance Receptors. *Cold Spring Harb Perspect. Biol.* **2,** a001941.

Bear, J. E. and Gertler, F. B. (2009). Ena/VASP: Towards Resolving a Pointed Controversy at the Barbed End. *J. Cell. Sci.* **122,** 1947-1953.

Bear, J. E., Rawls, J. F. and Saxe, *C.* L.,3rd. (1998). SCAR, a WASP-Related Protein, Isolated as a Suppressor of Receptor Defects in Late Dictyostelium Development. *J. Cell Biol.* **142,** 1325-1335.

Becker, T., Loch, G., Beyer, M., Zinke, I., Aschenbrenner, A. *C.*, Carrera, P., Inhester, T., Schultze, J. L. and Hoch, M. (2010). FOXO-Dependent Regulation of Innate Immune Homeostasis. *Nature* **463,** 369-373.

Beli, P., Mascheroni, D., Xu, D. and Innocenti, M. (2008). WAVE and Arp2/3 Jointly Inhibit Filopodium Formation by Entering into a Complex with mDia2. *Nat. Cell Biol.* **10,** 849-857.

Bernadskaya, Y. Y., Patel, F. B., Hsu, H. T. and Soto, M. *C.* (2011). Arp2/3 Promotes Junction Formation and Maintenance in the *Caenorhabditis elegans* Intestine by Regulating Membrane Association of Apical Proteins. *Mol. Biol. Cell* **22,** 2886-2899.

Bettinger, J. *C.*, Lee, K. and Rougvie, A. E. (1996). Stage-Specific Accumulation of the Terminal Differentiation Factor LIN-29 during *Caenorhabditis elegans* Development. *Development* **122,** 2517-2527.

Bierne, H., Miki, H., Innocenti, M., Scita, G., Gertler, F. B., Takenawa, T. and Cossart, P. (2005). WASP-Related Proteins, Abi1 and Ena/VASP are Required for Listeria Invasion Induced by the Met Receptor. *J. Cell. Sci.* **118,** 1537-1547.

Birnbaum, D., Popovici, *C.* and Roubin, R. (2005). A Pair as a Minimum: The Two Fibroblast Growth Factors of the Nematode *Caenorhabditis elegans*. *Dev. Dyn.* **232,** 247-255.

Bischof, L. J., Kao, *C.* Y., Los, F. *C.*, Gonzalez, M. R., Shen, Z., Briggs, S. P., van der Goot, F. G. and Aroian, R. V. (2008). Activation of the Unfolded Protein Response is Required for Defenses Against Bacterial Pore-Forming Toxin in Vivo. *PLoS Pathog.* **4,** e1000176.

Blundell, M. P., Worth, A., Bouma, G. and Thrasher, A. J. (2010). The Wiskott-Aldrich Syndrome: The Actin Cytoskeleton and Immune Cell Function. *Dis. Markers* **29,** 157-175.

Boettner, D. R., Chi, R. J. and Lemmon, S. K. (2011). Lessons from Yeast for Clathrin-Mediated Endocytosis. *Nat. Cell Biol.* **14,** 2-10.

Bogdan, S., Grewe, O., Strunk, M., Mertens, A. and Klambt, *C.* (2004). Sra-1 Interacts with Kette and Wasp and is Required for Neuronal and Bristle Development in Drosophila. *Development* **131,** 3981-3989.

Bogdan, S. and Klambt, *C.* (2003). Kette Regulates Actin Dynamics and Genetically Interacts with Wave and Wasp. *Development* **130,** 4427-4437.

Bogdan, S., Stephan, R., Lobke, *C.*, Mertens, A. and Klambt, *C.* (2005). Abi Activates WASP to Promote Sensory Organ Development. *Nat. Cell Biol.* **7,** 977-984.

Bompard, G. and Caron, E. (2004). Regulation of WASP/WAVE Proteins: Making a Long Story Short. *J. Cell Biol.* **166,** 957-962.

Bosco, E. E., Mulloy, J. *C.* and Zheng, Y. (2009). Rac1 GTPase: A "Rac" of all Trades. *Cell Mol. Life Sci.* **66,** 370-374.

Branda, *C.* S. and Stern, M. J. (1999). Cell Migration and Axon Growth Cone Guidance in *Caenorhabditis elegans*. *Curr. Opin. Genet. Dev.* **9,** 479-484.

Brenner, S. (1974). The Genetics of *Caenorhabditis elegans*. *Genetics* **77,** 71-94.

Broderick, M. J. and Winder, S. J. (2005). Spectrin, Alpha-Actinin, and Dystrophin. *Adv. Protein Chem.* **70,** 203-246.

Bu, W., Chou, A. M., Lim, K. B., Sudhaharan, T. and Ahmed, S. (2009). The Toca-1-N-WASP Complex Links Filopodial Formation to Endocytosis. *J. Biol. Chem.* **284,** 11622-11636.

Bu, W., Lim, K. B., Yu, Y. H., Chou, A. M., Sudhaharan, T. and Ahmed, S. (2010). Cdc42 Interaction with N-WASP and Toca-1 Regulates Membrane Tubulation, Vesicle Formation and Vesicle Motility: Implications for Endocytosis. *PLoS One* **5,** e12153.

Budde, M. W. and Roth, M. B. (2011). The Response of *Caenorhabditis elegans* to Hydrogen Sulfide and Hydrogen Cyanide. *Genetics* **189,** 521-532.

Buechner, M. (2002). Tubes and the Single *C. elegans* Excretory Cell. *Trends Cell Biol.* **12,** 479-484.

Bulow, H. E., Boulin, T. and Hobert, O. (2004). Differential Functions of the *C. elegans* FGF Receptor in Axon Outgrowth and Maintenance of Axon Position. *Neuron* **42,** 367-374.

Burdine, R. D., Chen, E. B., Kwok, S. F. and Stern, M. J. (1997). Egl-17 Encodes an Invertebrate Fibroblast Growth Factor Family Member Required Specifically for Sex Myoblast Migration in *Caenorhabditis elegans*. *Proc. Natl. Acad. Sci. U. S. A.* **94,** 2433-2437.

Burglin, T. R. and Ruvkun, G. (2001). Regulation of Ectodermal and Excretory Function by the *C. elegans* POU Homeobox Gene Ceh-6. *Development* **128,** 779-790.

Burton, E. A., Pendergast, A. M. and Aballay, A. (2006). The *Caenorhabditis elegans* ABL-1 Tyrosine Kinase is Required for Shigella Flexneri Pathogenesis. *Appl. Environ. Microbiol.* **72,** 5043-5051.

Calixto, A., Chelur, D., Topalidou, I., Chen, X. and Chalfie, M. (2010a). Enhanced Neuronal RNAi in *C. elegans* using SID-1. *Nat. Methods* **7,** 554-559.

Calixto, A., Ma, *C.* and Chalfie, M. (2010b). Conditional Gene Expression and RNAi using MEC-8-Dependent Splicing in *C. elegans*. *Nat. Methods* **7,** 407-411.

Carlier, M. F., Nioche, P., Broutin-L'Hermite, I., Boujemaa, R., Le Clainche, *C.*, Egile, *C.*, Garbay, *C.*, Ducruix, A., Sansonetti, P. and Pantaloni, D. (2000). GRB2 Links Signaling to Actin Assembly by Enhancing Interaction of Neural Wiskott-Aldrich Syndrome Protein (N-WASp) with Actin-Related Protein (ARP2/3) Complex. *J. Biol. Chem.* **275,** 21946-21952.

Carlsson, E., Ranki, A., Sipila, L., Karenko, L., Abdel-Rahman, W. M., Ovaska, K., Siggberg, L., Aapola, U., Assamaki, R., Hayry, V. et al. (2012). Potential Role of a Navigator Gene NAV3 in Colorectal Cancer. *Br. J. Cancer* **106,** 517-524.

Carrette, F., Fabre, S. and Bismuth, G. (2009). FOXO1, T-Cell Trafficking and Immune Responses. *Adv. Exp. Med. Biol.* **665,** 3-16.

Castro, F. A., Forsti, A., Buch, S., Kalthoff, H., Krauss, *C.*, Bauer, M., Egberts, J., Schniewind, B., Broering, D. *C.*, Schreiber, S. et al. (2011). TLR-3 Polymorphism is an Independent Prognostic Marker for Stage II Colorectal Cancer. *Eur. J. Cancer*.

Chan, S. S., Zheng, H., Su, M. W., Wilk, R., Killeen, M. T., Hedgecock, E. M. and Culotti, J. G. (1996). UNC-40, a *C. elegans* Homolog of DCC (Deleted in Colorectal Cancer), is Required in Motile Cells Responding to UNC-6 Netrin Cues. *Cell* **87,** 187-195.

Chang, *C.*, Adler, *C.* E., Krause, M., Clark, S. G., Gertler, F. B., Tessier-Lavigne, M. and Bargmann, *C.* I. (2006). MIG-10/lamellipodin and AGE-1/PI3K Promote Axon Guidance and Outgrowth in Response to Slit and Netrin. *Curr. Biol.* **16,** 854-862.

Chang, H. *C.*, Paek, J. and Kim, D. H. (2011). Natural Polymorphisms in *C. elegans* HECW-1 E3 Ligase Affect Pathogen Avoidance Behaviour. *Nature* **480,** 525-529.

Charlie, N. K., Schade, M. A., Thomure, A. M. and Miller, K. G. (2006). Presynaptic UNC-31 (CAPS) is Required to Activate the G Alpha(s) Pathway of the *Caenorhabditis elegans* Synaptic Signaling Network. *Genetics* **172,** 943-961.

Chen, *C.* S., Bellier, A., Kao, *C.* Y., Yang, Y. L., Chen, H. D., Los, F. *C.* and Aroian, R. V. (2010). WWP-1 is a Novel Modulator of the DAF-2 Insulin-Like Signaling Network Involved in Pore-Forming Toxin Cellular Defenses in *Caenorhabditis elegans*. *PLoS One* **5,** e9494.

Chen, E. B., Branda, *C.* S. and Stern, M. J. (1997). Genetic Enhancers of Sem-5 Define Components of the Gonad-Independent Guidance Mechanism Controlling Sex Myoblast Migration in *Caenorhabditis elegans* Hermaphrodites. *Dev. Biol.* **182,** 88-100.

Choi, J. and Newman, A. P. (2006). A Two-Promoter System of Gene Expression in *C. elegans*. *Dev. Biol.* **296,** 537-544.

Clagett-Dame, M. and Knutson, D. (2011). Vitamin A in Reproduction and Development. *Nutrients* **3,** 385-428.

Clark, S. G., Shurland, D. L., Meyerowitz, E. M., Bargmann, *C.* I. and van der Bliek, A. M. (1997). A Dynamin GTPase Mutation Causes a Rapid and Reversible Temperature-Inducible Locomotion Defect in *C. elegans*. *Proc. Natl. Acad. Sci. U. S. A.* **94,** 10438-10443.

Colavita, A. and Culotti, J. G. (1998). Suppressors of Ectopic UNC-5 Growth Cone Steering Identify Eight Genes Involved in Axon Guidance in *Caenorhabditis elegans*. *Dev. Biol.* **194,** 72-85.

Collington, S. J., Williams, T. J. and Weller, *C.* L. (2011). Mechanisms Underlying the Localisation of Mast Cells in Tissues. *Trends Immunol.* **32,** 478-485.

Comer, A. R., Ahern-Djamali, S. M., Juang, J. L., Jackson, P. D. and Hoffmann, F. M. (1998). Phosphorylation of Enabled by the Drosophila Abelson Tyrosine Kinase Regulates the in Vivo Function and Protein-Protein Interactions of Enabled. *Mol. Cell. Biol.* **18,** 152-160.

Cook, D. N., Pisetsky, D. S. and Schwartz, D. A. (2004). Toll-Like Receptors in the Pathogenesis of Human Disease. *Nat. Immunol.* **5,** 975-979.

Cordes, S., Frank, *C.* A. and Garriga, G. (2006). The *C. elegans* MELK Ortholog PIG-1 Regulates Cell Size Asymmetry and Daughter Cell Fate in Asymmetric Neuroblast Divisions. *Development* **133,** 2747-2756.

Couillault, *C.*, Pujol, N., Reboul, J., Sabatier, L., Guichou, J. F., Kohara, Y. and Ewbank, J. J. (2004). TLR-Independent Control of Innate Immunity in *Caenorhabditis elegans* by the TIR Domain Adaptor Protein TIR-1, an Ortholog of Human SARM. *Nat. Immunol.* **5,** 488-494.

Courtney, K. D., Grove, M., Vandongen, H., Vandongen, A., LaMantia, A. S. and Pendergast, A. M. (2000). Localization and Phosphorylation of Abl-Interactor Proteins, Abi-1 and Abi-2, in the Developing Nervous System. *Mol. Cell. Neurosci.* **16,** 244-257.

Coy, J. F., Wiemann, S., Bechmann, I., Bachner, D., Nitsch, R., Kretz, O., Christiansen, H. and Poustka, A. (2002). Pore Membrane and/or Filament Interacting Like Protein 1 (POMFIL1) is Predominantly Expressed in the Nervous System and Encodes Different Protein Isoforms. *Gene* **290,** 73-94.

Dai, Z. and Pendergast, A. M. (1995). Abi-2, a Novel SH3-Containing Protein Interacts with the c-Abl Tyrosine Kinase and Modulates c-Abl Transforming Activity. *Genes Dev.* **9,** 2569-2582.

De Arras, L., Yang, I. V., Lackford, B., Riches, D. W., Prekeris, R., Freedman, J. H., Schwartz, D. A. and Alper, S. (2012). Spatiotemporal Inhibition of Innate Immunity Signaling by the Tbc1d23 RAB-GAP. *J. Immunol.* **188,** 2905-2913.

de Jong, L., Meng, Y., Dent, J. and Hekimi, S. (2004). Thiamine Pyrophosphate Biosynthesis and Transport in the Nematode *Caenorhabditis elegans*. *Genetics* **168,** 845-854.

de la Torre, J. R., Hopker, V. H., Ming, G. L., Poo, M. M., Tessier-Lavigne, M., Hemmati-Brivanlou, A. and Holt, *C.* E. (1997). Turning of Retinal Growth Cones in a Netrin-1 Gradient Mediated by the Netrin Receptor DC*C. Neuron* **19,** 1211-1224.

Delaney, J. R. and Mlodzik, M. (2006). TGF-Beta Activated Kinase-1: New Insights into the Diverse Roles of TAK1 in Development and Immunity. *Cell. Cycle* **5,** 2852-2855.

Dent, E. W., Gupton, S. L. and Gertler, F. B. (2011). The Growth Cone Cytoskeleton in Axon Outgrowth and Guidance. *Cold Spring Harb Perspect. Biol.* **3,** 10.1101/cshperspect.a001800.

DeVeale, B., Brummel, T. and Seroude, L. (2004). Immunity and Aging: The Enemy within? *Aging Cell.* **3,** 195-208.

DeVore, D. L., Horvitz, H. R. and Stern, M. J. (1995). An FGF Receptor Signaling Pathway is Required for the Normal Cell Migrations of the Sex Myoblasts in *C. elegans* Hermaphrodites. *Cell* **83,** 611-620.

Dierking, K., Polanowska, J., Omi, S., Engelmann, I., Gut, M., Lembo, F., Ewbank, J. J. and Pujol, N. (2011). Unusual Regulation of a STAT Protein by an SLC6 Family Transporter in *C. elegans* Epidermal Innate Immunity. *Cell. Host Microbe* **9,** 425-435.

Disanza, A. and Scita, G. (2008). Cytoskeletal Regulation: Coordinating Actin and Microtubule Dynamics in Membrane Trafficking. *Curr. Biol.* **18,** R873-5.

Dixon, S. J., Alexander, M., Chan, K. K. and Roy, P. J. (2008). Insulin-Like Signaling Negatively Regulates Muscle Arm Extension through DAF-12 in *Caenorhabditis elegans*. *Dev. Biol.* **318,** 153-161.

Dixon, S. J., Alexander, M., Fernandes, R., Ricker, N. and Roy, P. J. (2006). FGF Negatively Regulates Muscle Membrane Extension in *Caenorhabditis elegans*. *Development* **133,** 1263-1275.

Dolphin, *C.* T. and Hope, I. A. (2006). *Caenorhabditis elegans* Reporter Fusion Genes Generated by Seamless Modification of Large Genomic DNA Clones. *Nucleic Acids Res.* **34,** e72.

Du, L. and Pertsemlidis, A. (2011). Cancer and Neurodegenerative Disorders: Pathogenic Convergence through microRNA Regulation. *J. Mol. Cell. Biol.* **3,** 176-180.

Duerr, J. S. (2006). Immunohistochemistry. *WormBook*, 1-61.

Dunbar, T. L., Yan, Z., Balla, K. M., Smelkinson, M. G. and Troemel, E. R. (2012). *C. elegans* Detects Pathogen-Induced Translational Inhibition to Activate Immune Signaling. *Cell. Host Microbe* **11,** 375-386.

Echarri, A., Lai, M. J., Robinson, M. R. and Pendergast, A. M. (2004). Abl Interactor 1 (Abi-1) Wave-Binding and SNARE Domains Regulate its Nucleocytoplasmic Shuttling, Lamellipodium Localization, and Wave-1 Levels. *Mol. Cell. Biol.* **24,** 4979-4993.

Ehrlich, J. S., Hansen, M. D. and Nelson, W. J. (2002). Spatio-Temporal Regulation of Rac1 Localization and Lamellipodia Dynamics during Epithelial Cell-Cell Adhesion. *Dev. Cell.* **3,** 259-270.

El-Omar, E. M., Ng, M. T. and Hold, G. L. (2008). Polymorphisms in Toll-Like Receptor Genes and Risk of Cancer. *Oncogene* **27,** 244-252.

Evans, E. A., Chen, W. *C.* and Tan, M. W. (2008a). The DAF-2 Insulin-Like Signaling Pathway Independently Regulates Aging and Immunity in *C. elegans*. *Aging Cell.* **7,** 879-893.

Evans, E. A., Kawli, T. and Tan, M. W. (2008b). Pseudomonas Aeruginosa Suppresses Host Immunity by Activating the DAF-2 Insulin-Like Signaling Pathway in *Caenorhabditis elegans*. *PLoS Pathog.* **4,** e1000175.

Ewbank, J. J. (2006). Signaling in the Immune Response. *WormBook*, 1-12.

Ewbank, J. J. and Zugasti, O. (2011). *C. elegans*: Model Host and Tool for Antimicrobial Drug Discovery. *Dis. Model. Mech.* **4,** 300-304.

Fares, H. and Grant, B. (2002). Deciphering Endocytosis in *Caenorhabditis elegans*. *Traffic* **3,** 11-19.

Fares, H. and Greenwald, I. (2001). Genetic Analysis of Endocytosis in *Caenorhabditis elegans*: Coelomocyte Uptake Defective Mutants. *Genetics* **159,** 133-145.

Ferrandon, D., Imler, J. L., Hetru, *C.* and Hoffmann, J. A. (2007). The Drosophila Systemic Immune Response: Sensing and Signalling during Bacterial and Fungal Infections. *Nat. Rev. Immunol.* **7,** 862-874.

Firat-Karalar, E. N. and Welch, M. D. (2011). New Mechanisms and Functions of Actin Nucleation. *Curr. Opin. Cell Biol.* **23,** 4-13.

Fleming, T., Chien, S. *C.*, Vanderzalm, P. J., Dell, M., Gavin, M. K., Forrester, W. *C.* and Garriga, G. (2010). The Role of *C. elegans* Ena/VASP Homolog UNC-34 in Neuronal Polarity and Motility. *Dev. Biol.* **344,** 94-106.

Fleming, T. *C.*, Wolf, F. W. and Garriga, G. (2005). Sensitized Genetic Backgrounds Reveal a Role for *C. elegans* FGF EGL-17 as a Repellent for Migrating CAN Neurons. *Development* **132,** 4857-4867.

Foley, E. and O'Farrell, P. H. (2004). Functional Dissection of an Innate Immune Response by a Genome-Wide RNAi Screen. *PLoS Biol.* **2,** E203.

Frangioni, J. V. and Neel, B. G. (1993). Solubilization and Purification of Enzymatically Active Glutathione S-Transferase (pGEX) Fusion Proteins. *Anal. Biochem.* **210,** 179-187.

Fricke, R., Gohl, *C.*, Dharmalingam, E., Grevelhorster, A., Zahedi, B., Harden, N., Kessels, M., Qualmann, B. and Bogdan, S. (2009). Drosophila Cip4/Toca-1 Integrates Membrane Trafficking and Actin Dynamics through WASP and SCAR/WAVE. *Curr. Biol.* **19,** 1429-1437.

Fujisawa, K., Wrana, J. L. and Culotti, J. G. (2007). The Slit Receptor EVA-1 Coactivates a SAX-3/Robo Mediated Guidance Signal in *C. elegans*. *Science* **317,** 1934-1938.

Fukata, M., Hernandez, Y., Conduah, D., Cohen, J., Chen, A., Breglio, K., Goo, T., Hsu, D., Xu, R. and Abreu, M. T. (2009). Innate Immune Signaling by Toll-Like Receptor-4 (TLR4) Shapes the Inflammatory Microenvironment in Colitis-Associated Tumors. *Inflamm. Bowel Dis.* **15,** 997-1006.

Funato, Y., Terabayashi, T., Suenaga, N., Seiki, M., Takenawa, T. and Miki, H. (2004). IRSp53/Eps8 Complex is Important for Positive Regulation of Rac and Cancer Cell motility/invasiveness. *Cancer Res.* **64,** 5237-5244.

Fung, S. J., Sivagnanasundaram, S. and Weickert, *C.* S. (2011). Lack of Change in Markers of Presynaptic Terminal Abundance Alongside Subtle Reductions in Markers of Presynaptic Terminal Plasticity in Prefrontal Cortex of Schizophrenia Patients. *Biol. Psychiatry* **69,** 71-79.

Galkin, V. E., Orlova, A., Fattoum, A., Walsh, M. P. and Egelman, E. H. (2006). The CH-Domain of Calponin does Not Determine the Modes of Calponin Binding to F-Actin. *J. Mol. Biol.* **359,** 478-485.

Gallagher, L. A. and Manoil, *C.* (2001). Pseudomonas Aeruginosa PAO1 Kills *Caenorhabditis elegans* by Cyanide Poisoning. *J. Bacteriol.* **183,** 6207-6214.

Galletta, B. J. and Cooper, J. A. (2009). Actin and Endocytosis: Mechanisms and Phylogeny. *Curr. Opin. Cell Biol.* **21,** 20-27.

Galletta, B. J., Mooren, O. L. and Cooper, J. A. (2010). Actin Dynamics and Endocytosis in Yeast and Mammals. *Curr. Opin. Biotechnol.* **21,** 604-610.

Galovic, M., Xu, D., Areces, L. B., van der Kammen, R. and Innocenti, M. (2011). Interplay between N-WASP and CK2 Optimizes Clathrin-Mediated Endocytosis of EGFR. *J. Cell. Sci.* **124,** 2001-2012.

Garigan, D., Hsu, A. L., Fraser, A. G., Kamath, R. S., Ahringer, J. and Kenyon, *C.* (2002). Genetic Analysis of Tissue Aging in *Caenorhabditis elegans*: A Role for Heat-Shock Factor and Bacterial Proliferation. *Genetics* **161,** 1101-1112.

Garsin, D. A., Sifri, *C.* D., Mylonakis, E., Qin, X., Singh, K. V., Murray, B. E., Calderwood, S. B. and Ausubel, F. M. (2001). A Simple Model Host for Identifying Gram-Positive Virulence Factors. *Proc. Natl. Acad. Sci. U. S. A.* **98,** 10892-10897.

Garsin, D. A., Villanueva, J. M., Begun, J., Kim, D. H., Sifri, *C.* D., Calderwood, S. B., Ruvkun, G. and Ausubel, F. M. (2003). Long-Lived *C. elegans* Daf-2 Mutants are Resistant to Bacterial Pathogens. *Science* **300,** 1921.

Ghenea, S., Boudreau, J. R., Lague, N. P. and Chin-Sang, I. D. (2005). The VAB-1 Eph Receptor Tyrosine Kinase and SAX-3/Robo Neuronal Receptors Function Together during *C. elegans* Embryonic Morphogenesis. *Development* **132,** 3679-3690.

Gietz, R. D. and Schiestl, R. H. (2007). Quick and Easy Yeast Transformation using the LiAc/SS Carrier DNA/PEG Method. *Nat. Protoc.* **2,** 35-37.

Gimona, M., Djinovic-Carugo, K., Kranewitter, W. J. and Winder, S. J. (2002). Functional Plasticity of CH Domains. *FEBS Lett.* **513,** 98-106.

Gimona, M. and Mital, R. (1998). The Single CH Domain of Calponin is neither Sufficient nor Necessary for F-Actin Binding. *J. Cell. Sci.* **111 (Pt 13),** 1813-1821.

Giot, L., Bader, J. S., Brouwer, *C.*, Chaudhuri, A., Kuang, B., Li, Y., Hao, Y. L., Ooi, *C.* E., Godwin, B., Vitols, E. et al. (2003). A Protein Interaction Map of Drosophila Melanogaster. *Science* **302,** 1727-1736.

Giuliani, *C.*, Troglio, F., Bai, Z., Patel, F. B., Zucconi, A., Malabarba, M. G., Disanza, A., Stradal, T. B., Cassata, G., Confalonieri, S. et al. (2009). Requirements for F-BAR Proteins TOCA-1 and TOCA-2 in Actin Dynamics and Membrane Trafficking during *Caenorhabditis elegans* Oocyte Growth and Embryonic Epidermal Morphogenesis. *PLoS Genet.* **5,** e1000675.

Goodman, S. J., Branda, *C.* S., Robinson, M. K., Burdine, R. D. and Stern, M. J. (2003). Alternative Splicing Affecting a Novel Domain in the *C. elegans* EGL-15 FGF Receptor Confers Functional Specificity. *Development* **130,** 3757-3766.

Grant, B. and Hirsh, D. (1999). Receptor-Mediated Endocytosis in the *Caenorhabditis elegans* Oocyte. *Mol. Biol. Cell* **10,** 4311-4326.

Grant, B. D. and Sato, M. (2006). Intracellular Trafficking. *WormBook*, 1-9.

Gravato-Nobre, M. J. and Hodgkin, J. (2005). *Caenorhabditis elegans* as a Model for Innate Immunity to Pathogens. *Cell. Microbiol.* **7,** 741-751.

Greener, T., Grant, B., Zhang, Y., Wu, X., Greene, L. E., Hirsh, D. and Eisenberg, E. (2001). *Caenorhabditis elegans* Auxilin: A J-Domain Protein Essential for Clathrin-Mediated Endocytosis in Vivo. *Nat. Cell Biol.* **3,** 215-219.

Grove, M., Demyanenko, G., Echarri, A., Zipfel, P. A., Quiroz, M. E., Rodriguiz, R. M., Playford, M., Martensen, S. A., Robinson, M. R., Wetsel, W. *C.* et al. (2004). ABI2-Deficient Mice Exhibit Defective Cell Migration, Aberrant Dendritic Spine Morphogenesis, and Deficits in Learning and Memory. *Mol. Cell. Biol.* **24,** 10905-10922.

Guillemot, F. and Zimmer, *C.* (2011). From Cradle to Grave: The Multiple Roles of Fibroblast Growth Factors in Neural Development. *Neuron* **71,** 574-588.

Hahm, J. H., Kim, S. and Paik, Y. K. (2011). GPA-9 is a Novel Regulator of Innate Immunity Against Escherichia Coli Foods in Adult *Caenorhabditis elegans*. *Aging Cell.* **10,** 208-219.

Hahtola, S., Burghart, E., Puputti, M., Karenko, L., Abdel-Rahman, W. M., Vakeva, L., Jeskanen, L., Virolainen, S., Karvonen, J., Salmenkivi, K. et al. (2008). Cutaneous T-Cell Lymphoma-Associated Lung Cancers show Chromosomal Aberrations Differing from Primary Lung Cancer. *Genes Chromosomes Cancer* **47,** 107-117.

Hanson, P. I. and Whiteheart, S. W. (2005). AAA+ Proteins: Have Engine, Will Work. *Nat. Rev. Mol. Cell Biol.* **6,** 519-529.

Hao, J. *C.*, Yu, T. W., Fujisawa, K., Culotti, J. G., Gengyo-Ando, K., Mitani, S., Moulder, G., Barstead, R., Tessier-Lavigne, M. and Bargmann, *C.* I. (2001). *C. elegans* Slit Acts in Midline, Dorsal-Ventral, and Anterior-Posterior Guidance Via the SAX-3/Robo Receptor. *Neuron* **32,** 25-38.

Hardin, J. and King, R. S. (2008). The Long and the Short of Wnt Signaling in *C. elegans*. *Curr. Opin. Genet. Dev.* **18,** 362-367.

Harris, T. W., Hartwieg, E., Horvitz, H. R. and Jorgensen, E. M. (2000). Mutations in Synaptojanin Disrupt Synaptic Vesicle Recycling. *J. Cell Biol.* **150,** 589-600.

Haskins, K. A., Russell, J. F., Gaddis, N., Dressman, H. K. and Aballay, A. (2008). Unfolded Protein Response Genes Regulated by CED-1 are Required for *Caenorhabditis elegans* Innate Immunity. *Dev. Cell.* **15,** 87-97.

Hedgecock, E. M., Culotti, J. G. and Hall, D. H. (1990). The Unc-5, Unc-6, and Unc-40 Genes Guide Circumferential Migrations of Pioneer Axons and Mesodermal Cells on the Epidermis in *C. elegans*. *Neuron* **4,** 61-85.

Hekimi, S. and Kershaw, D. (1993). Axonal Guidance Defects in a *Caenorhabditis elegans* Mutant Reveal Cell-Extrinsic Determinants of Neuronal Morphology. *J. Neurosci.* **13,** 4254-4271.

Henderson, S. T. and Johnson, T. E. (2001). Daf-16 Integrates Developmental and Environmental Inputs to Mediate Aging in the Nematode *Caenorhabditis elegans*. *Curr. Biol.* **11,** 1975-1980.

Hetru, *C.* and Hoffmann, J. A. (2009). NF-kappaB in the Immune Response of Drosophila. *Cold Spring Harb Perspect. Biol.* **1,** a000232.

Hirao, N., Sato, S., Gotoh, T., Maruoka, M., Suzuki, J., Matsuda, S., Shishido, T. and Tani, K. (2006). NESH (Abi-3) is Present in the Abi/WAVE Complex but does Not Promote c-Abl-Mediated Phosphorylation. *FEBS Lett.* **580,** 6464-6470.

Hobert, O. (2002). PCR Fusion-Based Approach to Create Reporter Gene Constructs for Expression Analysis in Transgenic *C. elegans*. *BioTechniques* **32,** 728-730.

Hoebe, K., Janssen, E. and Beutler, B. (2004). The Interface between Innate and Adaptive Immunity. *Nat. Immunol.* **5,** 971-974.

Hoeven, R., McCallum, K. *C.*, Cruz, M. R. and Garsin, D. A. (2011). Ce-Duox1/BLI-3 Generated Reactive Oxygen Species Trigger Protective SKN-1 Activity Via p38 MAPK Signaling during Infection in *C. elegans*. *PLoS Pathog.* **7,** e1002453.

Hoffmann, M., Segbert, *C.*, Helbig, G. and Bossinger, O. (2010). Intestinal Tube Formation in *Caenorhabditis elegans* Requires Vang-1 and Egl-15 Signaling. *Dev. Biol.* **339,** 268-279.

Hong, K., Hinck, L., Nishiyama, M., Poo, M. M., Tessier-Lavigne, M. and Stein, E. (1999). A Ligand-Gated Association between Cytoplasmic Domains of UNC5 and DCC Family Receptors Converts Netrin-Induced Growth Cone Attraction to Repulsion. *Cell* **97,** 927-941.

Horng, T. and Medzhitov, R. (2001). Drosophila MyD88 is an Adapter in the Toll Signaling Pathway. *Proc. Natl. Acad. Sci. U. S. A.* **98,** 12654-12658.

Hosono, R. and Kamiya, Y. (1991). Additional Genes which Result in an Elevation of Acetylcholine Levels by Mutations in *Caenorhabditis elegans*. *Neurosci. Lett.* **128,** 243-244.

Hotez, P. J., Savioli, L. and Fenwick, A. (2012). Neglected Tropical Diseases of the Middle East and North Africa: Review of their Prevalence, Distribution, and Opportunities for Control. *PLoS Negl Trop. Dis.* **6,** e1475.

Hu, S., Pawson, T. and Steven, R. M. (2011). UNC-73/trio RhoGEF-2 Activity Modulates *Caenorhabditis elegans* Motility through Changes in Neurotransmitter Signaling Upstream of the GSA-1/Galphas Pathway. *Genetics* **189,** 137-151.

Huang, *C.* G., Lamitina, T., Agre, P. and Strange, K. (2007). Functional Analysis of the Aquaporin Gene Family in *Caenorhabditis elegans*. *Am. J. Physiol. Cell. Physiol.* **292,** C1867-73.

Huber, A. B., Kolodkin, A. L., Ginty, D. D. and Cloutier, J. F. (2003). Signaling at the Growth Cone: Ligand-Receptor Complexes and the Control of Axon Growth and Guidance. *Annu. Rev. Neurosci.* **26,** 509-563.

Hurwitz, M. E., Vanderzalm, P. J., Bloom, L., Goldman, J., Garriga, G. and Horvitz, H. R. (2009). Abl Kinase Inhibits the Engulfment of Apoptotic [Corrected] Cells in *Caenorhabditis elegans*. *PLoS Biol.* **7,** e99.

Ibarra, N., Pollitt, A. and Insall, R. H. (2005). Regulation of Actin Assembly by SCAR/WAVE Proteins. *Biochem. Soc. Trans.* **33,** 1243-1246.

Innocenti, M., Gerboth, S., Rottner, K., Lai, F. P., Hertzog, M., Stradal, T. E., Frittoli, E., Didry, D., Polo, S., Disanza, A. et al. (2005). Abi1 Regulates the Activity of N-WASP and WAVE in Distinct Actin-Based Processes. *Nat. Cell Biol.* **7,** 969-976.

Innocenti, M., Tenca, P., Frittoli, E., Faretta, M., Tocchetti, A., Di Fiore, P. P. and Scita, G. (2002). Mechanisms through which Sos-1 Coordinates the Activation of Ras and Rac. *J. Cell Biol.* **156,** 125-136.

Innocenti, M., Zucconi, A., Disanza, A., Frittoli, E., Areces, L. B., Steffen, A., Stradal, T. E., Di Fiore, P. P., Carlier, M. F. and Scita, G. (2004). Abi1 is Essential for the Formation and Activation of a WAVE2 Signalling Complex. *Nat. Cell Biol.* **6,** 319-327.

Inoue, H., Hisamoto, N., An, J. H., Oliveira, R. P., Nishida, E., Blackwell, T. K. and Matsumoto, K. (2005). The *C. elegans* p38 MAPK Pathway Regulates Nuclear Localization of the Transcription Factor SKN-1 in Oxidative Stress Response. *Genes Dev.* **19,** 2278-2283.

Insall, R. H. and Machesky, L. M. (2009). Actin Dynamics at the Leading Edge: From Simple Machinery to Complex Networks. *Dev. Cell.* **17,** 310-322.

Irazoqui, J. E., Ng, A., Xavier, R. J. and Ausubel, F. M. (2008). Role for Beta-Catenin and HOX Transcription Factors in *Caenorhabditis elegans* and Mammalian Host Epithelial-Pathogen Interactions. *Proc. Natl. Acad. Sci. U. S. A.* **105,** 17469-17474.

Irazoqui, J. E., Troemel, E. R., Feinbaum, R. L., Luhachack, L. G., Cezairliyan, B. O. and Ausubel, F. M. (2010a). Distinct Pathogenesis and Host Responses during Infection of *C. elegans* by P. Aeruginosa and S. Aureus. *PLoS Pathog.* **6,** e1000982.

Irazoqui, J. E., Urbach, J. M. and Ausubel, F. M. (2010b). Evolution of Host Innate Defence: Insights from *Caenorhabditis elegans* and Primitive Invertebrates. *Nat. Rev. Immunol.* **10,** 47-58.

Ishii, N., Wadsworth, W. G., Stern, B. D., Culotti, J. G. and Hedgecock, E. M. (1992). UNC-6, a Laminin-Related Protein, Guides Cell and Pioneer Axon Migrations in *C. elegans*. *Neuron* **9,** 873-881.

Iwasaki, K., Staunton, J., Saifee, O., Nonet, M. and Thomas, J. H. (1997). Aex-3 Encodes a Novel Regulator of Presynaptic Activity in *C. elegans*. *Neuron* **18,** 613-622.

James, P., Halladay, J. and Craig, E. A. (1996). Genomic Libraries and a Host Strain Designed for Highly Efficient Two-Hybrid Selection in Yeast. *Genetics* **144,** 1425-1436.

Janeway, *C.* A.,Jr and Medzhitov, R. (2002). Innate Immune Recognition. *Annu. Rev. Immunol.* **20,** 197-216.

Jia, K., Thomas, *C.*, Akbar, M., Sun, Q., Adams-Huet, B., Gilpin, *C.* and Levine, B. (2009). Autophagy Genes Protect Against Salmonella Typhimurium Infection and Mediate Insulin Signaling-Regulated Pathogen Resistance. *Proc. Natl. Acad. Sci. U. S. A.* **106,** 14564-14569.

Jockusch, B. M., Rothkegel, M. and Schwarz, G. (2004). Linking the Synapse to the Cytoskeleton: A Breath-Taking Role for Microfilaments. *Neuroreport* **15,** 1535-1538.

Jordan, B. R. (2004). How Consistent are Expression Chip Platforms? *Bioessays* **26,** 1236-1242.

Jorgensen, E. M. (2005). Gaba. *WormBook*, 1-13.

Juang, J. L. and Hoffmann, F. M. (1999). Drosophila Abelson Interacting Protein (dAbi) is a Positive Regulator of Abelson Tyrosine Kinase Activity. *Oncogene* **18,** 5138-5147.

Kage-Nakadai, E., Uehara, T. and Mitani, S. (2011). H+/myo-Inositol Transporter Genes, Hmit-1.1 and Hmit-1.2, have Roles in the Osmoprotective Response in *Caenorhabditis elegans*. *Biochem. Biophys. Res. Commun.* **410,** 471-477.

Kamath, R. S., Martinez-Campos, M., Zipperlen, P., Fraser, A. G. and Ahringer, J. (2001). Effectiveness of Specific RNA-Mediated Interference through Ingested Double-Stranded RNA in *Caenorhabditis elegans*. *Genome Biol.* **2,** RESEARCH0002.

Kaneko, T. and Silverman, N. (2005). Bacterial Recognition and Signalling by the Drosophila IMD Pathway. *Cell. Microbiol.* **7,** 461-469.

Karenko, L., Hahtola, S., Paivinen, S., Karhu, R., Syrja, S., Kahkonen, M., Nedoszytko, B., Kytola, S., Zhou, Y., Blazevic, V. et al. (2005). Primary Cutaneous T-Cell Lymphomas show a Deletion Or Translocation Affecting NAV3, the Human UNC-53 Homologue. *Cancer Res.* **65,** 8101-8110.

Karin, M., Lawrence, T. and Nizet, V. (2006). Innate Immunity Gone Awry: Linking Microbial Infections to Chronic Inflammation and Cancer. *Cell* **124,** 823-835.

Katso, R. M., Pardo, O. E., Palamidessi, A., Franz, *C.* M., Marinov, M., De Laurentiis, A., Downward, J., Scita, G., Ridley, A. J., Waterfield, M. D. et al. (2006). Phosphoinositide 3-Kinase C2beta Regulates Cytoskeletal Organization and Cell Migration Via Rac-Dependent Mechanisms. *Mol. Biol. Cell* **17,** 3729-3744.

Kawai, K., Saito, A., Sudo, T. and Osada, H. (2008). Specific Regulation of Cytokine-Dependent p38 MAP Kinase Activation by p62/SQSTM1. *J. Biochem.* **143,** 765-772.

Kawai, T. and Akira, S. (2007). Signaling to NF-kappaB by Toll-Like Receptors. *Trends Mol. Med.* **13,** 460-469.

Kawai, T. and Akira, S. (2011). Toll-Like Receptors and their Crosstalk with Other Innate Receptors in Infection and Immunity. *Immunity* **34,** 637-650.

Kawli, T. and Tan, M. W. (2008). Neuroendocrine Signals Modulate the Innate Immunity of *Caenorhabditis elegans* through Insulin Signaling. *Nat. Immunol.* **9,** 1415-1424.

Kawli, T., Wu, *C.* and Tan, M. W. (2010). Systemic and Cell Intrinsic Roles of Gqalpha Signaling in the Regulation of Innate Immunity, Oxidative Stress, and Longevity in *Caenorhabditis elegans*. *Proc. Natl. Acad. Sci. U. S. A.* **107,** 13788-13793.

Kellenberger, S. and Schild, L. (2002). Epithelial Sodium channel/degenerin Family of Ion Channels: A Variety of Functions for a Shared Structure. *Physiol. Rev.* **82,** 735-767.

Kennedy, B. P., Aamodt, E. J., Allen, F. L., Chung, M. A., Heschl, M. F. and McGhee, J. D. (1993). The Gut Esterase Gene (Ges-1) from the Nematodes *Caenorhabditis elegans* and *Caenorhabditis* Briggsae. *J. Mol. Biol.* **229,** 890-908.

Kennedy, S., Wang, D. and Ruvkun, G. (2004). A Conserved siRNA-Degrading RNase Negatively Regulates RNA Interference in *C. elegans*. *Nature* **427,** 645-649.

Kennedy, T. E., Serafini, T., de la Torre, J. R. and Tessier-Lavigne, M. (1994). Netrins are Diffusible Chemotropic Factors for Commissural Axons in the Embryonic Spinal Cord. *Cell* **78,** 425-435.

Kerry, S., TeKippe, M., Gaddis, N. *C.* and Aballay, A. (2006). GATA Transcription Factor Required for Immunity to Bacterial and Fungal Pathogens. *PLoS One* **1,** e77.

Khan, M. L., Ali, M. Y., Siddiqui, Z. K., Shakir, M. A., Ohnishi, H., Nishikawa, K. and Siddiqui, S. S. (2000). *C. elegans* KLP-11/OSM-3/KAP-1: Orthologs of the Sea Urchin Kinesin-II, and Mouse KIF3A/KIFB/KAP3 Kinesin Complexes. *DNA Res.* **7,** 121-125.

Killeen, M. T. and Sybingco, S. S. (2008). Netrin, Slit and Wnt Receptors Allow Axons to Choose the Axis of Migration. *Dev. Biol.* **323,** 143-151.

Kim, D. (2008). Studying Host-Pathogen Interactions and Innate Immunity in *Caenorhabditis elegans*. *Dis. Model. Mech.* **1,** 205-208.

Kim, D. H., Feinbaum, R., Alloing, G., Emerson, F. E., Garsin, D. A., Inoue, H., Tanaka-Hino, M., Hisamoto, N., Matsumoto, K., Tan, M. W. et al. (2002). A Conserved p38 MAP Kinase Pathway in *Caenorhabditis elegans* Innate Immunity. *Science* **297,** 623-626.

Kim, D. H., Liberati, N. T., Mizuno, T., Inoue, H., Hisamoto, N., Matsumoto, K. and Ausubel, F. M. (2004). Integration of *Caenorhabditis elegans* MAPK Pathways Mediating Immunity and Stress Resistance by MEK-1 MAPK Kinase and VHP-1 MAPK Phosphatase. *Proc. Natl. Acad. Sci. U. S. A.* **101,** 10990-10994.

Kim, J., Lee, A. R., Kawasaki, I., Strome, S. and Shim, Y. H. (2009). A Mutation of Cdc-25.1 Causes Defects in Germ Cells but Not in Somatic Tissues in *C. elegans*. *Mol. Cells* **28,** 43-48.

Kishi, M., Kummer, T. T., Eglen, S. J. and Sanes, J. R. (2005). LL5beta: A Regulator of Postsynaptic Differentiation Identified in a Screen for Synaptically Enriched Transcripts at the Neuromuscular Junction. *J. Cell Biol.* **169,** 355-366.

Klein, *C.*, Mikutta, J., Krueger, J., Scholz, K., Brinkmann, J., Liu, D., Veerkamp, J., Siegel, D., Abdelilah-Seyfried, S. and le Noble, F. (2011). Neuron Navigator 3a Regulates Liver Organogenesis during Zebrafish Embryogenesis. *Development* **138,** 1935-1945.

Korenbaum, E. and Rivero, F. (2002). Calponin Homology Domains at a Glance. *J. Cell. Sci.* **115,** 3543-3545.

Krause, M., Dent, E. W., Bear, J. E., Loureiro, J. J. and Gertler, F. B. (2003). Ena/VASP Proteins: Regulators of the Actin Cytoskeleton and Cell Migration. *Annu. Rev. Cell Dev. Biol.* **19,** 541-564.

Krause, M., Leslie, J. D., Stewart, M., Lafuente, E. M., Valderrama, F., Jagannathan, R., Strasser, G. A., Rubinson, D. A., Liu, H., Way, M. et al. (2004). Lamellipodin, an Ena/VASP Ligand, is Implicated in the Regulation of Lamellipodial Dynamics. *Dev. Cell.* **7,** 571-583.

Krens, S. F., Spaink, H. P. and Snaar-Jagalska, B. E. (2006). Functions of the MAPK Family in Vertebrate-Development. *FEBS Lett.* **580,** 4984-4990.

Kumar, H., Kawai, T. and Akira, S. (2009). Toll-Like Receptors and Innate Immunity. *Biochem. Biophys. Res. Commun.* **388,** 621-625.

Kumar, H., Kawai, T. and Akira, S. (2011). Pathogen Recognition by the Innate Immune System. *Int. Rev. Immunol.* **30,** 16-34.

Kurisu, S. and Takenawa, T. (2009). The WASP and WAVE Family Proteins. *Genome Biol.* **10,** 226.

Kurisu, S. and Takenawa, T. (2010). WASP and WAVE Family Proteins: Friends Or Foes in Cancer Invasion? *Cancer. Sci.* **101,** 2093-2104.

Larkin, J. E., Frank, B. *C.*, Gavras, H., Sultana, R. and Quackenbush, J. (2005). Independence and Reproducibility Across Microarray Platforms. *Nat. Methods* **2,** 337-344.

Larsen, P. L., Albert, P. S. and Riddle, D. L. (1995). Genes that Regulate both Development and Longevity in *Caenorhabditis elegans*. *Genetics* **139,** 1567-1583.

Leinweber, B. D., Leavis, P. *C.*, Grabarek, Z., Wang, *C.* L. and Morgan, K. G. (1999). Extracellular Regulated Kinase (ERK) Interaction with Actin and the Calponin Homology (CH) Domain of Actin-Binding Proteins. *Biochem. J.* **344 Pt 1,** 117-123.

Lemaitre, B., Kromer-Metzger, E., Michaut, L., Nicolas, E., Meister, M., Georgel, P., Reichhart, J. M. and Hoffmann, J. A. (1995). A Recessive Mutation, Immune Deficiency (Imd), Defines Two Distinct Control Pathways in the Drosophila Host Defense. *Proc. Natl. Acad. Sci. U. S. A.* **92,** 9465-9469.

Leng, Y., Zhang, J., Badour, K., Arpaia, E., Freeman, S., Cheung, P., Siu, M. and Siminovitch, K. (2005). Abelson-Interactor-1 Promotes WAVE2 Membrane Translocation and Abelson-Mediated Tyrosine Phosphorylation Required for WAVE2 Activation. *Proc. Natl. Acad. Sci. U. S. A.* **102,** 1098-1103.

Levy-Strumpf, N. and Culotti, J. G. (2007). VAB-8, UNC-73 and MIG-2 Regulate Axon Polarity and Cell Migration Functions of UNC-40 in *C. elegans*. *Nat. Neurosci.* **10,** 161-168.

Li, *C.* and Kim, K. (2008). Neuropeptides. *WormBook*, 1-36.

Liberati, N. T., Fitzgerald, K. A., Kim, D. H., Feinbaum, R., Golenbock, D. T. and Ausubel, F. M. (2004). Requirement for a Conserved Toll/interleukin-1 Resistance Domain Protein in the *Caenorhabditis elegans* Immune Response. *Proc. Natl. Acad. Sci. U. S. A.* **101,** 6593-6598.

Lin, K., Hsin, H., Libina, N. and Kenyon, *C.* (2001). Regulation of the *Caenorhabditis elegans* Longevity Protein DAF-16 by insulin/IGF-1 and Germline Signaling. *Nat. Genet.* **28,** 139-145.

Lin, T. Y., Huang, *C.* H., Kao, H. H., Liou, G. G., Yeh, S. R., Cheng, *C.* M., Chen, M. H., Pan, R. L. and Juang, J. L. (2009). Abi Plays an Opposing Role to Abl in Drosophila Axonogenesis and Synaptogenesis. *Development* **136,** 3099-3107.

Liu, L., Walker, E. A., Kissane, S., Khan, I., Murray, P. I., Rauz, S. and Wallace, G. R. (2011). Gene Expression and miR Profiles of Human Corneal Fibroblasts in Response to Dexamethasone. *Invest. Ophthalmol. Vis. Sci.* **52,** 7282-7288.

Los, F. *C.*, Kao, *C.* Y., Smitham, J., McDonald, K. L., Ha, *C.*, Peixoto, *C.* A. and Aroian, R. V. (2011). RAB-5- and RAB-11-Dependent Vesicle-Trafficking Pathways are Required for Plasma Membrane Repair After Attack by Bacterial Pore-Forming Toxin. *Cell. Host Microbe* **9,** 147-157.

Lowery, L. A. and Van Vactor, D. (2009). The Trip of the Tip: Understanding the Growth Cone Machinery. *Nat. Rev. Mol. Cell Biol.* **10,** 332-343.

Lundquist, E. A. (2003). Rac Proteins and the Control of Axon Development. *Curr. Opin. Neurobiol.* **13,** 384-390.

Lundquist, E. A. (2006). Small GTPases. *WormBook*, 1-18.

Lundquist, E. A., Reddien, P. W., Hartwieg, E., Horvitz, H. R. and Bargmann, *C.* I. (2001). Three *C. elegans* Rac Proteins and several Alternative Rac Regulators Control Axon Guidance, Cell Migration and Apoptotic Cell Phagocytosis. *Development* **128,** 4475-4488.

Luo, L. (2000). Rho GTPases in Neuronal Morphogenesis. *Nat. Rev. Neurosci.* **1,** 173-180.

Machesky, L. M. and Insall, R. H. (1998). Scar1 and the Related Wiskott-Aldrich Syndrome Protein, WASP, Regulate the Actin Cytoskeleton through the Arp2/3 Complex. *Curr. Biol.* **8,** 1347-1356.

Maduzia, L. L., Gumienny, T. L., Zimmerman, *C.* M., Wang, H., Shetgiri, P., Krishna, S., Roberts, A. F. and Padgett, R. W. (2002). Lon-1 Regulates *Caenorhabditis elegans* Body Size Downstream of the Dbl-1 TGF Beta Signaling Pathway. *Dev. Biol.* **246,** 418-428.

Maes, T., Barcelo, A. and Buesa, *C.* (2002). Neuron Navigator: A Human Gene Family with Homology to Unc-53, a Cell Guidance Gene from *Caenorhabditis elegans*. *Genomics* **80,** 21-30.

Mah, A. K., Armstrong, K. R., Chew, D. S., Chu, J. S., Tu, D. K., Johnsen, R. *C.*, Chen, N., Chamberlin, H. M. and Baillie, D. L. (2007). Transcriptional Regulation of AQP-8, a *Caenorhabditis elegans* Aquaporin Exclusively Expressed in the Excretory System, by the POU Homeobox Transcription Factor CEH-6. *J. Biol. Chem.* **282,** 28074-28086.

Mah, A. K., Tu, D. K., Johnsen, R. *C.*, Chu, J. S., Chen, N. and Baillie, D. L. (2010). Characterization of the Octamer, a Cis-Regulatory Element that Modulates Excretory Cell Gene-Expression in *Caenorhabditis elegans*. *BMC Mol. Biol.* **11,** 19.

Mahoney, T. R., Luo, S. and Nonet, M. L. (2006). Analysis of Synaptic Transmission in *Caenorhabditis elegans* using an Aldicarb-Sensitivity Assay. *Nat. Protoc.* **1,** 1772-1777.

Maliniemi, P., Carlsson, E., Kaukola, A., Ovaska, K., Niiranen, K., Saksela, O., Jeskanen, L., Hautaniemi, S. and Ranki, A. (2011). NAV3 Copy Number Changes and Target Genes in Basal and Squamous Cell Cancers. *Exp. Dermatol.* **20,** 926-931.

Mallo, G. V., Kurz, *C.* L., Couillault, *C.*, Pujol, N., Granjeaud, S., Kohara, Y. and Ewbank, J. J. (2002). Inducible Antibacterial Defense System in *C. elegans*. *Curr. Biol.* **12,** 1209-1214.

Maloof, J. N., Whangbo, J., Harris, J. M., Jongeward, G. D. and Kenyon, *C.* (1999). A Wnt Signaling Pathway Controls Hox Gene Expression and Neuroblast Migration in *C. elegans*. *Development* **126,** 37-49.

Manser, J., Roonprapunt, *C.* and Margolis, B. (1997). *C. elegans* Cell Migration Gene Mig-10 Shares Similarities with a Family of SH2 Domain Proteins and Acts Cell Nonautonomously in Excretory Canal Development. *Dev. Biol.* **184,** 150-164.

Manser, J. and Wood, W. B. (1990). Mutations Affecting Embryonic Cell Migrations in *Caenorhabditis elegans*. *Dev. Genet.* **11,** 49-64.

Marcus-Gueret, N., Schmidt, K. L. and Stringham, E. G. (2012). Distinct Cell Guidance Pathways Controlled by the Rac and Rho GEF Domains of UNC-73/TRIO in *Caenorhabditis elegans*. *Genetics* **190,** 129-142.

Marsh, E. K. (2010). Host-Pathogen Interactions in the Innate Immune Response of the Nematode *Caenorhabditis elegans*. *Ph. D. thesis, University of Birmingham*.

Marsh, E. K., van den Berg, M. *C.* and May, R. *C.* (2011). A Two-Gene Balance Regulates Salmonella Typhimurium Tolerance in the Nematode *Caenorhabditis elegans*. *PLoS One* **6,** e16839.

Martinez-Lopez, M. J., Alcantara, S., Mascaro, *C.*, Perez-Branguli, F., Ruiz-Lozano, P., Maes, T., Soriano, E. and Buesa, *C.* (2005). Mouse Neuron Navigator 1, a Novel Microtubule-Associated Protein Involved in Neuronal Migration. *Mol. Cell. Neurosci.* **28,** 599-612.

Mattingly, B. *C.* and Buechner, M. (2011). The FGD Homologue EXC-5 Regulates Apical Trafficking in *C. elegans* Tubules. *Dev. Biol.* **359,** 59-72.

McGhee, J. D. (2007). The *C. elegans* Intestine. *WormBook*, 1-36.

McGhee, J. D., Fukushige, T., Krause, M. W., Minnema, S. E., Goszczynski, B., Gaudet, J., Kohara, Y., Bossinger, O., Zhao, Y., Khattra, J. et al. (2009). ELT-2 is the Predominant Transcription Factor Controlling Differentiation and Function of the *C. elegans* Intestine, from Embryo to Adult. *Dev. Biol.* **327,** 551-565.

McKay, S. J., Johnsen, R., Khattra, J., Asano, J., Baillie, D. L., Chan, S., Dube, N., Fang, L., Goszczynski, B., Ha, E. et al. (2003). Gene Expression Profiling of Cells,

Tissues, and Developmental Stages of the Nematode *C. elegans*. *Cold Spring Harb. Symp. Quant. Biol.* **68,** 159-169.

McNeill, E. M., Roos, K. P., Moechars, D. and Clagett-Dame, M. (2010). Nav2 is Necessary for Cranial Nerve Development and Blood Pressure Regulation. *Neural Dev.* **5,** 6.

McShea, M. A., Schmidt, K. L., Dubuke, M. L., Baldiga, *C.* E., Zhang, S., O'Toole S.M., Gosselin, J., Kuhlwein, M., Hashmi, S., Stringham, E. G. et al. (2012). Abelson Interactor-1 (ABI-1) Interacts with MRL Adaptor Protein MIG-10 and is Required in Guided Cell Migrations and Process Outgrowth in *C.elegans*. *Submitted*.

Merrifield, *C.* J., Qualmann, B., Kessels, M. M. and Almers, W. (2004). Neural Wiskott Aldrich Syndrome Protein (N-WASP) and the Arp2/3 Complex are Recruited to Sites of Clathrin-Mediated Endocytosis in Cultured Fibroblasts. *Eur. J. Cell Biol.* **83,** 13-18.

Merrill, R. A., Plum, L. A., Kaiser, M. E. and Clagett-Dame, M. (2002). A Mammalian Homolog of Unc-53 is Regulated by all-Trans Retinoic Acid in Neuroblastoma Cells and Embryos. *Proc. Natl. Acad. Sci. U. S. A.* **99,** 3422-3427.

Miller, K. G., Emerson, M. D. and Rand, J. B. (1999). Goalpha and Diacylglycerol Kinase Negatively Regulate the Gqalpha Pathway in *C. elegans*. *Neuron* **24,** 323-333.

Mitchell, K. J., Doyle, J. L., Serafini, T., Kennedy, T. E., Tessier-Lavigne, M., Goodman, *C.* S. and Dickson, B. J. (1996). Genetic Analysis of Netrin Genes in Drosophila: Netrins Guide CNS Commissural Axons and Peripheral Motor Axons. *Neuron* **17,** 203-215.

Mizuno, T., Fujiki, K., Sasakawa, A., Hisamoto, N. and Matsumoto, K. (2008). Role of the *Caenorhabditis elegans* Shc Adaptor Protein in the c-Jun N-Terminal Kinase Signaling Pathway. *Mol. Cell. Biol.* **28,** 7041-7049.

Mizuno, T., Hisamoto, N., Terada, T., Kondo, T., Adachi, M., Nishida, E., Kim, D. H., Ausubel, F. M. and Matsumoto, K. (2004). The *Caenorhabditis elegans* MAPK Phosphatase VHP-1 Mediates a Novel JNK-Like Signaling Pathway in Stress Response. *EMBO J.* **23,** 2226-2234.

Mohamed, A. M., Boudreau, J. R., Yu, F. P., Liu, J. and Chin-Sang, I. D. (2012). The *Caenorhabditis elegans* Eph Receptor Activates NCK and N-WASP, and Inhibits Ena/VASP to Regulate Growth Cone Dynamics during Axon Guidance. *PLoS Genet.* **8,** e1002513.

Mohamed, A. M. and Chin-Sang, I. D. (2011). The *C. elegans* Nck-1 Gene Encodes Two Isoforms and is Required for Neuronal Guidance. *Dev. Biol.* **354,** 55-66.

Morisato, D. and Anderson, K. V. (1995). Signaling Pathways that Establish the Dorsal-Ventral Pattern of the Drosophila Embryo. *Annu. Rev. Genet.* **29,** 371-399.

Muley, P. D., McNeill, E. M., Marzinke, M. A., Knobel, K. M., Barr, M. M. and Clagett-Dame, M. (2008). The atRA-Responsive Gene Neuron Navigator 2 Functions in Neurite Outgrowth and Axonal Elongation. *Dev. Neurobiol.* **68,** 1441-1453.

Murphy, *C.* T., Lee, S. J. and Kenyon, *C.* (2007). Tissue Entrainment by Feedback Regulation of Insulin Gene Expression in the Endoderm of *Caenorhabditis elegans*. *Proc. Natl. Acad. Sci. U. S. A.* **104,** 19046-19050.

Murphy, *C.* T., McCarroll, S. A., Bargmann, *C.* I., Fraser, A., Kamath, R. S., Ahringer, J., Li, H. and Kenyon, *C.* (2003). Genes that Act Downstream of DAF-16 to Influence the Lifespan of *Caenorhabditis elegans*. *Nature* **424,** 277-283.

Nelson, F. K., Albert, P. S. and Riddle, D. L. (1983). Fine Structure of the *Caenorhabditis elegans* Secretory-Excretory System. *J. Ultrastruct. Res.* **82,** 156-171.

Nelson, F. K. and Riddle, D. L. (1984). Functional Study of the *Caenorhabditis elegans* Secretory-Excretory System using Laser Microsurgery. *J. Exp. Zool.* **231,** 45-56.

Neumann-Haefelin, E., Qi, W., Finkbeiner, E., Walz, G., Baumeister, R. and Hertweck, M. (2008). SHC-1/p52Shc Targets the insulin/IGF-1 and JNK Signaling Pathways to Modulate Life Span and Stress Response in *C. elegans*. *Genes Dev.* **22,** 2721-2735.

Nizet, V. and Johnson, R. S. (2009). Interdependence of Hypoxic and Innate Immune Responses. *Nat. Rev. Immunol.* **9,** 609-617.

Nobes, *C.* and Hall, A. (1994). Regulation and Function of the Rho Subfamily of Small GTPases. *Curr. Opin. Genet. Dev.* **4,** 77-81.

Nobes, *C.* D. and Hall, A. (1995). Rho, Rac and cdc42 GTPases: Regulators of Actin Structures, Cell Adhesion and Motility. *Biochem. Soc. Trans.* **23,** 456-459.

Nobes, *C.* D., Hawkins, P., Stephens, L. and Hall, A. (1995). Activation of the Small GTP-Binding Proteins Rho and Rac by Growth Factor Receptors. *J. Cell. Sci.* **108 (Pt 1),** 225-233.

Noda, Y. and Sasaki, S. (2008). The Role of Actin Remodeling in the Trafficking of Intracellular Vesicles, Transporters, and Channels: Focusing on Aquaporin-2. *Pflugers Arch.* **456,** 737-745.

Nonet, M. L., Staunton, J. E., Kilgard, M. P., Fergestad, T., Hartwieg, E., Horvitz, H. R., Jorgensen, E. M. and Meyer, B. J. (1997). *Caenorhabditis elegans* Rab-3 Mutant Synapses Exhibit Impaired Function and are Partially Depleted of Vesicles. *J. Neurosci.* **17,** 8061-8073.

Nord, H., Hartmann, *C.*, Andersson, R., Menzel, U., Pfeifer, S., Piotrowski, A., Bogdan, A., Kloc, W., Sandgren, J., Olofsson, T. et al. (2009). Characterization of Novel and Complex Genomic Aberrations in Glioblastoma using a 32K BAC Array. *Neuro Oncol.* **11,** 803-818.

Norris, A. D., Dyer, J. O. and Lundquist, E. A. (2009). The Arp2/3 Complex, UNC-115/abLIM, and UNC-34/Enabled Regulate Axon Guidance and Growth Cone Filopodia Formation in *Caenorhabditis elegans*. *Neural Dev.* **4,** 38.

Norris, A. D. and Lundquist, E. A. (2011). UNC-6/netrin and its Receptors UNC-5 and UNC-40/DCC Modulate Growth Cone Protrusion in Vivo in *C. elegans*. *Development* **138,** 4433-4442.

Nurnberg, A., Kitzing, T. and Grosse, R. (2011). Nucleating Actin for Invasion. *Nat. Rev. Cancer.* **11,** 177-187.

Oh, S. W., Mukhopadhyay, A., Svrzikapa, N., Jiang, F., Davis, R. J. and Tissenbaum, H. A. (2005). JNK Regulates Lifespan in *Caenorhabditis elegans* by Modulating Nuclear Translocation of Forkhead Transcription factor/DAF-16. *Proc. Natl. Acad. Sci. U. S. A.* **102,** 4494-4499.

Olkkonen, V. M. and Stenmark, H. (1997). Role of Rab GTPases in Membrane Traffic. *Int. Rev. Cytol.* **176,** 1-85.

O'Rourke, D., Baban, D., Demidova, M., Mott, R. and Hodgkin, J. (2006). Genomic Clusters, Putative Pathogen Recognition Molecules, and Antimicrobial Genes are Induced by Infection of *C. elegans* with M. Nematophilum. *Genome Res.* **16,** 1005-1016.

Palmer, T. D., Ashby, W. J., Lewis, J. D. and Zijlstra, A. (2011). Targeting Tumor Cell Motility to Prevent Metastasis. *Adv. Drug Deliv. Rev.* **63,** 568-581.

Palmitessa, A. and Benovic, J. L. (2010). Arrestin and the Multi-PDZ Domain-Containing Protein MPZ-1 Interact with Phosphatase and Tensin Homolog (PTEN) and Regulate *Caenorhabditis elegans* Longevity. *J. Biol. Chem.* **285,** 15187-15200.

Pan, *C.* L. and Garriga, G. (2008). Fresh Air is Good for Nerves: Hypoxia Disturbs Axon Guidance. *Nat. Neurosci.* **11,** 859-861.

Pan, *C.* L., Howell, J. E., Clark, S. G., Hilliard, M., Cordes, S., Bargmann, *C.* I. and Garriga, G. (2006). Multiple Wnts and Frizzled Receptors Regulate Anteriorly Directed Cell and Growth Cone Migrations in *Caenorhabditis elegans*. *Dev. Cell.* **10,** 367-377.

Paone, A., Galli, R., Gabellini, *C.*, Lukashev, D., Starace, D., Gorlach, A., De Cesaris, P., Ziparo, E., Del Bufalo, D., Sitkovsky, M. V. et al. (2010). Toll-Like Receptor 3 Regulates Angiogenesis and Apoptosis in Prostate Cancer Cell Lines through Hypoxia-Inducible Factor 1 Alpha. *Neoplasia* **12,** 539-549.

Paquette, N., Broemer, M., Aggarwal, K., Chen, L., Husson, M., Erturk-Hasdemir, D., Reichhart, J. M., Meier, P. and Silverman, N. (2010). Caspase-Mediated Cleavage, IAP Binding, and Ubiquitination: Linking Three Mechanisms Crucial for Drosophila NF-kappaB Signaling. *Mol. Cell* **37,** 172-182.

Park, H., Chan, M. M. and Iritani, B. M. (2010). Hem-1: Putting the "WAVE" into Actin Polymerization during an Immune Response. *FEBS Lett.* **584,** 4923-4932.

Partridge, F. A., Gravato-Nobre, M. J. and Hodgkin, J. (2010). Signal Transduction Pathways that Function in both Development and Innate Immunity. *Dev. Dyn.* **239,** 1330-1336.

Patel, F. B., Bernadskaya, Y. Y., Chen, E., Jobanputra, A., Pooladi, Z., Freeman, K. L., Gally, *C.*, Mohler, W. A. and Soto, M. *C.* (2008). The WAVE/SCAR Complex Promotes Polarized Cell Movements and Actin Enrichment in Epithelia during *C. elegans* Embryogenesis. *Dev. Biol.* **324,** 297-309.

Pawson, T., Gish, G. D. and Nash, P. (2001). SH2 Domains, Interaction Modules and Cellular Wiring. *Trends Cell Biol.* **11,** 504-511.

Peeters, P. J., Baker, A., Goris, I., Daneels, G., Verhasselt, P., Luyten, W. H., Geysen, J. J., Kass, S. U. and Moechars, D. W. (2004). Sensory Deficits in Mice Hypomorphic for a Mammalian Homologue of Unc-53. *Brain Res. Dev. Brain Res.* **150,** 89-101.

Perry, M. D., Li, W., Trent, *C.*, Robertson, B., Fire, A., Hageman, J. M. and Wood, W. B. (1993). Molecular Characterization of the Her-1 Gene Suggests a Direct Role in Cell Signaling during *Caenorhabditis elegans* Sex Determination. *Genes Dev.* **7,** 216-228.

Petalcorin, M. I., Joshua, G. W., Agapow, P. M. and Dolphin, *C.* T. (2005). The Fmo Genes of *Caenorhabditis elegans* and *C.* Briggsae: Characterisation, Gene Expression and Comparative Genomic Analysis. *Gene* **346,** 83-96.

Piccinini, A. M. and Midwood, K. S. (2010). DAMPening Inflammation by Modulating TLR Signalling. *Mediators Inflamm.* **2010,** 672395. Epub 2010 Jul 13.

Pilipiuk, J., Lefebvre, *C.*, Wiesenfahrt, T., Legouis, R. and Bossinger, O. (2009). Increased IP3/Ca2+ Signaling Compensates Depletion of LET-413/DLG-1 in *C. elegans* Epithelial Junction Assembly. *Dev. Biol.* **327,** 34-47.

Pradel, E., Zhang, Y., Pujol, N., Matsuyama, T., Bargmann, *C.* I. and Ewbank, J. J. (2007). Detection and Avoidance of a Natural Product from the Pathogenic Bacterium Serratia Marcescens by *Caenorhabditis elegans*. *Proc. Natl. Acad. Sci. U. S. A.* **104,** 2295-2300.

Pujol, N., Cypowyj, S., Ziegler, K., Millet, A., Astrain, A., Goncharov, A., Jin, Y., Chisholm, A. D. and Ewbank, J. J. (2008). Distinct Innate Immune Responses to Infection and Wounding in the *C. elegans* Epidermis. *Curr. Biol.* **18,** 481-489.

Pujol, N., Link, E. M., Liu, L. X., Kurz, *C.* L., Alloing, G., Tan, M. W., Ray, K. P., Solari, R., Johnson, *C.* D. and Ewbank, J. J. (2001). A Reverse Genetic Analysis of Components of the Toll Signaling Pathway in *Caenorhabditis elegans*. *Curr. Biol.* **11,** 809-821.

Pujol, N., Zugasti, O., Wong, D., Couillault, *C.*, Kurz, *C.* L., Schulenburg, H. and Ewbank, J. J. (2008). Anti-Fungal Innate Immunity in *C. elegans* is Enhanced by Evolutionary Diversification of Antimicrobial Peptides. *PLoS Pathog.* **4,** e1000105.

Qadota, H., Inoue, M., Hikita, T., Koppen, M., Hardin, J. D., Amano, M., Moerman, D. G. and Kaibuchi, K. (2007). Establishment of a Tissue-Specific RNAi System in *C. elegans*. *Gene* **400,** 166-173.

Quinn, *C. C.*, Pfeil, D. S., Chen, E., Stovall, E. L., Harden, M. V., Gavin, M. K., Forrester, W. *C.*, Ryder, E. F., Soto, M. *C.* and Wadsworth, W. G. (2006). UNC-6/netrin and SLT-1/slit Guidance Cues Orient Axon Outgrowth Mediated by MIG-10/RIAM/lamellipodin. *Curr. Biol.* **16,** 845-853.

Quinn, *C. C.*, Pfeil, D. S. and Wadsworth, W. G. (2008). CED-10/Rac1 Mediates Axon Guidance by Regulating the Asymmetric Distribution of MIG-10/lamellipodin. *Curr. Biol.* **18,** 808-813.

Quinn, *C. C.* and Wadsworth, W. G. (2008). Axon Guidance: Asymmetric Signaling Orients Polarized Outgrowth. *Trends Cell Biol.* **18,** 597-603.

Rand, J. B. (2007). Acetylcholine. *WormBook*, 1-21.

Reddy, K. *C.*, Andersen, E. *C.*, Kruglyak, L. and Kim, D. H. (2009). A Polymorphism in Npr-1 is a Behavioral Determinant of Pathogen Susceptibility in *C. elegans*. *Science* **323,** 382-384.

Reebye, V., Frilling, A., Hajitou, A., Nicholls, J. P., Habib, N. A. and Mintz, P. J. (2012). A Perspective on Non-Catalytic Src Homology (SH) Adaptor Signalling Proteins. *Cell. Signal.* **24,** 388-392.

Reichhart, J. M., Georgel, P., Meister, M., Lemaitre, B., Kappler, *C.* and Hoffmann, J. A. (1993). Expression and Nuclear Translocation of the rel/NF-Kappa B-Related Morphogen Dorsal during the Immune Response of Drosophila. *C. R. Acad. Sci. III.* **316,** 1218-1224.

Ren, M., Feng, H., Fu, Y., Land, M. and Rubin, *C.* S. (2009). Protein Kinase D is an Essential Regulator of *C. elegans* Innate Immunity. *Immunity* **30,** 521-532.

Rivera, G. M., Briceno, *C.* A., Takeshima, F., Snapper, S. B. and Mayer, B. J. (2004). Inducible Clustering of Membrane-Targeted SH3 Domains of the Adaptor Protein Nck Triggers Localized Actin Polymerization. *Curr. Biol.* **14,** 11-22.

Robertson, H. M. and Thomas, J. H. (2006). The Putative Chemoreceptor Families of *C. elegans*. *WormBook*, 1-12.

Roelens, I. (2002). Complementary Pathways Control Directional Migration of the Excretory Canals in *Caenorhabditis elegans*. *Ph. D. thesis, Ghent University*.

Rohlfing, A. K., Miteva, Y., Hannenhalli, S. and Lamitina, T. (2010). Genetic and Physiological Activation of Osmosensitive Gene Expression Mimics Transcriptional Signatures of Pathogen Infection in *C. elegans*. *PLoS One* **5,** e9010.

Romagnolo, B., Jiang, M., Kiraly, M., Breton, *C.*, Begley, R., Wang, J., Lund, J. and Kim, S. K. (2002). Downstream Targets of Let-60 Ras in *Caenorhabditis elegans*. *Dev. Biol.* **247,** 127-136.

Rottner, K., Hanisch, J. and Campellone, K. G. (2010). WASH, WHAMM and JMY: Regulation of Arp2/3 Complex and Beyond. *Trends Cell Biol.* **20,** 650-661.

Rutschmann, S., Jung, A. *C.*, Zhou, R., Silverman, N., Hoffmann, J. A. and Ferrandon, D. (2000). Role of Drosophila IKK Gamma in a Toll-Independent Antibacterial Immune Response. *Nat. Immunol.* **1,** 342-347.

Ryu, J. R., Echarri, A., Li, R. and Pendergast, A. M. (2009). Regulation of Cell-Cell Adhesion by Abi/Diaphanous Complexes. *Mol. Cell. Biol.* **29,** 1735-1748.

Sagasti, A., Hisamoto, N., Hyodo, J., Tanaka-Hino, M., Matsumoto, K. and Bargmann, *C.* I. (2001). The CaMKII UNC-43 Activates the MAPKKK NSY-1 to Execute a Lateral Signaling Decision Required for Asymmetric Olfactory Neuron Fates. *Cell* **105,** 221-232.

Saifee, O., Wei, L. and Nonet, M. L. (1998). The *Caenorhabditis elegans* Unc-64 Locus Encodes a Syntaxin that Interacts Genetically with Synaptobrevin. *Mol. Biol. Cell* **9,** 1235-1252.

Sakaguchi, A., Matsumoto, K. and Hisamoto, N. (2004). Roles of MAP Kinase Cascades in *Caenorhabditis elegans*. *J. Biochem.* **136,** 7-11.

Salminen, A., Ojala, J., Huuskonen, J., Kauppinen, A., Suuronen, T. and Kaarniranta, K. (2008). Interaction of Aging-Associated Signaling Cascades: Inhibition of NF-kappaB Signaling by Longevity Factors FoxOs and SIRT1. *Cell Mol. Life Sci.* **65,** 1049-1058.

Sato, Y., Goto, Y., Narita, N. and Hoon, D. S. (2009). Cancer Cells Expressing Toll-Like Receptors and the Tumor Microenvironment. *Cancer. Microenviron* **2 Suppl 1,** 205-214.

Savage-Dunn, *C.* (2005). TGF-Beta Signaling. *WormBook*, 1-12.

Savage-Dunn, *C.*, Maduzia, L. L., Zimmerman, *C.* M., Roberts, A. F., Cohen, S., Tokarz, R. and Padgett, R. W. (2003). Genetic Screen for Small Body Size Mutants in *C. elegans* Reveals Many TGFbeta Pathway Components. *Genesis* **35,** 239-247.

Sawa, M., Suetsugu, S., Sugimoto, A., Miki, H., Yamamoto, M. and Takenawa, T. (2003). Essential Role of the *C. elegans* Arp2/3 Complex in Cell Migration during Ventral Enclosure. *J. Cell. Sci.* **116,** 1505-1518.

Sawa, M. and Takenawa, T. (2006). *Caenorhabditis elegans* WASP-Interacting Protein Homologue WIP-1 is Involved in Morphogenesis through Maintenance of WSP-1 Protein Levels. *Biochem. Biophys. Res. Commun.* **340,** 709-717.

Schmidt, K. L., Marcus-Gueret, N., Adeleye, A., Webber, J., Baillie, D. and Stringham, E. G. (2009). The Cell Migration Molecule UNC-53/NAV2 is Linked to the ARP2/3 Complex by ABI-1. *Development* **136,** 563-574.

Schmitz, *C.*, Kinge, P. and Hutter, H. (2007). Axon Guidance Genes Identified in a Large-Scale RNAi Screen using the RNAi-Hypersensitive *Caenorhabditis elegans* Strain Nre-1(hd20) Lin-15b(hd126). *Proc. Natl. Acad. Sci. U. S. A.* **104,** 834-839.

Schulenburg, H., Hoeppner, M. P., Weiner, J.,3rd and Bornberg-Bauer, E. (2008). Specificity of the Innate Immune System and Diversity of C-Type Lectin Domain (CTLD) Proteins in the Nematode *Caenorhabditis elegans*. *Immunobiology* **213,** 237-250.

Schuske, K. R., Richmond, J. E., Matthies, D. S., Davis, W. S., Runz, S., Rube, D. A., van der Bliek, A. M. and Jorgensen, E. M. (2003). Endophilin is Required for Synaptic Vesicle Endocytosis by Localizing Synaptojanin. *Neuron* **40,** 749-762.

Scita, G., Nordstrom, J., Carbone, R., Tenca, P., Giardina, G., Gutkind, S., Bjarnegard, M., Betsholtz, *C.* and Di Fiore, P. P. (1999). EPS8 and E3B1 Transduce Signals from Ras to Rac. *Nature* **401,** 290-293.

Sechi, A. S. and Wehland, J. (2000). The Actin Cytoskeleton and Plasma Membrane Connection: PtdIns(4,5)P(2) Influences Cytoskeletal Protein Activity at the Plasma Membrane. *J. Cell. Sci.* **113 Pt 21,** 3685-3695.

Serafini, T., Kennedy, T. E., Galko, M. J., Mirzayan, *C.*, Jessell, T. M. and Tessier-Lavigne, M. (1994). The Netrins Define a Family of Axon Outgrowth-Promoting Proteins Homologous to *C. elegans* UNC-6. *Cell* **78,** 409-424.

Shakir, M. A., Jiang, K., Struckhoff, E. *C.*, Demarco, R. S., Patel, F. B., Soto, M. *C.* and Lundquist, E. A. (2008). The Arp2/3 Activators WAVE and WASP have Distinct Genetic Interactions with Rac GTPases in *Caenorhabditis elegans* Axon Guidance. *Genetics* **179,** 1957-1971.

Shao, Z., Zhang, Y. and Powell-Coffman, J. A. (2009). Two Distinct Roles for EGL-9 in the Regulation of HIF-1-Mediated Gene Expression in *Caenorhabditis elegans*. *Genetics* **183,** 821-829.

Shao, Z., Zhang, Y., Ye, Q., Saldanha, J. N. and Powell-Coffman, J. A. (2010). *C. elegans* SWAN-1 Binds to EGL-9 and Regulates HIF-1-Mediated Resistance to the Bacterial Pathogen Pseudomonas Aeruginosa PAO1. *PLoS Pathog.* **6,** e1001075.

Shapira, M., Hamlin, B. J., Rong, J., Chen, K., Ronen, M. and Tan, M. W. (2006). A Conserved Role for a GATA Transcription Factor in Regulating Epithelial Innate Immune Responses. *Proc. Natl. Acad. Sci. U. S. A.* **103,** 14086-14091.

Shapira, M. and Tan, M. W. (2008). Genetic Analysis of *Caenorhabditis elegans* Innate Immunity. *Methods Mol. Biol.* **415,** 429-442.

Sheffield, M., Loveless, T., Hardin, J. and Pettitt, J. (2007). *C. elegans* Enabled Exhibits Novel Interactions with N-WASP, Abl, and Cell-Cell Junctions. *Curr. Biol.* **17,** 1791-1796.

Shen, *C.*, Nettleton, D., Jiang, M., Kim, S. K. and Powell-Coffman, J. A. (2005). Roles of the HIF-1 Hypoxia-Inducible Factor during Hypoxia Response in *Caenorhabditis elegans*. *J. Biol. Chem.* **280,** 20580-20588.

Shen, L. L., Wang, Y. and Wang, D. Y. (2007). Involvement of Genes Required for Synaptic Function in Aging Control in *C. elegans*. *Neurosci. Bull.* **23,** 21-29.

Shi, Y., Alin, K. and Goff, S. P. (1995). Abl-Interactor-1, a Novel SH3 Protein Binding to the Carboxy-Terminal Portion of the Abl Protein, Suppresses v-Abl Transforming Activity. *Genes Dev.* **9,** 2583-2597.

Shioya, M., Obayashi, S., Tabunoki, H., Arima, K., Saito, Y., Ishida, T. and Satoh, J. (2010). Aberrant microRNA Expression in the Brains of Neurodegenerative Diseases: MiR-29a Decreased in Alzheimer Disease Brains Targets Neurone Navigator 3. *Neuropathol. Appl. Neurobiol.* **36,** 320-330.

Shivers, R. P., Kooistra, T., Chu, S. W., Pagano, D. J. and Kim, D. H. (2009). Tissue-Specific Activities of an Immune Signaling Module Regulate Physiological Responses to Pathogenic and Nutritional Bacteria in *C. elegans*. *Cell. Host Microbe* **6,** 321-330.

Shivers, R. P., Pagano, D. J., Kooistra, T., Richardson, *C.* E., Reddy, K. *C.*, Whitney, J. K., Kamanzi, O., Matsumoto, K., Hisamoto, N. and Kim, D. H. (2010). Phosphorylation of the Conserved Transcription Factor ATF-7 by PMK-1 p38 MAPK Regulates Innate Immunity in *Caenorhabditis elegans*. *PLoS Genet.* **6,** e1000892.

Shukla, A. K., Xiao, K. and Lefkowitz, R. J. (2011). Emerging Paradigms of Beta-Arrestin-Dependent Seven Transmembrane Receptor Signaling. *Trends Biochem. Sci.* **36,** 457-469.

Siddiqui, S. S. and Culotti, J. G. (1991). Examination of Neurons in Wild Type and Mutants of *Caenorhabditis elegans* using Antibodies to Horseradish Peroxidase. *J. Neurogenet.* **7,** 193-211.

Sieburth, D., Madison, J. M. and Kaplan, J. M. (2007). PKC-1 Regulates Secretion of Neuropeptides. *Nat. Neurosci.* **10,** 49-57.

Silverman, N., Paquette, N. and Aggarwal, K. (2009). Specificity and Signaling in the Drosophila Immune Response. *Invertebrate Surviv. J.* **6,** 163-174.

Simmer, F., Moorman, *C.*, van der Linden, A. M., Kuijk, E., van den Berghe, P. V., Kamath, R. S., Fraser, A. G., Ahringer, J. and Plasterk, R. H. (2003). Genome-Wide RNAi of *C. elegans* using the Hypersensitive Rrf-3 Strain Reveals Novel Gene Functions. *PLoS Biol.* **1,** E12.

Singh, V. and Aballay, A. (2006). Heat-Shock Transcription Factor (HSF)-1 Pathway Required for *Caenorhabditis elegans* Immunity. *Proc. Natl. Acad. Sci. U. S. A.* **103,** 13092-13097.

Singh, V. and Aballay, A. (2009). Regulation of DAF-16-Mediated Innate Immunity in *Caenorhabditis elegans*. *J. Biol. Chem.* **284,** 35580-35587.

So, *C.* W., So, *C.* K., Cheung, N., Chew, S. L., Sham, M. H. and Chan, L. *C.* (2000). The Interaction between EEN and Abi-1, Two MLL Fusion Partners, and Synaptojanin and Dynamin: Implications for Leukaemogenesis. *Leukemia* **14,** 594-601.

Soete, G., Betist, M. *C.* and Korswagen, H. *C.* (2007). Regulation of *Caenorhabditis elegans* Body Size and Male Tail Development by the Novel Gene Lon-8. *BMC Dev. Biol.* **7,** 20.

Sonnemann, K. J. and Bement, W. M. (2011). Wound Repair: Toward Understanding and Integration of Single-Cell and Multicellular Wound Responses. *Annu. Rev. Cell Dev. Biol.* **27,** 237-263.

Soto, M. *C.*, Qadota, H., Kasuya, K., Inoue, M., Tsuboi, D., Mello, *C. C.* and Kaibuchi, K. (2002). The GEX-2 and GEX-3 Proteins are Required for Tissue Morphogenesis and Cell Migrations in *C. elegans*. *Genes Dev.* **16,** 620-632.

Spiering, D. and Hodgson, L. (2011). Dynamics of the Rho-Family Small GTPases in Actin Regulation and Motility. *Cell. Adh Migr.* **5,** 170-180.

Springer, W., Hoppe, T., Schmidt, E. and Baumeister, R. (2005). A *Caenorhabditis elegans* Parkin Mutant with Altered Solubility Couples Alpha-Synuclein Aggregation to Proteotoxic Stress. *Hum. Mol. Genet.* **14,** 3407-3423.

Steffen, A., Rottner, K., Ehinger, J., Innocenti, M., Scita, G., Wehland, J. and Stradal, T. E. (2004). Sra-1 and Nap1 Link Rac to Actin Assembly Driving Lamellipodia Formation. *EMBO J.* **23,** 749-759.

Stephan, R., Grevelhorster, A., Wenderdel, S., Klambt, *C.* and Bogdan, S. (2008). Abi Induces Ectopic Sensory Organ Formation by Stimulating EGFR Signaling. *Mech. Dev.* **125,** 183-195.

Sternberg, P. W. (2005). Vulval Development. *WormBook*, 1-28.

Steven, R., Kubiseski, T. J., Zheng, H., Kulkarni, S., Mancillas, J., Ruiz Morales, A., Hogue, *C.* W., Pawson, T. and Culotti, J. (1998). UNC-73 Activates the Rac GTPase and is Required for Cell and Growth Cone Migrations in *C. elegans*. *Cell* **92,** 785-795.

Steven, R., Zhang, L., Culotti, J. and Pawson, T. (2005). The UNC-73/Trio RhoGEF-2 Domain is Required in Separate Isoforms for the Regulation of Pharynx Pumping and Normal Neurotransmission in *C. elegans*. *Genes Dev.* **19,** 2016-2029.

Stiernagle, T. (2006). Maintenance of *C. elegans*. *WormBook*, 1-11.

Stradal, T., Courtney, K. D., Rottner, K., Hahne, P., Small, J. V. and Pendergast, A. M. (2001). The Abl Interactor Proteins Localize to Sites of Actin Polymerization at the Tips of Lamellipodia and Filopodia. *Curr. Biol.* **11,** 891-895.

Stradal, T., Kranewitter, W., Winder, S. J. and Gimona, M. (1998). CH Domains Revisited. *FEBS Lett.* **431,** 134-137.

Stradal, T. E., Rottner, K., Disanza, A., Confalonieri, S., Innocenti, M. and Scita, G. (2004). Regulation of Actin Dynamics by WASP and WAVE Family Proteins. *Trends Cell Biol.* **14,** 303-311.

Stringham, E., Pujol, N., Vandekerckhove, J. and Bogaert, T. (2002). Unc-53 Controls Longitudinal Migration in *C. elegans*. *Development* **129,** 3367-3379.

Stringham, E. G., Dixon, D. K., Jones, D. and Candido, E. P. (1992). Temporal and Spatial Expression Patterns of the Small Heat Shock (hsp16) Genes in Transgenic *Caenorhabditis elegans*. *Mol. Biol. Cell* **3,** 221-233.

Stringham, E. G. and Schmidt, K. L. (2009). Navigating the Cell: UNC-53 and the Navigators, a Family of Cytoskeletal Regulators with Multiple Roles in Cell Migration, Outgrowth and Trafficking. *Cell. Adh Migr.* **3,** 342-346.

Struckhoff, E. *C.* and Lundquist, E. A. (2003). The Actin-Binding Protein UNC-115 is an Effector of Rac Signaling during Axon Pathfinding in *C. elegans*. *Development* **130,** 693-704.

Styer, K. L., Singh, V., Macosko, E., Steele, S. E., Bargmann, *C.* I. and Aballay, A. (2008). Innate Immunity in *Caenorhabditis elegans* is Regulated by Neurons Expressing NPR-1/GPCR. *Science* **322,** 460-464.

Sudo, T., Maruyama, M. and Osada, H. (2000). P62 Functions as a p38 MAP Kinase Regulator. *Biochem. Biophys. Res. Commun.* **269,** 521-525.

Sun, H., Bristow, B. N., Qu, G. and Wasserman, S. A. (2002). A Heterotrimeric Death Domain Complex in Toll Signaling. *Proc. Natl. Acad. Sci. U. S. A.* **99,** 12871-12876.

Symons, A., Beinke, S. and Ley, S. *C.* (2006). MAP Kinase Kinase Kinases and Innate Immunity. *Trends Immunol.* **27,** 40-48.

Symons, M. (1996). Rho Family GTPases: The Cytoskeleton and Beyond. *Trends Biochem. Sci.* **21,** 178-181.

Tabara, H., Sarkissian, M., Kelly, W. G., Fleenor, J., Grishok, A., Timmons, L., Fire, A. and Mello, *C. C.* (1999). The Rde-1 Gene, RNA Interference, and Transposon Silencing in *C. elegans*. *Cell* **99,** 123-132.

Takenawa, T. and Suetsugu, S. (2007). The WASP-WAVE Protein Network: Connecting the Membrane to the Cytoskeleton. *Nat. Rev. Mol. Cell Biol.* **8,** 37-48.

Taki, T., Shibuya, N., Taniwaki, M., Hanada, R., Morishita, K., Bessho, F., Yanagisawa, M. and Hayashi, Y. (1998). ABI-1, a Human Homolog to Mouse Abl-Interactor 1, Fuses the MLL Gene in Acute Myeloid Leukemia with t(10;11)(p11.2;q23). *Blood* **92,** 1125-1130.

Tan, M. W. and Shapira, M. (2011). Genetic and Molecular Analysis of Nematode-Microbe Interactions. *Cell. Microbiol.* **13,** 497-507.

Tanaka-Hino, M., Sagasti, A., Hisamoto, N., Kawasaki, M., Nakano, S., Ninomiya-Tsuji, J., Bargmann, *C.* I. and Matsumoto, K. (2002). SEK-1 MAPKK Mediates Ca2+ Signaling to Determine Neuronal Asymmetric Development in *Caenorhabditis elegans*. *EMBO Rep.* **3,** 56-62.

Tani, K., Sato, S., Sukezane, T., Kojima, H., Hirose, H., Hanafusa, H. and Shishido, T. (2003). Abl Interactor 1 Promotes Tyrosine 296 Phosphorylation of Mammalian Enabled (Mena) by c-Abl Kinase. *J. Biol. Chem.* **278,** 21685-21692.

Tanos, B. E. and Pendergast, A. M. (2007). Abi-1 Forms an Epidermal Growth Factor-Inducible Complex with Cbl: Role in Receptor Endocytosis. *Cell. Signal.* **19,** 1602-1609.

Tauszig-Delamasure, S., Bilak, H., Capovilla, M., Hoffmann, J. A. and Imler, J. L. (2002). Drosophila MyD88 is Required for the Response to Fungal and Gram-Positive Bacterial Infections. *Nat. Immunol.* **3,** 91-97.

Tenor, J. L. and Aballay, A. (2008). A Conserved Toll-Like Receptor is Required for *Caenorhabditis elegans* Innate Immunity. *EMBO Rep.* **9,** 103-109.

Thomas, J. H. and Robertson, H. M. (2008). The *Caenorhabditis* Chemoreceptor Gene Families. *BMC Biol.* **6,** 42.

Trent, *C.*, Tsuing, N. and Horvitz, H. R. (1983). Egg-Laying Defective Mutants of the Nematode *Caenorhabditis elegans*. *Genetics* **104,** 619-647.

Troemel, E. R., Chu, S. W., Reinke, V., Lee, S. S., Ausubel, F. M. and Kim, D. H. (2006). P38 MAPK Regulates Expression of Immune Response Genes and Contributes to Longevity in *C. elegans*. *PLoS Genet.* **2,** e183.

Tross, D., Petrenko, L., Klaschik, S., Zhu, Q. and Klinman, D. M. (2009). Global Changes in Gene Expression and Synergistic Interactions Induced by TLR9 and TLR3. *Mol. Immunol.* **46,** 2557-2564.

Valanne, S., Kallio, J., Kleino, A. and Ramet, M. (2011). Large-Scale RNAi Screens Add both Clarity and Complexity to Drosophila NF-kappaB Signaling. *Dev. Comp. Immunol.*

van Haren, J., Draegestein, K., Keijzer, N., Abrahams, J. P., Grosveld, F., Peeters, P. J., Moechars, D. and Galjart, N. (2009). Mammalian Navigators are Microtubule Plus-End Tracking Proteins that can Reorganize the Cytoskeleton to Induce Neurite-Like Extensions. *Cell Motil. Cytoskeleton* **66,** 824-838.

Vance, R. E., Isberg, R. R. and Portnoy, D. A. (2009). Patterns of Pathogenesis: Discrimination of Pathogenic and Nonpathogenic Microbes by the Innate Immune System. *Cell. Host Microbe* **6,** 10-21.

Vartiainen, S., Pehkonen, P., Lakso, M., Nass, R. and Wong, G. (2006). Identification of Gene Expression Changes in Transgenic *C. elegans* Overexpressing Human Alpha-Synuclein. *Neurobiol. Dis.* **22,** 477-486.

Viswanathan, M., Kim, S. K., Berdichevsky, A. and Guarente, L. (2005). A Role for SIR-2.1 Regulation of ER Stress Response Genes in Determining *C. elegans* Life Span. *Dev. Cell.* **9,** 605-615.

Wadsworth, W. G. (2002). Moving Around in a Worm: Netrin UNC-6 and Circumferential Axon Guidance in *C. elegans*. *Trends Neurosci.* **25,** 423-429.

Wang, K. Z., Wara-Aswapati, N., Boch, J. A., Yoshida, Y., Hu, *C.* D., Galson, D. L. and Auron, P. E. (2006). TRAF6 Activation of PI 3-Kinase-Dependent Cytoskeletal Changes is Cooperative with Ras and is Mediated by an Interaction with Cytoplasmic Src. *J. Cell. Sci.* **119,** 1579-1591.

Wang, L. and Ligoxygakis, P. (2006). Pathogen Recognition and Signalling in the Drosophila Innate Immune Response. *Immunobiology* **211,** 251-261.

Wang, Y., Chen, T., Han, *C.*, He, D., Liu, H., An, H., Cai, Z. and Cao, X. (2007). Lysosome-Associated Small Rab GTPase Rab7b Negatively Regulates TLR4 Signaling in Macrophages by Promoting Lysosomal Degradation of TLR4. *Blood* **110,** 962-971.

Watari-Goshima, N., Ogura, K., Wolf, F. W., Goshima, Y. and Garriga, G. (2007). *C. elegans* VAB-8 and UNC-73 Regulate the SAX-3 Receptor to Direct Cell and Growth-Cone Migrations. *Nat. Neurosci.* **10,** 169-176.

Welch, H. *C.*, Coadwell, W. J., Stephens, L. R. and Hawkins, P. T. (2003). Phosphoinositide 3-Kinase-Dependent Activation of Rac. *FEBS Lett.* **546,** 93-97.

White, M. F. and Kahn, *C.* R. (1994). The Insulin Signaling System. *J. Biol. Chem.* **269,** 1-4.

Wightman, B., Baran, R. and Garriga, G. (1997). Genes that Guide Growth Cones Along the *C. elegans* Ventral Nerve Cord. *Development* **124,** 2571-2580.

Wightman, B., Clark, S. G., Taskar, A. M., Forrester, W. *C.*, Maricq, A. V., Bargmann, *C.* I. and Garriga, G. (1996). The *C. elegans* Gene Vab-8 Guides Posteriorly Directed Axon Outgrowth and Cell Migration. *Development* **122,** 671-682.

Windoffer, R., Beil, M., Magin, T. M. and Leube, R. E. (2011). Cytoskeleton in Motion: The Dynamics of Keratin Intermediate Filaments in Epithelia. *J. Cell Biol.* **194,** 669-678.

Withee, J., Galligan, B., Hawkins, N. and Garriga, G. (2004). *Caenorhabditis elegans* WASP and Ena/VASP Proteins Play Compensatory Roles in Morphogenesis and Neuronal Cell Migration. *Genetics* **167,** 1165-1176.

Witte, H., Neukirchen, D. and Bradke, F. (2008). Microtubule Stabilization Specifies Initial Neuronal Polarization. *J. Cell Biol.* **180,** 619-632.

Wolf, F. W. (1998). Posterior Migration Guidance in *Caenorhabditis elegans*. *Doctor Dissertation, University of California, Berkeley*.

Wolf, F. W., Hung, M. S., Wightman, B., Way, J. and Garriga, G. (1998). Vab-8 is a Key Regulator of Posteriorly Directed Migrations in *C. elegans* and Encodes a Novel Protein with Kinesin Motor Similarity. *Neuron* **20,** 655-666.

Wolf, M., Nunes, F., Henkel, A., Heinick, A. and Paul, R. J. (2008). The MAP Kinase JNK-1 of *Caenorhabditis elegans*: Location, Activation, and Influences Over Temperature-Dependent Insulin-Like Signaling, Stress Responses, and Fitness. *J. Cell. Physiol.* **214,** 721-729.

Wong, D., Bazopoulou, D., Pujol, N., Tavernarakis, N. and Ewbank, J. J. (2007). Genome-Wide Investigation Reveals Pathogen-Specific and Shared Signatures in the Response of *Caenorhabditis elegans* to Infection. *Genome Biol.* **8,** R194.

Wu, Y. *C.*, Cheng, T. W., Lee, M. *C.* and Weng, N. Y. (2002). Distinct Rac Activation Pathways Control *Caenorhabditis elegans* Cell Migration and Axon Outgrowth. *Dev. Biol.* **250,** 145-155.

Youngman, M. J., Rogers, Z. N. and Kim, D. H. (2011). A Decline in p38 MAPK Signaling Underlies Immunosenescence in *Caenorhabditis elegans*. *PLoS Genet.* **7,** e1002082.

Yu, T. W., Hao, J. *C.*, Lim, W., Tessier-Lavigne, M. and Bargmann, *C.* I. (2002). Shared Receptors in Axon Guidance: SAX-3/Robo Signals Via UNC-34/Enabled and a Netrin-Independent UNC-40/DCC Function. *Nat. Neurosci.* **5,** 1147-1154.

Zallen, J. A., Yi, B. A. and Bargmann, *C.* I. (1998). The Conserved Immunoglobulin Superfamily Member SAX-3/Robo Directs Multiple Aspects of Axon Guidance in *C. elegans*. *Cell* **92,** 217-227.

Zhang, G. and Ghosh, S. (2001). Toll-Like Receptor-Mediated NF-kappaB Activation: A Phylogenetically Conserved Paradigm in Innate Immunity. *J. Clin. Invest.* **107,** 13-19.

Zhang, Y. and Kubiseski, T. J. (2010). *Caenorhabditis elegans* Wsp-1 Regulation of Synaptic Function at the Neuromuscular Junction. *J. Biol. Chem.* **285,** 23040-23046.

Zhang, Y. L. and Dong, *C.* (2005). MAP Kinases in Immune Responses. *Cell. Mol. Immunol.* **2,** 20-27.

Zhao, Z., Fang, L., Chen, N., Johnsen, R. *C.*, Stein, L. and Baillie, D. L. (2005). Distinct Regulatory Elements Mediate Similar Expression Patterns in the Excretory Cell of *Caenorhabditis elegans*. *J. Biol. Chem.* **280,** 38787-38794.

Zhou, Z., Caron, E., Hartwieg, E., Hall, A. and Horvitz, H. R. (2001). The *C. elegans* PH Domain Protein CED-12 Regulates Cytoskeletal Reorganization Via a Rho/Rac GTPase Signaling Pathway. *Dev. Cell.* **1,** 477-489.

Ziegler, K., Kurz, *C.* L., Cypowyj, S., Couillault, *C.*, Pophillat, M., Pujol, N. and Ewbank, J. J. (2009). Antifungal Innate Immunity in *C. elegans*: PKCdelta Links G Protein Signaling and a Conserved p38 MAPK Cascade. *Cell. Host Microbe* **5,** 341-352.

Zugasti, O. and Ewbank, J. J. (2009). Neuroimmune Regulation of Antimicrobial Peptide Expression by a Noncanonical TGF-Beta Signaling Pathway in *Caenorhabditis elegans* Epidermis. *Nat. Immunol.* **10,** 249-256.